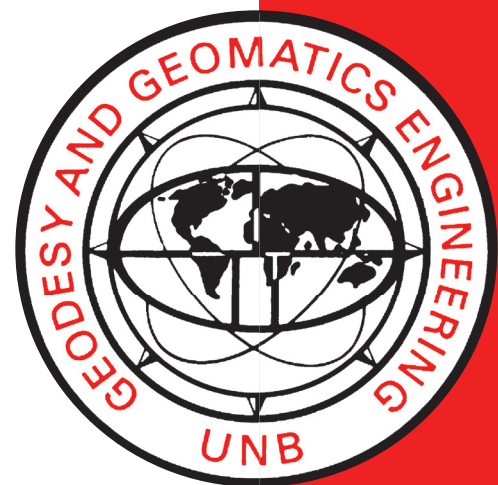


# **PHOTOGRAMMETRY: THE CONCEPTS**

**E. E. DERENYI**

**September 1996**



**LECTURE NOTES  
NO. 57**

# **PHOTOGRAMMETRY: THE CONCEPTS**

E. E. Derenyi

Department of Geodesy and Geomatics Engineering  
University of New Brunswick  
P.O. Box 4400  
Fredericton, N.B.  
Canada  
E3B 5A3

September 1996

## PREFACE

In order to make our extensive series of lecture notes more readily available, we have scanned the old master copies and produced electronic versions in Portable Document Format. The quality of the images varies depending on the quality of the originals. The images have not been converted to searchable text.

## **PREFACE**

These lecture notes present the concepts and principles of photogrammetry, both the analogue and the analytical. Emphasis is placed on the analytical procedures, which are time invariant and provide the most rigorous solutions. Analogue photogrammetry was invented to physically model the geometric relationships between image, model and object space at the time when the computational solution of the complex mathematical expressions was practically impossible. This is no longer the case, and the use of analogue photogrammetry is declining rapidly.

The technology and practice of photogrammetry is very dynamic, and new instruments and techniques are constantly being introduced. Therefore, instruments and techniques are only treated in general terms without reference to particular makes or models. The reader is referred to the scientific literature for the most up-to-date information.

Eugene E. Derenyi

### **NOTE**

Certain material in these lecture notes has been copied under license from CANCOPY. Resale or further copying of this material is strictly prohibited.

## 1. INTRODUCTION

The objectives of *surveying engineering* are the acquisition, processing, rendering, dissemination and management of *spatial information* on or near the surface of the earth. The word “spatial” indicates that the location of the information is known in three-dimensional space. In other words, the information is *geographically referenced* in a three-dimensional coordinate system. Locating features, objects and phenomena in three-dimensional space, combining these data with their attributes and arrange them in a form that is convenient and functional for utilization by interested parties is a primary responsibility of surveying engineers. In certain cases, time may also be of importance and is included as the fourth dimension. The name *geomatics* has now been chosen to represent the above activities. It is an abbreviated form of *geoinformatics* (geoinformation) and incorporates both the qualitative and quantitative information pertaining to the earth (geos).

The two fundamental elements (measurements) used to derive spatial positions are: *direction* and *distance*. These elements can be obtained either by direct observation, or indirectly, by measuring a quantity which is a function of these elements. Measurements made with a theodolite, a level or a tape are direct observations of the fundamental elements. The measurement of distances with an electronic distance measuring (EDM) device is indirect observation, since the distances are derived by recording the time of propagation of the electromagnetic wave between two points. Positioning by the global positioning system (GPS) is done by means of distances to satellites which are based on accurate observations of the time of travel of the electromagnetic signal. Images can also be used for spatial positioning, and measurements made in images are also considered indirect observations with respect to the two fundamental elements.

*Image* means likeness, a representation of reality. Images are created by *projection*, a process or technique of reproducing a spatial object upon a plane or curved surface by straight lines (rays) which originate at the object and are intersected by the surface. If two points are joined by a straight line, one point is said to be projected upon the other.

Projection is a subset of *transformation*, which means a change in position, size, shape and orientation. Projection is also considered *mapping*, which means to assign to every element of a set a corresponding element in another set.

Projections can be constructed *mathematically*, *graphically* and *physically*. The physical construction of projections is performed by various optical or mechanical devices, such as a photographic camera.

An image latently contains one or both fundamental elements of spatial positioning. In fact all imaging devices operate on either the direction or the distance measuring (ranging) principle. The relative position of points in an image is a function of either the direction in which the corresponding object point was observed by the imaging device, or of the distance between the imaging device and the object point or both. A photographic camera is a directional imaging device; a side-looking airborne radar (SLAR), and a side-scan sonar are ranging devices; while a plane positional indicator (PPI) radar (navigation radar) measures both range and direction.

In physical imaging, the projecting ray is the electromagnetic or accoustic energy reflected or emitted by an object. Imaging devices that capable of sensing and recording this radiation are often referred to as *sensors*. The observation of objects by a sensor occurs from a certain distance without getting into contact with them. Therefore, this type of data acquisition is referred to as *remote sensing*.

Images provide much more information than what is required for spatial positioning. In fact they comprise three distinct kinds of data:

- *geometric data* (direction and distance), which indicate the spatial relationship between image and object points and are used to reconstruct spatial positions;
- *radiometric data* (grey level), which indicate the intensity of the electromagnetic radiation which was reflected or emitted from objects, and received by a sensor. These data are used to identify objects and their qualitative characteristics;
- *spectral data* (colour), which indicate the dominant wavelength of the radiation emanating from objects, and are also used for qualitative analysis.

Images are recorded in either *analogue* (physical) or *digital* form. Analogue images are 'hard copies', where the intensity of radiation received by the sensor is visualized in grey levels or in shades of color on photographic paper or film. Digital

images are 'soft copies' and record the radiance of objects numerically in small, regularly spaced area elements. These values are stored as a matrix, an element of which is called picture element or *pixel*.

Images are utilized in two distinct manner: by performing either *metric or interpretative analysis*. In the metric analysis, quantitative measurements are made in the image and then geometric information, such as spatial position, distance, area, shape, size, volume, distribution of objects are derived. This operation is called *photogrammetry*. The definition of photogrammetry is therefore: the science of obtaining reliable measurements by means of images for the determination of the geometric properties of objects.

The principal application of photogrammetry is to determine the spatial position of the natural and man-made features situated on the earth's surface (*topographic* application). Photogrammetry is also used as a measuring tool in architecture, industrial design, deformation studies of structures, accident investigation, medicine etc. These operations are referred to as *non-topographic* applications.

According to the location of the sensor during data acquisition, there are three branches of photogrammetry: *Terrestrial* photogrammetry means that the images are acquired by a ground based stationary sensor. *Aerial* photogrammetry deals with images taken with sensors mounted on airborne platforms. *Space* photogrammetry embraces the processing of images recorded of the earth or of other planets from satellites. *Close-range* photogrammetry is a sub-branch of terrestrial photogrammetry implying that the sensor is situated in the close vicinity of the object to be imaged.

There are two methods available for performing the photogrammetric measurements and processing the data. One method employs complex instruments, which physically model the geometric relationship that existed between the image and the object at the time of data acquisition. These instruments act as analogue computers and the method is called *analogue or instrumental photogrammetry*.

Photogrammetric operations can also be performed by mathematical modelling. This method is called *analytical, numerical or computational* photogrammetry. The utilization of digital images is a special case in analytical photogrammetry, because of the type of instrumentation used and the wide range of data processing operations that are

available compared to working with hard copy images. This class is called *digital or soft copy photogrammetry*.

Regardless of the data processing method employed in photogrammetry, the spatial position of points is determined by the fundamental geometric operation of *intersection*. Two rays which meet in space produce an intersection and define a point.

In the interpretative evaluation of images, *qualitative* observations are made to detect the presence of certain phenomenon, identify and classify objects and to ascertain their physical condition, state and properties. This category forms the science and art of *image interpretation* or *image analysis*. The two types of evaluation processes are not mutually exclusive. Image interpretation may require that some measurements be made to facilitate the interpretation. Conversely, in photogrammetry a certain amount of interpretation must be performed during mapping to assign attributes to objects .

It is evident from the preceding discussion that the objectives of surveying engineering can be met equally well by utilizing images of a scene to be surveyed rather than making on-site measurements. In fact, imaging fits much better the meaning of the word surveying than the observations made in the field. The primary dictionary definition “surveying” is to look over; to view as from a high place; to take a broad general view.

Imaging has distinct advantages over data acquisition by direct, on-site, measurement.

- An image is a complete, *comprehensive record* of a scene or situation as it existed at the instant of acquisition.
- It is a *multilevel data* set which can provide both quantitative and qualitative information.
- Data acquisition can be accomplished within a short time over large areas by imaging from the air or space.
- Processing and analysis of this data can be made at an appropriate time and place, distant from the scene and can be repeated or augmented at will.
- The direct observation of directions and distances means point-by-point measurement, while on images *continuous measurements* can be made by tracing or delineating objects.

Nevertheless, certain limitations of photogrammetry must also be recognized.

- The *weather* and the *seasons* can place severe restrictions on the primary data acquisition. On the other hand, under favorable conditions, images can be acquired over a large tract of land within a short period of time from the air or from space.
- It is not feasible to use aerial photography for the survey of small areas.
- Equipment needed for the acquisition and processing of the data is *more expensive* and more *complex* to operate than those used for surveying on site.
- Photogrammetry is not an entirely *self sufficient* spatial positioning process. A certain amount of on-site observations are needed to control and verify the analysis.
- At the current state of the art, direct in situ measurements can provide the highest possible accuracy for determining spatial positions.

The choice of using direct observations or imaging to solve a particular spatial positioning problem should be decided through a *pre-analysis* in which all requirements, conditions, circumstances are carefully considered.

## 2. GEOMETRIC TRANSFORMATIONS

The relative position of points in space are defined by coordinates in a reference system. Frequently used reference systems are the:

- *polar* coordinate system ( $r, \theta$ , in a two-dimensional space);
- *geodetic* (geographic) coordinate system (latitude  $\phi$ , longitude  $\lambda$  and the height above the ellipsoid  $h$ );
- *Cartesian* (rectangular) coordinate system ( $x, y, z$ ).

Most photogrammetric operations are performed in a right-handed Cartesian coordinate system.

Geometric transformations change the position, size, shape and orientation of objects by changing their coordinates according to the functions:

$$x' = f_1(x, y, z) ,$$

$$y' = f_2(x, y, z) ,$$

$$z' = f_3(x, y, z).$$

The discussion is restricted to *point transformations*, which constitute the simplest class of geometric transformations. These transformations let the point persist as a space element, i.e., the transformation brings every point into correspondence with another point. In contrast, some other transformations carry the point over into other space elements, such as a straight line, a plane, a sphere, etc.

The transition brought about by transformation can be interpreted geometrically in a *passive* and in an *active* way. The passive interpretation is a change in the coordinate system while the object remains stationary. A new set of coordinates  $x', y', z'$  are then assigned to every point with coordinates  $x, y, z$  in the original system. In contrast, the active interpretation regards the coordinate system fixed and changes the location of the object in space. Points with coordinates  $x, y, z$  are moved to a new location  $x', y', z'$  in space.

In photogrammetry, measurements are made on physical objects, in real or virtual models, instruments, images, maps, etc., each with their own reference system. Therefore, transformation from one coordinate system to another is a frequent requirement.

## 2.1 Fundamental Transformations

There are four fundamental transformations. Expressed mathematically in two-dimensional space, they are as follows:

1. *Translation* by constant  $a$  and  $b$  means:

$$x' = x + a, \quad y' = y + b. \quad (2-1)$$

2. *Rotation* through an angle  $\beta$  means:

$$\begin{aligned} x' &= x \cos \beta + y \sin \beta, \\ y' &= -x \sin \beta + y \cos \beta. \end{aligned} \quad (2-2)$$

3. *Reflection* in one of the axes is:

$$x' = x, \quad y' = -y \quad \text{or} \quad x' = -x, \quad y' = y. \quad (2-3)$$

4. *Scale change* by a factor of  $S$  means:

$$x' = Sx, \quad y' = Sy. \quad (2-4)$$

Reflection is not used in photogrammetry and will not be considered any further.

The passive interpretation of translation means shifting the origin of the coordinate system in the direction of the axes. Rotation means that the origin remains fixed while the axes are displaced. Scale change means a change in the unit of measure.

The active interpretation of the fundamental transformations is also rather simple. Translation means a shift of the object parallel with the coordinate axes. Rotation means all possible displacement of a rigid object, with one of its points is kept fixed. Therefore, if an object is displaced so that the new position of one of its points is the same as its initial position, the displacement is a rotation. A scale change actively interpreted is an expansion or contraction of the object in the direction of the coordinate axes, while the unit of measure remains the same.

A combination of the above fundamental transformations generates a variety of changes in the coordinates. The various possibilities are now summarized for the passive case in two dimensions.

## 2.2 Transformations of the Coordinate System in Two-Dimensional Space

- a) Rotation is expressed in matrix form as:

$$\begin{pmatrix} x' \\ y' \end{pmatrix} = \begin{pmatrix} \cos \beta & \sin \beta \\ -\sin \beta & \cos \beta \end{pmatrix} \begin{pmatrix} x \\ y \end{pmatrix} \quad (2-5)$$

or  $\bar{x}' = M \bar{x}$ ,

where  $M$  is called the *rotation matrix* and the bar represents the vector of coordinates. The rotation matrix is orthogonal, whereby its inverse is equal to its transpose. Therefore, the inverse transformation becomes

$$\begin{pmatrix} x \\ y \end{pmatrix} = \begin{pmatrix} \cos \beta & -\sin \beta \\ \sin \beta & \cos \beta \end{pmatrix} \begin{pmatrix} x' \\ y' \end{pmatrix}, \quad (2-6)$$

or  $\bar{x} = M^{-1} x' = M^T \bar{x}'$ .

b) Rotation and uniform scale change are combined as

$$\begin{pmatrix} x' \\ y' \end{pmatrix} = \begin{pmatrix} s \cos \beta & s \sin \beta \\ -s \sin \beta & s \cos \beta \end{pmatrix} \begin{pmatrix} x \\ y \end{pmatrix} \quad (2-7)$$

or in parametric form

$$\begin{pmatrix} x' \\ y' \end{pmatrix} = \begin{pmatrix} a & b \\ -b & a \end{pmatrix} \begin{pmatrix} x \\ y \end{pmatrix} \quad (2-8)$$

This is a *two-parameter* transformation. The inverse relationship is

$$\begin{pmatrix} x \\ y \end{pmatrix} = \frac{1}{a^2+b^2} \begin{pmatrix} a & -b \\ b & a \end{pmatrix} \begin{pmatrix} x' \\ y' \end{pmatrix} \quad (2-9)$$

c) The combination of rotation, translation and scale change becomes in parametric form

$$\begin{pmatrix} x' \\ y' \end{pmatrix} = \begin{pmatrix} a & b \\ -b & a \end{pmatrix} \begin{pmatrix} x \\ y \end{pmatrix} + \begin{pmatrix} c \\ d \end{pmatrix} \quad (2-10)$$

This is a *four-parameter* transformation, referred to as *two-dimensional similarity* or *linear conformal* transformation. It preserves the magnitude of the angles. Similarity transformation is often used in imaging and mapping because it includes a change of scale. The inverse transformation is

$$\begin{pmatrix} x \\ y \end{pmatrix} = \frac{1}{a^2 + b^2} \begin{pmatrix} a & -b \\ b & a \end{pmatrix} \begin{pmatrix} x' \\ y' \end{pmatrix} - \begin{pmatrix} c \\ d \end{pmatrix}. \quad (2-11)$$

d) A six-parameter transformation is obtained by expanding the four-parameter transformation by incorporating a non-uniform scale change and a differential rotation of one of the axes. The explicit form is

$$\begin{pmatrix} x' \\ y' \end{pmatrix} = \begin{pmatrix} \cos \beta & \sin \beta \\ -\sin \beta & \cos \beta \end{pmatrix} \begin{pmatrix} 1 & 0 \\ -\delta & 1 \end{pmatrix} \begin{pmatrix} s_x x \\ s_y y \end{pmatrix} + \begin{pmatrix} c_1 \\ c_2 \end{pmatrix} \quad (2-12)$$

The rotation matrix is therefore

$$M = M_{\beta} M_{\delta} = \begin{pmatrix} (\cos \beta - \delta \sin \beta) & \sin \beta \\ -(\sin \beta + \delta \cos \beta) & \cos \beta \end{pmatrix} \quad (2-13)$$

Note that  $M$  is **not** orthogonal. The transformation expressed in parametric form is

$$\begin{pmatrix} x' \\ y' \end{pmatrix} = \begin{pmatrix} a_1 & b_1 \\ a_2 & b_2 \end{pmatrix} \begin{pmatrix} x \\ y \end{pmatrix} + \begin{pmatrix} c_1 \\ c_2 \end{pmatrix} \quad (2-14)$$

The inverse transformation is

$$\begin{pmatrix} x \\ y \end{pmatrix} = \frac{1}{a_1 b_2 - a_2 b_1} \begin{pmatrix} b_2 & -b_1 \\ -a_2 & a_1 \end{pmatrix} \begin{pmatrix} x' \\ y' \end{pmatrix} - \begin{pmatrix} c_1 \\ c_2 \end{pmatrix} \quad (2-15)$$

This transformation is called *affine transformation*. It represents a common rotation of both axes by the same angle, a differential rotation of one of the two axes, two scale changes which differ in the direction of the two axes and two translations. Parallel lines remain parallel but the magnitude of angles is not preserved. It is used in photogrammetry to model and correct errors which destroy orthogonality and introduce a non-uniform scale.

e) The general two-dimensional polynomial transformation has the form

$$\begin{aligned} x' &= a_0 + a_1 x + a_2 y + a_3 xy + a_4 x^2 + a_5 y^2 + \dots \\ y' &= b_0 + b_1 x + b_2 y + b_3 xy + b_4 x^2 + b_5 y^2 + \dots \end{aligned} \quad (2-16)$$

f) The conformal two-dimensional polynomial transformation is derived from Equation (2-16) by enforcing the condition

$$\frac{\partial x'}{\partial x} = \frac{\partial y'}{\partial y} \quad \text{and} \quad \frac{\partial x'}{\partial y} = -\frac{\partial y'}{\partial x}$$

whereby the transformation becomes

$$\begin{aligned}x' &= A_0 + A_1x + A_2y + A_3(x^2 - y^2) + A_4(2xy) + \dots \\x' &= B_0 - A_2x + A_1y - A_4(x^2 - y^2) + A_3(2xy) + \dots\end{aligned}\quad (2-17)$$

The transformations are now extended to three-dimensional space.

## 2.3 Transformations in Three-Dimensional Space

Here the transition of a three-dimensional right-hand Cartesian coordinate system takes place  $(x, y, z)$ . By combining the three fundamental transformations the most general transformation possible includes three rotations, three translations and three scale changes. First the rotations are dealt with.

### 2.3.1 Rotating a three-dimensional coordinate system

In photogrammetry as in surveying the  $xy$  axes are assumed to lie in the horizontal plane and the  $z$ -axis is vertical. A rotation around the  $x$  axis is denoted by the Greek letter  $\omega$ , the rotation around  $y$  is  $\phi$  and around  $z$  is  $\kappa$ . Looking from the positive end of an axis towards the origin, an anti-clockwise rotation is considered a positive rotation around that axis. Conversely, a clockwise rotations when viewed at the origin in the positive direction of an axis is considered positive (Figure 2-1).

Based on the derivation of the rotation in two-dimensional space, the following three rotation matrices express the individual rotations in space around the three axes:

$$\begin{aligned}M_\omega \text{ or } M_x &= \begin{bmatrix} 1 & 0 & 0 \\ 0 & \cos \omega & \sin \omega \\ 0 & -\sin \omega & \cos \omega \end{bmatrix} \\M_\phi \text{ or } M_y &= \begin{bmatrix} \cos \phi & 0 & -\sin \phi \\ 0 & 1 & 0 \\ \sin \phi & 0 & \cos \phi \end{bmatrix} \\M_\kappa \text{ or } M_z &= \begin{bmatrix} \cos \kappa & \sin \kappa & 0 \\ -\sin \kappa & \cos \kappa & 0 \\ 0 & 0 & 1 \end{bmatrix}\end{aligned}\quad (2-18)$$

where the subscripts  $\omega, \phi, \kappa$  represent the angles of rotation and the subscripts  $x, y, z$  designate the axis around which the rotation occurs.

Sequential rotations can be combined into a single 3x3 rotation matrix by multiplication. Since matrix multiplication is not commutative, the sequence in which the rotations are introduced must be considered. The first rotation matrix must be pre-multiplied by the second rotation and then by the third rotation, etc. If, for example, the y and z axes are rotated first around the x axis by  $\omega$ , and then the x axis and the previously rotated z are rotated around the once rotated y axis by  $\phi$ , and finally the previously rotated x and y axes are rotated about the twice rotated z by  $\kappa$ , then the resultant rotation matrix is formed as

$$M_r = M_\kappa M_\phi M_\omega$$

or 
$$M_r = M_z M_y M_x \quad (2-19)$$

By performing the multiplication the resultant matrix becomes

$$M_r = \begin{bmatrix} \cos \phi \cos \kappa & \cos \omega \sin \kappa + \sin \omega \sin \phi \cos \kappa & \sin \omega \sin \kappa - \cos \omega \sin \phi \cos \kappa \\ -\cos \phi \sin \kappa & \cos \omega \cos \kappa - \sin \omega \sin \phi \sin \kappa & \sin \omega \cos \kappa + \cos \omega \sin \phi \sin \kappa \\ \sin \phi & -\sin \omega \cos \phi & \cos \omega \cos \phi \end{bmatrix} \quad (2-20)$$

The matrix  $M_r$  is orthogonal since each of the three matrices used to form it are orthogonal. The general form of  $M_r$  is:

$$M_r = \begin{pmatrix} m_{11} & m_{12} & m_{13} \\ m_{21} & m_{22} & m_{23} \\ m_{31} & m_{32} & m_{33} \end{pmatrix}.$$

There are a total of  $3! = 3 \times 2 = 6$  possible sequences for the multiplication of the three matrices. The effect of combining rotations in different sequences can be visualized by an experiment performed with a dice as shown in Figure 2-2.

The rotation angles can be computed from the known numerical values of the nine elements of  $M_r$  by equating them with corresponding elements in the trigonometric form of the matrix. For example, for the matrix in Equation (2-20) the angles are computed as:

$$\begin{aligned} \phi &= \arcsin m_{31} \\ \omega &= \arcsin \frac{-m_{32}}{m_{33}} \\ \kappa &= \arcsin \frac{-m_{21}}{m_{11}} \end{aligned}$$

### 2.3.2 First order approximation of the rotation matrix

The sin function of a small angle is approximately equal to the angle in radians and the cos of this angle is approximately equal to unity. Thereby the first order approximation of the three rotation matrices becomes

$$M_x = \begin{bmatrix} 1 & 0 & 0 \\ 0 & 1 & \omega \\ 0 & -\omega & 1 \end{bmatrix} = I + \begin{bmatrix} 0 & 0 & 0 \\ 0 & 0 & \omega \\ 0 & -\omega & 0 \end{bmatrix} = I + \bar{M}_x \quad (2-21)$$

$$M_y = \begin{bmatrix} 1 & 0 & -\phi \\ 0 & 1 & 0 \\ \phi & 0 & 1 \end{bmatrix} = I + \begin{bmatrix} 0 & 0 & -\phi \\ 0 & 0 & 0 \\ \phi & 0 & 0 \end{bmatrix} = I + \bar{M}_y \quad (2-22)$$

$$M_z = \begin{bmatrix} 1 & \kappa & 0 \\ -\kappa & 1 & 0 \\ 0 & 0 & 1 \end{bmatrix} = I + \begin{bmatrix} 0 & \kappa & 0 \\ -\kappa & 0 & 0 \\ 0 & 0 & 0 \end{bmatrix} = I + \bar{M}_z \quad (2-23)$$

The resultant first order approximation of the rotation matrix for the sequence of rotation used in Equation (2-19) can be formed as

$$M_r = (I + \bar{M}_z)(I + \bar{M}_y)(I + \bar{M}_x) = I + \bar{M}_z + \bar{M}_y + \bar{M}_x$$

The products of the Ms are small and are omitted. The resultant matrix is

$$M_r = \begin{bmatrix} 1 & \kappa & -\phi \\ -\kappa & 1 & \omega \\ \phi & -\omega & 1 \end{bmatrix} \quad (2-24)$$

It should be noted that the form of the first approximation of the rotation matrix is independent of the sequence in which the three rotations are introduced. This matrix is not truly orthogonal.

### 2.3.3 Rotation of an object in a fixed system

Keeping with the sign convention for the rotations as stated in Section 2.3.1, the three rotation matrices that express the rotation of a rigid object around a fixed set of axes becomes:

$$\begin{pmatrix} 1 & 0 & 0 \\ 0 & \cos \omega & -\sin \omega \\ 0 & \sin \omega & \cos \omega \end{pmatrix} = M_{\omega}^T \text{ or } M_x^T \quad (2-29)$$

$$\begin{pmatrix} \cos \phi & 0 & \sin \phi \\ 0 & 1 & 0 \\ -\sin \phi & 0 & \cos \phi \end{pmatrix} = M_{\phi}^T \text{ or } M_y^T \quad (2-30)$$

$$\begin{pmatrix} \cos \kappa & -\sin \kappa & 0 \\ \sin \kappa & \cos \kappa & 0 \\ 0 & 0 & 1 \end{pmatrix} = M_{\kappa}^T = M_z^T \quad (2-31)$$

The active rotation matrix is the transpose of the passive matrix.

In some applications a combination of rotating the object as well as the axes may be necessary. The following is an example. Consider the case when the axes  $x, y, z$  are rotated from the original orientation by a matrix  $R$  to assume the orientation  $x', y', z'$ , as shown in Figure 2-3.  $P$  is a point with coordinates  $x, y, z$  in the original system. This point is then rotated by matrix  $A$  to the position  $P_1$ .

$$\text{Rotated point in the fixed system } P_1 = A^T P$$

$$\text{Fixed point in the rotated system: } P' = R P$$

The combination of the two types of rotations results in the following expressions of the spatial position of  $P$ .

$$P_1' = R P_1 = A^T R P = A^T P'$$

If a point is rotated about one set of axes the coordinates of that point can be found with respect to another set of axes provided that the relationship between the two sets of axes is known.

Note, that in a fully analytical solution of a photogrammetric problem the general form of the rotation matrix can be freely chosen, as long as the same form of the matrix is used consistently throughout the solution. In this case it is unimportant whether the axis or the object is rotating, and in what sequence the three rotation matrices are combined. The definition of the rotation matrix must be known, however, if rotation angles are taken from a previous solution. It is safer to take over the numerical values of the matrix.

### 2.3.4 The parametric form of the rotation matrix

Rotations around three mutually perpendicular axes can also be expressed by three independent parameters instead of using the rotation angles themselves. An orthogonal rotation matrix  $M$  can be formed as

$$M = (I + S) (I - S)^{-1},$$

where  $S$  is a real skew symmetric matrix. The above equation is called *Caley's formula*.

To prove that  $M$  formed in this manner is a proper rotation matrix, first it has to be proven that  $(I-S)^{-1}$  exists. This is done by proving that  $|I-S| \neq 0$ .

If  $S$  is chosen to be

$$S = \frac{1}{2} \begin{bmatrix} 0 & -c & b \\ c & 0 & -a \\ -b & a & 0 \end{bmatrix} \quad (2-25)$$

then

$$I - S = \begin{bmatrix} 1 & c/2 & -b/2 \\ -c/2 & 1 & a/2 \\ b/2 & -a/2 & 1 \end{bmatrix}$$

Therefore

$$\begin{aligned} |I-S| &= 1 \left(1 + \frac{a^2}{4}\right) - \frac{c}{2} \left(-\frac{c}{2} - \frac{a}{2} \frac{b}{2}\right) - \frac{b}{2} \left(\frac{c}{2} \frac{a}{2} - \frac{b}{2}\right) \\ &= 1 + \frac{a^2}{4} + \frac{c^2}{4} + \frac{c}{2} \frac{a}{2} \frac{b}{2} - \frac{b}{2} \frac{c}{2} \frac{a}{2} + \frac{b^2}{4} \\ &= 1 + \frac{a^2}{4} + \frac{b^2}{4} + \frac{c^2}{4} \\ &= 1 + \frac{1}{4} (a^2 + b^2 + c^2) \end{aligned}$$

$|I-S|$  can never be zero, as all terms are positive.

Next it must be proven that M is orthogonal by proving that  $M^T M = I$ .

$$\begin{aligned} M^T M &= [(I+S) (I-S)^{-1}]^T [(I+S) (I-S)^{-1}] \\ &= (I-S)^{-1T} (I+S)^T (I+S) (I-S)^{-1} \\ &= (I+S)^{-1} (I-S) (I+S) (I-S)^{-1} \end{aligned}$$

To facilitate the proof of orthogonality it is now proven that

$$(I-S) (I+S) = (I+S) (I-S)$$

$$(I-S)(I+S) = \begin{pmatrix} 1 & c/2 & -b/2 \\ -c/2 & 1 & a/2 \\ b/2 & -a/2 & 1 \end{pmatrix} \begin{pmatrix} 1 & -c/2 & b/2 \\ c/2 & 1 & -a/2 \\ -b/2 & a/2 & 1 \end{pmatrix}$$

$$= \begin{pmatrix} 1+c^2/4+b^2/4 & -b/2 a/2 & -c/2 a/2 \\ -b/2 a/2 & 1+c^2/4+a^2/4 & -c/2 b/2 \\ -c/2 a/2 & -c/2 b/2 & 1+a^2/4+b^2/4 \end{pmatrix}$$

$$(I+S) (I-S) = \begin{pmatrix} 1 & -c/2 & b/2 \\ c/2 & 1 & -a/2 \\ -b/2 & a/2 & 1 \end{pmatrix} \begin{pmatrix} 1 & c/2 & -b/2 \\ -c/2 & 1 & a/2 \\ b/2 & -a/2 & 1 \end{pmatrix}$$

$$= \begin{pmatrix} 1+c^2/4+b^2/4 & -b/2 a/2 & -c/2 a/2 \\ -b/2 a/2 & 1+c^2/4+a^2/4 & -c/2 b/2 \\ -c/2 a/2 & -c/2 b/2 & 1+a^2/4+b^2/4 \end{pmatrix}$$

Therefore,  $(I-S)(I+S) = (I+S)(I-S)$

Completion of proof for  $M^T M = I$  is:

$$\begin{aligned} M^T M &= (I+S)^{-1} (I-S) (I+S) (I-S)^{-1} \\ &= (I+S)^{-1} (I+S) (I-S) (I-S)^{-1} \\ &= (I) (I) = I. \end{aligned}$$

It can also be proven in a similar way that  $(I+S)^{-1} (I-S)$  is orthogonal, by proving that  $MM^T = I$ .

$$\begin{aligned} MM^T &= (I+S)^{-1} (I-S) [(I+S)^{-1} (I-S)]^T \\ &= (I+S)^{-1} (I-S) (I-S)^{-1T} \\ &= (I+S)^{-1} (I-S) (I+S) (I-S)^{-1} \\ &= (I+S)^{-1} (I+S) (I-S) (I-S)^{-1} \\ &= (I) (I) = I. \end{aligned}$$

The matrix  $M$  is now formed by using Cayley's Formula:  $M = (I+S) (I-S)^{-1}$ .

$$(I-S)^{-1} = \frac{1}{1 + \frac{1}{4}(a^2+b^2+c^2)} \begin{pmatrix} 1+a^2/4 & a/2 b/2-c/2 & a/2 c/2+b/2 \\ a/2 b/2+c/2 & 1+b^2/4 & b/2 c/2-a/2 \\ a/2 c/2-b/2 & b/2 c/2+a/2 & 1+c^2/4 \end{pmatrix}$$

If  $1 + \frac{1}{4}(a^2+b^2+c^2) = |I-S| = \Delta$  then

$$\begin{aligned} M &= \frac{1}{\Delta} \begin{pmatrix} 1 & -c/2 & b/2 \\ c/2 & 1 & -a/2 \\ -b/2 & a/2 & 1 \end{pmatrix} \begin{pmatrix} 1+a^2/4 & ab/4 - c/2 & ac/4 + b/2 \\ ab/4 + c/2 & 1 + b^2/4 & bc/4 - a/2 \\ ac/4 - b/2 & bc/4 + a/2 & 1+c^2/4 \end{pmatrix} \\ &= \frac{1}{\Delta} \begin{pmatrix} 1+a^2/4-b^2/4-c^2/4 & -c + ab/2 & b + ac/2 \\ c + ab/2 & 1-a^2/4+b^2/4-c^2/4 & -a + bc/2 \\ -b + ac/2 & a + bc/2 & 1-a^2/4-b^2/4+c^2/4 \end{pmatrix} \quad (2-26) \end{aligned}$$

Let  $\Delta' = (1 - \frac{1}{4}(a^2 + b^2 + c^2))$ , then

$$M = \frac{1}{\Delta} \begin{pmatrix} \Delta'+a^2/2 & -c + ab/2 & b + ac/2 \\ c + ab/2 & \Delta'+b^2/2 & -a + bc/2 \\ -b + ac/2 & a + bc/2 & \Delta'+c^2/2 \end{pmatrix} \quad (2-27)$$

The rotation matrix  $M$  formed by the three independent parameters  $a$ ,  $b$  and  $c$  is known as the *Rodrigues matrix*.

The first order approximation of the Rodrigues matrix is

$$M = \begin{pmatrix} 1 & -c & b \\ c & 1 & -a \\ -b & a & 1 \end{pmatrix} \quad (2-28)$$

### **2.3.5 Rotations in a gimbal system**

In instruments, rotations in a three-dimensional coordinate system are introduced by employing a gimbal suspension. In this system, a rotation about one axis may upset the orientation of the other axes. Therefore, to know the manner in which the three axes are suspended and support one another is of utmost importance. For example, in the case shown in Figure 2-4, axis A is fixed and supports B which in turn supports axis C. Consequently

A is the primary axis,

B is the secondary axis, and

C is the tertiary axis.

A rotation introduced around the primary axis will also rotate the secondary and the tertiary axes. The rotation around the secondary axis will only affect the orientation of the tertiary axis. While a rotation of an object around the tertiary axis does not change the setting of any of the axes. Rotations around A, B then C in this sequence means that the rotation around B will be around an axis displaced by the primary rotation. The rotation around C will be around an axis which is displaced twice, first by the primary rotation and then by the secondary rotation.

The gimbal suspension can be visualized by imagining that the telescope of a theodolite can rotate around its axis. The rotation of the telescope leaves all three axes stationary; a rotation about the horizontal axis will also rotate the telescope and its axis while the rotation around the vertical axis will rotate the telescope with its axis and also the horizontal axis. Therefore, the vertical axis is the primary, the horizontal axis the secondary and the telescope axis the tertiary axis of the theodolite.

Mathematically these rotations can be dealt with in the following way: A fixed system of axes (X, Y, Z) is taken coincident with the initial position of the gimbal axes A, B, C respectively. The rotation of a body around the primary, secondary and tertiary

gimbal axes can be expressed by rotations around the fixed system of axes (X, Y, Z), by forming the resultant rotation matrix  $M_R$  as:

$$M_R = M_P M_S M_T \quad (2-32)$$

where  $M_P$ ,  $M_S$  and  $M_T$  are the matrices of the rotation around the primary, secondary and tertiary axes respectively.

The hierarchy of axes is an important factor in analogue photogrammetry if the rotations that are happening in instruments are to be expressed analytically. Such is the case when pre-computed rotations are set in instruments or when rotations that had been made in instruments are used in subsequent mathematical computations. The ranking of the axes depends on the way the projector is supported and must be learned from the operator's manual or by examining the instrument. The direction of the positive and negative rotation must be ascertained in the same manner. For example, in instruments manufactured by the Wild (Leica) firm, Z is the tertiary, X is the secondary and Y the primary axes. The same applies to the Balplex and Kelsh plotters. The resultant matrix is therefore formed as

$$M_R = M_Y M_X M_Z = M_\phi M_\omega M_\kappa .$$

In instruments of the Zeiss firm the order is

$$M_R = M_X M_Y M_Z = M_\omega M_\phi M_\kappa .$$

In purely analytical solutions the ranking of the axes is unimportant as long as all rotation matrices in a particular solution are consistently formed in the same manner.

### **2.3.6 Three-dimensional similarity transformation**

The most frequently used coordinate transformation in three-dimensional space is a seven parameter transformation which introduces a uniform scale change, three rotations and three translations. It has the form

$$\begin{pmatrix} x' \\ y' \\ z' \end{pmatrix} = S M_R \begin{pmatrix} x \\ y \\ z \end{pmatrix} + \begin{pmatrix} x_T \\ y_T \\ z_T \end{pmatrix} \quad (2-33)$$

where S is the scale factor,  $x_T$ ,  $y_T$ ,  $z_T$  are the translation constants and  $M_R$  is the resultant matrix of the rotations around the three axes.  $M_R$  must be formed in accordance with the sequence in which rotations are introduced or according to the hierarchy of the axes.

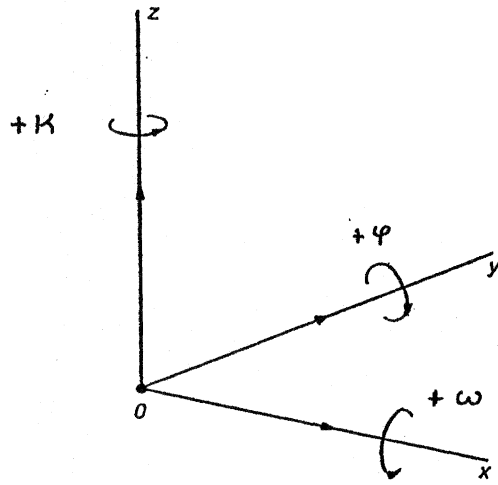


Figure 2-1

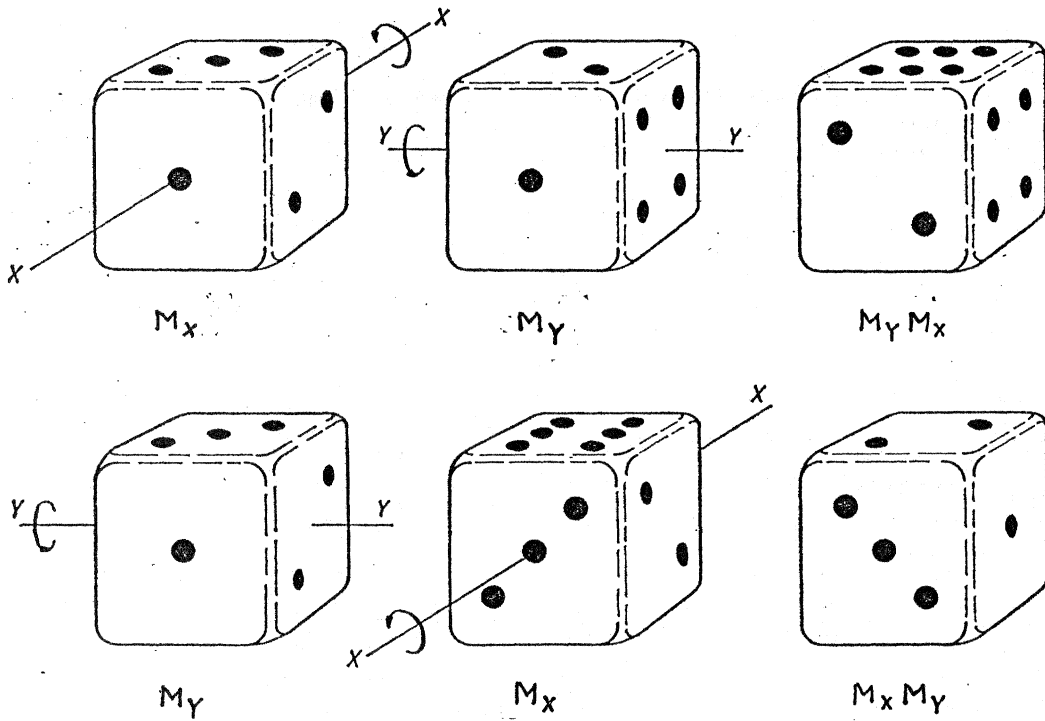


Figure 2-2

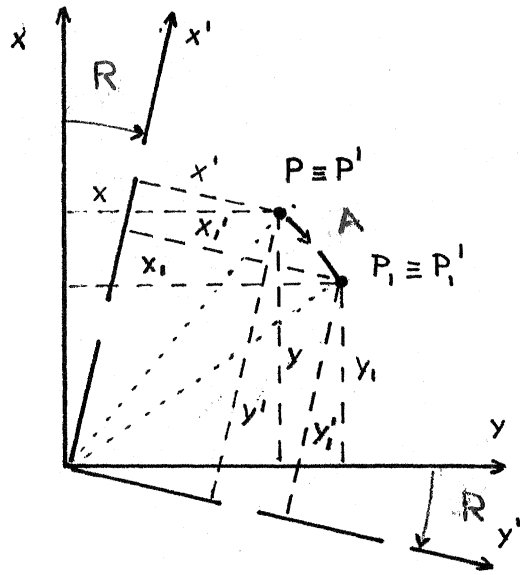


Figure 2-3

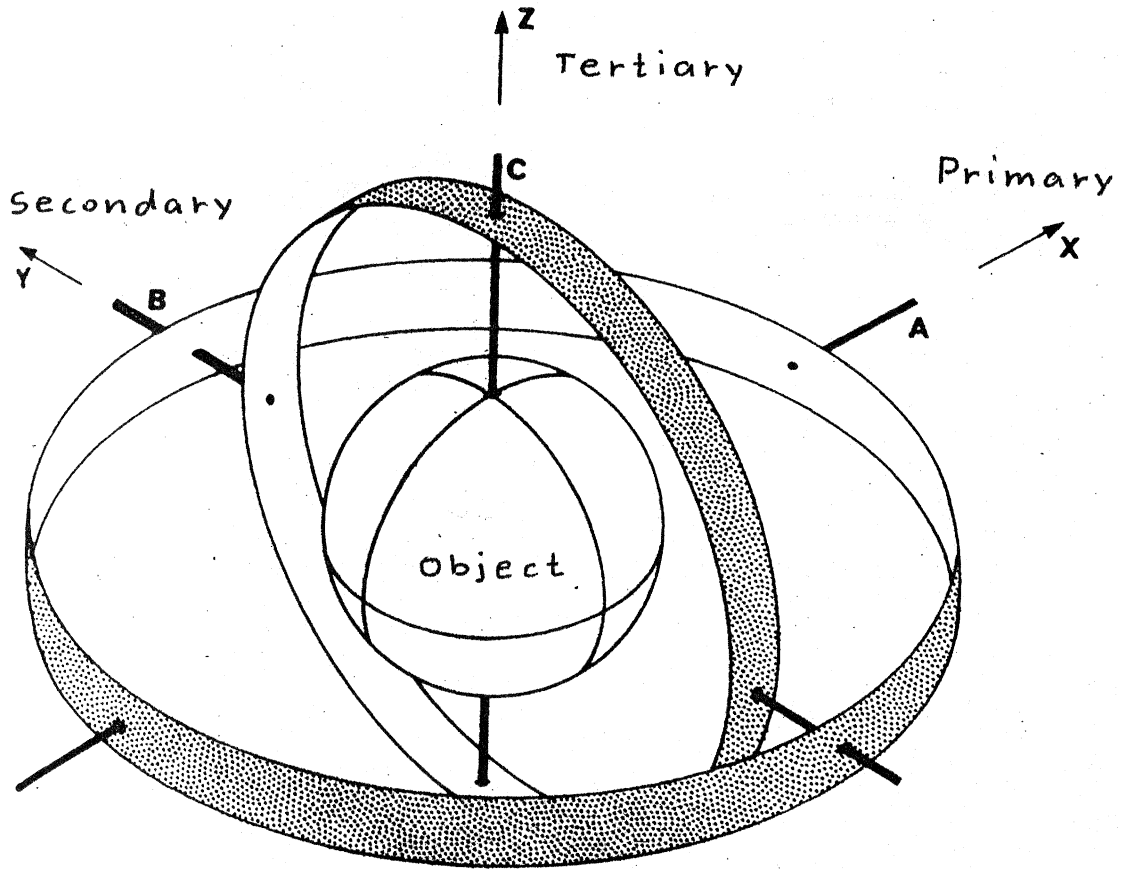


Figure 2-4

### 3. PHOTOGRAMMETRIC MEASUREMENTS

#### 3.1 Instrumentation

The most fundamental observations made in photogrammetry are the measurements of x,y coordinates of points in the image. An image is the original photogrammetric data set, which is a comprehensive record of a scene as it existed at a particular instant of time. A selective retrieval is made from this data source during the measurements. The negative is the original, first generation data set. A positive images, which is printed on film, paper or occasionally on glass plate, are high quality, second generation copies. Positive images which are printed on transparent material are called *diapositives*.

The positive copies are either produced by *contact printing* or by *projection printing*. In contact printing, the emulsion side of the negative is placed in direct contact with the unexposed emulsion of the printing material and is exposed by illuminating this assembly through the negative in a contact printer. The scale of the positive image produced in this manner is identical to that of the negative.

In projection printing, the negative is placed in a projector with the emulsion facing the projector lens. The light source then projects the negative image through the projector lens onto the printing material placed emulsion side up on an easel (table) at some distance from the projector. By varying the ratio of the distances from the projector lens to the negative and to the easel, the scale of the positive print is changed with respect to the negative. Thus, enlargements and reductions can be made (Figure 3-1).

It is important that the interior orientation established at the time of the primary data acquisition be maintained during the printing process. In other words the bundle of rays associated with the print must be congruent to that of the negative. In contact printing this is assured by the technique employed. In projection printers the optical axis of the lens must pass through the principal point of the negative during printing. The fiducial centre of the negative is substituted as a close approximation of the principal point for this purpose. Precision projection printers also have fiducial marks etched on the stage plate (negative holder), centered on the optical axis. The interior orientation is maintained by aligning the fiducial marks on the negative with these marks.

Instruments specifically constructed for the measurement image coordinates are called *comparators*. There are *monocomparators* and *stereocomparators*. In monocomparators the measurements are made on one image at a time. In stereocomparators measurements are made simultaneously on two overlapping images under stereoscopic viewing. The discussion in this chapter is restricted to monoscopic measurements. There are other instruments such as the analytical plotter and the various stereoscopic restitution instruments which can also provide image coordinates, but will be discussed later. Photogrammetric measurements are also made in stereoscopic models, which is again discussed in another chapter.

The principle of operation of a monocomparator is shown in Figure 3-2a. The main components are a stage attached to a carriage on which the image to be measured is mounted; a binocular microscope for viewing the image under magnification; two hand wheels which move the photo carriage in two mutually perpendicular directions and a light source to illuminate the image. Sometimes the stage can be rotated in azimuth. A measuring mark in the shape of a dot or cross is placed in the optical path of the viewing system. Measurements are made by moving the carriage with the hand wheels until the measuring mark sits on the image point of interest. The amount of movement introduced in the  $x$  and  $y$  directions is measured by precision lead screws, by a combination of a precision grid plate and an optical micrometer or by rotary or linear encoders. The measurements are displayed on a counter or on an electronic display device, are recorded on a printer, entered into a computer or stored on disk or tape. In some instruments servo motors facilitate the movement of the carriage. Precision comparators can provide measurements to the nearest micrometer (0.001 mm).

### **3.2 Processing of the Measurements**

Initially the measurements are referenced to the  $x$ ,  $y$  axes of the comparator and to the zero mark of the counter as an arbitrary origin. These values must be transformed to the image coordinate system for further computations. Therefore, readings are also taken on the fiducial marks, in order to define the relationship between the comparator and the fiducial coordinate system. The measurements are then transformed into the fiducial system.

If the fiducial axes were aligned parallel to the comparator axes before the measurements, (Figure 3-2a) then a translation is sufficient to transform the readings into the fiducial system as

$$\begin{aligned}
 x_a &= x'_a - \frac{x'_{F1} + x'_{F2} + x'_{F3} + x'_{F4}}{4} = x'_a - x'_{F0} \\
 y_a &= y'_a - \frac{y'_{F1} + y'_{F2} + y'_{F3} + y'_{F4}}{4} = y'_a - y'_{F0}
 \end{aligned}
 \tag{3-1}$$

where  $x_a, y_a$  are image coordinates of point  $a$  in the fiducial system;  $x'_a, y'_a$  are coordinates in the comparator system,  $x_{F1}$  to  $x_{F4}$  and  $y_{F1}$  to  $y_{F4}$  are the measured coordinates of the fiducial marks in the comparator system and  $x'_{F0}, y'_{F0}$  are the coordinates of the fiducial centre in the comparator system.

The comparator and the fiducial axes can be aligned by rotating the stage. This is a trial and error operation and is not favoured when precision measurements are required. Instead, the alignment is done only approximately and the orientation of the fiducial axes in the comparator system are defined mathematically as (Figure 3-2b)

$$\tan \theta = \frac{y_{F2} - y_{F1}}{x_{F2} - x_{F1}} \tag{3-2}$$

where  $\theta$  is the angle of rotation of the comparator axes to the fiducial axes. The coordinates of all measured points, including the fiducial marks, are then transformed to a coordinate system which is parallel to the fiducial system, by the equation

$$\begin{aligned}
 x_a &= x'_a \cos \theta + y'_a \sin \theta \\
 y_a &= -x'_a \sin \theta + y'_a \cos \theta
 \end{aligned}$$

Finally, the rotated coordinates are translated to the fiducial system using Equation (3-1).

### **3.3 Correction of Measured Image Coordinates**

The measured image coordinates contain random and systematic errors from various sources, which perturb the collinearity condition. The effect of the random errors can be minimized by repeated observations. One way of dealing with the systematic errors is to model them mathematically and then applying corrections to the measurements. This operation is often referred to as refinement of the image coordinates. Another method is to include them as unknown parameters in the photogrammetric solution. This approach is the topic of another course. The major sources of the systematic errors are:

- displacement of the principal point;
- comparator errors;
- deformations of the photographic material;
- distortions caused by the optics of the camera;

- atmospheric refraction, and
- the curvature of the earth.

### **3.3.1 Displacement of the principal point**

The principal point does not necessarily coincide with the intersection of the fiducial mark lines. The actual position of the principal point is determined through camera calibration and is specified by its coordinates  $(x_0, y_0)$  in the fiducial system, as shown in Figure 3-3. The transformation from the fiducial centre to the principal point as the origin of the coordinate system is done by the translation

$$x_p = x' - x_0$$

$$y_p = y' - y_0$$

where  $x_p, y_p$  and  $x', y'$  are coordinates in systems with the principal point and the fiducial centre as the origin respectively, and  $x_0, y_0$  are the coordinates of the principal point in the fiducial system. In precision mapping cameras the two points only differ by a few micrometres.

### **3.3.2 Comparator errors**

Non-uniform scale along the x and y axes, nonorthogonality of the two axes and curvature of the axes are errors inherent in measuring instruments. These errors are determined by calibration and then appropriate corrections are applied to the measurements. The calibration is performed by observing the grid intersections on precision grid plates and comparing these with the known positions. The most convenient way of applying the corrections to the measurements is by determining the parameters of an appropriate transformation equation, such as affine transformation, based on the results of the calibration. Thereafter all measurements are subjected to this transformation.

Measuring instruments with long lead screws usually exhibit larger errors than those with master grid plates or encoders. Long lead screws are also sensitive to changes in temperature and must be kept in an air conditioned environment.

### **3.3.3 Deformation of the photographic material**

This deformation stems from dimensional changes in the base of the photographic emulsion, which occur after the exposure. It is often referred to as *film distortion* since the emulsion base of the images used in photogrammetric work is usually a film material. This deformation is the largest contributor to the systematic errors associated with precision photogrammetric measurements. It is also the most complex to deal with since these

deformations are in part irregular throughout the images. This distortion affects the imaging rays indirectly by displacing the image points from its location established at the instant of data acquisition.

Dimensional changes in the emulsion base are caused by inherent properties of the material and by external influences. Although the polyethylene terephthalate bases used for aerial films have high dimensional stability, some changes still occur. Glass has a very high dimensional stability, but it is inconvenient to handle. Photographic paper has poor stability and is not used for precise photogrammetric work. The dimensional changes are either temporary reversible or permanent irreversible.

Temporary changes are caused by:

- (a) Temperature variations which expands or contracts the base.
- (b) Humidity variations which again expands or contracts the base

Temporary dimensional changes can be minimized by storing the film under controlled atmospheric conditions. When the film is removed from storage to the work place, it is important to allow sufficient time for it to acclimatize to the new environment before the measurement commence.

Permanent changes are caused by:

- (a) Plastic flow of the base. The emulsion exerts a compressive force on the base which results in permanent shrinkage. Tension in film processing machines causes longitudinal stretching and lateral contraction of roll films. This action is aggravated by the softening of the film caused by the heat and the chemicals.
- (b) Aging. The internal strain that is present in the film due to the manufacturing process is slowly released with time and some loss in moisture will also occur. The base will shrink as the result .

The geometric effects on the image caused by the deformation of the film base fall into three categories:

- (1) *Uniform scale change*, which is an overall dimensional change and can be expressed by a single scale factor.
- (2) *Affine scale change*, which is different in longitudinal and in transverse direction of the film roll. Two scale factors are needed to define this change.
- (3) *Non uniform or irregular change*, which varies in direction and magnitude from point to point in the image.

The simplest method of correcting the uniform and the affine distortions is by comparing the known (calibrated) and the measured distances between opposite fiducial marks. The ratio of the two distances gives a scale factor in x and y direction and the coordinates of all measured points are corrected as:

$$x = S_x x'$$

$$y = S_y y'$$

where x, y and x', y' are the corrected and measured coordinates respectively and  $S_x$ ,  $S_y$  are the scale factors.

A more sophisticated method is to evaluate the parameters of an affine or projective transformation equation based on the measured and calibrated coordinates of the fiducial marks and then transform the coordinates of the image points. By this method all measured coordinates in the comparator system can be transformed into the fiducial system and at the same time correct for the film deformation.

The most elaborate method of correction utilizes the images of a control grid called *reseau*. There are two kinds of reseau. The one consists of an array of fine crosses etched on the surface of a glass plate, mounted in the focal plane of the camera, in contact with the emulsion. These marks will be photographed on the image at the instant of exposure. The second type of reseau consists of a pattern of small holes drilled through a metal platen situated in the focal plane behind the film. The reseau marks are projected through these holes and through the film base onto the emulsion at the instant of exposure.

The simplest way of utilizing the reseau marks is to include the measurement of the mark which is closest to each point into the measuring program. The difference between the measured and calibrated coordinates of these marks is applied as correction to a particular point. The correction expressed mathematically is

$$x = x' + (xr_c - xr)$$

$$y = y' + (yr_c - yr)$$

where x, y and x', y' are the corrected and observed coordinates of an image point respectively and  $xr_c$ ,  $yr_c$  and  $xr$ ,  $yr$  are the calibrated and measured coordinates of a reseau mark.

A more general procedure is to observe a number of marks distributed over the image and use these data together with the calibrated coordinates to evaluate the parameters of a polynomial transformation equation. The coordinates of all other measured points are

then transformed from the comparator to the reseau system. This method is more advantageous if many points have been observed.

### 3.3.3 Lens imperfections

The imperfections in the optics of imaging devices fall into two categories. The *aberrations*, which degrade the pictorial quality or sharpness of the image and the *distortions*, which degrade the geometric fidelity or positional accuracy.

The primary lens aberrations are the spherical aberration, coma, astigmatism, curvature of field and the chromatic aberration. *Spherical aberration* effects the formation of images in the optical axis (Figure 3-3a). It means that rays originating from a point in the optical axis and entering the lens near its outer edge will come to focus closer to the lens than rays which enter the lens near to its centre. The image of a point object thus becomes a small circle or blur. *Coma* is similar to spherical aberration except that it affects the imaging of off-axis objects. The resulting image of these points becomes a convex-shaped blur. The spherical aberration and the coma are caused by imperfect grinding of the spherical surface of the lens.

The effect of *astigmatism* is that rays of object points that are situated on two mutually perpendicular lines will come to focus at two different image distances (Figure 3-3b). With an astigmatic lens, rays originating at the same object distance but striking the lens at varying incidence angle will come to focus at different image distances. This condition is called *curvature of field*.

*Chromatic aberration* is caused by varying refractive characteristics of the different wavelength which make up the visible light (Figure 3-3c). Short wavelength radiation (blue light) is refracted more and comes to focus closer to the lens than the longer wavelength red light.

Lens aberrations can be minimized by multi-element lens assemblies consisting of positive and negative lenses and made of glass with different refractive index. Some aberrations can also be reduced by reducing the lens opening.

Lens distortions occur when light rays on the image side do not emerge from the lens parallel to the path of the incident rays on the object side (Figure 3-4). In other words, the angle of refraction of the lens assembly is not equal to the angle of incidence. There are

three types of lens distortions: symmetric radial, usually referred to simply as radial lens distortion, asymmetric radial and tangential.

Radial distortion, as implied by its name, displaces the image points in a radial direction from the principal point. Outward displacement is considered positive. *Symmetric radial distortion* means that the displacement has the same magnitude and sign in any direction around the centre, at a certain radial distance. The *asymmetric radial distortion* is a residual variation from the symmetric displacement as a function of the radial direction. *Tangential distortion* is the displacement of the image point in a direction normal to the radial line through the point. Lens distortions are caused by imperfect grinding and centering of the lens elements. The symmetric radial distortion of lenses manufactured for photogrammetric work seldom exceeds 10  $\mu\text{m}$  and the magnitude of the other two distortions is considerably less. Therefore, only the symmetric radial distortion is discussed further.

The determination of lens distortion is an integral part of the camera calibration. It is specified graphically, in tabular form or by a mathematical model. The graphical presentation is a plot which shows the distortions as ordinates and angular or radial distances as abscissa. It is referred to as the *radial distortion curve*. (Figure 3-5). The tabular presentation lists the numerical values of the distortion at regular intervals of the radial distance. The mathematical model of the symmetric radial lens distortion is an odd-power polynomial of the form.

$$\Delta r = k_0 r + k_1 r^3 + k_2 r^5 + \dots \quad (3-3)$$

where  $\Delta r$  is the radial distortion,  $r$  is the radial distance and  $k_0$   $k_1$   $k_2$  are coefficients which are obtained through camera calibration.

The first step in correcting the image coordinates for radial lens distortion is to compute the radial distance as

$$r = (x'^2 + y'^2)^{1/2}$$

where  $x'$  and  $y'$  are the coordinates of a point in the image coordinate system. Then the value of  $\Delta r$  is determined from one of the three presentations of the distortion data. Finally, the  $\Delta r$  is resolved into the  $x$  and  $y$  components and applied to the coordinates, as

$$\begin{aligned} x &= x' \left(1 - \frac{\Delta r}{r}\right) \\ y &= y' \left(1 - \frac{\Delta r}{r}\right) \end{aligned} \quad (3-4)$$

### 3.3.4 Atmospheric refraction

The density and hence the index of refraction of the atmosphere decreases as the altitude increases. Therefore, light rays which project objects onto the image plane are not straight lines but follow a curved path. The image of an object will appear where the tangent to the curved ray path at the perspective centre intersects the image plane (Figure 3-6). This means that image points are displaced radially outward from the principal point as compared to the projection by a straight ray path. The angle between the correct and the actual ray path is the angle of refraction  $\Delta\theta$ . The magnitude of this angle is a function of the altitude of the camera above sea level  $H$ , the elevation of the ground above sea level  $h$ , and of the angle of incidence  $\theta$ , of the imaging ray.

The index of refraction for standard atmosphere, was defined by Bertram in 1965 as:

$$K = \frac{2410 H}{H^2 - 6H + 250} - \frac{2410 h}{h^2 - 6h + 250} \frac{h}{H} \quad (3-5)$$

If both  $H$  and  $h$  are expressed in kilometres, then  $K$  is in  $\mu\text{rad}$ .

Based on Figure 3-6 the radial distance of an image point is

$$r = f \tan \theta .$$

The effect of a small change in  $\theta$  on  $r$  can be obtained by differentiating the above expression with respect to  $\theta$  as

$$\frac{\partial r}{\partial \theta} = \frac{f}{\cos^2 \theta} d\theta$$

whereby the radial displacement of an image point caused by the atmospheric refraction is

$$\Delta r = \frac{f}{\cos^2 \theta} \Delta \theta \quad (3-6)$$

where

$$\Delta \theta = K \tan \theta = K \frac{r}{f} \quad (3-7)$$

whereby

$$\Delta r = K \frac{f}{\cos^2 \theta} \frac{r}{f}$$

Based on Figure 3-6

$$\cos \theta = \frac{f}{(r^2 + f^2)^{1/2}}$$

and

$$\cos^2 \theta = \frac{f^2}{r^2 + f^2}$$

so that the final form of the displacement becomes

$$\Delta r = K \left( r + \frac{r^3}{f^2} \right) \quad (3-8)$$

K should be in radians ( $K \times 10^{-6}$ ). Equation (3-6) was derived for vertical photography.

This displacement occurs radially outward, from the principal point.

Another approach for determining this correction is to calculate  $\Delta\theta$ , the angle of refraction, first and then use equation (3-6) to obtain the correction to the radial distance. The angle  $\Delta\theta$  can be calculated from the formula

$$\Delta\theta = \tan \theta \left( c_1 + \frac{1}{2} c_2 \sec^2\theta \right) . \quad (3-9)$$

The first term of this equation is identical to equation (3-7) while the second term expresses the effect of the earth curvature. The  $c_1$  and  $c_2$  values are listed in Tables 3-1 and 3-2 for a  $\theta$  angle of  $45^\circ$  and for various flying heights and terrain elevations. The  $c$  values for unlisted flying heights and terrain elevations can be obtained by linear interpolation. The  $c_2$  values are very small in comparison to  $c_1$ , so that the contribution of the earth curvature to the refraction can be neglected in most cases. Based on the  $c$  values listed in the two tables the unit of angle  $\Delta\theta$  is microradians ( $\mu\text{rad.}$ ).

According to Table 3-1, the coefficient of refraction reaches its maximum value at around 16 km above sea level and decreases thereafter. The explanation of this phenomenon is that a transition occurs at this altitude from the troposphere, where the refractive index is larger than one, to the stratosphere where the refractive index is approximately equal to one. Figure 3-7 illustrates this fact and explains its effect on  $\Delta\theta$ . This displacement always occurs radially outward, from the principal point, thus it has a positive sign.

### **3.3.5 Earth curvature**

When the object space coordinates used in aerial or space photogrammetry are defined in a three-dimensional XYZ Cartesian coordinate system, then the effect of the earth curvature must be considered. On the earth, the elevation of a point is measured along the normal to the curved equipotential surface at sea level. In Figure 3-8, A is an object point on the surface of the earth, while A' is the corresponding point on the mapping plane which contains the XY axes. The corresponding points projected onto the image plane through the perspective centre L are a and a'. Point a is the actual image position, and a' is the theoretical location. The distance between the two is  $\Delta r$ , which is the displacement due to the earth's curvature. It can be calculated from the equation:

$$\Delta r = \frac{Hr^3}{2Rf^2} \quad (3-10)$$

where H is the flying height above the terrain, r is the radial distance from the principal point to the image point, f is the principal distance and R is the radius of the earth which can be taken as 6,372 km. This displacement always occurs radially inward, towards the principal point, thus it has a negative sign.

The effect of earth curvature should not be considered as an error since it only occurs when a flat mapping plane is used for defining the object space coordinates. This displacement is not present when the object points are referenced in a geocentric coordinate system.

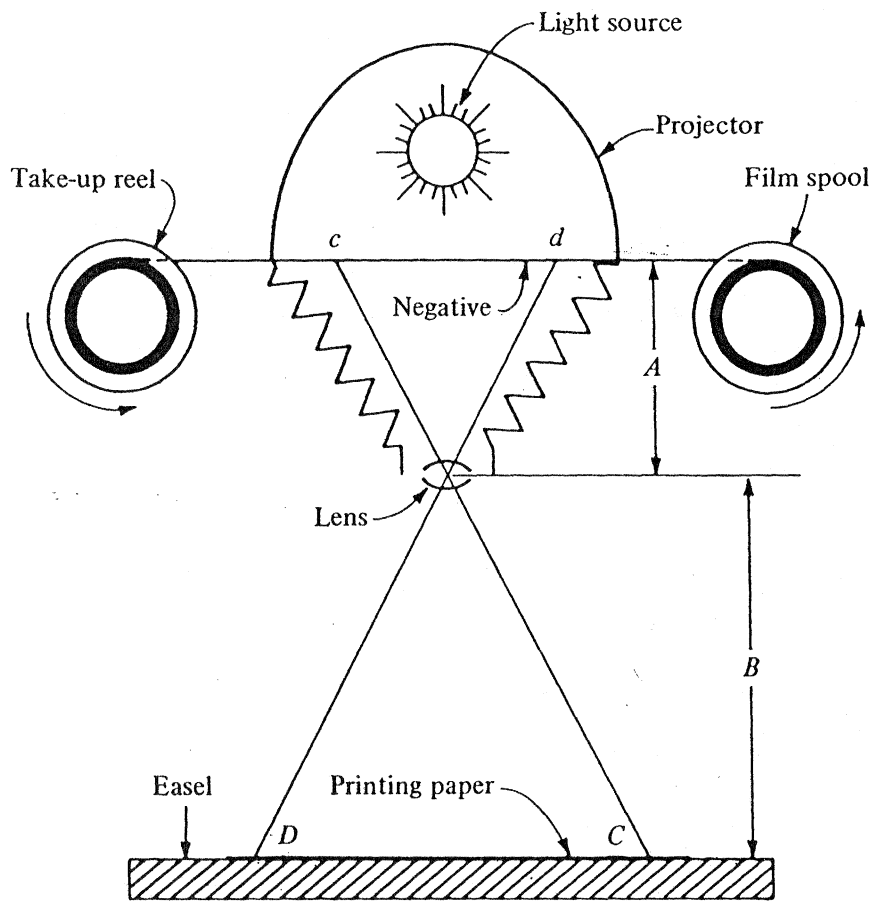


Figure 3-1

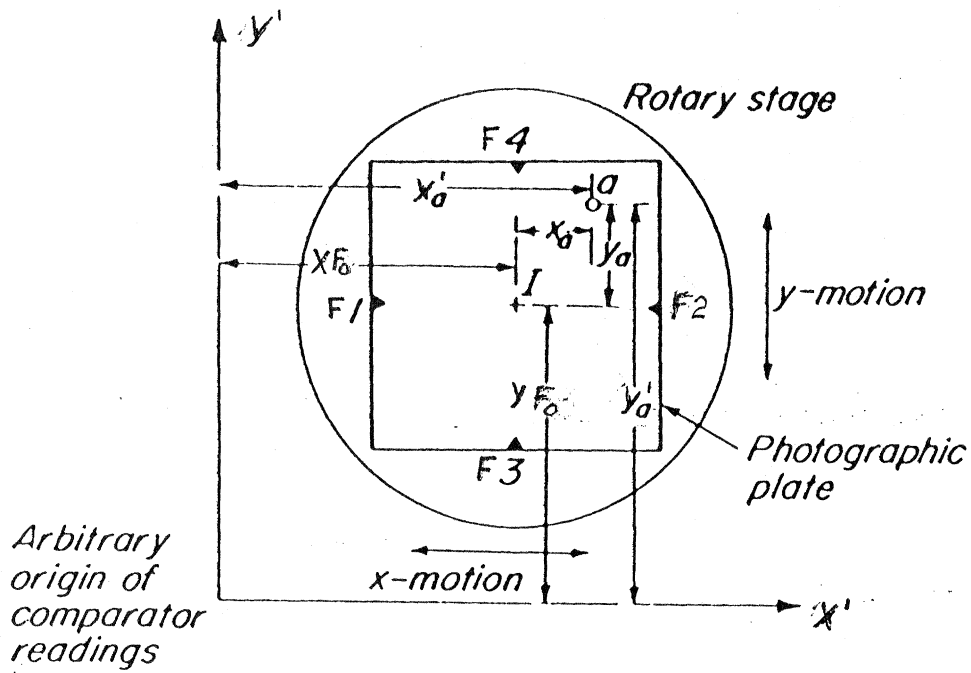


Figure 3-2a

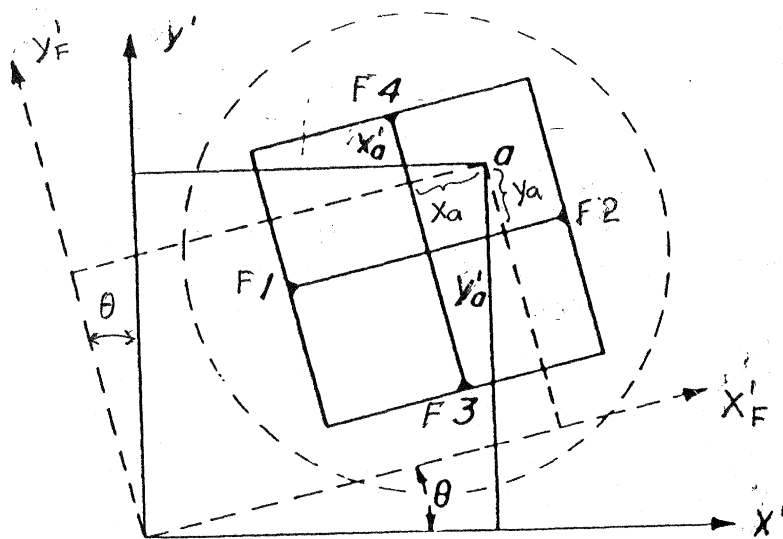


Figure 3-2b

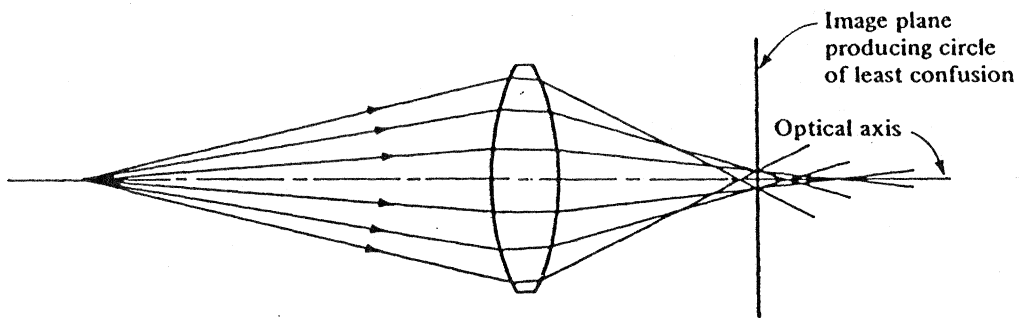


FIGURE 3-3a  
Spherical aberration.

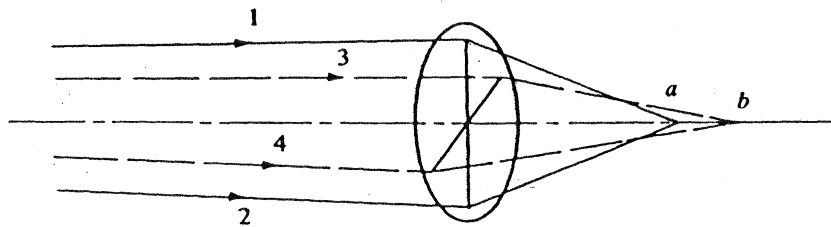


FIGURE 3-3b  
Astigmatism.

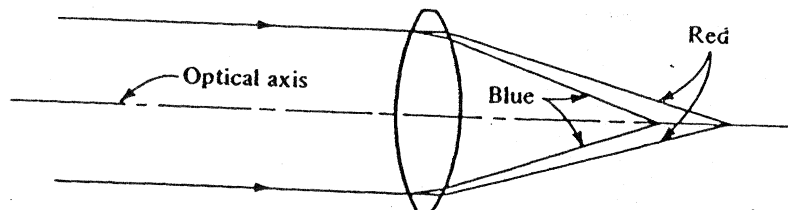


FIGURE 3-3c  
Chromatic aberration.

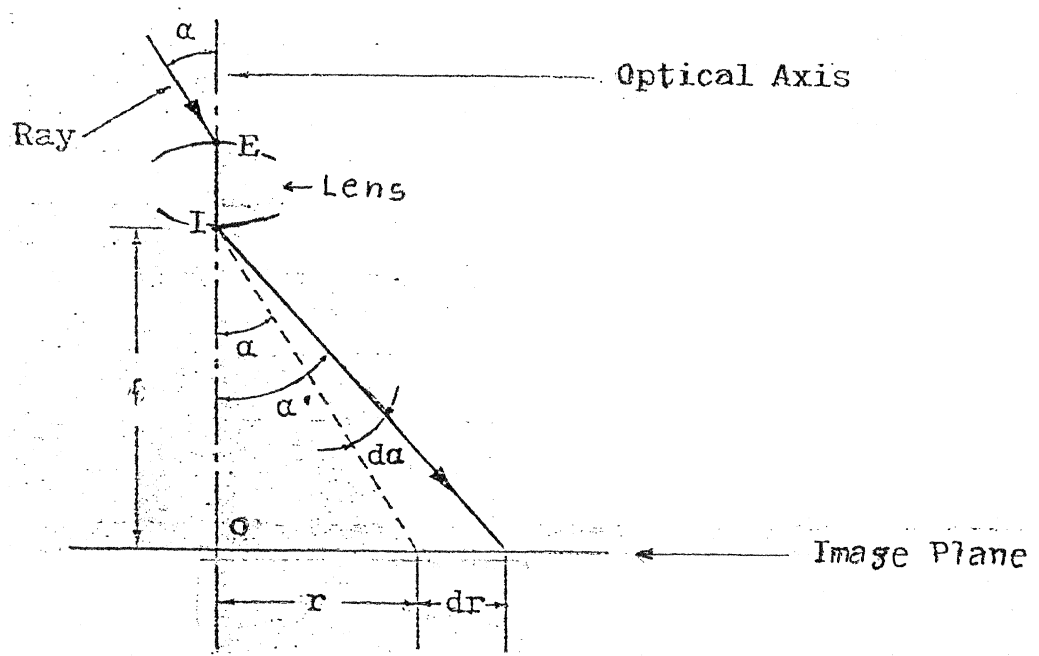


Figure 3-4

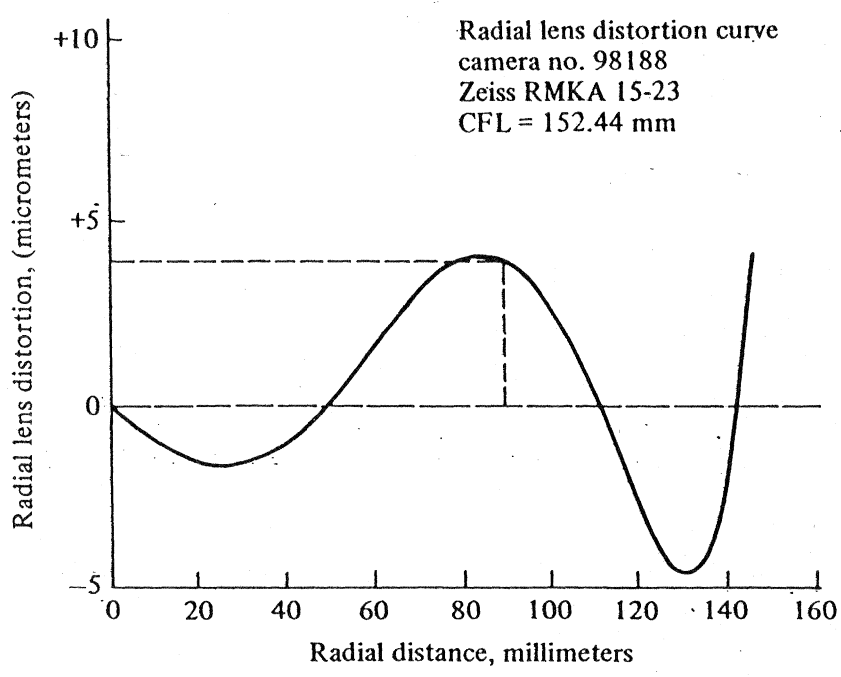


Figure 3-5

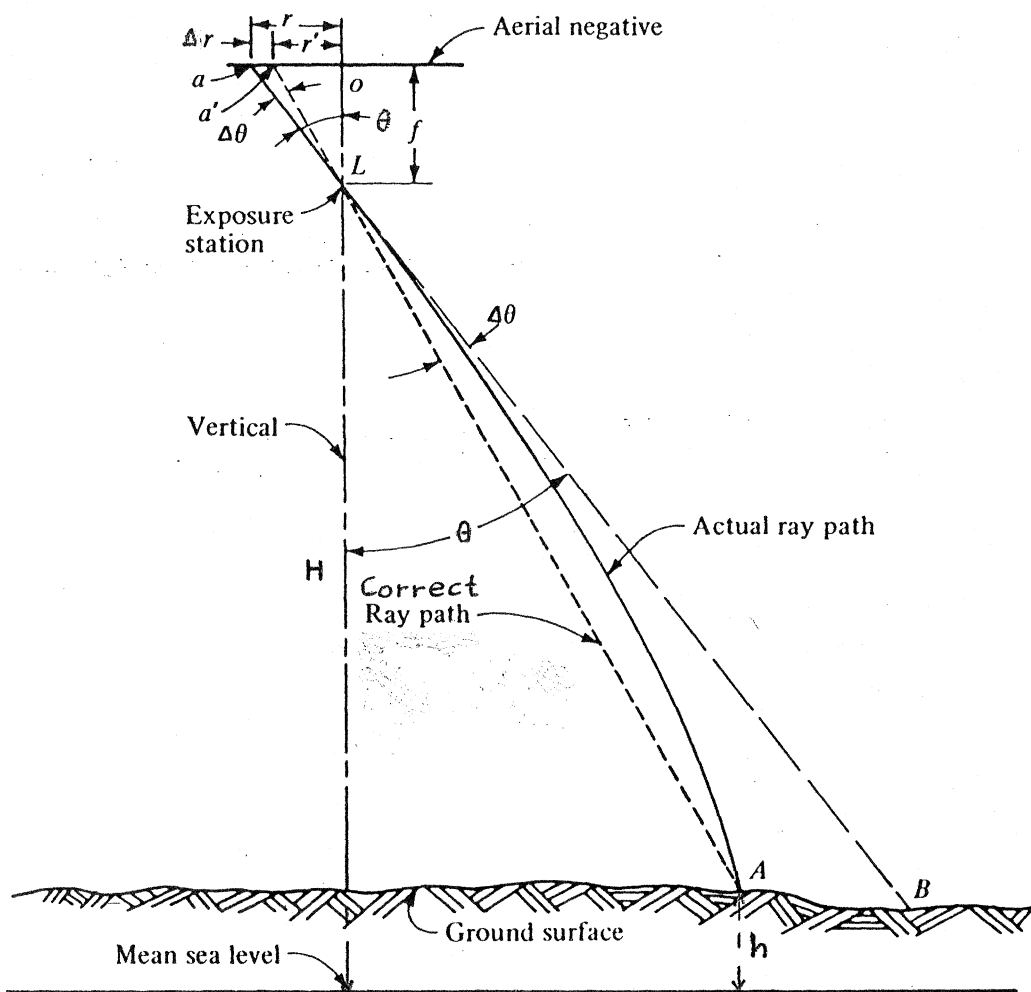
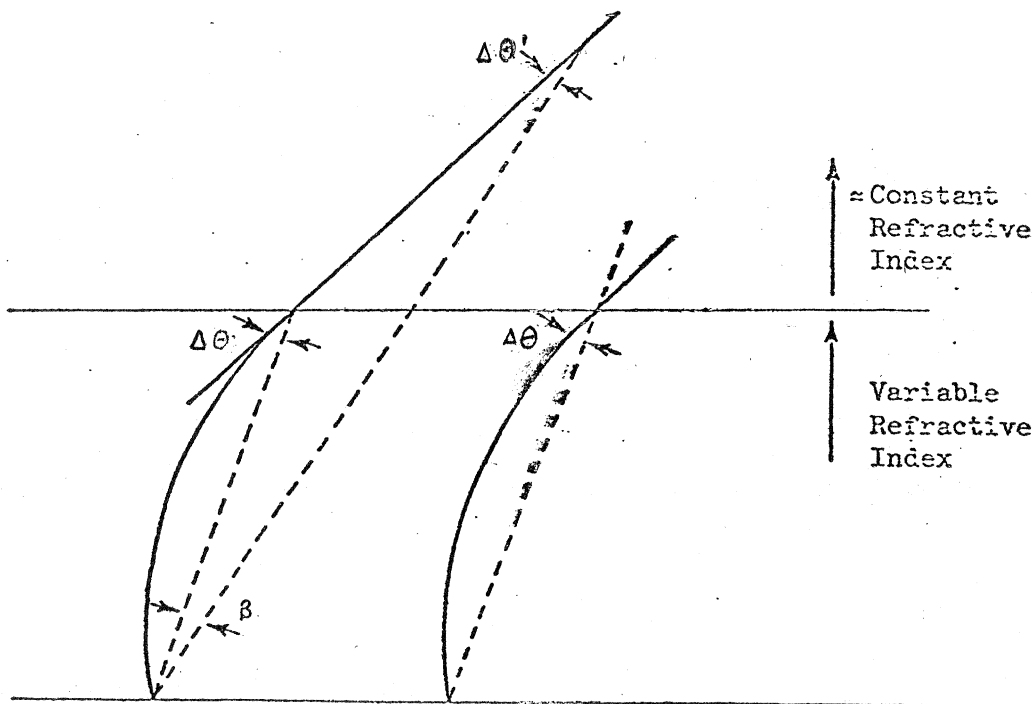
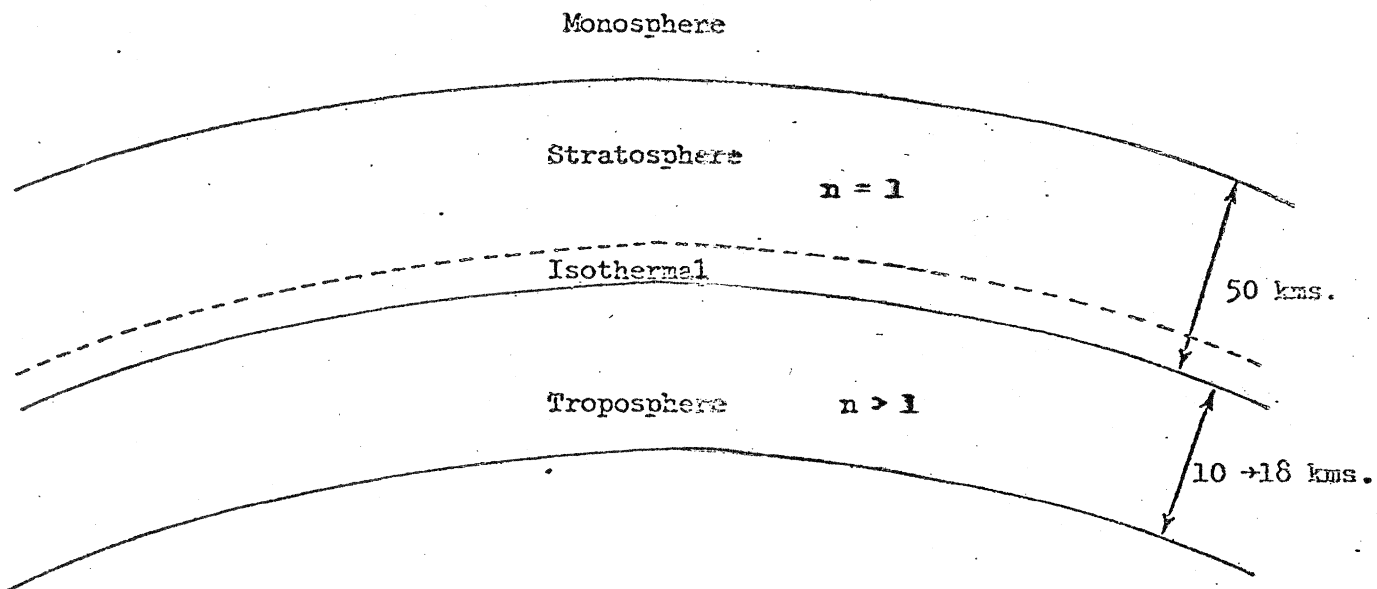


Figure 3-6



$$\Delta\theta = \Delta\theta' + \beta, \quad \therefore \Delta\theta' < \Delta\theta$$

Figure 3-7

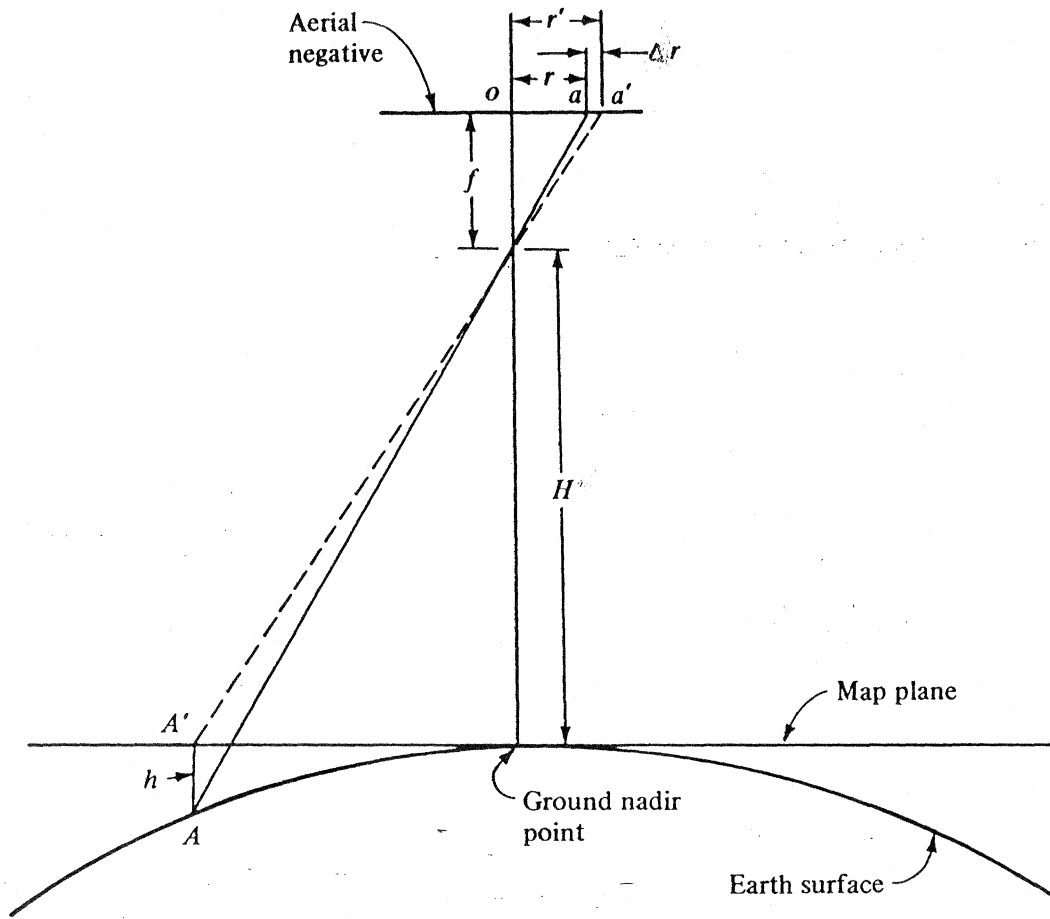


Figure 3-8

Table 3-1 Photogrammetric refraction in microradians for a ray at 45° with the vertical in the U. S. Standard Atmosphere, 1962

Flying height above sea level	Photogrammetric refraction for ground heights of				Flying height above sea level	Photogrammetric refraction for ground heights of			
	0.0 km	1.0 km	2.0 km	4.0 km		0.0 km	1.0 km	2.0 km	4.0 km
0.5 km	6.5				13.5 km	91.3	82.0	73.2	57.0
1.0	12.6	0.0			14.0	92.2	83.0	74.2	58.2
1.5	18.5	6.0			14.5	92.8	83.7	75.1	59.2
2.0	24.1	11.7	0.0		15.0	93.3	84.2	75.7	60.1
2.5	29.3	17.1	5.6		15.5	93.5	84.6	76.2	60.7
3.0	34.3	22.3	10.9		16.0	93.6	84.8	76.5	61.2
3.5	39.0	27.1	15.9		16.5	93.6	84.9	76.6	61.5
4.0	43.5	31.7	20.6	0.0	17.0	93.4	84.8	76.6	61.7
4.5	47.7	36.1	25.1	4.7	17.5	93.2	84.6	76.6	61.8
5.0	51.6	40.2	29.3	9.2	18.0	92.8	84.3	76.4	61.8
5.5	55.3	44.0	33.3	13.5	18.5	92.3	84.0	76.1	61.7
6.0	58.8	47.6	37.0	17.5	19.0	91.8	83.5	75.7	61.5
6.5	62.1	51.0	40.6	21.3	19.5	91.2	83.0	75.3	61.3
7.0	65.1	54.2	43.9	24.8	20.0	90.5	82.4	74.8	61.0
7.5	67.9	57.2	47.0	28.2	21.0	89.1	81.2	73.8	60.3
8.0	70.6	59.9	49.8	31.3	22.0	87.5	79.8	72.6	59.4
8.5	73.0	62.5	52.5	34.2	23.0	85.8	78.3	71.2	58.4
9.0	75.2	64.9	55.0	37.0	24.0	84.0	76.7	69.8	57.2
9.5	77.3	67.1	57.4	39.5	25.0	82.2	75.0	68.2	56.0
10.0	79.2	69.1	59.5	41.9	26.0	80.3	73.4	66.7	54.8
10.5	80.9	70.9	61.5	44.1	27.0	78.4	71.6	65.1	53.5
11.0	82.5	72.6	63.3	46.1	28.0	76.6	69.8	63.6	52.2
11.5	85.0	75.2	66.0	49.0	29.0	74.7	68.2	62.0	50.9
12.0	87.1	77.4	68.3	51.5	30.0	72.9	66.5	60.5	49.6
12.5	88.8	79.3	70.2	53.7	31.0	71.1	64.8	59.0	48.4
13.0	90.2	80.8	71.8	55.5	32.0	69.4	63.2	57.5	47.1

Table 3-1 cont'd.

Flying height above sea level	Photogrammetric refraction for ground heights of		Flying height above sea level	Photogrammetric refraction for ground heights of	
	0.0 km	2.0 km		0.0 km	2.0 km
32 km	69.4	57.5	62 km	37.7	30.6
34	66.1	54.7	64	36.5	29.6
36	63.1	52.1	66	35.4	28.7
38	60.1	49.6	68	34.4	27.8
40	57.4	47.3	70	33.4	27.0
42	54.9	45.1	72	32.5	26.2
44	52.6	43.1	74	31.6	25.5
46	50.4	41.3	76	30.8	24.8
48	48.4	39.6	78	30.0	24.2
50	46.5	38.0	80	29.3	23.6
52	44.8	36.5	82	28.5	23.0
54	43.2	35.2	84	27.9	22.4
56	41.7	33.9	86	27.2	21.9
58	40.3	32.7	88	26.6	21.4
60	38.9	31.6	90	26.0	20.9
			Z > 90	<u>2340.5</u>	<u>1837.4</u>
				Z	Z - 2

Table 3-2 Contribution of earth curvature to refraction for a ray at 45° with the vertical, in microradians

Flying height above sea level	Contribution to the refraction for ground heights of			
	0.0 km	1.0 km	2.0 km	4.0 km
5.0 km	0.03	0.02	0.01	0.00
10.0	0.10	0.07	0.06	0.03
15.0	0.18	0.15	0.12	0.08
20.0	0.26	0.23	0.19	0.14
25.0	0.33	0.29	0.25	0.18
30.0	0.39	0.34	0.30	0.22

## 4. THE GEOMETRY OF IMAGING

### 4.1 Definitions

Images are created by projection. Joining two points by a straight line means that one point is projected upon the other. This straight line is also termed a *ray*. From a geometrical standpoint, there are different kinds of projections. If points situated on a straight line in a plane or in a three-dimensional figure, are projected upon a single point located outside the figure in question, a so called *central projection*, *central perspective* or *perspective projection* occurs. The point located outside the figures, is called the *projection centre* or *perspective centre*. If the rays of projection are intersected by a line, a plane or by a three-dimensional figure, then an image of the original point group is obtained. A special case of the central projection is the *parallel projection*, which has its projection centre at infinity. If a line or plane intersects these projecting rays at right angle, then the parallel projection becomes an *orthogonal* or *orthographic projection*. Maps are orthographic projections.

Directional imaging devices form central perspectives. A notable example of such a device is the photographic camera, which is the most frequently used data acquisition tool in photogrammetry. The geometry associated with image formation in a photographic camera is now discussed in detail.

The optical centre of the camera lens is the perspective centre and the image plane is the plane of projection. In reality there are two projection centres in a photographic camera: the *exterior projection centre*, at the *front nodal point* of the objective lens, where all rays coming from the object intersect and the *interior projection centre* at the *rear nodal point* from where the rays diverge towards the image plane (Figure 4-1). Theoretically, rays on the object and image side of the lens run parallel to one another and therefore, mathematically the two projection centres can be represented as a single point. The physical reality is, however, different as explained in Chapter 4. The region between the perspective centre and the image plane is referred to as *image space*. The region outside the camera occupied by the object is called *object space* (see Figures 4-1 and 4-2).

The image space coordinate system has its origin at the *principal point*, which is the foot of the perpendicular dropped from the perspective centre onto the image plane. The  $x$  and  $y$  axes lie in the image plane and the positive  $z$ -axis is perpendicular to this plane. The three axes constitute a right-handed Cartesian coordinate system. The distance between the perspective centre and the principal point, or in other words, the length of the perpendicular dropped from the perspective centre to the image plane, is called the *principal distance* or *camera constant*. (Figures 4-1, 4-2 and 4-3). The principal distance is often referred to, erroneously, as *focal length* although, the two quantities are not identical. Focal length is an optical quantity. It is the distance from the optical centre of a lens measured along the optical axis to the point where rays coming from infinity intersect (focus or focal point). It is an inherent property of the lens assembly only and not of the camera assembly. It is determined by optical test procedures. The principal distance on the other hand is a geometric quantity pertaining to the entire camera assembly and is determined by camera calibration. To add to the confusion, in many literature, both quantities are denoted as "f". Therefore, it is preferred to use the term *camera constant* denoted as "c". In fact the principal distance is more closely related to the optical quantity image distance, which appears in the lens equation, than to the focal length. As the camera is focused to various object distances, the image distance is changing and so does, by definition, the principal distance, while the focal length remains constant. For cameras focused to infinity the three quantities are very nearly the same since the image plane is in the focal plane.

The exact location of the principal point cannot be established physically. Therefore, the focal plane or image plane frame of cameras specifically manufactured for photogrammetric work (metric or cartographic cameras) contains four or more reference marks, called *fiducial marks*. These marks are located either at the half way point along each side of the frame or in the four corners and also appear on the image. The intersection of lines connecting opposite fiducial marks is called the *fiducial centre*, and the connecting lines of neighboring marks form the  $x$  and  $y$  axes of the *fiducial coordinate system* (Figure 4-2 and 4-3).

It should be emphasized that the principal point and the fiducial centre are not identical, although in metric cameras the two are physically inseparable. The fiducial centre is established with the help of fiducial marks, while the location of the principal point is determined by camera calibration and are specified by their  $x$  and  $y$  coordinates in the fiducial system. The fiducial and the image or photo coordinate axes are parallel to one another. In analogue photogrammetry the fiducial system is accepted as a close approximation of the image coordinate system.

In Figure 4-3 the  $F_s$  are the fiducial marks,  $F_c$  is the fiducial centre,  $O$  is the principal point with coordinates  $x_o, y_o$  in the fiducial system,  $L$  is the perspective centre,  $f$  is the principal distance and  $a$  is a point in the image with coordinates  $x_a, y_a$  in the fiducial system. The image space coordinates of  $L$  are  $x_o, y_o, f$ .

The geometric relationship between the perspective centre and the image plane is established by the *interior or inner orientation*. The three fundamental elements of interior orientation are the two coordinates of the principal point  $x_o, y_o$  in the fiducial system, and the principal distance  $f$  (figure 4-3). There are other factors that have an effect on interior orientation which will be dealt with later. Interior orientation defines the shape and dimension of the bundle rays in image space.

A three-dimensional right-handed Cartesian coordinate system  $X, Y, Z$  is used as a reference system in object space, as shown in Figure 4-3 and 4-4. The object space coordinates of the projection centre  $L$  are  $X_L, Y_L, Z_L$ , and the coordinates of an object point  $A$  are  $X_A, Y_A, Z_A$ . The projection centre is often referred to as *exposure station* in object space.

The geometric relationship between image and object is established by the *exterior orientation*. It defines the position and orientation of the image in object space. The six elements of exterior orientation are the three object space coordinates  $X_L, Y_L, Z_L$  of the perspective centre (exposure station) and the three orientation angles  $\omega, \phi, \kappa$  of the image space coordinate axes with respect to the object space system (See Figure 4-4). These angular elements are also referred to as *X-tilt, Y-tilt* and *swing* respectively to signify the axes around which the rotations occur, or as *roll, pitch* and *yaw* in terms of the attitude changes of the sensor platform: .

Images are classified as follows according to the angular orientation of the optical axis of the sensor :

- *Truly vertical image* means that the sensor is pointing accurately vertically downward;
- *Nearly vertical image* means that the sensor is pointing unintentionally away from the vertical by up to  $5^\circ$ ;
- *Oblique image* means that the sensor is pointing intentionally away from the vertical ;
- *Horizontal image* means that the sensor is pointing in an exact horizontal direction;
- *Upward or downward-directed image* means that the sensor is pointing intentional upward or downward from the horizontal;

- *Zenith image* has the sensor is pointing vertically upward.

The characteristic elements of a tilted photograph are as follows ( Figure 4-5):

- *Principal axis* is a line through the perspective centre which is perpendicular to the image plane;
- *Angle of tilt* is the angle at the perspective centre formed by the principal axis and the plumb line;
- *Plumb line* is a vertical line through the perspective centre;
- *Principal line* is the line of greatest slope on the image plane which passes through the principal point;
- *Principal plane* is the vertical plane defined by the principal line and the perspective centre;
- *Nadir point* is the point of intersection of the plumb line with the image plane;
- *Isocentre* is the point of intersection of the bisector of principal axis and plumb line with the image plane.

The nine elements of interior and exterior orientations uniquely define the geometric relationship between an object and its image. Knowing these elements, it becomes possible to reconstruct the spatial position of an object from its image.

#### 4.2 Analytical Projective Relations

Imaging by central projection is based on the fundamental theorem that at the instant of projection the perspective centre L, the image point a, and the object point A, lie on a straight line. In other words the image vector,  $\bar{a}$  and the object vector  $\bar{A}$  are *collinear*.(Figure 4-4). This so-called *collinearity condition* is valid for every ray in an imaging bundle and forms the basis of imaging with all types of sensors and for the reconstruction of objects from their images.

Two vectors are collinear if one is a scalar multiple of the other. Whereby

$$\bar{a} = k \bar{A}$$

where k is a scale factor. The components of  $\bar{a}$  in the image space coordinate system are

$$\bar{a} = \begin{pmatrix} x_a - x_o \\ y_a - y_o \\ -f \end{pmatrix} \quad (4-1)$$

and the components of  $\bar{A}$  in the object space system are:

$$\bar{A} = \begin{pmatrix} X_A - X_L \\ Y_A - Y_L \\ Z_A - Z_L \end{pmatrix} \quad (4-2)$$

The two vectors are now referred to a common coordinate system by transforming  $\bar{A}$  from the object space system to the image space with the help of the orientation matrix  $M$ . Thus

$$\bar{a} = kM \bar{A}$$

or

$$\begin{pmatrix} x_a - x_o \\ y_a - y_o \\ -f \end{pmatrix} = kM \begin{pmatrix} X_A - X_L \\ Y_A - Y_L \\ Z_A - Z_L \end{pmatrix} = k \begin{pmatrix} U \\ V \\ W \end{pmatrix} \quad (4-3)$$

By expanding  $M$ , performing the multiplication and dropping subscripts  $a$  and  $A$  results in the equation

$$\begin{aligned} x - x_o &= k[m_{11}(X - X_L) + m_{12}(Y - Y_L) + m_{13}(Z - Z_L)] \\ y - y_o &= k[m_{21}(X - X_L) + m_{22}(Y - Y_L) + m_{23}(Z - Z_L)] \\ -f &= k[m_{31}(X - X_L) + m_{32}(Y - Y_L) + m_{33}(Z - Z_L)] \end{aligned} \quad (4-4)$$

The scalar  $k$ , which is different for each ray in a bundle, can be eliminated by dividing the first two equations with the third one. The final form of the equation is obtained as:

$$\begin{aligned} x - x_o &= -f \frac{m_{11}(X - X_L) + m_{12}(Y - Y_L) + m_{13}(Z - Z_L)}{m_{31}(X - X_L) + m_{32}(Y - Y_L) + m_{33}(Z - Z_L)} = -f \frac{U}{W} \\ y - y_o &= -f \frac{m_{21}(X - X_L) + m_{22}(Y - Y_L) + m_{23}(Z - Z_L)}{m_{31}(X - X_L) + m_{32}(Y - Y_L) + m_{33}(Z - Z_L)} = -f \frac{V}{W} \end{aligned} \quad (4-5)$$

The inverse relationship is

$$\bar{A} = \frac{1}{k} M^T \bar{a}$$

or

$$\begin{pmatrix} X - X_L \\ Y - Y_L \\ Z - Z_L \end{pmatrix} = \frac{1}{k} M^T \begin{pmatrix} x - x_0 \\ y - y_0 \\ -f \end{pmatrix} = \frac{1}{k} \begin{pmatrix} u \\ v \\ w \end{pmatrix} \quad (4-6)$$

In the expanded form it is written as

$$X = X_L + (Z - Z_L) \frac{m_{11}(x - x_0) + m_{21}(y - y_0) + m_{31}(-f)}{m_{13}(x - x_0) + m_{23}(y - y_0) + m_{33}(-f)} = X_L + (Z - Z_L) \frac{u}{w}$$

$$Y = Y_L + (Z - Z_L) \frac{m_{12}(x - x_0) + m_{22}(y - y_0) + m_{32}(-f)}{m_{13}(x - x_0) + m_{23}(y - y_0) + m_{33}(-f)} = Y_L + (Z - Z_L) \frac{v}{w} \quad (4-7)$$

Equations (4-5) and (4-7) are called the *collinearity equations* and are used extensively in analytical photogrammetry to establish the relationship between coordinates in image and object space. The direct relationship (equation 4-5), referred to as the *projection case*, expresses image space coordinates of an object point as a function of the interior and exterior orientation elements and the object space coordinates of that point, such as

$$x_i = F_1(x_0, f, X_L, Y_L, Z_L, \omega, \phi, \kappa, X_i, Y_i, Z_i) ,$$

$$y_i = F_2(y_0, f, X_L, Y_L, Z_L, \omega, \phi, \kappa, X_i, Y_i, Z_i) . \quad (4-8)$$

The inverse relationship (equation 4-6), referred to as *reprojection* expresses the planimetric coordinates of a point in object space as a function of the interior and exterior orientation elements, the image space coordinates of that point and of the elevation of the point above datum, such as

$$X_i = F'_1(x_o, f, x_i, y_i, X_L, Y_L, Z_L, \omega, \varphi, \kappa, Z_i)$$

$$Y_i = F'_2(y_o, f, x_i, y_i, X_L, Y_L, Z_L, \omega, \varphi, \kappa, Z_i) \quad (4-9)$$

The collinearity equation is the most fundamental equation in spatial positioning. In fact it can be used for solving any spatial positioning problem associated with directional data acquisition systems. Several examples are now presented.

The six elements of exterior orientation can be determined if the interior orientation is known and the image and object space coordinates of at least three points are given. This operation is analogous to resection in geodetic surveying, where the coordinates of the instrument station are determined by sighting points with known coordinates. Therefore, this operation is referred to as *space resection*.

The collinearity equation can, in fact, accommodate angles as observations since

$$\tan \beta = \frac{x-x_o}{f} \quad \text{and} \quad \tan \gamma = \frac{y-y_o}{f}$$

where  $\beta$  and  $\gamma$  are angles formed by a ray and the optical axis of the camera in the  $xz$  and  $yz$  planes respectively. Thus, one can also introduce in the collinearity equation horizontal and vertical angles observed with a theodolite and then solve a *three-dimensional geodetic problem*. An interesting point to note is, that by retaining the three orientation elements as unknowns, the mislevelling of the theodolite can also be dealt with.

A special case of space resection is the *determination* of the *perspective centre* of projection instruments used in analogue photogrammetry. The image and object space coordinates are obtained by observing a precision grid plate. More details provided about this in the numerical photogrammetry course.

The interior orientation elements can also be treated as unknowns and so called additional parameters can be included, which model various distortions affecting the imaging process. In this form, the collinearity equation is used for *sensor calibration*.

The projection form of the collinearity equation (equation 4-5) indicates that to every object point corresponds a single image point. The reprojection form (equation 4-6) on the other hand indicates that infinite number of object points belong to every image point as a function of the  $Z$  object space coordinate. Conversely, object points which have the same planimetric position ( $X, Y$ ) but are at different elevations will be projected to a different

location in the image. This phenomenon is a fundamental characteristic of central perspectives and is called *relief displacement*.

It is evident, therefore, that a single image is insufficient to reconstruct the spatial position of a three-dimensional object. A single image allows only to recover the direction of a ray extending from the perspective centre through an image point towards the object point. The length of the ray remains undefined. Either a second image of the same object, taken from a different location is needed, or the Z coordinates of the object points must be known to obtain a complete solution. The first case leads to the *space intersection*, where collinearity equations pertaining to two or more images are solved simultaneously to find the object space coordinates of a point. This operation will be discussed in detail later. A real or assumed knowledge of the Z coordinate forms the basis of *rectification*.

Rectification means the transformation of a so-called tilted image, one with a coordinate system not parallel to the object space coordinate system, unto an equivalent non-tilted image, taken from the same exposure station. In airborne and spaceborne data acquisition this means the transformation of an image taken with a non-vertical sensor orientation onto an equivalent image with vertical sensor orientation so that the image plane becomes horizontal. It is a transformation from one plane to another and the new product remains a central perspective. Knowing the interior and exterior orientation elements, the reprojection form of the collinearity equation can be used for this purpose by setting the projection plane at a certain elevation with respect to the datum. In other words, the same Z value is assigned to each object point. It is recommended to set Z at the average elevation of the object points to minimize the effect of the fluctuation in elevation on the position of the image points. The exterior orientation elements can, of course, be determined by space resection if they are unknown at the outset of the rectification process.

#### **4.4 Solution of the Collinearity Equation**

It should be noted that the collinearity equations are non-linear. The equations must, therefore, be linearized, initial approximations assumed for all unknowns and an iterative solution followed. Linearization is performed by applying Taylor's series expansion, as discussed in Appendix I, Section C-4 (page 622 in the textbook).

The collinearity condition (equation 4-5) written in functional form is

$$F_1 = (x-x_0) [m_{31}(X-X_L) + m_{32}(Y-Y_L) + m_{33}(Z-Z_L)] + f [m_{11}(X-X_L) + m_{12}(Y-Y_L) + m_{13}(Z-Z_L)] = 0 \quad (4-10)$$

$$F_2 = (y-y_0) [m_{31}(X-X_L) + m_{32}(Y-Y_L) + m_{33}(Z-Z_L)] + f [m_{21}(X-X_L) + m_{22}(Y-Y_L) + m_{23}(Z-Z_L)] = 0$$

Usually the image coordinates  $x, y$  are observed quantities, the interior orientation elements  $x_0, y_0, f$  are considered known from camera calibration and the remaining nine variables  $X_L, Y_L, Z_L, \omega, \phi, \kappa, X, Y, Z$  are treated as unknowns. Equation (5-3) is therefore partially differentiated with respect to each of these variables. Differentiation with respect to the three angles means differentiating the rotation matrix. Further detail are provided in Appendix I, Sections C-6 and 10-3 (or pages 625 and 309 in the reference book).

Initial approximations for the six exterior orientation elements can be obtained from data acquisition records, and by simple measurements and calculations. For nearly vertical images, the rotation angles  $\phi$  and  $\omega$  is initially assumed to be zero. For intentionally tilted images, the nominal value of the tilt is used.

The  $\kappa$  angle depends on the azimuth of the flight direction with respect to the object space coordinate system. It is the angle measured counterclockwise from the object space X-axis to the image x-axis. If the flight direction is due east or west then  $\kappa$  is  $0^\circ$  or  $180^\circ$ , respectively. If the line runs due north or south then  $\kappa$  is  $+90^\circ$  or  $-90^\circ$ , respectively. Otherwise, an approximate value of  $\kappa$  can be computed as the difference between the azimuths of a control line (the line connecting two control points) as

$$\kappa = \alpha_P - \alpha_G,$$

where  $\alpha_G$  and  $\alpha_P$  are the azimuths of the control line in the object space and image coordinate systems respectively.

If the azimuth of the flight line  $\alpha_L$  is known, then  $\kappa$  can be obtained as

$$\kappa = 90^\circ - \alpha_L.$$

The flying height above datum is assumed as the initial value for  $Z_L$ . It can also be obtained from the scale of the image, which in turn can be calculated as the ratio of the length of a control line in the image and on the ground. Thereby

$$Z_L = f SF$$

where SF is the scale factor.

Initial values for  $X_L$  and  $Y_L$  can be calculated by substituting the initial approximations for  $Z_L$  and for the angular orientation elements into equation (4-7). For nearly vertical photographs

$$\begin{aligned} X_L &= X + (Z-Z_L) \frac{x-x_0}{f} \\ Y_L &= Y + (Z-Z_L) \frac{y-y_0}{f} \end{aligned} \quad (4-11)$$

#### 4.4 Projective Transformation

From the reprojection form all the collinearity equations (equation 4-7) a parameter form can be developed for projecting points from one plane onto another through a projection centre. By setting  $Z = 0$  and rearranging the equation results in:

$$\begin{aligned} X &= \frac{(X_L m_{13} - Z_L m_{11})x + (X_L m_{23} - Z_L m_{21})y +}{m_{13}x + m_{23}y + (-m_{13}x_0 - m_{23}y_0 - m_{33}f)} \\ &+ \frac{[(X_L m_{33} - Z_L m_{31})(-f) + (-X_L m_{13} + Z_L m_{11})x_0 + (-X_L m_{23} + Z_L m_{21})y_0]}{m_{13}x + m_{23}y + (-m_{13}x_0 - m_{23}y_0 - m_{33}f)} \end{aligned}$$

The equation for Y can be rearranged similarly.

By introducing the notations

$$a_1^1 = X_L m_{13} - Z_L m_{11}$$

$$b_1^1 = X_L m_{23} - Z_L m_{21}$$

etc.

the two equations become

$$X = \frac{a_1^1 x + b_1^1 y + c_1^1}{a_o^1 x + b_o^1 y + c_o^1}$$

$$Y = \frac{a_2^1 x + b_2^1 y + c_2^1}{a_o^1 x + b_o^1 y + c_o^1} \quad (4-12)$$

After both equations are divided by  $c_o^1$  the final form is obtained as:

$$X = \frac{a_1 x + b_1 y + c_1}{a_o x + b_o y + 1}$$

$$Y = \frac{a_2 x + b_2 y + c_2}{a_o x + b_o y + 1} \quad (4-13)$$

The inverse transformation is

$$x = \frac{(b_2 - b_o Y)(X - c_1) - (b_1 - b_o X)(Y - c_2)}{(a_1 - a_o X)(b_2 - b_o Y) - (b_1 - b_o X)(a_2 - a_o Y)}$$

$$y = \frac{(a_1 - a_o X)(Y - c_2) - (a_2 - a_o Y)(X - c_1)}{(a_1 - a_o X)(b_2 - b_o Y) - (b_1 - b_o X)(a_2 - a_o Y)} \quad (4-14)$$

Equations (4-11) and (4-12) are called *projective transformation* equations. To every point  $x, y$  in one plane there corresponds a point  $X, Y$  in the other plane, provided that the common denominator is not zero. If the denominator becomes zero then the corresponding point moves to infinity. It is called the vanishing point. The projective transformation is not conformal. A one-to-one correspondence of points and lines remains, but neither the magnitude of angles nor the parallelity of lines is preserved. The shape of figures is changed.

The projective transformation is useful for modelling and correcting errors which distort the shape of a figure and for analytical rectification. There are eight independent parameters. Thus the coordinates of four corresponding points (control points) must be known in both planes to evaluate them. Thereafter, all other points can be transformed from one plane onto the other. The accuracy of rectifying images of a three-dimensional scene in this manner can be improved by referencing the X,Y coordinates of all control points to a plane, set at the average terrain height, before evaluating the transformation parameters.

The advantage of analytical rectification by projective transformation versus using the collinearity equation (equation 4-7) is that it can be performed without the knowledge of interior orientation and only planimetric control points are needed. Rectification by the collinearity equation, on the other hand, can be performed with a minimum of three control points.

## 4.5 Analogue Rectification

In analogue photogrammetry, the projective relationship that exists between image and object is modeled physically with the help of instruments, that act as analogue computers. In these devices, the collinearity condition, which is the most fundamental projective relationship, is modeled optically by light rays or mechanically by metal rods. Transformations are solved by physical rotations and translations.

### 4.5.1 Perspective rectification instruments

Perspective rectification transforms an image with an arbitrary orientation in space onto another image which is oriented parallel to the datum plane. This means, in the case of aerial photography, the transformation of a tilted photograph onto an equivalent truly vertical photograph and changing the scale to a desired, usually enlarged, scale, as shown in Figure 4-7. (See also the description of rectification in Appendix II.)

The letters  $o$ ,  $i$ , and  $n$  in this figure designate the principal point, isocentre and the nadir point on the photographs in various states, while  $O$ ,  $I$  and  $N$  are the positions of these points on the ground. The tilted and the equivalent vertical photos intersect along the axis of tilt that passes through the isocentre. The tilt angle is indicated as  $\tau$ . Perspective

rectification only eliminates the tilt displacement, and the displacements caused by relief still remain. This product is still a central perspective.

The instrument used for perspective rectification is called *rectifier*. It is essentially a photographic enlarger or projection printer with auxiliary movements added. Its main components are the

- illumination system which is a light source with a reflector; a stage plate for mounting the negative image;
- projector lens; and
- projection table or easel on which the rectified image appears (see Figure 4-8 and 4-9).

The optical projector enforces physically the collinearity condition whereby a point in the negative placed on the stage plate, its projection on the easel and the optical center of the projector lens form a straight ray. Rectifiers provide an analog solution or physical modelling of the projective transformation equation.

Certain constraints imposed by the optical-mechanical solution of the projective transformation must be dealt with by satisfying two optical and a geometric condition in order to obtain a sharp and geometrically correct rectified image.

a) The first optical condition requires that the lens equation be satisfied in order to produce a sharp image on the easel plane. The rectifier has to be set so that

$$\frac{1}{i} + \frac{1}{p} = \frac{1}{F}$$

where  $i$  is the image distance (the distance from the negative plane to the lens plane),  $p$  the projection distance (the distance from the easel plane to the lens plane) and  $F$  the focal length of the rectifier lens.

b) If both the negative (stage) plane and the projection (easel) plane are tilted during rectification as shown in Figure 4-8, then both the image and the projections distances vary throughout the image. To maintain a sharp focus at all image points in spite of this setup, the Scheimpflug condition must be satisfied. The Scheimpflug condition states that, in projecting images through a lens from one plane to another which are not parallel, the two planes and the lens plane must intersect along a common line to satisfy the lens equation at every point. This means, in case of a rectifier, that the negative, the lens and the easel

planes must intersect along a common line, as shown in Figure 4-10, to keep all projected image points in sharp focus on the easel. This is the second optical condition.

In Figure 4-10 points  $a'$  and  $b'$  are so located on the easel that

$$\frac{1}{i_a} + \frac{1}{p_a} = \frac{1}{F} \quad \text{and} \quad \frac{1}{i_b} + \frac{1}{p_b} = \frac{1}{F}$$

The line of intersection of the three planes passes through  $S$ .

c) Enlargement is introduced by changing the image distance to projection height ratio, so that

$$m = \frac{p}{i}$$

where  $m$  is the magnification factor.

Figure 4-11 illustrates two possibilities for introducing magnification.

In case (a) the image distance is set to  $f$ , the principal distance of the photographic camera. This gives a fixed magnification factor of  $p/f$ , where  $p$  is constrained by the lens equation as a function of  $F$ , the focal length of the lens used.

In case (b), the magnification factor is changed freely as the ratio  $p/i$ . As a consequence, the bundle of rays in the rectifier are no longer congruent to the bundle of rays in the camera that took the photographs. In other words, the interior orientation of the image acquisition system is no longer maintained.

The challenge is to maintain the correct geometric relationship between corresponding points in the original (negative) and the rectified and enlarged images without maintaining the interior orientation. The geometry of the rectification is shown in Figure 4-12, which is a side view in the principal plane.

In this figure  $G$  represents a horizontal plane in object space (ground);  $P$  is the negative plane. The angle  $\tau$  formed at  $S$  by the intersection of these two planes is the angle of tilt of the photograph to be rectified. Image points  $a$ ,  $b$ ,  $n$  and  $o$  are the projections of the object points  $A$ ,  $B$ ,  $N$  and  $O$  through projection center  $Lc$ , which represents the projection center of the camera. The point pairs  $n$  and  $N$  are the photo and ground nadir points, while  $o$  is the principal point and  $O$  is its projection on the ground. Thus the angle between the

rays  $nN$  and  $oO$  is also the tilt angle  $\tau$ .  $V$  is the vanishing point, the image of an object located at infinity. (The ray  $LcV$  is parallel to  $G$  and the angle  $LcVP$  is also  $\tau$  ).

Now line  $V Lc$  is rotated around  $V$  by angle  $\delta$  to establish a new projection center  $Lr$ , and the image points are re projected onto a tilted plane  $E$ , which has been rotated around  $S$  by the same angle  $\delta$ , with respect to the horizontal. The points  $A', B', N'$  and  $O'$  are in fact the intersections of arcs drawn around  $S$  as the center with radii  $SA, SB, SN$  and  $SO$  respectively. Thus point groups  $A', B', N', O'$  are equivalent to point groups  $A, B, N, O$  although the bundle of the projection rays passing through center  $Lr$  are not congruent to those through center  $Lc$ .  $Lr$  is the projection center of the rectifier,  $R$  is the rectifier lens plane and  $E$  is the easel plane. The perpendicular through  $Lr$  onto  $R$  is the optical axis of the rectifier lens which intersects the negative and the easel planes at points  $c$  and  $C$  respectively. The perpendicular dropped from  $V$  onto  $R$  is the focal length  $F$  of the rectifier lens.

Note that the principal point  $o$  is not located at the intersection of the rectifier optical axis with the negative plane but separated by a distance  $d$ . Therefore, the rectifier has to be set up as follows:

- The negative is placed on the stage plate and centered on the optical axis of the rectifier lens.
- The stage plate is rotated until the principal plane of the negative lies in the principal plane of the rectifier.
- The negative is then shifted through a distance  $d$  in the direction of the principal line of the rectifier. (The principal line runs perpendicular to the tilt axis of the rectifier.) A positive shift is upward.

The last step is the geometric condition which assures that the projective relationship between the negative and the rectified enlargement is identical to the projective relationship between the negative and the object planes, although the interior orientation has not been maintained. The magnitude of the shift of the negative can be computed as

$$d = \frac{f}{\sin \tau} \left( \cos \tau \frac{\cos \beta}{\cos \alpha} \right)$$

where  $f$  is the principal distance of the camera lens that produced the negative, and  $\alpha$  and  $\beta$  are the inclinations of the negative and the easel planes respectively.

Rectifiers may have a total of ten degrees of freedom as follows:

- shifts in two directions ( $x,y$ ) and a rotation of the negative in its own plane;
- shifts in two directions ( $X,Y$ ) and a rotation of the enlarging paper on the easel;
- tilt of the negative and easel planes with respect to the lens plane by the angles  $\alpha$  and  $\beta$  respectively;
- change of the image distance  $i$  and the projection distance  $p$ .

Of the above ten elements only eight are independent. The  $i$  and  $p$  settings are correlated through the lens equation and  $\alpha$  and  $\beta$  are interrelated by the Scheimpflug condition. These eight elements are the analog representation of the eight parameters of two dimensional projective transformation equation, which is used to perform analytical rectification without the knowledge of interior orientation.

If, as usual, the rectified enlargement is not referenced to an object space coordinate system in the rectifier, then three degrees of freedom can be eliminated. Thus most rectifiers are designed around the following five motions as shown in Figure 4-13:

- (a) change of magnification;
- (b) easel tilt around the  $x$  axis with respect to the lens plane;
- (c) a swing of the negative to bring the principal plane of the negative in the principal plane of the rectifier;
- (d) a shift of the negative in the direction of the principal line; and
- (e) a shift of the negative in the direction normal to the principal line.

Most rectifiers are so constructed that the lens equation and the Scheimpflug conditions are automatically satisfied with the help of mechanical devices called inverses. The Peaucellier (Figure 4-14) and the Pythagorean inversors are designed to maintain the lens equation, and the Carpentier inversor (Figure 4-15) satisfies the Scheimpflug condition.

Although the rectifier settings can be precalculated if the tilt of the photograph is known or has been predetermined, an empirical trial and error method of orientation is most often used in practice as follows:

- A minimum of four control points are plotted at the scale selected for the rectified photo.
- This plot is placed on the easel and the five rectifier motions are adjusted by trial and error until the projected images of the control points coincide with the corresponding plotted points.
- The plot is then replaced by photographic paper and exposed.

The result is a photograph free of tilt displacement. It remains, however, a central perspective and relief displacement is still present. The effect of the relief displacement can be minimized by setting the height of the datum plane for the rectified photo to the average terrain elevation. This is done by plotting the control points in a perspective projection on the selected reference plane as shown in Figure 4-16. The coordinates are displaced radially from the ground principal point (theoretically from the ground nadir point) as function of their elevation above or below the reference plane according to the equation:

$$d = \frac{rh}{H - h}$$

where  $d$  is the magnitude of the radial displacement,  $H$  is the flying height above the reference plane,  $r$  is the radial distance of the point from the ground principal point and  $h$  is the elevation of the control point with respect to the reference plane. A positive value for  $d$  means a displacement away from the ground principal point.

Rectified photographs can be used as map substitutes where the terrain is reasonably flat or when the effect of relief displacement can be tolerated. This displacement can be calculated by the above equation at any location of the rectified photo.

#### **4.5.2 Reflection type rectification instruments**

A simple device designed for the correction of tilt displacement in photographs is the *sketchmaster* which utilizes the *camera lucida* principle. This device does not produce a rectified photograph but provides correction for tilt displacement while manually transferring planimetric details from a tilted photo onto a map.

The principle of operation of the sketchmaster is shown in Figure 4-17. The photograph is placed on a holder in the instrument and the map or drafting paper on the table below the eye piece. The viewing system is a half-silvered mirror or a beam splitter. A large mirror, set at 45° to the photo holder, projects the photo onto the eye piece mirror and at the same time the map can be viewed directly through the semi-transparent mirror. Thus the photo and the map are viewed in superimposition.

The aim is to match selected features on the map or the control points plotted on the drafting sheet with corresponding photo images. Thereafter new features can be transferred from the photo onto the map by manual tracing. It is advisable to perform the matching and tracing in subsections of the photograph at a time to localize the effect of the

various distortions, including those caused by relief displacement. A minimum of three control features must be selected for matching which surround the area of interest.

There are various adjustments available to perform the superimposition. The ratio of the ray path length from eyepiece to map and eyepiece to photo can be changed using the adjustable legs, thus varying the magnification. The photograph can be tilted around two perpendicular axes with the help of the adjustable legs, and the map sheet can be shifted and rotated.

In another design of the sketchmaster the photograph is mounted on a vertical easel which can be tilted and rotated by means of a ball socket (Figure 4-18).

The most advanced design of the reflection type rectification devices is the zoom transfer scope. Zoom optics provide continuous variation in magnification. An anamorphic optical system allows the introduction of affine scale change, and image rotation is applied by means of rotating prisms.

The principal application of the reflection type rectification devices is in map revision and updating.

#### **4.6 First Order Approximation of the Collinearity Equation**

In the derivation of an approximation of equation (4-7) it is assumed that all points in object space are in the same plane so that  $Z = 0$ ; the image coordinates are referenced to the principal point, whereby  $x_0 = y_0 = 0$  and that the rotation angles are small enough to warrant the use of the first order approximation of the rotation matrix (Equation 2-23). Therefore the first order approximation of Equation (4-7) for  $X$  becomes

$$X = X_L - Z_L \frac{x - y\kappa - f\phi}{-x\phi + y\omega - f}$$

The second term of the above equation is now divided by  $-f$ , whereby

$$X = X_L - Z_L \frac{\frac{-x}{f} + \frac{y}{f} \kappa + \phi}{1 - \left(-\frac{x}{f} \phi + \frac{y}{f} \omega\right)}$$

An expansion of the second term according to the general formula

$$\frac{1}{1-a} = 1 + a + a^2 + \dots + a^n \quad \text{for } a < 1$$

and neglecting the 2nd and higher order terms of the rotations gives

$$X = X_L - Z_L \left( -\frac{x}{f} + \frac{x^2}{f^2} \varphi - \frac{xy}{f^2} \omega + \frac{y}{f} \kappa + \varphi \right)$$

Similarly

$$Y = Y_L - Z_L \left( -\frac{y}{f} - \frac{y^2}{f^2} \omega + \frac{xy}{f^2} \varphi - \frac{x}{f} \kappa - \omega \right)$$

By combining the two  $\varphi$  and  $\omega$  terms the final form of the equations is obtained as

$$X = X_L + Z_L \left( \frac{x}{f} - \left(1 + \frac{x^2}{f^2}\right) \varphi + \frac{xy}{f^2} \omega - \frac{y}{f} \kappa \right)$$

$$Y = Y_L + Z_L \left( \frac{y}{f} - \frac{xy}{f^2} \varphi + \left(1 + \frac{y^2}{f^2}\right) \omega + \frac{x}{f} \kappa \right) \quad (4-17)$$

where the exterior orientation elements are clearly separated.

Equation (4-15) is now developed further to express small changes in the position of a projected point as function of small changes in the exterior orientation elements, so that

$$X = X' + dX, \quad Y = Y' + dY, \quad Z = Z' + dZ,$$

where  $X'$ ,  $Y'$ ,  $Z'$  are approximate coordinates of the projected point and  $dX$ ,  $dY$ ,  $dZ$  are small changes in these coordinates introduced by small changes in the exterior orientation elements, i.e.  $dX_L$ ,  $dY_L$ ,  $dZ_L$ ,  $d\omega$ ,  $d\varphi$ ,  $d\kappa$ . The approximate value of small rotations is zero, whereby from equation (4-15)

$$X' = X_L + \frac{Z_L x}{f}, \quad Y' = Y_L + \frac{Z_L y}{f} \quad (4-16)$$

For large rotations,  $X'$ ,  $Y'$  can be obtained by inserting the estimated values of the rotation angles into equations (4-15) or (4-7). Equation (4-15) can now be written as

$$X' + dX = X'_L + dX_L + (Z'_L + dZ_L) \left( \frac{x}{f} - \left(1 + \frac{x^2}{f^2}\right) d\phi + \frac{xy}{f^2} d\omega - \frac{y}{f} d\kappa \right)$$

$$Y' + dY = Y'_L + dY_L + (Z'_L + dZ_L) \left( \frac{y}{f} - \frac{xy}{f^2} d\phi + \left(1 + \frac{y^2}{f^2}\right) d\omega + \frac{x}{f} d\kappa \right)$$

The multiplication is now performed and terms with products of small changes are omitted. Thereafter, a substitution of equation (4-16) will cancel  $X'$  and  $Y'$  and the result is

$$dX = dX_L + \frac{x}{f} dZ_L - \left(1 + \frac{x^2}{f^2}\right) Z'_L d\phi + \frac{xy}{f^2} Z'_L d\omega - \frac{y}{f} Z'_L d\kappa$$

$$dY = dY_L + \frac{y}{f} dZ_L - \frac{xy}{f^2} Z'_L d\phi + \left(1 + \frac{y^2}{f^2}\right) Z'_L d\omega + \frac{x}{f} Z'_L d\kappa$$

From equation (4-14) in the case that the origin of the coordinate system is at the projection of the perspective centre  $L$  ( $X'_L = Y'_L = 0$ ), the image coordinates can be expressed as

$$x = \frac{f}{Z'_L} X', \quad y = \frac{f}{Z'_L} Y'$$

A substitution of these expressions into the previous equations and dropping the prime superscript yields

$$dX = dX_L + \frac{X}{Z_L} dZ_L - \left(Z_L + \frac{X^2}{Z_L}\right) d\phi + \frac{XY}{Z_L} d\omega - Y d\kappa$$

$$dY = dY_L + \frac{Y}{Z_L} dZ_L - \frac{XY}{Z_L} d\phi + \left(Z_L + \frac{Y^2}{Z_L}\right) d\omega + X d\kappa \quad (4-17)$$

The above equations are the so-called *differential formulae*, which express the changes  $dX$ ,  $dY$  in the coordinates of a point in the projection plane as functions of small differential changes in the position of the perspective centre and angular orientation. These formulae are useful for developing simple numerical solutions for various photogrammetric problems and for studying the effects of various observational and operational errors on the spatial position of points.  $Z_L$  is actually the projection height.

The algebraic signs in equation (4-17) are in accordance to the sign convention of the rotations defined in Section 2.4.1. This should always be verified when the formulae are to be applied to a certain instrument.

In a similar way differential formulae can be derived for intentionally tilted images. For example if the approximate values of the rotations are

$$\varphi' = \varphi^{\circ}, \quad \omega' = 0^{\circ}, \quad \kappa' = 0^{\circ}$$

then the differential formulae become

$$\begin{aligned} dX = & dX_L + \frac{X}{Z_L} dZ_L - (Z_L + \frac{X^2}{Z_L})d\varphi + \frac{Y}{Z} (X \cos \varphi - Z_L \sin \varphi)d\omega \\ & - \frac{Y}{Z_L} (Z_L \cos \varphi - X \sin \varphi)d\kappa \end{aligned} \quad (4-18)$$

$$\begin{aligned} dY = & dY_L + \frac{Y}{Z_L} dZ_L - \frac{XY}{Z_L} d\varphi + [\frac{X}{Z_L} \sin \varphi + (Z_L + \frac{Y^2}{Z_L})\cos \varphi]d\omega \\ & + [X \cos \varphi - \sin \varphi (Z_L + \frac{Y^2}{Z_L})] d\kappa \end{aligned}$$

#### 4.7 Approximate Analytical Projective Relations

For truly vertical photographs or if the effect of tilt can be ignored and when the x and y image and ground coordinate axes are considered parallel, the rotation matrix M becomes a unit matrix. Thus the planimetric ground coordinates are computed according to equation (4-7) as

$$X = X_L + (Z - Z_L) \frac{x - x_0}{-f} \quad (3 - 17a)$$

$$Y = Y_L + (Z - Z_L) \frac{y - y_0}{f} \quad (3 - 17b)$$

If the image and ground  $x$  and  $y$  axes are not parallel, then a  $\kappa$  rotation must be included in the computation so that

$$X = X_L + (Z - Z_L) \frac{(x - x_o) \cos \kappa - (y - y_o) \sin \kappa}{-f} \quad (3 - 18a)$$

$$Y = Y_L + (Z - Z_L) \frac{(x - x_o) \sin \kappa + (y - y_o) \cos \kappa}{f} \quad (3 - 18b)$$

Equations (4-17) can be rearranged for the case of a particular terrain and image point pair  $A$  and  $a$ , as:

$$\frac{X - X_L}{x - x_o} = \frac{Y - Y_L}{y - y_o} = \frac{Z - Z_L}{-f} = \frac{Z_L - Z}{f}$$

The coordinate differences represent distances on the ground and in the image. Thus the ratios in the above formula express the *scale factor*,  $SF$  of the image. Since  $Z_L$  is  $H$  the flying height above the datum and  $Z$  is  $h$ , the elevation of a terrain point above datum, as shown in Figure 4-19, the scale factor can be expressed in general form as

$$SF = \frac{H - h}{f} \quad (3 - 19)$$

The scale of a vertical photograph varies according to the fluctuation of the terrain elevation represented by  $h$ . This is one of the principal differences between a photograph, which is a central projection, and a map which is an orthogonal projection. The average scale is the most convenient measure to describe the scale of a vertical photograph taken over variable terrain. In this case,  $h$  becomes the average terrain elevation  $h_{av}$ , as shown in Figure (4-19).

Another important difference between a map and a vertical photograph is that all points on the map are in their true relative planimetric position, while on a photograph all points which are above or below the selected datum are displaced radially from the fiducial center with respect to their true position, as shown in Figure 4-20. This displacement is called *relief displacement*. The tip of the tower  $A$ , at an elevation  $h_A$  above the datum and its orthogonal projection onto the datum  $A'$  occupy in reality the same planimetric position. On the photograph, however, they show up at two distinctly different image positions  $a$  and  $a'$  respectively.

From equation (4-17) it follows that

$$X_A - X_L = (Z_A - Z_L) \frac{x_a - x_o}{-f} \quad \text{and}$$

$$X_{A'} - X_L = (Z_{A'} - Z_L) \frac{x_{a'} - x_o}{f}$$

Since both  $A$  and  $A'$  have the same planimetric coordinates and  $A'$  is on the datum plane,

$$X_{A'} = X_A, \quad \text{and} \quad Z_{A'} = 0$$

whereby

$$Z_A \frac{x_a - x_o}{f} - Z_L \frac{x_a - x_o}{f} = -Z_L \frac{x_{a'} - x_o}{f}$$

from which

$$Z_A (x_a - x_o) = Z_L (x_a - x_o - x_{a'} + x_o) = Z_L (x_a - x_{a'}) = Z_L \Delta x$$

Thus the  $Z$  coordinate of  $A$  is

$$Z_A = \frac{Z_L \Delta x}{x_a - x_o}$$

or through a similar derivation using the  $Y$  coordinates

$$Z_A = \frac{Z_L \Delta y}{y_a - y_o}$$

Since in the similar triangles shown in Figure 4-21

$$\frac{x}{\Delta x} = \frac{y}{\Delta y} = \frac{r}{\Delta r}$$

therefore

$$Z_A = \frac{Z_L \Delta r}{r}$$

By changing the notations to obtain a general formula

$$h = \frac{Hd}{r}$$

where  $h$  is the height above datum of an object point,  $H$  is the flying height above the datum selected for measurement of  $h$ ,  $d$  is the relief displacement (the difference in the radial distance to the top and the base image of an object), and  $r$  is the radial distance on the photograph from the fiducial center to the displaced image. The above equation can also be derived by plane trigonometry based on Figure 4-20.

Equation (4-20) can be used to calculate the heights of objects such as buildings, trees, etc. if the image displacement of the top with respect to the base is known.

The relief displacement itself can be calculated by rearranging Equation (4-20) as

$$d = \frac{r h}{H}$$

All objects situated above the selected datum are displaced radially outward from the fiducial centre and all points below the datum plane are displaced radially inward.

If the camera axis unintentionally or intentionally deviates from the plumb line at the time of exposure, the photograph becomes tilted with respect to the horizontal datum plane. Image points are then displaced from their correct position, as shown in Figure 22. This displacement is called *tilt displacement*. The approximate value of this displacement caused by unintentional tilt of a few degrees can be calculated from the differential formulae (Equation 4-15). The exact value of this displacement and the effect of large intentional tilt has to be evaluated using the collinearity equation.

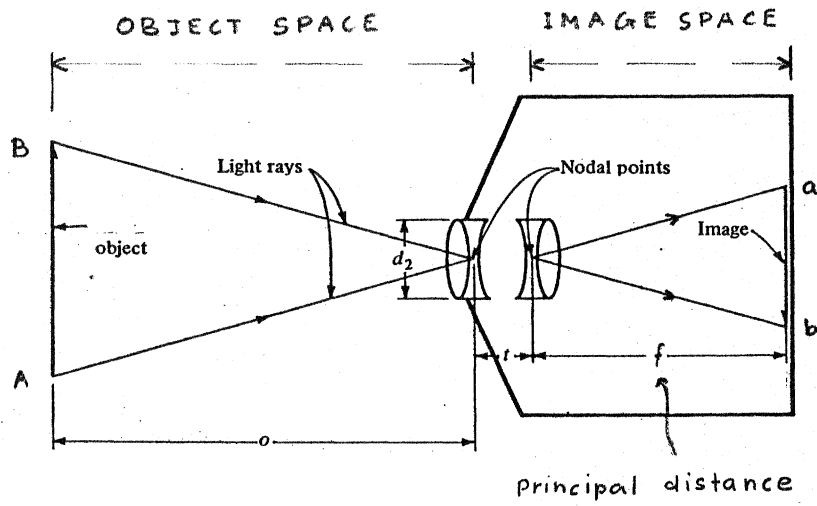


Figure 4-1

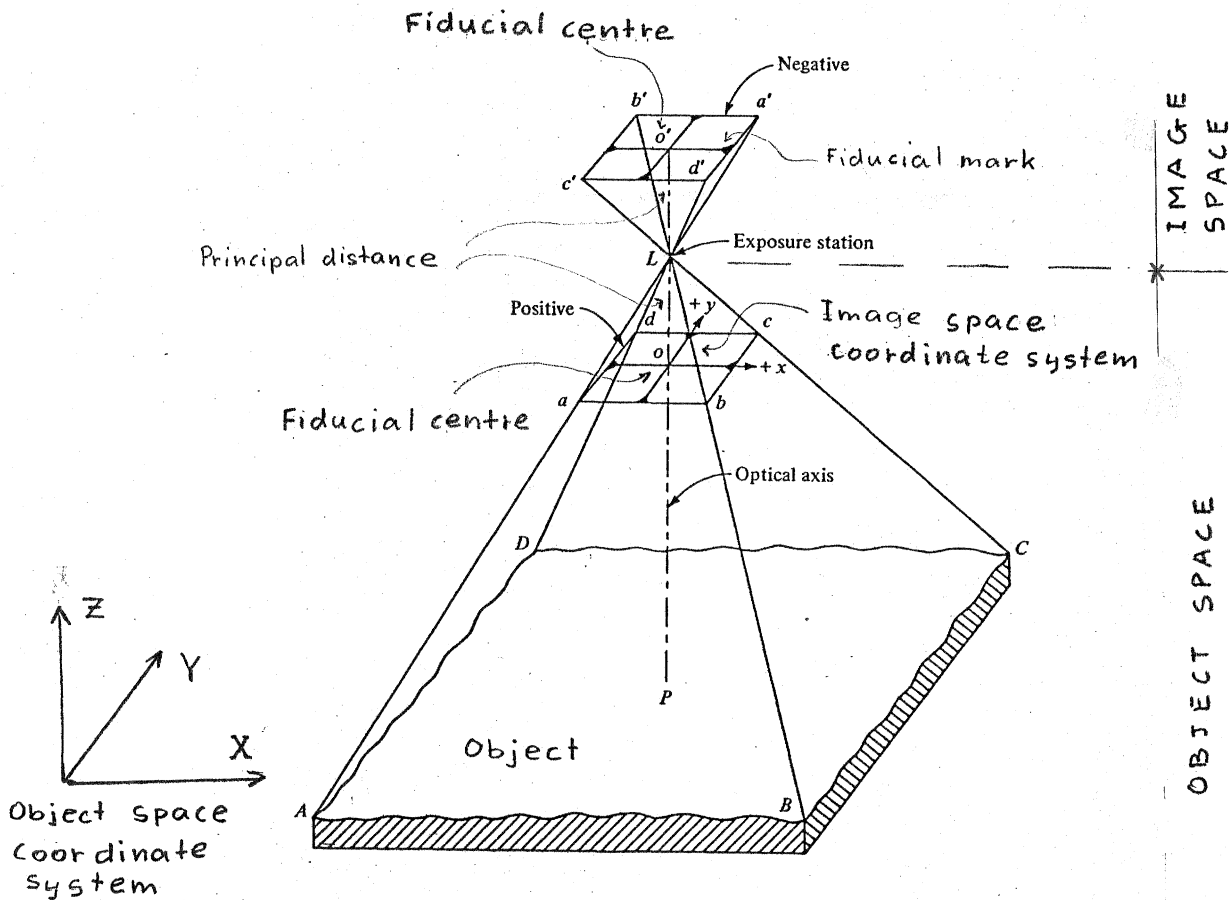


Figure 4-2

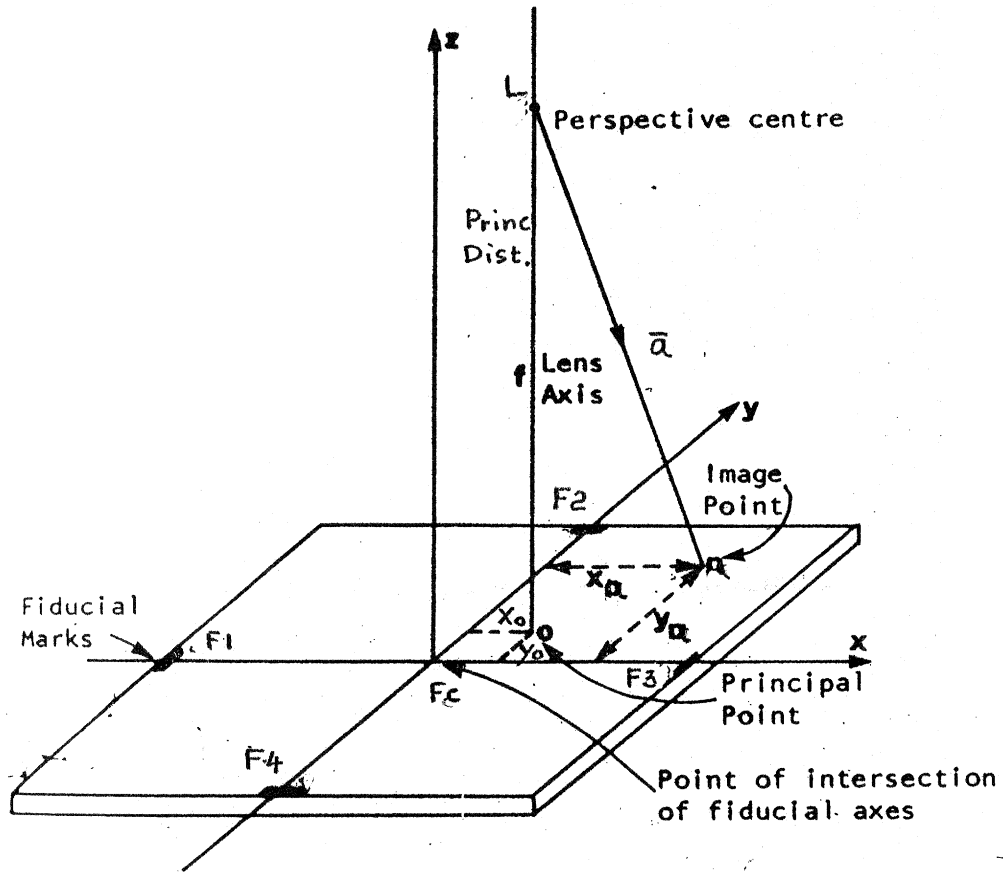


Figure 4-3

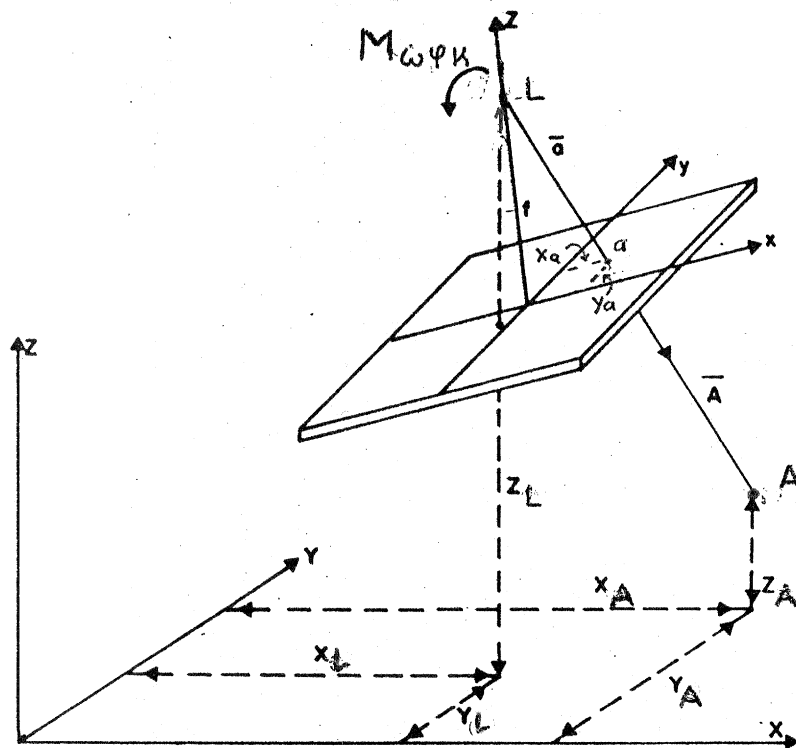
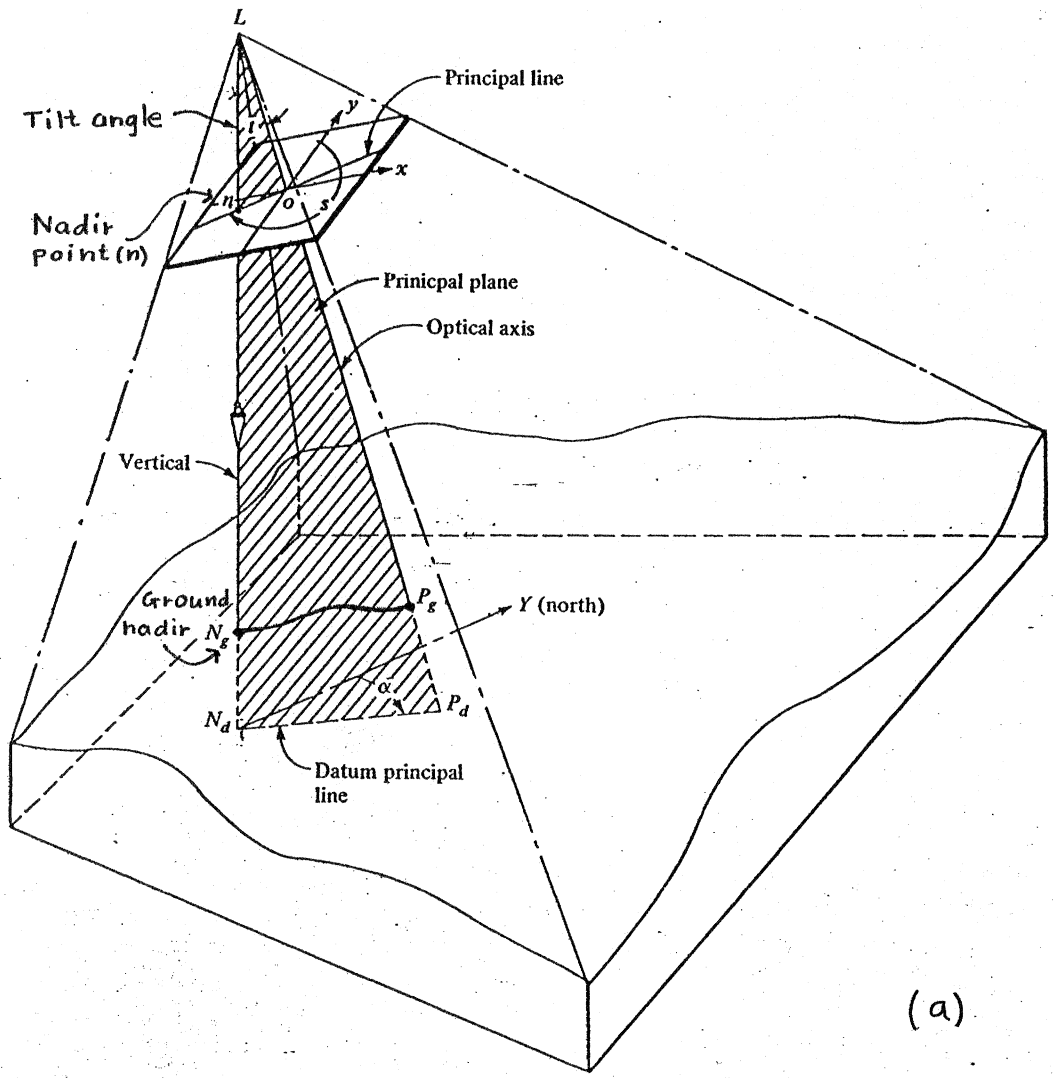
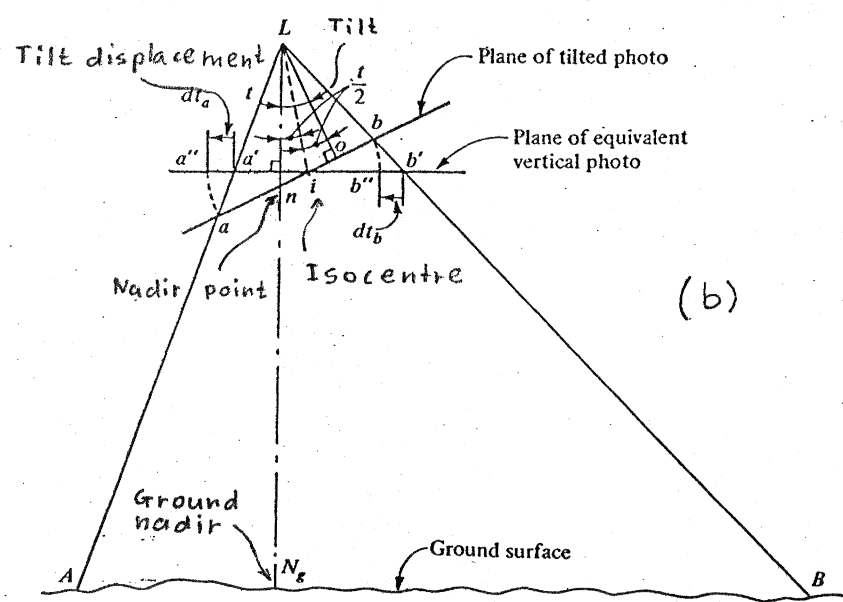


Figure 4-4



(a)



(b)

Figure 4-5

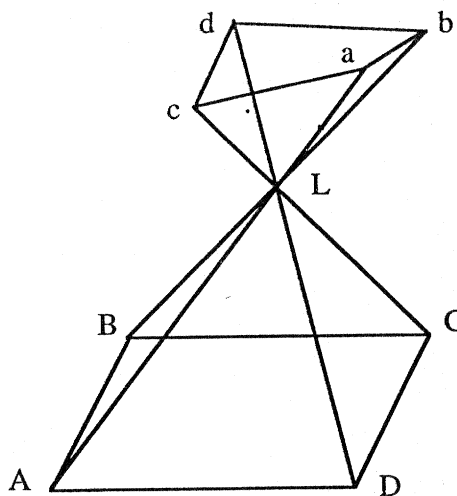


Figure 4-6

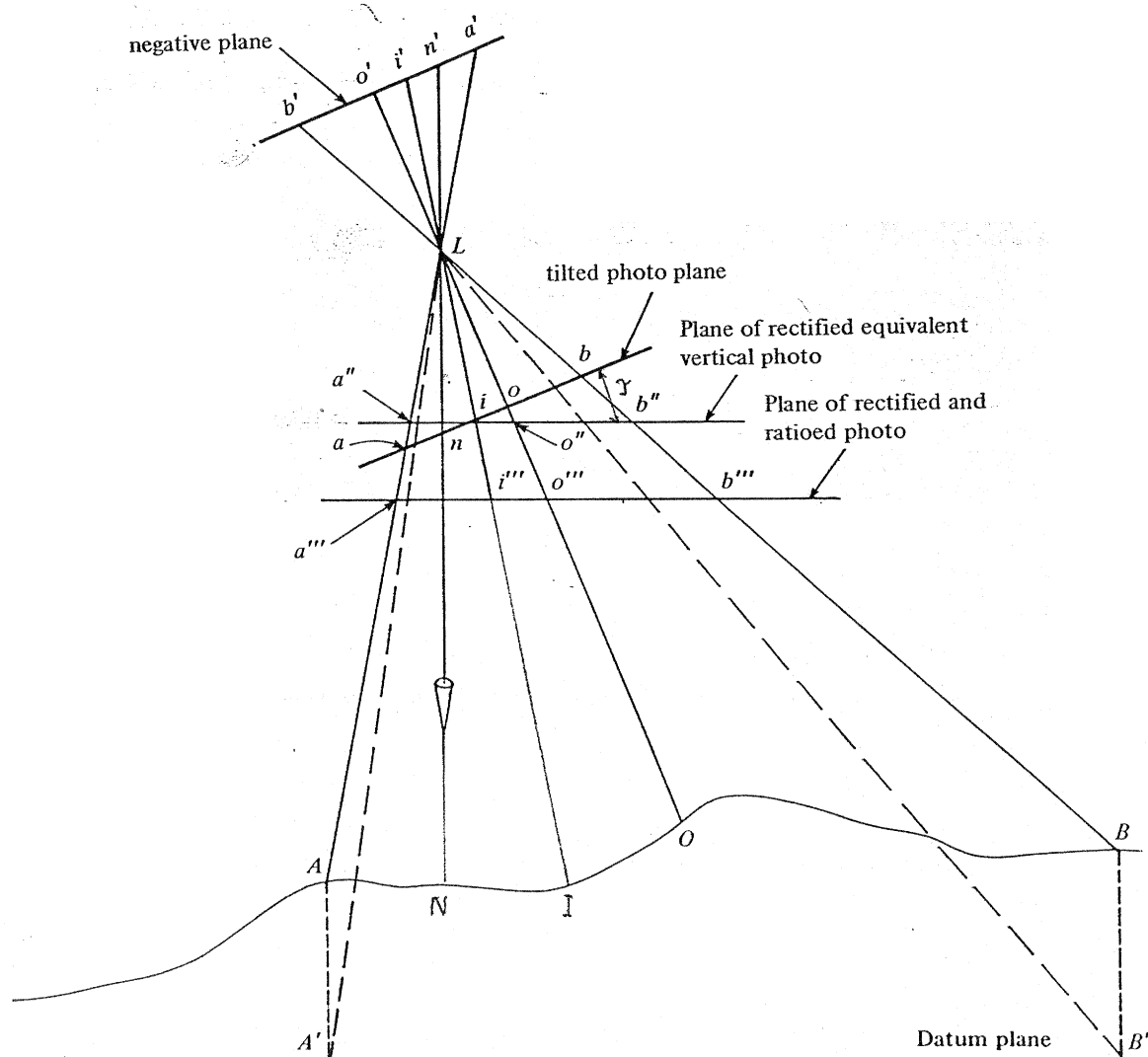


Figure 4-7

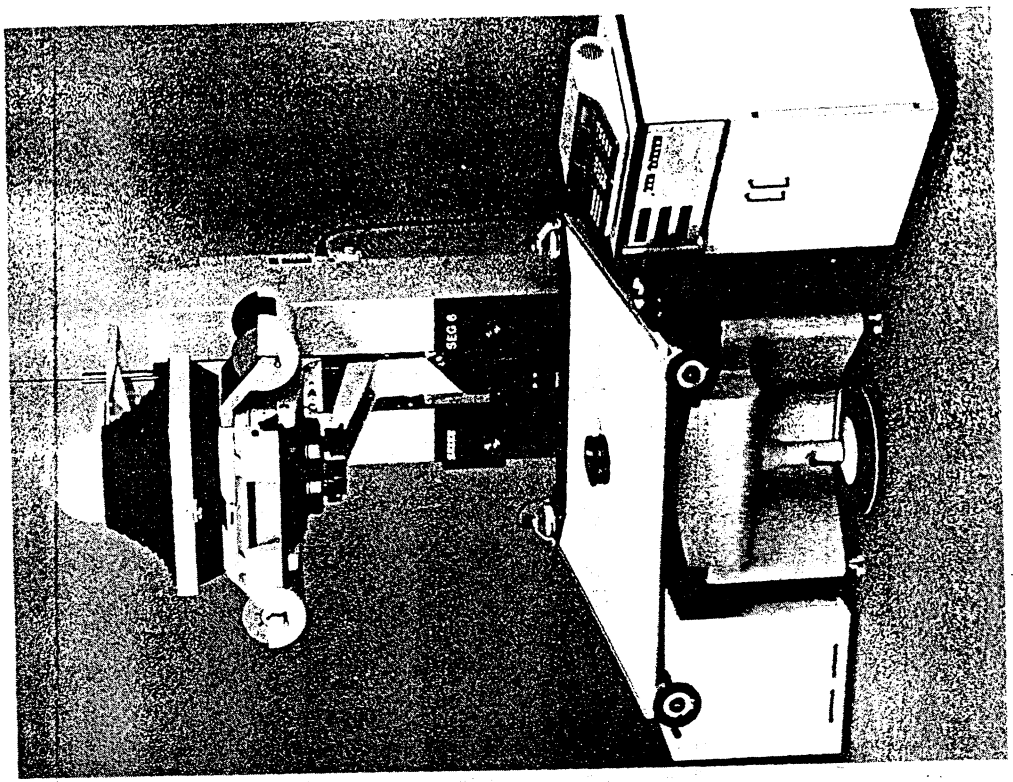


Figure 4-9 The SEG 6 automatic rectifier. (Courtesy Carl Zeiss, Oberkochen.)

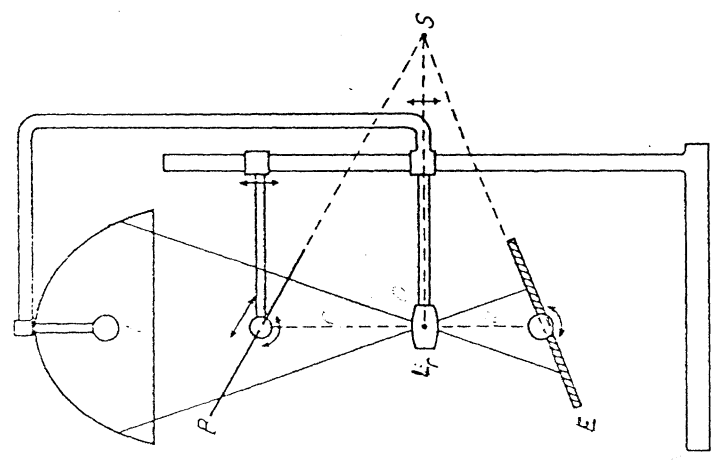


Figure 4-8

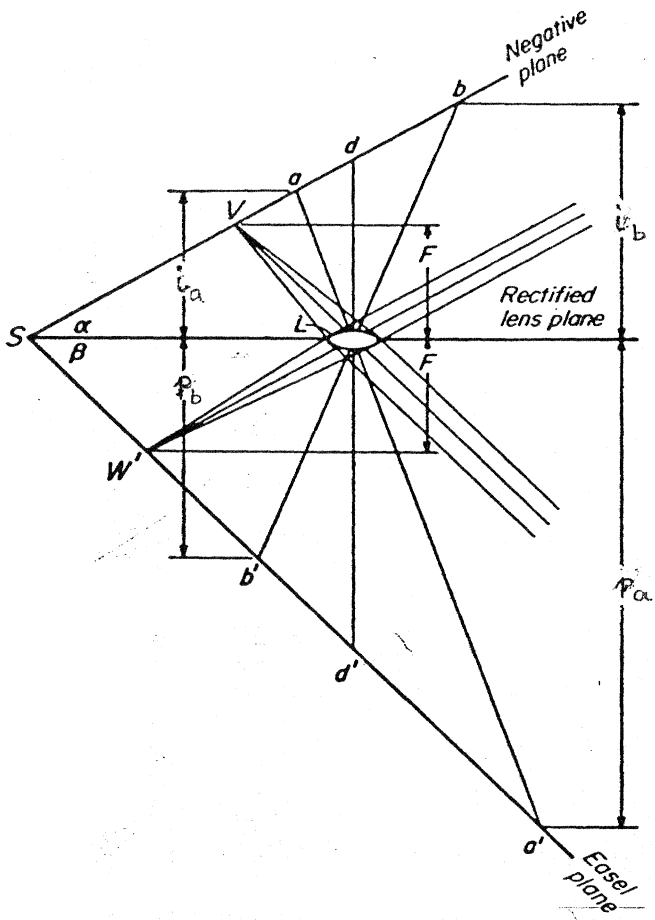


Figure 4-10

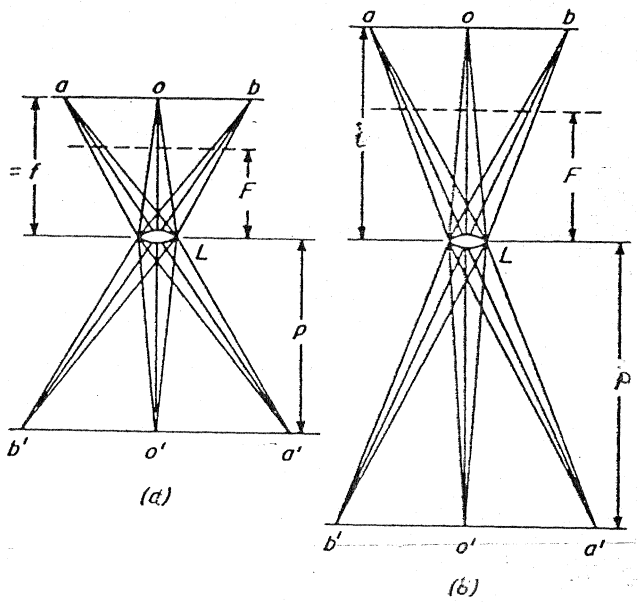


Figure 4-11



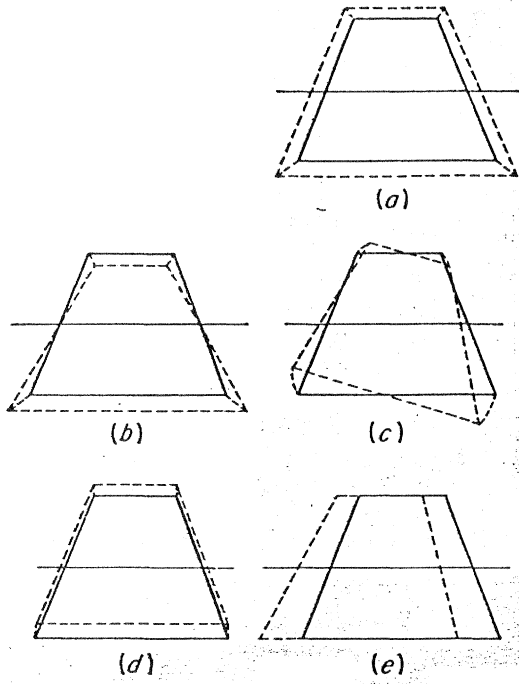


Figure 4-13

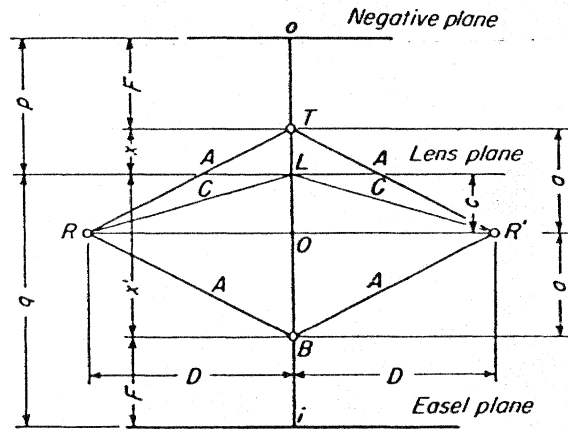


Figure 4-14. Peaucellier inverter.

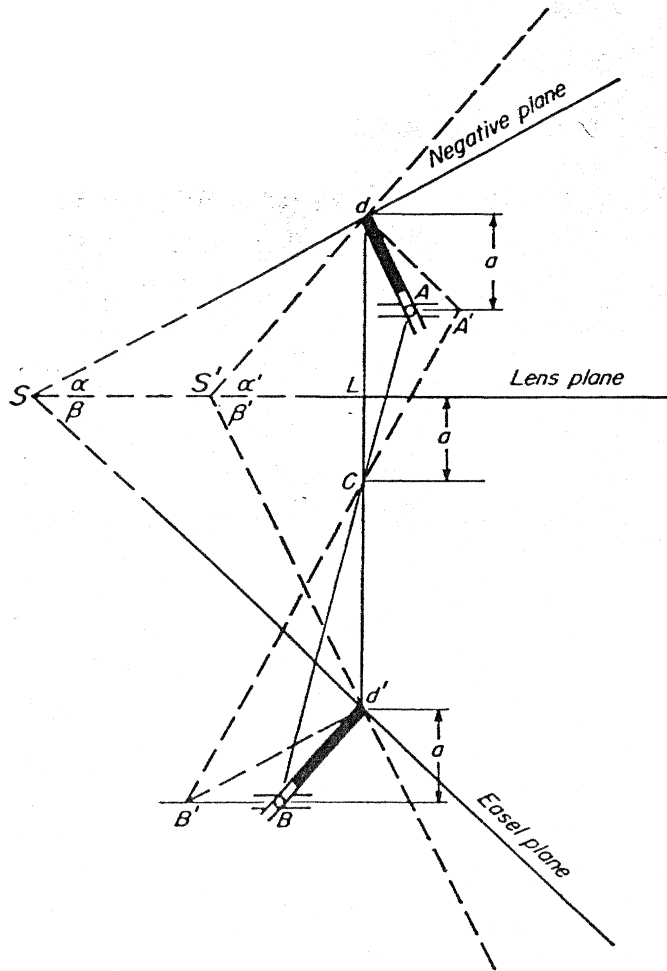


Figure 4-15. Carpentier inverter.

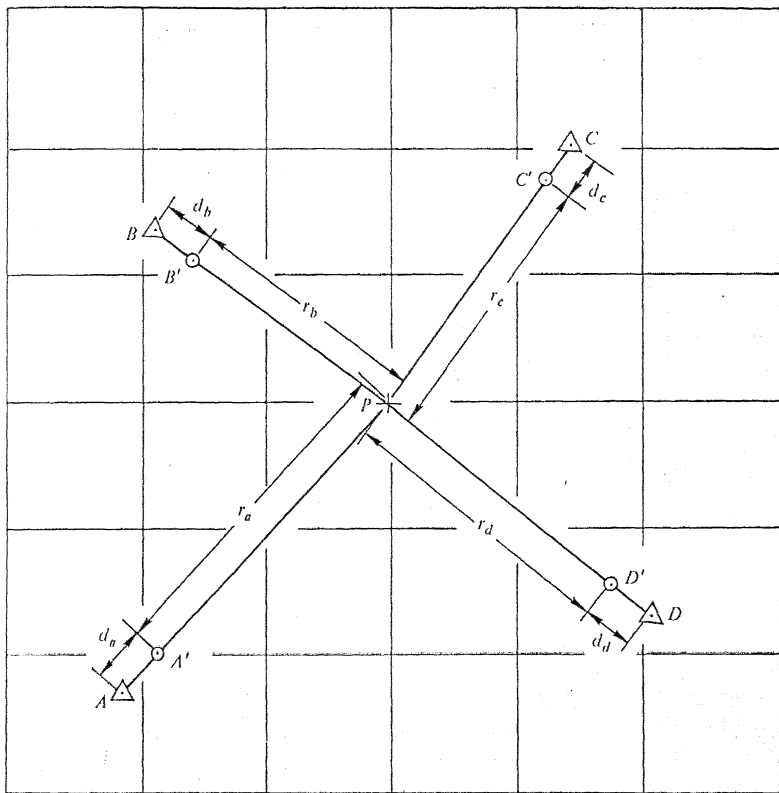


Figure 4-16

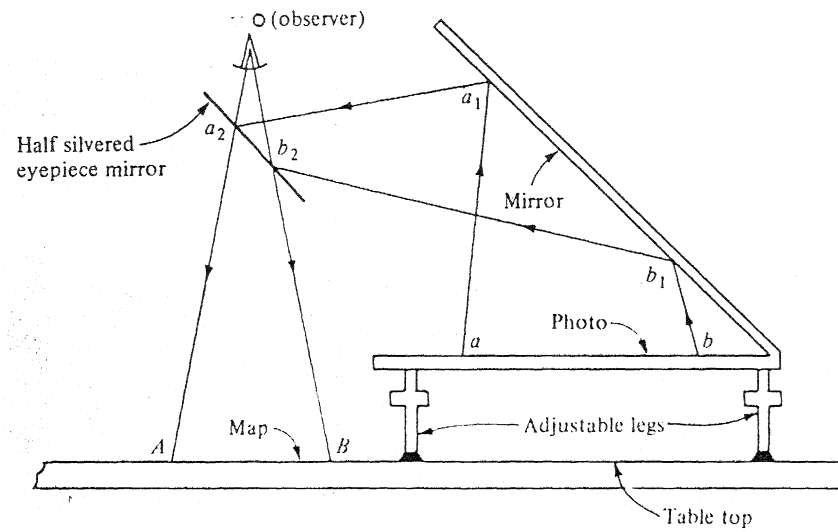


Figure 4-17

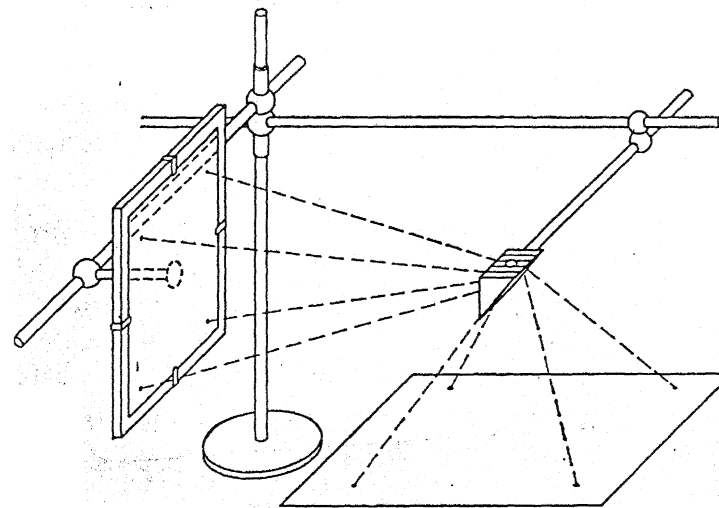


Figure 4-18

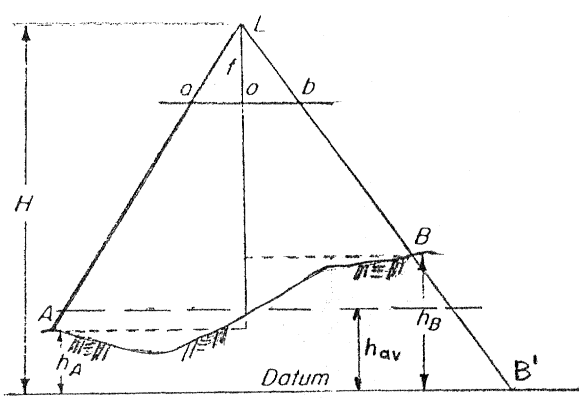


Figure 4-19

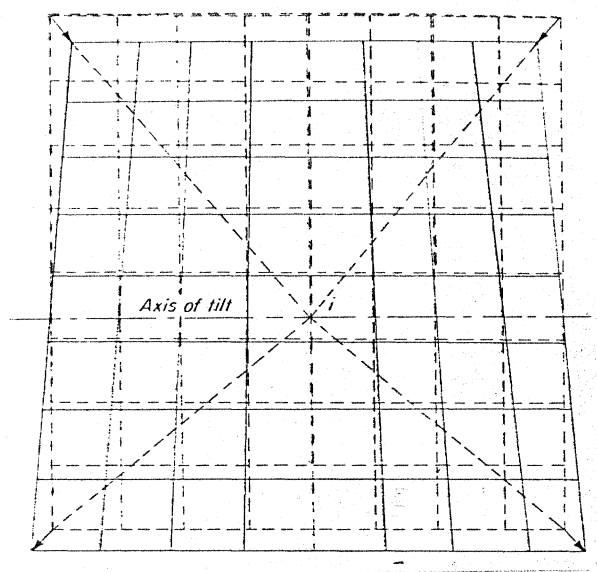


Figure 4-22

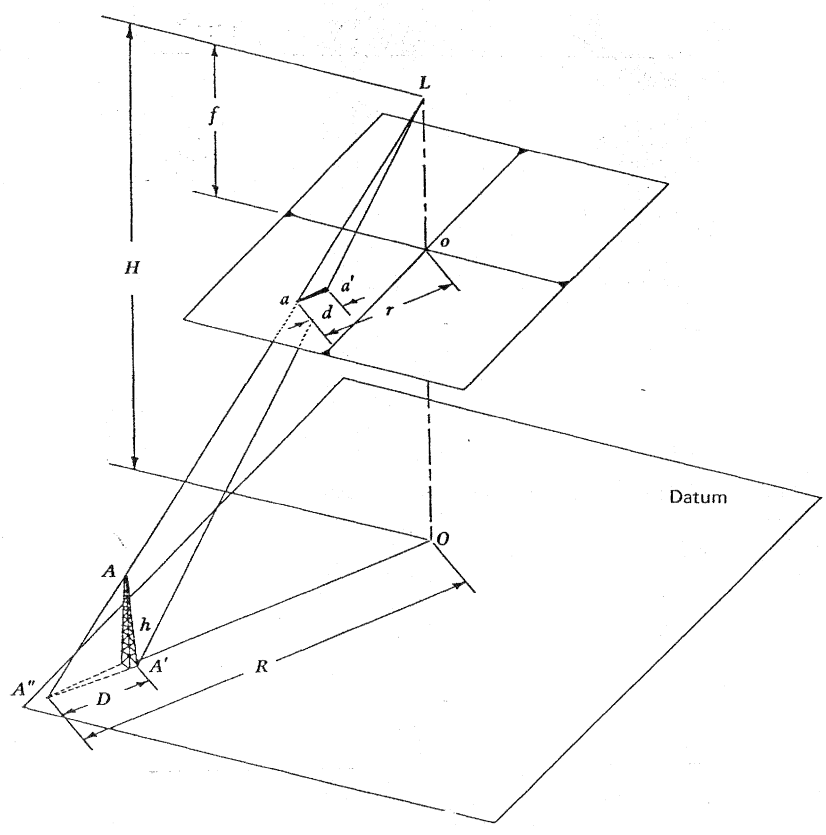


Figure 4-20

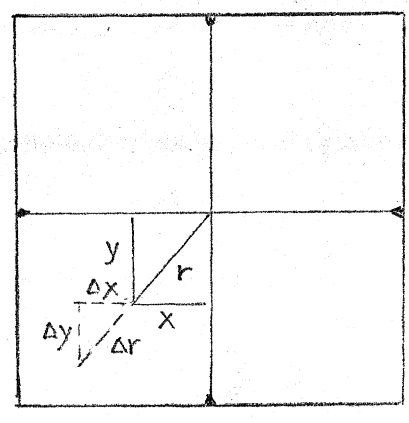


Figure 4-21

## 5. ANALYTICAL SPATIAL POSITIONING

An image is a two-dimensional representation of three-dimensional space. Therefore, a single image is insufficient to reconstruct fully a three-dimensional scene. A single image is only sufficient to recover the direction of a ray that extends from an image point through the perspective centre towards an object point. The length of that ray remains undefined. A single image is analogous to the observation of the direction to a point at only one theodolite station in geodetic surveying. Directions must be observed from at least two stations and determine the position of a point by intersection. In photogrammetry, this means that an object must be imaged from at least two sensor stations in order to determine its spatial position by intersecting collinear rays. This procedure is called *space intersection*.

The two images are referred to as *overlapping images*, *stereo images* or *stereo pairs*. The branch of photogrammetry which deals with obtaining the spatial position of objects from stereo images is called *stereo photogrammetry*.

The idea of spatial positioning based on images is illustrated in Figure 5-1. Object point A is projected onto an image plane through perspective centre (exposure station)  $L_1$  as points  $a_1$  and onto another image plane through  $L_2$  as  $a_2$ . When  $a_1$  and  $a_2$  are reprojected through  $L_1$  and  $L_2$ , the intersection of the two rays will define a point in space. The distance between the two perspective centres or exposure stations is referred to as the *stereo base B*.

### 5.1 Space Intersection

The analytical projective relation that exists between two image spaces and the object space is defined by the collinearity equations as

$$\bar{a}_1 = k_1 M_1 \bar{A}_1 \quad \text{and} \quad \bar{a}_2 = k_2 M_2 \bar{A}_2 \quad (5-1a)$$

The inverse relationship is

$$\bar{A}_1 = \frac{1}{k_1} M_1^T \bar{a}_1 \quad \text{and} \quad \bar{A}_2 = \frac{1}{k_2} M_2^T \bar{a}_2 \quad (5-1b)$$

Based on the reprojection form of the collinearity equation (equation 3-7), equation (5.1b) can be written as:

$$X = X_{L1} + (Z - Z_{L1}) \frac{u_1}{w_1} \quad (5-2a)$$

$$Y = Y_{L1} + (Z - Z_{L1}) \frac{v_1}{w_1} \quad (5-2b)$$

$$X = X_{L2} + (Z - Z_{L2}) \frac{u_2}{w_2} \quad (5-2c)$$

$$Y = Y_{L2} + (Z - Z_{L2}) \frac{v_2}{w_2} \quad (5-2d)$$

There are a total of 25 variables in equations (5-2a) (5-2d). These are: the three elements of the interior orientation and the six elements of exterior orientation of each of the two images, two coordinates of the projected point in each image and the three object space coordinates. If all variables except the three object space coordinates are known, then the three object space coordinates of a point, like A ( $X_A, Y_A, Z_A$ ), can be computed from the above four equations by least squares adjustment. This is space intersection.

A simpler solution can also be obtained by expressing  $Z$  from equations (5-2a) and (5-2c) as

$$Z = \frac{X_{L2}w_1w_2 - Z_{L2}u_2w_1 + Z_{L1}u_1w_2 - X_{L1}w_1w_2}{u_1w_2 - u_2w_1} \quad (5-3)$$

The  $X$  coordinate is then calculated by back substituting  $Z$  into equation (5-2a) or (5-2c). The  $Y$  coordinate can be obtained from either equation (5-2b) or (5-2d). The usual practice is to compute both values and accept the mean of the two as the final  $Y$  coordinate. The difference between the two  $Y$  values is due to observational errors and to the various distortions that affect the imaging process. It is referred to as residual  $Y$ -parallax.

The usual case is, however, that the 22 variables on the right hand side of equations (5-2a-d) must be determined before the space intersection can be performed. Therefore, spatial positioning involves the following steps:

1. The image coordinates of all control and new points are measured in both images, (4 variables per point pair; 2 per image).

2. The interior orientation elements of the two images are obtained from the camera calibration (6 variables; 3 per image) and are applied to the measurements. (It is possible to treat the interior orientation parameters as unknown, but then the solution of spatial positioning becomes more complex).
3. The exterior orientation elements of the two images are determined (12 variables; 6 per image).
5. The unknown object space coordinates are computed by space intersection.

The exterior orientation is determined by one of the following three procedures:

- Sequential space resection of the two images,
- Simultaneous space resection and intersection (Steps 3. and 5. are combined),
- A modular, three-step solution.

## **5.2 Sequential Resection**

The exterior orientation of each of each image is determined by space resection according to equation 3-5. There are a total of twelve unknowns:

in image 1:  $X_{L1}, Y_{L1}, Z_{L1}, \omega_1, \phi_1, \kappa_1$  and

in image 2:  $X_{L2}, Y_{L2}, Z_{L2}, \omega_2, \phi_2, \kappa_2$ .

The two resections are treated independently and a minimum of three ground control points are needed in each image. The control points, however, may be common or partially common. A least squares adjustment is performed if more than the minimum number of control points are available.

Thereafter the spatial position (X, Y, Z) of any new point is determined by space intersection as explained in Section 5.1. Figure 5-2 illustrates the geometry where  $P_1$  to  $P_4$  and control points are  $P_5, P_6$  are new points.

## **5.3 Simultaneous Resection**

In this procedure the exterior orientation of the two images in a stereopair are determined by a simultaneous least squares solution. The computation of the object space coordinates of new points is also included, whereby this procedure is a combined space resection and intersection. The solution is based on the collinearity condition. Each ray provides a pair of observation equations in the form of equation (3-5). The equations of

each ray associated with a control point contain six unknowns, which are the exterior orientation elements. A ray of a new point includes nine unknowns, the six exterior orientation elements, and the three object space coordinates of that point. Therefore, the total number of unknowns in a stereopair is equal to:  $12 + 3n$ , where  $n$  is the number of new points. Although, each new point introduces three new unknowns, it also provides four new observation equations. Therefore, the inclusion of new points in a simultaneous solution increases the redundancy. The mechanics of the least squares solutions will be discussed later.

#### **5.4 Three-Step Solution**

This is a modular solution of the exterior orientation elements. In the first step, each corresponding image ray is directed towards a common point in space, which represents the object point. This operation is performed in a assumed coordinate system. It essentially means the orientation of two bundles of rays in space with respect to each other so that all corresponding rays will intersect in space, when extended. This step is therefore called *relative orientation*.

In the second step, the relatively oriented bundles of rays are extended until they intersect in space. The point of intersection in space formed by two corresponding rays is called *model point* and the three-dimensional space in which these points are located is referred to as *model space*. The collection of the model points forms a *stereoscopic model* or *stereomodel*, which is a replica of the object at a reduced scale. This step is the *model formation*.

In the third and final step, the model is positioned, oriented, and scaled to fit the object in the object space coordinate system and is called *absolute orientation*. Each step is now discussed in detail.

##### **5.5.1 Relative orientation**

A corresponding point in a pair of overlapping images is formed by projecting the same object point through two perspective centres onto the two image planes. This in fact means that the two corresponding image and object vectors lie in one plane; they are *coplanar*. Relative orientation can therefore be achieved by enforcing the coplanarity of corresponding image vectors.

The geometry of two overlapping photographs is illustrated in Figure 5-1. Here,  $\bar{A}_1$  or  $L_1A$  and  $\bar{A}_2$  or  $L_2A$  are the two corresponding object space vectors associated with object point A;  $\bar{a}_1$  or  $L_1a_1$  and  $\bar{a}_2$  or  $L_2a_2$  are the two image vectors associated with the same object point, while  $\bar{B} = L_1L_2$  is the base vector. These vectors must all be coplanar. The plane which contains the base vector and a pair of image vectors is called the *epipolar plane*.

In order to arrive at a mathematical expression which enforces the collinearity of the two image vectors, it is first proven that the scalar triple product of three vectors ( $\bar{A}$ ,  $\bar{B}$  and  $\bar{C}$  in Figure 5-3) is the volume of a *parallelepiped*, in which  $|\bar{A}|$ ,  $|\bar{B}|$  and  $|\bar{C}|$  form adjacent corners. The triple product is written as

$$\bar{A} \cdot (\bar{B} \times \bar{C}).$$

The magnitude of the cross product is

$$|\bar{B} \times \bar{C}| = |\bar{B}| \cdot |\bar{C}| \sin \theta$$

which gives the area of the base parallelogram. The cross product itself is a vector which is perpendicular to the base parallelogram and is represented by unit vector  $\upsilon$ .

The dot or scalar product is

$$\bar{A} \cdot (\bar{B} \times \bar{C}) = |\bar{A}| (|\bar{B}| \cdot |\bar{C}| \sin \theta) \cos \phi.$$

However,  $|\bar{A}| \cos \phi$  is the height of the parallelepiped. Thus  $\bar{A} \cdot (\bar{B} \times \bar{C})$  represents the area of the base parallelogram of the parallelepiped multiplied by its height, which gives the volume.

The scalar triple product written in an expanded form is

$$\bar{A} \cdot (\bar{B} \times \bar{C}) = (B_y C_z - B_z C_y) A_x + (B_z C_x - B_x C_z) A_y + (B_x C_y - B_y C_x) A_z,$$

which can be written in a determinant form as

$$\bar{A} \cdot (\bar{B} \times \bar{C}) = \begin{vmatrix} A_x & A_y & A_z \\ B_x & B_y & B_z \\ C_x & C_y & C_z \end{vmatrix}. \quad (5-4)$$

If the three vectors are coplanar then the volume of the parallelepiped becomes zero, which means that their scalar triple product, shown in equation (5-4), is equal to zero. By applying this theory to the vectors of two overlapping images, the mathematical condition of coplanarity of two corresponding image vectors is expressed as

$$\bar{\mathbf{B}} \cdot (\bar{\mathbf{a}}_1 \times \bar{\mathbf{a}}_2) = 0. \quad (5-5)$$

The three vectors must be related to a common coordinate system. If the object space coordinate system is chosen for this purpose then the components of the stereo base  $\bar{\mathbf{B}}$  become

$$\bar{\mathbf{B}} = \begin{pmatrix} X_{L2} - X_{L1} \\ Y_{L2} - Y_{L1} \\ Z_{L2} - Z_{L1} \end{pmatrix} = \begin{pmatrix} B_x \\ B_y \\ B_z \end{pmatrix}$$

which are the components of the stereo base. The components of the two image vectors in the object space coordinate system are

$$\bar{\mathbf{a}}_1 = M_1^T \begin{pmatrix} x_1 - x_{01} \\ y_1 - y_{01} \\ -f_1 \end{pmatrix} = \begin{pmatrix} u_1 \\ v_1 \\ w_1 \end{pmatrix}$$

and

$$\bar{\mathbf{a}}_2 = M_2^T \begin{pmatrix} x_2 - x_{02} \\ y_2 - y_{02} \\ -f_2 \end{pmatrix} = \begin{pmatrix} u_2 \\ v_2 \\ w_2 \end{pmatrix}$$

where, in most cases  $f_1 = f_2 = f$ .

According to equation (5-4), the coplanarity of the base vector and the two image vectors is satisfied if

$$\begin{vmatrix} B_x & B_y & B_z \\ u_1 & v_1 & w_1 \\ u_2 & v_2 & w_2 \end{vmatrix} = 0 \quad (5-6)$$

Equation (5-6) is commonly known as the *coplanarity condition equation*. Equation (5-6) can be rearranged by expanding the determinant as

$$(v_1 B_z - w_1 B_y)u_2 - (u_1 B_z - w_1 B_x)v_2 + (u_1 B_y - v_1 B_x)w_2 = 0,$$

or written in matrix form,

$$(v_1 B_z - w_1 B_y \quad -u_1 B_z + w_1 B_x \quad +u_1 B_y - v_1 B_x) \begin{pmatrix} u_2 \\ v_2 \\ w_2 \end{pmatrix} = 0$$

and finally

$$(u_1 \ v_1 \ w_1) \begin{pmatrix} 0 & -B_z & B_y \\ B_z & 0 & -B_x \\ -B_y & B_x & 0 \end{pmatrix} \begin{pmatrix} u_2 \\ v_2 \\ w_2 \end{pmatrix} = 0. \quad (5-7)$$

By a substitution of the image coordinates of the two corresponding points reduced to the principal point as the origin, the coplanarity equation becomes

$$(x_1 \ y_1 \ -f) M_1 \begin{pmatrix} 0 & -B_z & B_y \\ B_z & 0 & -B_x \\ -B_y & B_x & 0 \end{pmatrix} M_2^T \begin{pmatrix} x_2 \\ y_2 \\ -f \end{pmatrix} = 0 \quad (5-8)$$

There are twelve unknown parameters in this equation, which are the six exterior orientation elements of the two images,

$$X_{L1}, Y_{L1}, Z_{L1}, \omega_1, \phi_1, \kappa_1, X_{L2}, Y_{L2}, Z_{L2}, \omega_2, \phi_2, \kappa_2.$$

For the purpose of relative orientation, however, it is sufficient to enforce the coplanarity of corresponding image vectors in an arbitrary coordinate system and to use an arbitrary scale, rather than working in the object space system. There are two commonly used schemes for selecting an arbitrary coordinate system and scale.

In Scheme 1, the image space coordinate system of one of the two images (say that of Image 1) is adopted as a provisional coordinate system. The X-component of the stereo base ( $B_x$ ) is assumed to have unit length, or some other preset value. It is advantageous to set  $B_x$  equal to the photo base ( $b$ ), whereby the scale of the base components and of the model coordinates will be similar to the scale of the image. Therefore, the coordinates of projection centre  $L_1$  become zero, matrix  $M_1$  reduces to a unit matrix and all coordinates in

Image 1 remain unchanged. The twelve elements of exterior orientation are now reduced to five independent differential elements. Differential means that the values of the orientation elements are not referenced to a fixed, exterior coordinate system but are only the differences in the exterior orientation of the two images. The coplanarity condition now becomes

$$\begin{vmatrix} 1 & by & bz \\ x_1 & y_1 & -f \\ u_2 & v_2 & w_2 \end{vmatrix} = 0 \quad (5-9)$$

or based on equation (5-8)

$$(x_1 \ y_1 \ -f) \begin{pmatrix} 0 & -bz & by \\ bz & 0 & -1 \\ -by & 1 & 0 \end{pmatrix} M_2^T \begin{pmatrix} x_2 \\ y_2 \\ -f \end{pmatrix} = 0. \quad (5-10)$$

The five unknowns are  $by$ ,  $bz$ ,  $d\omega_2$ ,  $d\phi_2$  and  $d\kappa_2$ , which define the position of projection centre  $L_2$  in relation to  $L_1$  and the orientation of the coordinate system of Image 2 with respect to the coordinate system of Image 1. This is the so-called *dependent pair* relative orientation. The orientation is performed by shifting and rotating Image 2 with respect to Image 1, which remains unchanged.

In Scheme 2, the origin of the provisional coordinate system is at  $L_1$ , the  $x$  axis is chosen to coincide with the base, whereby the  $y$  and  $z$  components of the base become zero. Again, the stereo base ( $B=B_x$ ) is assumed to have unit length or some other preset value. The orientation is performed by rotating both images. The coplanarity condition now becomes

$$\begin{vmatrix} 1 & 0 & 0 \\ u_1 & v_1 & w_1 \\ u_2 & v_2 & w_2 \end{vmatrix} = 0 \quad (5-11)$$

or according to equation (5-8)

$$(x_1 \ y_1 \ -f) M_1 \begin{pmatrix} 0 & 0 & 0 \\ 0 & 0 & -1 \\ 0 & 1 & 0 \end{pmatrix} M_2^T \begin{pmatrix} x_2 \\ y_2 \\ -f \end{pmatrix} = 0. \quad (5-12)$$

In this case the five unknowns are  $d\phi_1$ ,  $d\phi_2$ ,  $d\kappa_1$ ,  $d\kappa_2$  and  $d\omega_1$  or  $d\omega_2$ . The two omegas are not independent and only one of the two can be included in a particular solution. This is the so-called *independent pair method*.

Various other schemes can be devised which are variations of the previous two. It must be assured, however, that the five unknowns selected for the orientation are independent.

Each pair of corresponding rays gives one condition equation. Thus a minimum of five ray pairs, or corresponding image points, are required to solve for the five unknowns of relative orientation.

### **5.5.2 Model formation**

In this step the intersection of the coplanar corresponding rays are formed and the coordinates of the intersection points is computed in the arbitrary coordinate system. This is a space intersection operation which can be solved as explained in Section 5.1. The scale of the model is a function of the length assumed for  $b_x$ . It can be unity such as in equations (5-10) and (5-12), or some other value. For example, if  $b_x$  is set equal to the photo base (the distance between the principal and the corresponding principal points on the same image), then the scale of the model and that of the base components will approximately be equal to the scale of the image.

### **5.5.3 Absolute orientation**

After the relative orientation is accomplished, the stereo model must be scaled, translated and oriented with respect to the object space coordinate system (Figure 5-4). Mathematically, this operation is achieved by a seven parameter, three-dimensional similarity transformation of the model coordinates according to equation (2-33). This equation, when rewritten specifically for absolute orientation, becomes

$$\begin{pmatrix} X_G \\ Y_G \\ Z_G \end{pmatrix} = S M \begin{pmatrix} X_m \\ Y_m \\ Z_m \end{pmatrix} + \begin{pmatrix} X_T \\ Y_T \\ Z_T \end{pmatrix} \quad (5-12)$$

where  $X_G, Y_G, Z_G$  are the object space coordinates,  
 $X_m, Y_m, Z_m$  are model space coordinates,  
 $X_T, Y_T, Z_T$  are translation constants which define the object space coordinates of the origin of the model coordinate system,  
 $S$  is the scale change from model space to object space, and  
 $M$  is a three-dimensional orthogonal rotation matrix which defines the orientation of the model coordinate system with respect to the object space system. It is formed in as described in Section 2.3.1.

In this case the three rotations are denoted as common omega ( $\Omega$ ), which is the rotation around the X model axis, common phi ( $\Phi$ ) the rotation around the Y axis and common kappa ( $K$ ) the rotation around the model Z axis. The name "common" and the capital Greek letters indicate that the two projection systems (images) which form the stereo model are rotating simultaneously in the same direction and by the same amount, thus resulting in the rotation of the model. The lower case Greek letters  $\omega, \phi, \kappa$  designate the rotations of individual projection systems or images.

The expanded form of equation (5-12) yields three independent equations, such as:

$$\begin{aligned} X_G - S (m_{11}X_m + m_{12}Y_m + m_{13}Z_m) - X_T &= 0 \\ Y_G - S (m_{21}X_m + m_{22}Y_m + m_{23}Z_m) - Y_T &= 0 \\ Z_G - S (m_{31}X_m + m_{32}Y_m + m_{33}Z_m) - Z_T &= 0 \end{aligned} \quad (5-13)$$

There are a total of seven transformation elements in equation (5-12) and (5-13): a scale factor ( $S$ ), three translation constants ( $X_T, Y_T, Z_T$ ) and the three rotation angles ( $\Omega, \Phi, K$ ). Each coordinate of a point which is known in both the object space and model space, yields one of the equations in (5-13). Thus, the minimum control point data needed to perform an absolute orientation are:

- two control points with known X, Y coordinates (horizontal control points) and
- three control points with known Z coordinates (vertical control points).

The same point can serve as horizontal and vertical control point if all three of its coordinates are known.

### **5.5 Approximate Solution of Relative Orientation**

Rays, which reproject two corresponding image points through their respective perspective centres onto a horizontal plane will intersect on that plane only in the event that the two projection systems (images) are correctly oriented with respect to each other and when the projection plane is set at the correct distance from the perspective centres. If these conditions are not met, then two distinct points will appear on the projection plane. The separation between the two points is called *parallax* (Figure 5-6).

A more comprehensive definition of parallax is: the change in the direction in which an object is seen or imaged caused by a change in the position of the observer or the sensor. According to this definition, the primary measure of the parallax is an angle. It is the *parallactic angle*, which is the angle formed by the two viewing or imaging rays at the object viewed or imaged and subtended by the line connecting the two observation or imaging stations (stereo base). In Figure 5-5,  $\gamma_a$  and  $\gamma_b$  are parallactic angles. For a given base length, the magnitude of the parallactic angle varies inversely as a function of the distance from the base to the object. The closer the object is to the base the larger the parallactic angle becomes and vice versa. In fact, this change in the size of the parallactic angle forms the basis of stereoscopic depth perception.

A visualization of the parallax in linear sense occurs when the viewing or imaging rays are intersected by a projection plane, as seen in Figure 5-6. In this figure the separation between the two corresponding points A' and A'' on the projection plane is the *total parallax* ( $p$ ).

The separation between corresponding projected points measured in the direction parallel to the base is the x-component of the parallax or x-parallax ( $px$ ). The separation in the direction perpendicular to the base is the y-component or y-parallax ( $py$ ). The magnitude of  $px$  is directly proportional to the size of the parallactic angle and is utilized for the determination of the third dimension in space. This component can be eliminated by changing the distance of the projection plane from the projection centres. The y-parallax, on the other hand, is the consequence of incorrect mutual orientation of the two projection systems. It means that the corresponding rays are not coplanar; they bypass each other. Therefore, the elimination of the y-parallax is also a condition of relative orientation.

The parallax of an object or model point such as of A in Figures 5-5 and 5-6 with corresponding image points a' and a'' is expressed in terms of image coordinates as:

$$p_x = x'_a - x''_a$$

$$p_y = y'_a - y''_a$$

or in terms of the coordinates in the projection plane

$$pX = X'_A - X''_A \quad \text{and} \quad pY = Y'_A - Y''_A \quad .$$

The prime and double prime signify Image 1 (left image) and Image 2 (right image) of the stereoscopic pair.

Differences in the Y coordinate of corresponding points are caused by small changes in the exterior orientation from one images to the other. Therefore, the y-parallax can be expressed by the differential formulae (equation 3-15) as

$$\begin{aligned} pY = dY' - dY'' = & dBY' + \frac{Y}{Z} dBZ' + (Z + \frac{Y^2}{Z})d\omega' - \frac{XY}{Z} d\phi' + Xd\kappa' \\ & - dBY'' - \frac{Y}{Z} dBZ'' - (Z + \frac{Y^2}{Z})d\omega'' + \frac{(X-B)Y}{Z} d\phi'' - (X-B)d\kappa'' \end{aligned} \quad (5-16)$$

This equation has been set up with the understanding that the Y coordinates of the corresponding points on the projection plane are approximately the same and that the X coordinate of the point projected through the right perspective centre ( $L_2$ ) is  $(X-B)$ . Equation (5-16) is called the *y-parallax equation*.

If the y-parallax and the coordinates of sufficient number of points are measured or known, then the orientation elements can be computed from equation (5-14). There are a total of ten elements in this equation. However, relative orientation is defined by five independent orientation elements, as explained in section 5.5.1.

The y-parallax equations of  $i$  number of image points is shown by the following equation .



By including only one from each of the three correlated pairs of unknowns, the number of orientation elements is reduced from ten to seven. If  $dBY'$ ,  $dBZ'$  and  $d\omega'$  are selected, the y-parallax equation becomes as shown in equation 5-18.

$$\begin{array}{c}
 \left[ \begin{array}{c} pY_1 \\ pY_2 \\ \cdot \\ \cdot \\ \cdot \\ \cdot \\ pY_i \end{array} \right] = \begin{array}{c} \begin{array}{ccccccc} (1) & (2) & (3) & (4) & (5) & (6) & (7) \\ 1 & \frac{Y_1}{Z_1} & X_1 & -(X_1-B) & -\frac{X_1 Y_1}{Z_1} & \frac{(X_1-B) Y_1}{Z_1} & \frac{Y_1^2}{Z_1} + Z_1 \\ 1 & \frac{Y_2}{Z_2} & X_2 & -(X_2-B) & -\frac{X_2 Y_2}{Z_2} & \frac{(X_2-B) Y_2}{Z_2} & \frac{Y_2^2}{Z_2} + Z_2 \\ \cdot & \cdot & \cdot & \cdot & \cdot & \cdot & \cdot \\ \cdot & \cdot & \cdot & \cdot & \cdot & \cdot & \cdot \\ \cdot & \cdot & \cdot & \cdot & \cdot & \cdot & \cdot \\ 1 & \frac{Y_i}{Z_i} & X_i & -(X_i-B) & -\frac{X_i Y_i}{Z_i} & \frac{(X_i-B) Y_i}{Z_i} & \frac{Y_i^2}{Z_i} + Z_i \end{array} \\ \left[ \begin{array}{c} dBY' \\ dBZ' \\ d\kappa' \\ d\kappa'' \\ d\phi' \\ d\phi'' \\ d\omega' \end{array} \right]
 \end{array}
 \end{array} \quad (5-18)$$

Equation system (5-18) is still correlated since there is a relationship between columns (2), (5) and (6) as follows:

$$\text{column (2)} = -\frac{1}{B} [\text{column (5)} + \text{column (6)}].$$

This indicates a correlation between  $dBZ'$ ,  $\phi'$  and  $\phi''$  and only two of these three unknowns can be included in a particular solution. Columns (1), (3) and (4) are also interdependent since

$$\text{column (1)} = \frac{1}{B} [\text{column (3)} + \text{column (4)}].$$

This means that  $dBY'$ ,  $\kappa'$  and  $\kappa''$  are also correlated.

By selecting  $\phi'$ ,  $\phi''$ ,  $\kappa'$  and  $\kappa''$ , the number of unknowns is reduced to five rotations as shown in equation (5-17).

$$\begin{bmatrix} pY_1 \\ pY_2 \\ \cdot \\ \cdot \\ pY_i \end{bmatrix} = \begin{bmatrix} X_1 & -(X_1-B) & -\frac{X_1 Y_1}{Z_1} & \frac{(X_1-B)}{Z_1} Y_1 & \frac{Y_1^2}{Z_1} + Z_1 \\ X_2 & -(X_2-B) & -\frac{X_2 Y_2}{Z_2} & \frac{(X_2-B)}{Z_2} Y_2 & \frac{Y_2^2}{Z_2} + Z_2 \\ \cdot & \cdot & \cdot & \cdot & \cdot \\ \cdot & \cdot & \cdot & \cdot & \cdot \\ X_i & -(X_i-B) & -\frac{X_i Y_i}{Z_i} & \frac{(X_i-B)}{Z_i} Y_i & \frac{Y_i^2}{Z_i} + Z_i \end{bmatrix} \begin{bmatrix} d\kappa' \\ d\kappa'' \\ d\phi' \\ d\phi'' \\ d\omega' \end{bmatrix} \quad (5-19)$$

These are the five elements of the independent pair method of relative orientation. A similar equation system can be set up for the dependent pair method by selecting  $dBY''$ ,  $dBZ''$ ,  $d\kappa''$ ,  $d\phi''$  and  $d\omega''$ .

The computation can be simplified if the y-parallax is measured at six symmetrically distributed points, as shown in Figure 5-7 and if changes in the third dimension of the object are fairly small (moderate topography). In this figure, Point 1 is the projection of the principal point of the left-hand image, while Point 2 is the projection of the principal point of the right-hand image. Points 3, 4, 5 and 6 are at equidistant from points 1 and 2 in Y direction and are spaced at the same distance apart in X direction as points 1 and 2. Thus the six points form a grid pattern. Distances 1-3, 1-5, 2-4 and 2-6 are denoted as D and by definition the distances between 1-2, 3-4, and 5-6 are equal to the base B. Furthermore the Z coordinate of all points is assumed to be approximately equal, and the subscript is dropped. Therefore the coordinates of the six orientation points are:

Point	X	Y	Z
1	0	0	Z
2	B	0	Z
3	0	D	Z
4	B	D	Z
5	0	-D	Z
6	B	-D	Z

A substitution of these values into equation 5-19 yields the y-parallax equations of the six reallive orientation points as follows:

$pY_1$		0	B	0	0	Z	$d\kappa'$	
$pY_2$		B	0	0	0	Z	$d\kappa''$	
$pY_3$		0	B	0	$-\frac{BD}{Z}$	$(Z+\frac{D^2}{Z})$	$d\phi'$	
$pY_4$	=	B	0	$-\frac{BD}{Z}$	0	$(Z+\frac{D^2}{Z})$	$d\phi''$	..(5-20)
$pY_5$		0	B	0	$\frac{BD}{Z}$	$(Z+\frac{D^2}{Z})$	$d\omega'$	
$pY_6$		B	0	$\frac{BD}{Z}$	0	$(Z+\frac{D^2}{Z})$		
observations		coefficient matrix					unknowns	

The solution of equation (5-18) provides the following general expressions for the computation of the five independent pair relative orientation elements:

$$\begin{aligned}
d\omega' &= \frac{Z}{4D^2} (-2pY_1 - 2pY_2 + pY_3 + pY_4 + pY_5 + pY_6) \\
d\phi' &= \frac{Z}{2BD} (pY_6 - pY_4) \\
d\kappa' &= \frac{1}{3B} [pY_2 + pY_4 + pY_6 - (3Z + \frac{2D^2}{Z}) d\omega'] \\
d\phi'' &= \frac{Z}{2BD} (pY_5 - pY_3) \\
d\kappa'' &= \frac{1}{3B} [pY_1 + pY_3 + pY_5 - (3Z + \frac{2D^2}{Z}) d\omega']
\end{aligned} \tag{5-21}$$

Similarly, the five orientation elements of the dependent pair case can be obtained as follows, when Image 2 (the right image) is oriented to Image 1 (the left image):

$$\begin{aligned}
dB\gamma'' &= \frac{1}{3} (-pY_2 - pY_4 - pY_6) - (Z + \frac{2D^2}{3Z}) d\omega'' \\
dBZ'' &= \frac{Z}{2D} (-pY_4 + pY_6) \\
d\omega'' &= \frac{Z}{4D^2} (2pY_1 + 2pY_2 - pY_3 - pY_4 - pY_5 - pY_6) \\
d\phi'' &= \frac{Z}{2BD} (-pY_3 + pY_4 + pY_5 - pY_6) \\
d\kappa'' &= \frac{1}{3B} (pY_1 - pY_2 + pY_3 - pY_4 + pY_5 - pY_6)
\end{aligned} \tag{5-22}$$

The solution for orienting the left image to the right one is the same as above but with opposite algebraic signs for the parallaxes.

Equations (5-21) and (5-22) can be used for numerical relative orientation in stereoscopic plotting instruments.

### 5.8 Sequential Solution of Absolute Orientation

In this method the seven parameters of absolute orientation are determined in three steps. The advantage is that it leads to a direct solution without iteration.

In the **first step**, the scale of the stereomodel is determined by comparing corresponding distances between control points. Thus

$$SF = \frac{1}{n} \sum_{i=1}^{i=n} \frac{D_i}{d_i} \quad (5-23)$$

where SF is the scale factor of the model, n is the number of distances used,  $D_i$  is a distance in object space and  $d_i$  is the corresponding distance in model space. Thereafter all model coordinates are multiplied by SF to change them to the scale of the object, so that

$$\begin{pmatrix} X \\ Y \\ Z \end{pmatrix}_{sm} = SF \begin{pmatrix} X \\ Y \\ Z \end{pmatrix}_m \quad (5-24)$$

where m and sm signify the original and scaled model coordinates respectively.

In the **second step**, the model and object space coordinates are referenced to a common origin by subtracting in each system, the coordinates of one of the control points from the coordinates of all other points, whereby

$$\begin{pmatrix} X \\ Y \\ Z \end{pmatrix}_{tsm} = \begin{pmatrix} X \\ Y \\ Z \end{pmatrix}_{sm} - \begin{pmatrix} X \\ Y \\ Z \end{pmatrix}_t \quad (5-25)$$

and

$$\begin{pmatrix} X \\ Y \\ Z \end{pmatrix}_{TG} = \begin{pmatrix} X \\ Y \\ Z \end{pmatrix}_G - \begin{pmatrix} X \\ Y \\ Z \end{pmatrix}_T \quad (5-26)$$

where tsm denotes the translated and scaled model coordinates; G and TG signify the original and translated ground coordinates, while t and T indicate the point selected as the translation constants in the model and ground systems respectively.

In the **third** step, the model coordinate system is rotated parallel to the object space system so that

$$\begin{pmatrix} X \\ Y \\ Z \end{pmatrix}_{\text{rtsm}} = M \begin{pmatrix} X \\ Y \\ Z \end{pmatrix}_{\text{tsm}} \quad (5-27)$$

where rtsm designates coordinates in the shifted object space system (TG system).

The rotation matrix is formed according to the parameter form as derived in section 2.3.3.

$$M = (I-S)^{-1} (I+S) \quad (5-28)$$

where S is a skew symmetric matrix. A substitution into equation (5-27) gives

$$\begin{pmatrix} X \\ Y \\ Z \end{pmatrix}_{\text{rtsm}} = (I-S)^{-1} (I+S) \begin{pmatrix} X \\ Y \\ Z \end{pmatrix}_{\text{tsm}}$$

A pre-multiplication of both sides by (I-S) gives:

$$(I-S) \begin{pmatrix} X \\ Y \\ Z \end{pmatrix}_{\text{rtsm}} = (I+S) \begin{pmatrix} X \\ Y \\ Z \end{pmatrix}_{\text{tsm}}$$

If S is defined as

$$S = \frac{1}{2} \begin{pmatrix} 0 & -c & b \\ c & 0 & -a \\ -b & a & 0 \end{pmatrix}$$

then equation (5-2) becomes:

$$\frac{1}{2} \begin{pmatrix} 2 & c & -b \\ -c & 2 & a \\ b & -a & 2 \end{pmatrix} \begin{pmatrix} X \\ Y \\ Z \end{pmatrix}_{\text{rtsm}} = \frac{1}{2} \begin{pmatrix} 2 & -c & b \\ c & 2 & -a \\ -b & a & 2 \end{pmatrix} \begin{pmatrix} X \\ Y \\ Z \end{pmatrix}_{\text{tsm}}$$

After performing the multiplication, the results are

$$\begin{pmatrix} 2X & +Yc & -Zb \\ -Xc & +2Y & +Za \\ Xb & -Ya & +2Z \end{pmatrix}_{\text{rtsm}} = \begin{pmatrix} 2X & -Yc & +Zb \\ Xc & +2Y & -Za \\ -Xb & +Ya & +2Z \end{pmatrix}_{\text{tsm}}$$

which can be decomposed into the following three equations:

$$\begin{aligned} -(Z_{G'} + Z_{m'}) b + (Y_{G'} + Y_{m'}) c &= 2 (X_{m'} - X_{G'}) \\ (Z_{G'} + Z_{m'}) a - (X_{G'} + X_{m'}) c &= 2 (Y_{m'} - Y_{G'}) \\ -(Y_{G'} + Y_{m'}) a + (X_{G'} + X_{m'}) b &= 2 (Z_{m'} - Z_{G'}) \end{aligned} \quad (5-29)$$

where  $G'$  indicates coordinates in the shifted object space system (TG or rtsm system) and  $m'$  signifies the coordinates in the shifted and scaled model system (tsm system). The solution of the above linear equations yields the three transformation parameters  $a$ ,  $b$  and  $c$ . A rotation matrix is then formed according to equation (5-12) and (2-27) and the object space coordinates of all new model points are computed by the transformation equation

$$\begin{pmatrix} X \\ Y \\ Z \end{pmatrix}_G = M \begin{pmatrix} X \\ Y \\ Z \end{pmatrix}_{\text{tsm}} + \begin{pmatrix} X \\ Y \\ Z \end{pmatrix}_T \quad (5-30)$$

Each point with known  $X_G$ ,  $Y_G$ ,  $Z_G$  and  $X_m$ ,  $Y_m$ ,  $Z_m$  coordinates yields a set of three equations as listed in equation (5-13). It appears therefore, that a single control point is sufficient to solve for the three rotation parameters. In doing so, however, the coefficient matrix becomes singular. Furthermore at least two, but preferably more of the equations should be set up for the  $Z$  coordinate, since the rotation parameters actually define the orientation of a plane in space.

## 5.8 Approximate Spatial Positioning

It is assumed that both the left and right photographs are truly vertical, have the same flying height and that the  $x$  and  $y$  axis on both photos are parallel to the  $X$  and  $Y$  ground coordinate axes, and that the fiducial centre and the principal point coincide. (Figure 5-8) This means that:

$$X_{L2} = X_{L1} + B = X_L + B, \quad Y_{L1} = Y_{L2} = Y_L, \quad Z_{L1} = Z_{L2} = Z_L$$

where  $B$  is the air base.

Based on equation system (5-2) the  $X$  and  $Y$  ground coordinates are computed as :

$$X = X_L + (Z - Z_L) \frac{x'}{-f} \quad (5-31a)$$

$$Y = Y_L + (Z - Z_L) \frac{y'}{-f} \quad (5-31b)$$

$$X = X_L + B + (Z - Z_L) \frac{x''}{-f} \quad (5-31c)$$

$$Y = Y_L + (Z - Z_L) \frac{y''}{-f} \quad (5-31d)$$

From equations (5-31a) and (5-31c),

$$X_L + (Z - Z_L) \frac{x'}{-f} = X_L + B + (Z - Z_L) \left( \frac{x''}{-f} \right)$$

and therefore

$$(Z - Z_L) \left( \frac{x'}{-f} - \frac{x''}{-f} \right) = B$$

and

$$Z - Z_L = B \frac{-f}{x' - x''}$$

Since the difference of the left and right  $x$  image coordinates is the  $x$ -parallax

$$Z = Z_L - \frac{Bf}{px} \quad (5-32a)$$

or since  $Z$  is the height of a point above datum and  $Z_L$  is the flying height, this equation can also be written as

$$h = H - \frac{Bf}{px}$$

The Xcoordinate is calculated by back substituting Z into equation (5-31a) or (5-31c) and the Y coordinate can be obtained from equations (5-31b) or (5-31d), whereby

$$X = X_L + B \frac{x'}{px} \quad (5 - 32b)$$

$$Y = Y_L + B \frac{y'}{px} \text{ or } Y = Y_L + B \frac{y''}{px} \quad (5 - 32c)$$

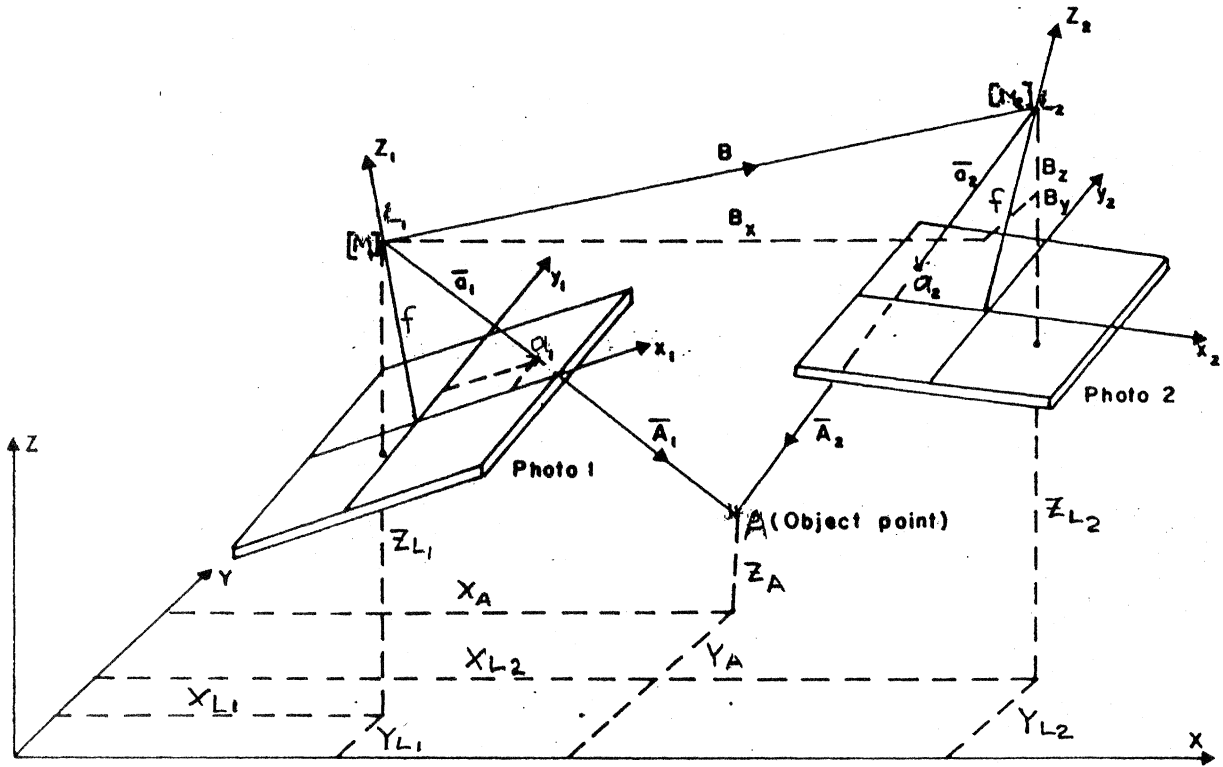


Figure 5-1

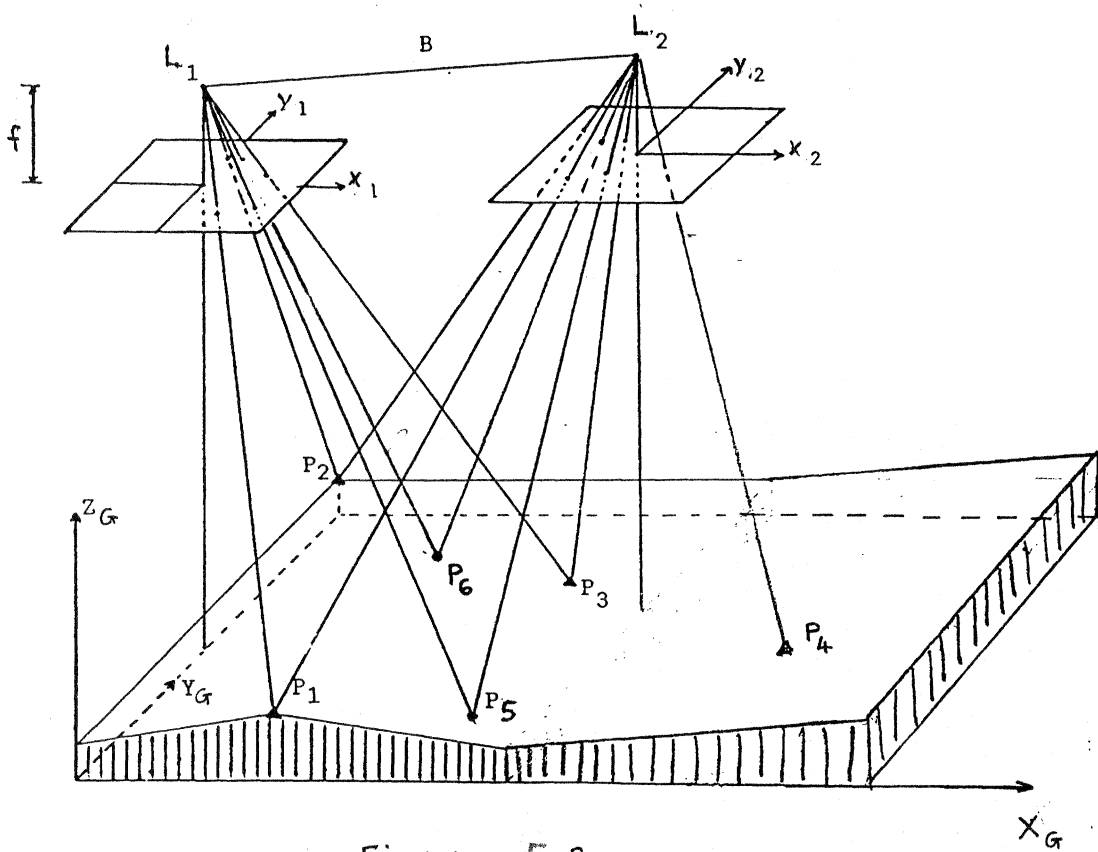


Figure 5-2

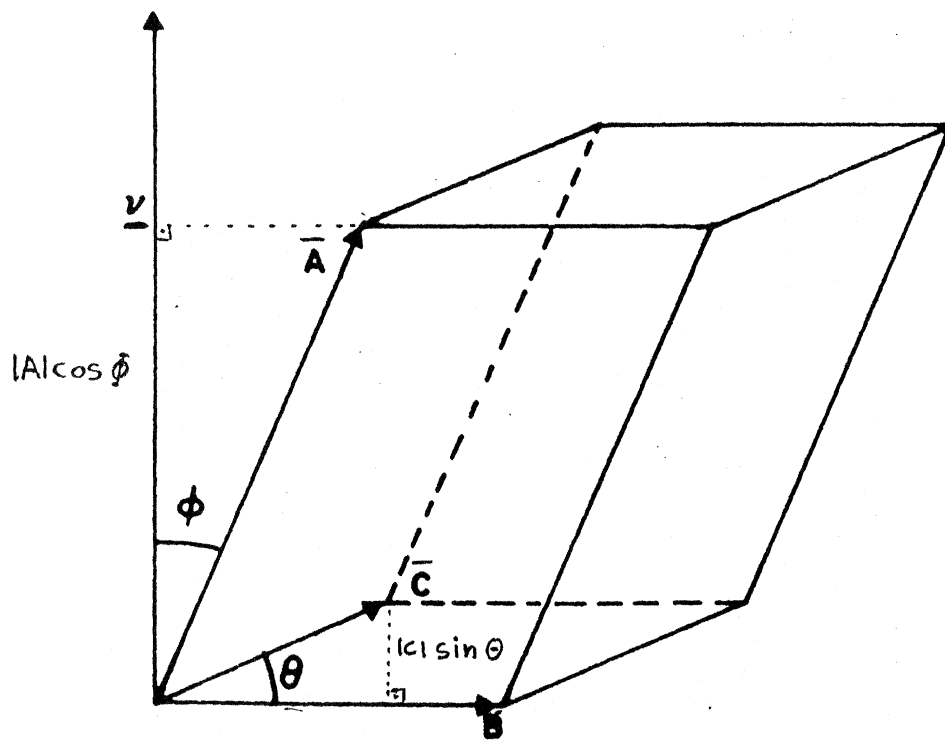


Figure 5-3

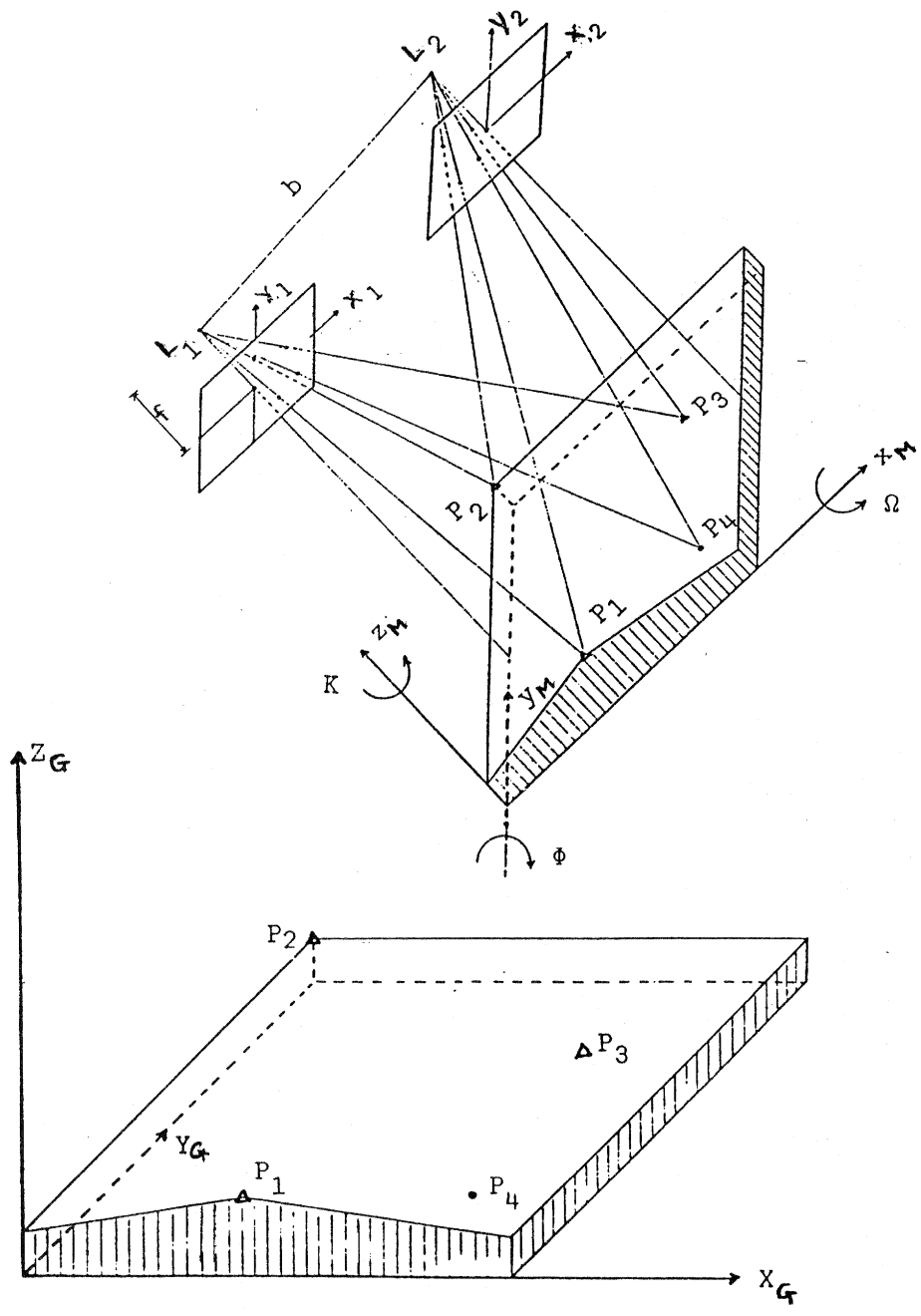


Figure 5-4

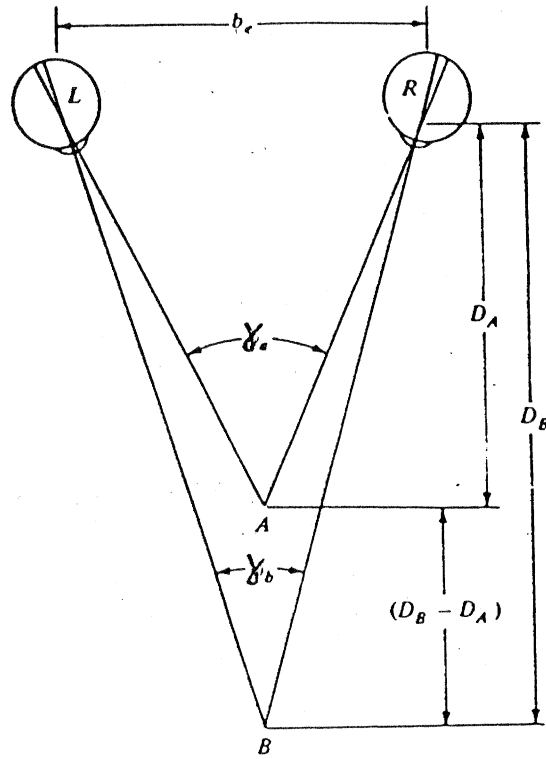


Figure 5-5a

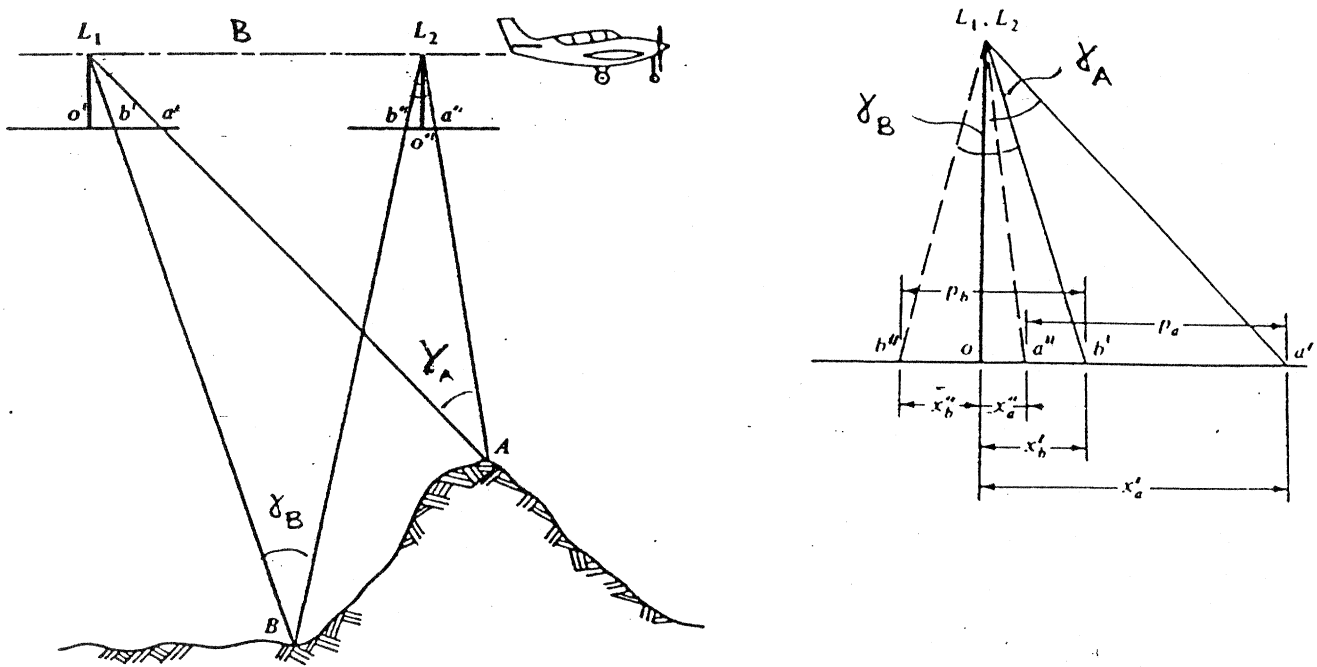


Figure 5-5b

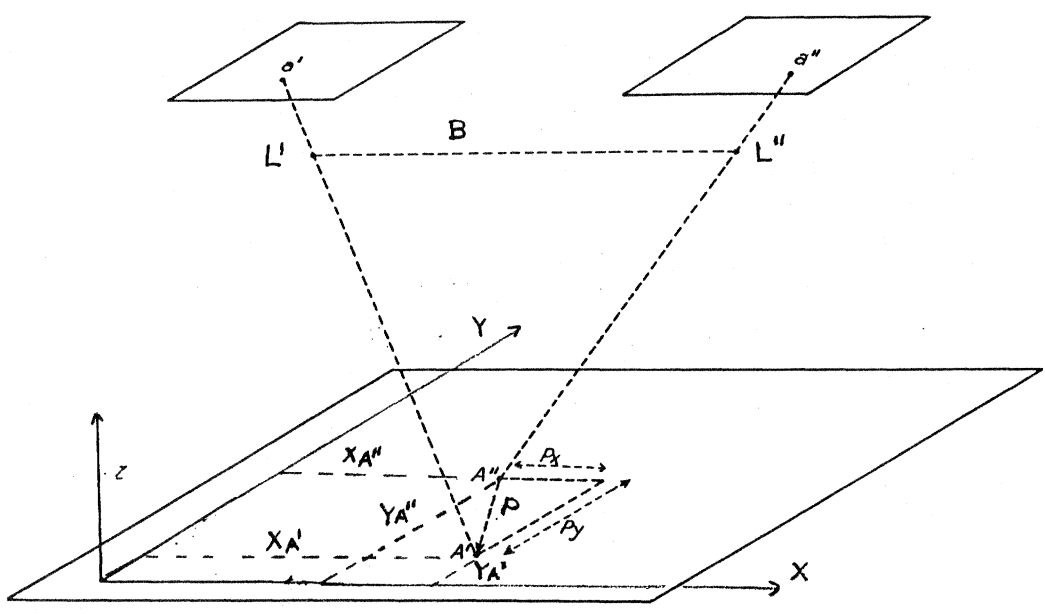


Figure 5-6a

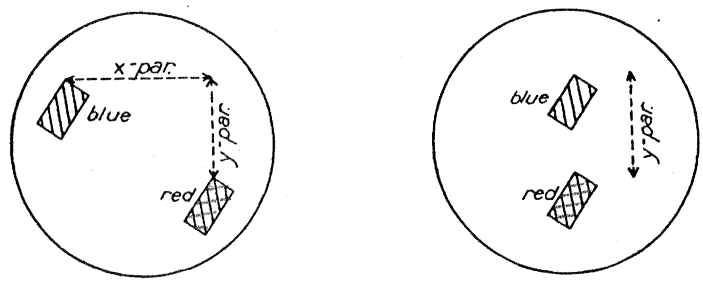


Figure 5-6b

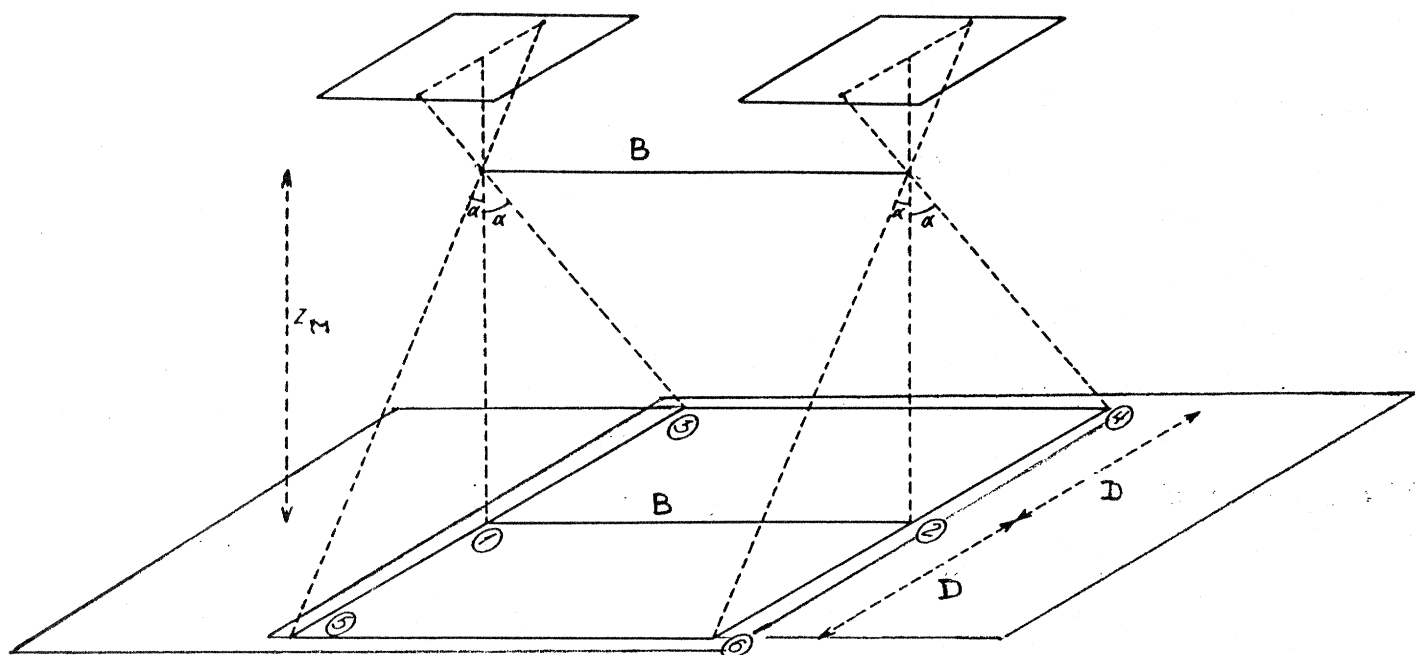


Figure 5-7a

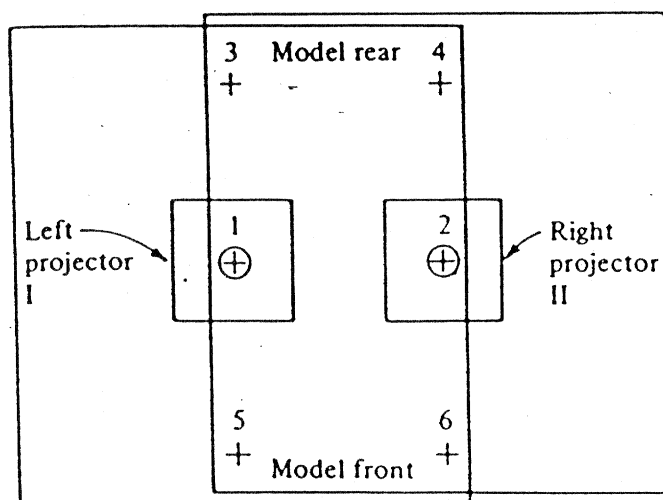


Figure 5-7b

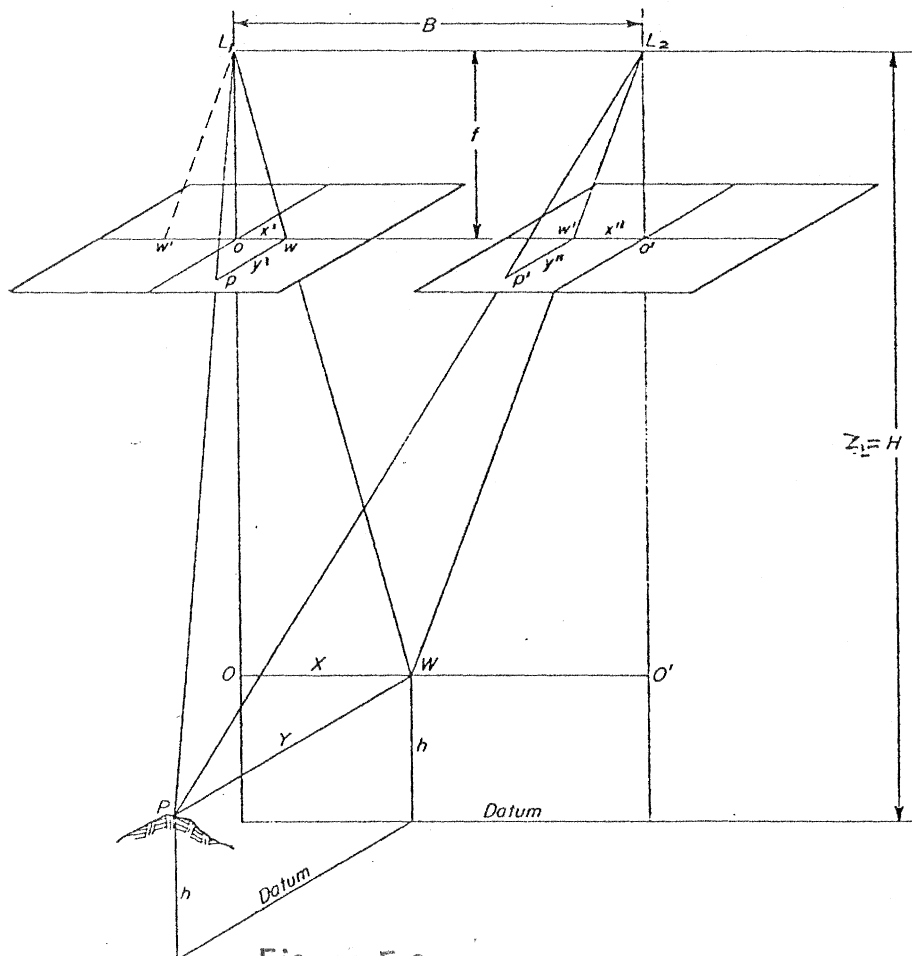


Figure 5-8  
Ground coordinates from parallax measurements.

## 6. STEREOSCOPY

Stereoscopic vision or stereo vision is the ability to perceive objects in three dimensions and judge distance. It is a necessary prerequisite for most photogrammetric measurements. Stereo vision is only possible by the full use of both eyes (*binocular* vision). It is true, that some sense of the third dimension may also exist when viewing with one eye (*monocular* vision) but this only occurs on the basis of relative size of objects, partially hidden objects, shadows and by past experience.

The human eye functions in a similar manner as an electronic camera (Figure 6-1). The incident light rays pass through the *cornea* which is a protective coating, enter the eye through a circular opening called the *pupil* and strike the lens. A diaphragm called *iris* regulates the diameter of the pupil (lens opening) and controls the amount of light that passes through the lens. It ranges from 2 to 8 mm in diameter. The iris is the colored part of the eye. The cornea and the lens refract the light rays which then pass through the jelly-like *vitreous* and come to focus on the *retina*. The retina has about 137 million light-receptor cells, which change light into electrical impulses just like the charge coupled devices (CCDs) do in an electronic camera. The optical nerve carries the electrical impulses to the brain, where the image is formed. The *fovea centralis*, which is situated around the place of intersection by the optical axis of the lens, is the most sensitive spot of the retina,

### 6.1 Natural Stereoscopic Vision

The three-dimensional impression gained of the surrounding by viewing it with the naked eyes is *direct* or *natural* stereoscopic vision. First the eye converges on the object or area viewed. This is achieved by changing the direction of the eye balls with the muscles. The eyes then focus on the object by changing the shape of the lens. The image distance of the eyes is fixed (about 23mm) while the focal length varies as the shape of the lens changes, to satisfy the lens equation. The instantaneous field of view of the eye, where it has a complete sharpness of vision is only  $1^\circ$  to  $2^\circ$ , while the total field of view covered by scanning movements, is about  $170^\circ$  (panoramic).

The two eyes are separated by 63 to 68mm (*eye base*), and each views an object from a slightly different direction. The angle formed by the two viewing rays at an object is the *parallax angle*  $\gamma$  (Figure 6-2). When an object like a pencil is held at arms length is

front of the eyes and the gaze is fixed on a spot far in the background, then two images appear. The left image is formed by the right eye and the right image by the left eye. The separation of the two images is the *parallax*. The existence of the two images becomes more apparent if the object is viewed by alternatively blinking with the eyes. The object appears jumping sideways, back and forth. The separation between the two images (the jump) will increase as the object is moved closer to the eyes and vice versa.

Parallax, as already defined in section 4.7, is the change in the direction in which an object is seen or imaged cause by a change in the position of the observer or the sensor. When the eyes sight two objects  $A$  and  $B$  at different distances away ( see Figure 6-2 ), the brain automatically and unconsciously associate distances  $D_A$  and  $D_B$  with the corresponding parallax angles  $\gamma_A$  and  $\gamma_B$ . The two points are imaged at slightly different spots on the retina. The separation between these two spots is the parallax difference  $\Delta p$  which is associated with the difference in the two parallax angles  $\Delta\gamma = \gamma_A - \gamma_B$ , and forms the basis of sensing the difference in distance  $\Delta D = D_B - D_A$ .

The largest parallax angle formed by the eyes, as determined by the eye base and the minimum distance of clear vision (25cm), is approximately  $15^\circ$ . The smallest change in the parallax angle ( $\Delta\gamma$ ) which the eye can sense is approximately  $10''$  of arc. Thus the accuracy of estimating the third dimension (*binocular* or *stereoscopic visual acuity*) is about  $15\ \mu\text{m}$  at a distance of 25 cm. In comparison the angular resolution of a single eye ranges from  $30''$  to  $1'$  of arc, which corresponds to an average linear resolution of 40 to  $80\ \mu\text{m}$  at a distance of 25 cm (*monocular visual acuity*). This figure represents the smallest separation between objects or lines which the eye can discern. Thus the ability of the human vision to sense the third dimension is significantly better than its two-dimensional resolving power.

## 6.2 Indirect Stereoscopic Vision

Direct stereoscopic vision can be substituted by viewing two photographs of a scene taken from two different stations as shown in Figure 6-3. The three requirements for this so called *indirect stereoscopic* vision are as follows:

1. The two photographs must be viewed at the same time.
2. Each eye must view only one of the two photographs.
3. The two photographs must be aligned in such a way that the extension of the viewing rays passing through the corresponding image points in the left and right photographs intersect in space.

At the intersection of the viewing rays a virtual spatial view appears of the photographed scene. At every intersection of the viewing rays a parallactic angle is formed and the vision system senses the third dimension in the same manner as in direct stereo viewing.

The first requirement is easy to meet. The second requirement, however, poses difficulties. It means that the photographs must be viewed with the axis of both eyes set almost parallel just like when viewing a distant object and at the same time the eyes must focus on an object close by. This is contrary to the natural ways in which the human vision function. Several instrumental aids are available to solve this problem.

### 6.3 Stereoscopic Viewing Aids

The simplest stereoscopic viewing aid is the *pocket stereoscope*. It consists of two lenses mounted in a frame on a stand at the normal eye separation. The lenses focus each eye on one of the photographs. The lenses may also provide some magnification. (Figure 6-4)

The *mirror stereoscope* provides for a wider separation of the images so that the 230 by 230 mm size aerial photographs can easily be accommodated. The viewing rays are diverted sideways and then downward towards the photographs by two pairs of mirrors mounted at  $45^\circ$  to the ray path, as shown in Figure 6-6. A binocular viewer attachment can provide magnification.

In the *anaglyphic viewing* system each of the two images are printed or projected in one of two complementary colours, usually red and blue-green, onto a white background. Each eye sees only one of the two images when viewing through glasses of the same complementary colours. The principal of anaglyphic viewing is illustrated in Figure 6-6.

The *polarization viewing* system is based on the same principal as the anaglyphic except that horizontal and vertical polarization filters are employed for projecting and viewing the images instead of colour. This makes the stereo viewing of colour photographs possible.

In the stereo *image alternator* system, a rotating shutter is mounted in front of the projector lenses as shown in Figure 6-7. The two shutters are rotating out of phase by exactly a quarter cycle ( $90^\circ$ ) thus only one of the two images are projected at any one time. The two shutters in the viewer are also rotating out of phase by  $90^\circ$  and are synchronized with the projector shutters, so that the left projector and viewer shutters open at the same

time and vice versa. The speed of rotation of the shutters is sufficiently fast to present a continuous stereoscopic view without any jitters.

#### 6.4 Alignment of the Photographs

The rigorous alignment of the two photographs for stereoscopic viewing (third requirement) means to perform the relative orientation. When viewing nearly vertical photographs under a stereoscope, however, an approximate method of orientation is usually satisfactory since the eye can accommodate small misalignments (residual y-parallaxes). This orientation is performed in the following steps (Figure 6-8):

1. The fiducial center is located in each photograph by joining opposite fiducial marks with a straight line. The intersection of the lines is the fiducial centre.

2. The location of the fiducial centres are marked on the adjacent overlapping photos. This may be done by observing corresponding details on the adjacent photos that surround the fiducial centers. The distance between the fiducial centre and the transferred fiducial centre is the photo base,  $b$ .

3. The photos are placed on a flat surface in the order they were taken. Aerial photos are numbered consecutively along the flight line.

4. The two photos are aligned so that the four points (the fiducial center and the transferred fiducial center on each photo) lie along a straight line as shown in Figure 6-8. This line indicates the ground track of the flight line.

6. The two photos are separated by about the same distance as the centres of the lenses in the pocket stereoscope or the centres of the wing mirrors of the mirror stereoscope, and fastened down.

The above procedure for aligning the photographs is an imperfect relative orientation because it is performed on a plane rather than in space and thus ignores the effect of tilt on the y-parallaxes. It only removes the effect of the  $d\kappa$ ,  $dy$  and the constant part of  $d\omega$ . It is equivalent to the first two steps of the empirical relative orientation in stereoplotters (see section 6.3). The centre of the overlap becomes free of  $py$  but residual y-parallaxes remain towards the edges. Therefore a corrective realignment may be necessary when viewing in these areas.

A pseudoscopic inverted view results if the photos are aligned in the opposite order as they were taken. This means that valleys look like ridges and hills appear as depressions.

### 6.5 Vertical Exaggeration

When the stereo viewing base-height ratio is smaller than the photographic base-height ratio, then the vertical scale of the stereoscopic view appears larger than the horizontal scale, i.e., the vertical dimension of objects appear exaggerated, as shown in Figure 6-9. This scale disparity is called *vertical exaggeration*. The following formula gives a close approximation of the vertical exaggeration factor,  $V$ :

$$V = \frac{B}{H} \frac{h}{b}$$

where  $B$  is the air base (distance between the two exposure station),  $H$  is the flying height above the average terrain elevation,  $h$  is the distance from the eye to the point where the intersection of corresponding viewing rays is perceived in space, and  $b$  is the eye base (distance between two eyes).

The  $B/H$  ratio depends for a given flying height on the field of view of the camera lens and on the percentage of the forward overlap of the photographs. The exact value of the  $b/h$  ratio is somewhat difficult to ascertain. For stereoscopes with different magnifying power this ratio ranges from 0.11 to 0.19. Thus 0.15 may be taken as an average value.

The vertical exaggeration should not be interpreted as a geometric distortion of the spatial model. It is only a psychological phenomenon which aids in the perception of the third dimension.

### 6.6 Parallax Measurement

Assume that a mark of the same size and shape etched on transparent material, is superimposed on each of the two overlapping photographs. The two marks, also called half-marks, fuse into a single mark when viewed stereoscopically which appears floating in space, as seen in Figure 6-10. Therefore, this mark is called the *floating mark*. If the spacing between the two marks is changed by shifting one with respect to the other sideways then the mark appears to have lowered or raised its position in space. When the two marks sit on corresponding image points in the left and right photographs then the

fused mark appears to be in contact with that point in the stereoscopic view. A change in spacing between the two marks alters the size of the parallax angle formed by the viewing rays which is the basis of depth perception.

Based on the principle of the floating mark, parallaxes of image points can be measured stereoscopically. A simple device called *parallax bar* can serve this purpose. It consists of a metal bar to which the two half marks, etched on a transparent material, are fastened, as shown in Figure 6-11. The right half mark can be moved with respect to the left mark (fixed mark) by turning a micrometer screw and the change in the separation between the two marks can be measured. From the micrometer readings, parallaxes or differences in parallaxes are obtained in the following way:

The parallax bar is placed on the photographs which are properly aligned for stereoscopic viewing. The micrometer is turned to approximately the middle of the scale range. The fixed mark is unclamped and the separation between the marks is changed until the floating mark sits on a terrain point of average elevation, when viewed through a stereoscope. The fixed mark is then clamped. The parallax bar is now ready to be moved to the points where the parallax is to be measured.

At every point the floating mark is set, under stereo vision, on the object or terrain surface by changing the separation between the two half marks, and the micrometer is read. Based on Figure 6-11, the parallax  $px_a$  of a point  $a$  is determined as:

$$px_a = x'_a - x''_a = D - (K - r_a) = (D - K) + r_a$$

where  $x_a$  and  $x'_a$  are the  $x$  image coordinates of  $a$ ,  $D$  is the spacing between the left and right fiducial centers,  $K$  is the distance from the index mark of the micrometer to the fixed mark and  $r_a$  is the micrometer reading (the distance from the index mark to the movable mark). Once the photos are fastened down and the fixed mark is clamped,  $D$  and  $K$  remain constant so that the term  $(D-K)$  becomes  $C$ , the parallax bar constant for that setup, so that the expression becomes

$$px_a = c = r_a$$

The constant  $C$  is obtained by first taking a micrometer reading ( $r$ ) with the floating mark set on an image point and then determining the parallax of that point as a difference of the  $x$  image coordinates measured monoscopically.

$$px = x - x'$$

The value of  $C$  is then calculated as:

$$c = px - r$$

It is convenient to use the fiducial centres for this purpose since the parallax of these points is equal to the photo base  $b$ , so that

$$C = b - r.$$

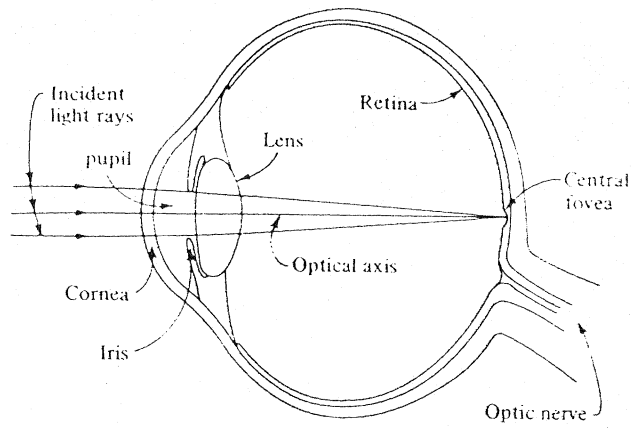


Figure 6-1

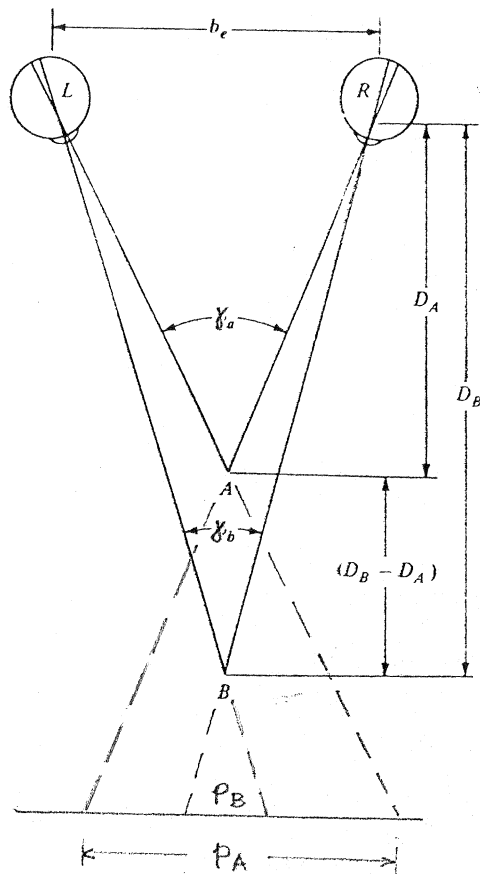
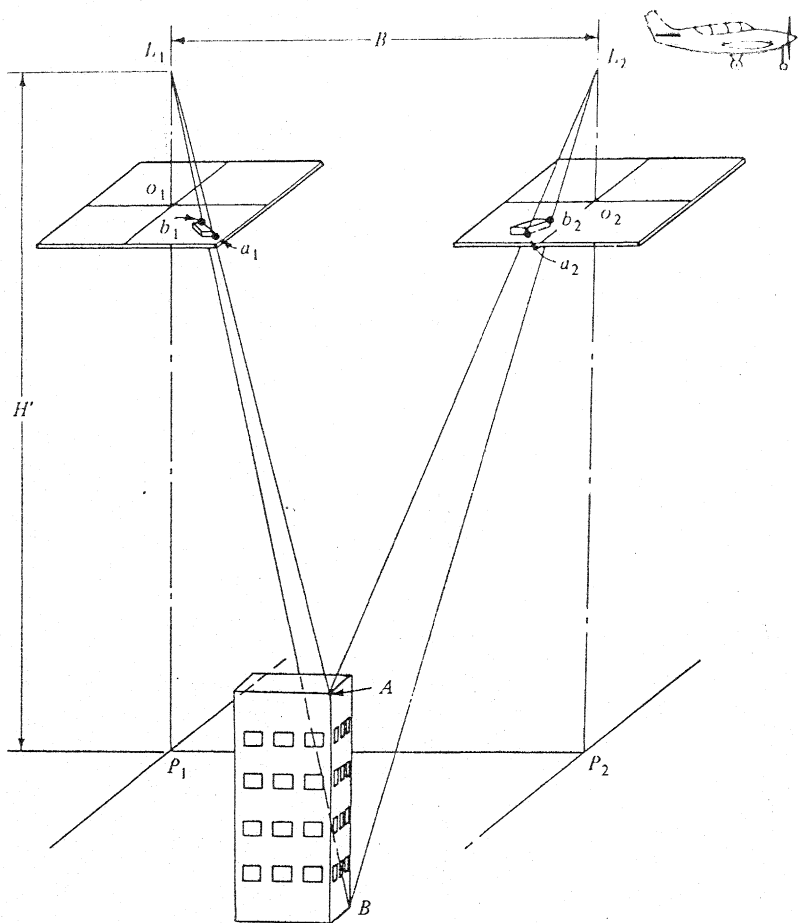
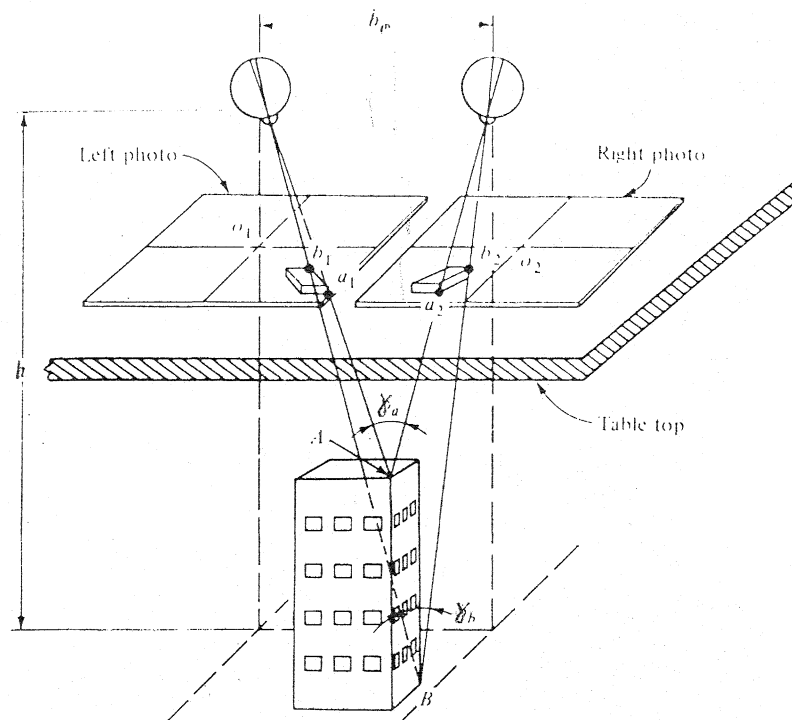


Figure 6-2



(a) Photographs from two exposure stations with building in common overlap area.



(B) Viewing the building stereoscopically.

Figure 5-3

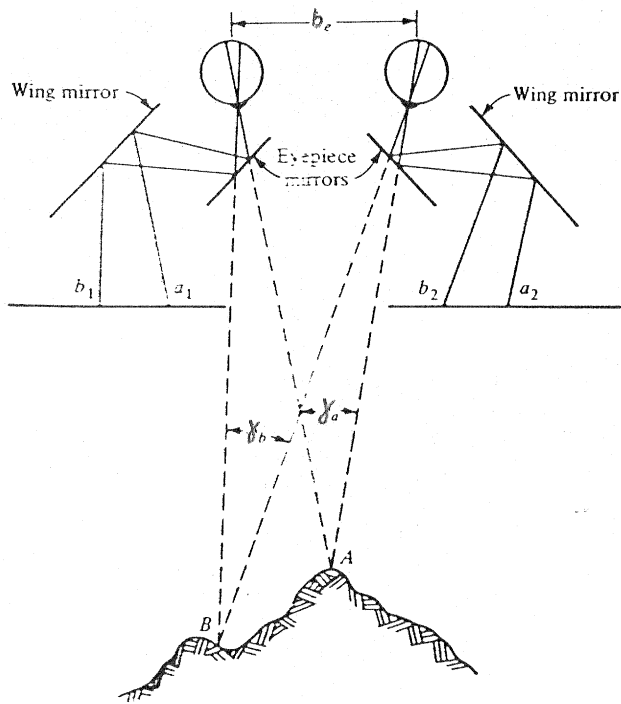


Figure 6-5

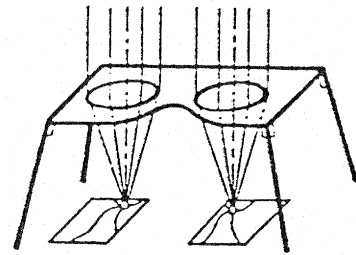


Figure 6-4

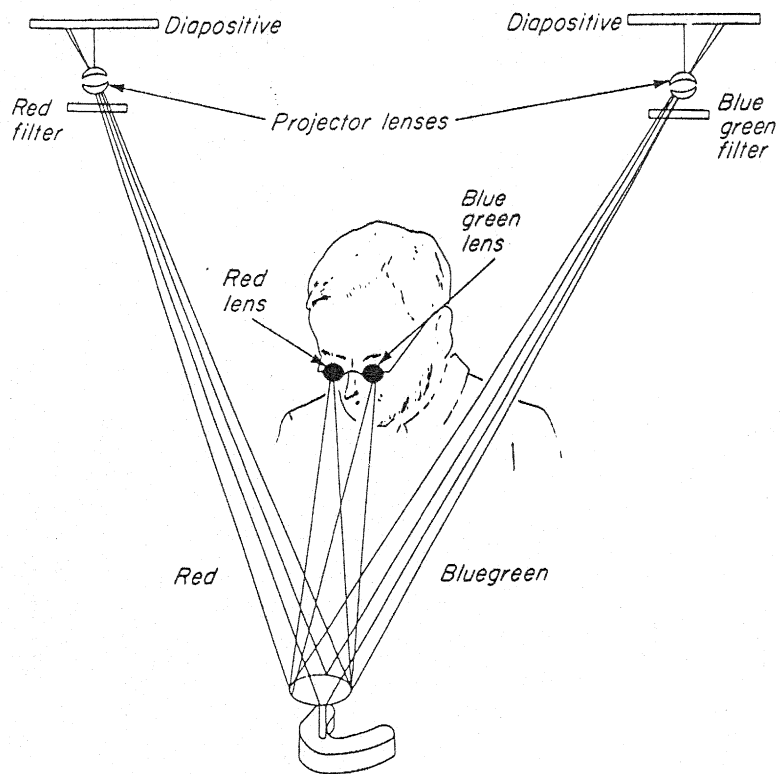


Figure 6-6 Anaglyphic viewing.

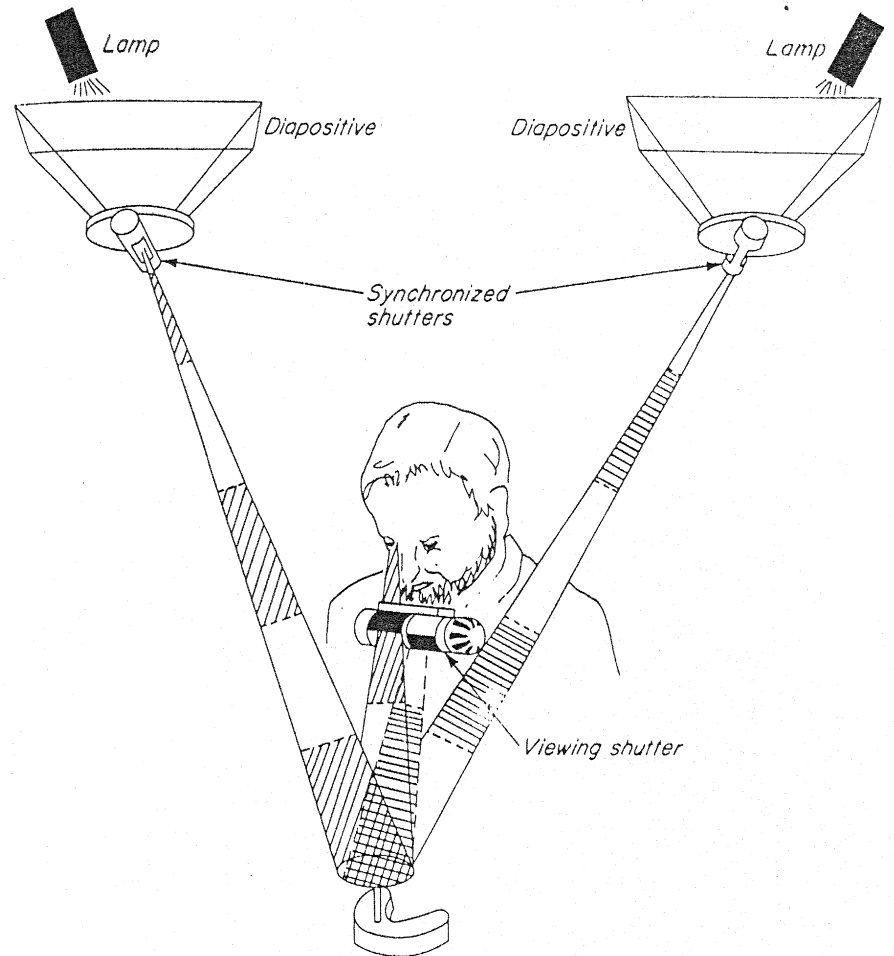
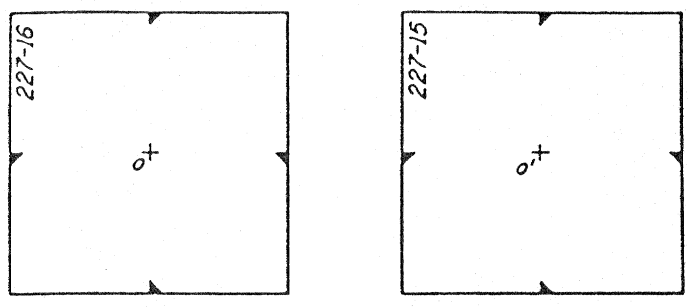
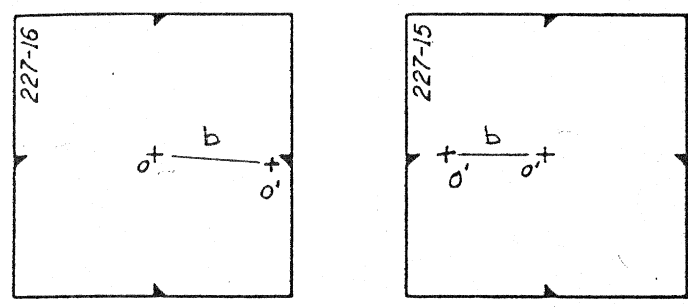


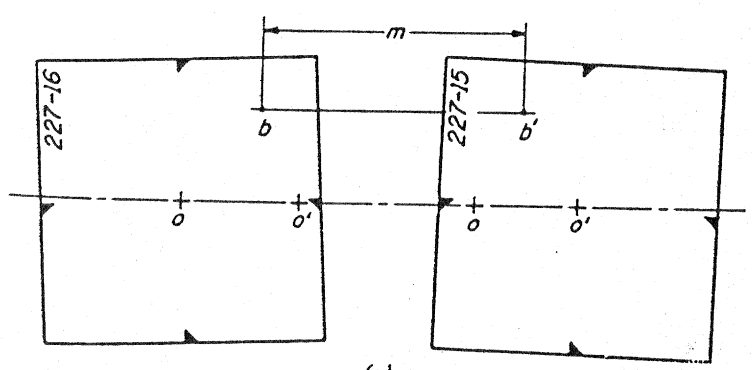
Figure 6-7. Principle of stereo image alternator (SIA).



(a)



(b)



(c)

Figure 6-8 Orienting photographs for viewing under stereoscope.

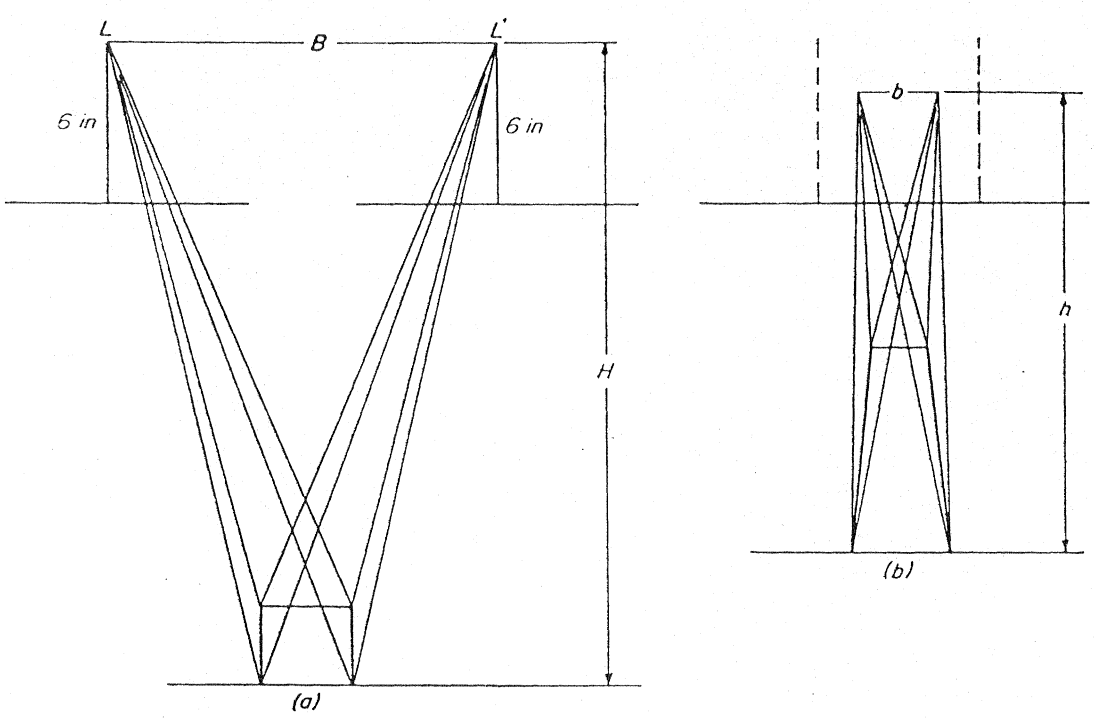
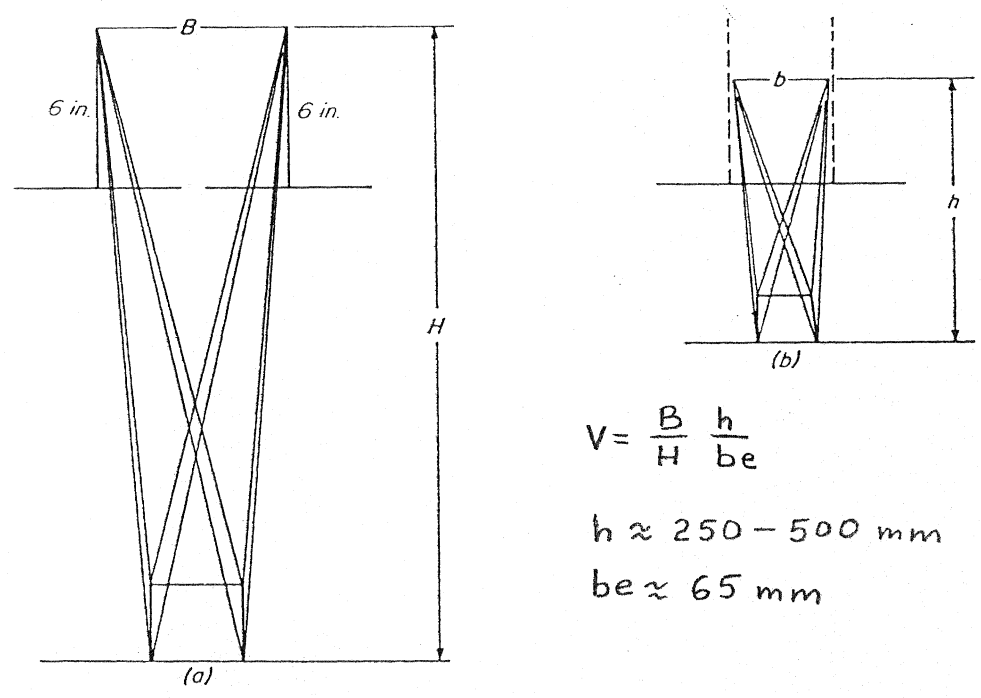


Figure 6-9a Vertical exaggeration,  $B/H = 0.60$ .



$$V = \frac{B}{H} \frac{h}{be}$$

$h \approx 250 - 500\text{ mm}$

$be \approx 65\text{ mm}$

Figure 6-9b Vertical exaggeration,  $B/H = 0.30$ .

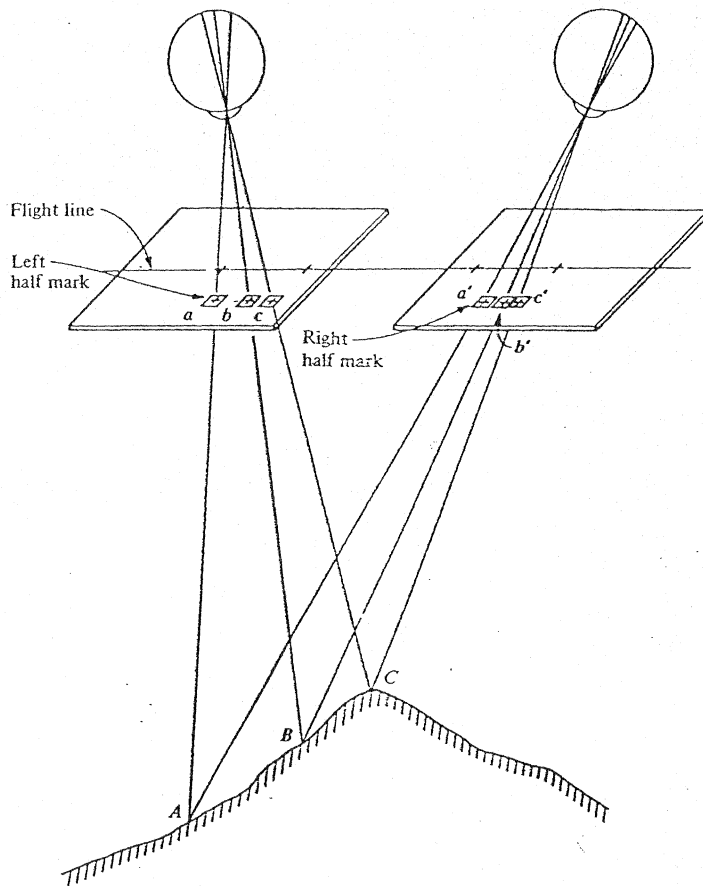


FIGURE 6-10  
The principle of the floating mark.

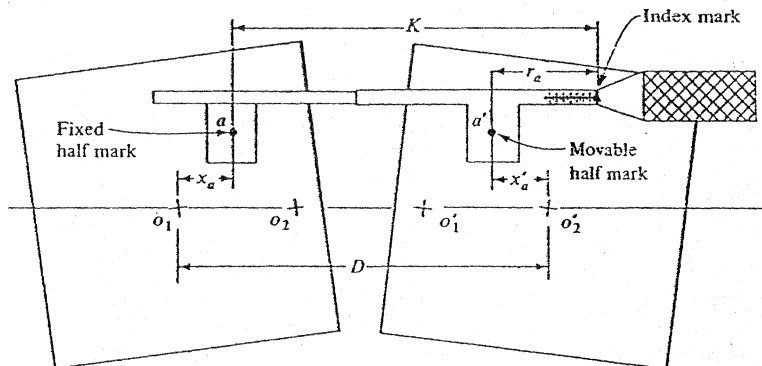


FIGURE 6-11  
Schematic diagram of the parallax bar.

## 7. PHOTOGRAMMATIC INSTRUMENTS FOR SPATIAL POSITIONING

### 7.1 Analogue Instruments

Determination of the spatial position of objects by analogue photogrammetric means is performed in *stereoscopic plotting instruments*. These devices, often called *stereoplotters* or simply *plotters*, provide an analogue solution for the construction of a spatial model of a three-dimensional scene from images of that scene appearing on two overlapping photographs and provide means to make measurements in this model for the purpose of determining the spatial position ( $X, Y, Z$ ) of objects. These devices function as analogue computers.

The design of stereoplotters is based on the concept illustrated in Figure 7-1. Part (a) of this figure illustrates the imaging of a portion of the terrain on a pair of overlapping aerial photographs. As the aircraft carrying a photographic camera proceeds along the flight line, terrain point  $A$  is projected through perspective centres  $L_1$  and  $L_2$  at the two exposure stations onto the image plane of the camera to record the corresponding points  $a_1$  and  $a_2$  on the two negatives. Positive transparencies (*diapositives*) made of the negatives are placed into two projectors to reverse the projection process, as shown in Part (b) of the figure. By the intersection of rays that reproject corresponding image points appearing on the two diapositives, a three dimensional, spatial model (also called *stereo model*) is formed of the terrain.  $A'$  is the model point of terrain point  $A$ . (See also the description of stereoplotters in Appendix II.)

Stereoplotters have three distinct components. These are: (1) the *projection system*, which forms the stereo model; (2) the *viewing system*, which makes it possible to see this model; and (3) a *measuring and/or tracing system* which enables measurements to be made in the model and to record these measurements graphically or digitally.

#### 7.1.1 Projection System

The projection system projects through a perspective centre the corresponding image points situated on a pair of overlapping diapositives into model space. The two most often employed projection systems are the *optical* and the *mechanical*. The concept of these two is shown in Figure 7-2. A rather uncommon projection system is the *optical-mechanical*, which will not be discussed.

In the optical projection system (Figures 7-2a and c) the the projection and intersection are modeled entirely by optical rays. The optical center of the objective lens is the perspective center and the image distance matches the principal distance associated with the diapositive.

The mechanical projection system employs a pair of metal rods, called *space rods*, in gimbal suspension to model the projection and intersection of rays. The intersection of the rotation axes in the two gimbal joints represent the perspective centers and horizontal tie rods connected to the space rods from the two *effective image planes*. The distance between these planes and the gimbal centers coincides with the principal distance associated with the diapositives. (Figure 7-2b)

### 7.1.2 Viewing System

The function of the viewing system is to provide a three-dimensional view of the stereo model. Stereoviewing is only possible if each eye views only one of the two images in the overlap area. A detailed description of stereovision is provided in Chapter 5.

Two kinds of viewing system is employed in the optical projector type plotters, the *direct viewing* and the *goniometric viewing*. In the direct viewing kind the corresponding images are projected onto a small horizontal platten in model space (Figure 7-3a). Color filters, polarization filters or image alternators are employed to facilitate stereo viewing. The lens equation must be satisfied to obtain a sharp image on the platten, so that

$$\frac{1}{F} = \frac{1}{p} + \frac{1}{h}$$

where  $F$  is the focal length of the projector lens,  $p$  is the principal distance of the projectors (distance from the image plane to the rear nodal point or interior projection center of the projector lens), and  $h$  is the projection distance (distance from the front nodal point or exterior projection center of the projector lens to the plane of optimum focus). These instruments have a fixed principal distance of a different value than the focal length of the projector lens. The intersection of corresponding projected rays must occur at a projection distance within the depth of field of the projector to maintain an acceptable sharpness. The design of these plotters is very simple, but they have significant physical limitations.

In the goniometric viewing optical projection instruments the corresponding images are projected onto a pair of mirrors as shown in Figure 7-3b. The rays are reflected by the mirrors into two optical trains and are viewed through binoculars. The focal length of the projector lens

is equal to the nominal principal distance associated with the diapositive and therefore the projected rays emerge from the lens parallel. An auxiliary lens system (Bauersfeld lens system) placed in the path of the rays assures that the projected image is in perfect focus on the mirrors regardless of the projection distance. (See details in Figure 7-4)

In the mechanical projection instruments the corresponding image points are projected orthogonally by lenses onto a prism in the effective image planes, and then directed to the eyepieces by an optical train (Figure 7-5). Both the principal distance and the projection height can be changed within a wide range without the constraints of optical conditions. This is a very versatile design and has been favoured by most manufacturers. (See details Figure 7-7.)

### 7.1.3. Measuring and Tracing System

Model coordinates are obtained by placing a *measuring* or *floating mark* in stereo vision on the model point to be observed and determining, with the help of counters the magnitude of the movement needed to do so. In the direct viewing optical projection instruments the floating mark is a single tiny luminous spot in the centre of a white platen onto which the images are projected. The platen forms part of a device called *tracing table*. (Figure 7-7) Raising and lowering the platen along a spindle by turning a thumb screw creates the impression of the measuring mark moving vertically in model space. Horizontal movement of the measuring mark is affected by free-hand shift of the tracing table. The position of a point in the model is measured by moving the platen horizontally and vertically until the floating mark appears to rest on the point in question. The elevation is then read directly from a counter connected to the spindle. Planimetric coordinates can only be measured if the tracing table is connected to a XY coordinotograph. The position of the point can, however, be plotted on a drafting sheet placed on the reference table by lowering a pencil point installed vertically beneath the measuring mark. Line features are plotted by guiding the floating mark with the tracing table along the feature while changing the height of the platen to keep the floating mark in contact with the feature. The pencil thereby inscribes a continuous trace of the feature on the paper. Contours are drawn by setting the mark at the elevation of the desired contour and then moving the tracing table about, keeping the floating mark on the surface of the terrain model.

In the goniometric viewing type optical projection instruments an identical measuring mark (half mark) is projected onto each of the viewing mirrors which are moved in X and Y direction along precision lead screws by turning hand wheels and in Z direction by rotating a foot disk. These movements are imparted to the auxiliary optics which then rotates under the projector lens about its front model point so that different parts of the diapositive can be viewed.

The two marks fuse into a single mark, floating in space, when viewed stereoscopically through the eyepieces. A correct setting of the floating mark on the surface of the terrain model or on an object means that the two projection rays intersect the diapositives at the corresponding image points. Thus the left and right measuring marks appear superimposed on the corresponding image location in the diapositives.

In the mechanical projection type instruments the X, Y and Z motions induce the pivoting of the space rods about the gimbal. These rotations, in turn, move the orthogonal viewing systems with the measuring marks, connected to the upper ends of the space rods, in a plane parallel to the plane of the diapositives (the effective image plane). The X and Y controls rotate both space rods and moves both measuring marks in the same direction so that different parts of the diapositive can be viewed and measured. The Z control rotates the rods and moves the two measuring marks in an opposite direction whereby the mark appears to move vertically in space and the height of the intersection point of the space rods changes in model space.

In some mechanical projection instruments the two space rods actually intersect on the *tracing stand* which can be moved freehand in X and Y direction (Figure 7-8). The height of the intersection point is changed by a vertical movement along the Z column. In other designs the space rods do not physically intersect, but are separated by the so called *base bridge* whose length is  $s - b$ , where  $s$  is a constant representing the distance between the two gimbal joints and  $b$  is the stereo model base. The separation of the two space rods along the base bridge and the distance along the right space rod from the connection to the base bridge and the gimbal joint are two sides of a parallelogram called the *Zeiss parallelogram* (Figure 7-9).

When tracing is done directly from the stereo model by a pencil attached to the tracing stand, then the map has the same scale as the model (Figure 7-10a). The scale from model to map manuscript can be changed by connecting a pantograph to the tracing stand (Figure 7-10b). A more versatile solution is to transfer the movements in the stereo model to a plotting table where the map manuscript is drawn. The plotting table is essentially a coordinatograph. Scale of the manuscript is changed through a gear box which connects the table to the main instrument (Figure 10c). In instruments with more advanced design, rotary or linear encoders are used to measure the X, Y and Z movements and display these electronically. In this case the movements in the stereo model can be transferred electronically to the plotting table and the pencil is driven by servo motors.

Distinction must be made between stereo model and stereo view. Stereo model is a geometrically correct spatial representation of the photographed object. It is created by mathematically or physically modeling the intersection of corresponding rays. Stereo view is a three dimensional perception of the photographed object and is created through a mental process. In the direct view optical projection instruments the stereo model is created by actual intersection of the optical rays and is viewable. In the other instruments only a stereo view is provided through the viewing optics. The stereo model is formed by the projection system.

#### 7.1.4 Setting up a Stereo Model

The setting up a stereo model means to establish the correct interior and exterior orientation of both projection systems.

##### 7.1.4.1 Interior orientation

Interior orientation reconstructs the shape of the bundle of rays that produced the image. The operational steps involved are as follows:

1. Preparing the diapositives to the correct size
2. Compensating for the image distortions
3. Centering the principal point of the diapositives over the projection center of the lens
4. Setting the principal distance of the camera in the instrument.

Most stereoplotters can accommodate diapositives which have the same size as the negative. These are prepared by either contact printing or by 1 to 1 projection printing. If this is not the case, then the size of the diapositive must be reduced or enlarged. The change in size must be according to the ratios

$$\frac{d}{d'} = \frac{f}{p}$$

where  $d$  and  $d'$  are the dimensions of the negative and the diapositive respectively, and  $f$  and  $p$  are the principal distances of the photographic camera and of the plotter respectively.

Physical limitations of most instruments only allow to compensate for the symmetric radial lens distortion and for the regular film distortion. Note that in analytical photogrammetry a more complete compensation for the image distortions is possible, as described in Chapter 7. Compensation for the radial lens distortion may be accomplished in one of the following three ways:

1. Printing the diapositives through a *correction plate* in the projection printer.
2. Projecting or viewing the diapositives through a *correction plate* in the plotter.
3. Varying the principal distance of projection system by a mechanical device called *cam*.
4. Using a projector lens whose distortion characteristics negate the distortion of the camera lens.

A correction plate is an aspheric glass plate the curvature of which models the lens distortion curve and deviates the ray path accordingly. (Figure 7-11) An aspheric cam mechanically raises and lowers the projection lens (or the diapositive) so that, the projected rays form the same angle with the optical axis of the projector as did the imaging rays with the optical axis of the camera on the object side.

The effect of radial lens distortion on the position of an image point is shown in Figure 7-12. Angle  $\alpha$  is the correct angle of refraction of the ray which is deviated by  $\Delta\alpha$ . The corresponding displacement in the radial distance  $r$  of an image point is  $\Delta r$ . This displacement can be corrected either by correcting the direction of the ray path directly or by changing  $f$  by  $\Delta f$  since

$$\Delta r = \frac{r}{f} \Delta f \quad \text{and} \quad \Delta f = \frac{f}{r} \Delta r$$

It should be noted that all the above optical and mechanical devices can only compensate for the distortions of a particular lens design e.g. Zeiss Pleogon, Wild Aviogon, etc. but not for the residual distortions of the lens in a particular camera. This is only possible by analytical means based on camera calibration.

The regular film deformation (shrinkage) can also be corrected by changing the principal distance. This deformation is actually a scale error as shown in Figure 7-13. It can be corrected by changing the principal distance to

$$f' = \frac{s'}{s} f$$

where  $s$  is the correct dimension of the image and  $s'$  is the actual dimension. These values are obtained from the calibrated and the measured distances between the fiducial marks.

#### 7.1.4.2 Relative orientation

The exterior orientation of the two photographs is defined by twelve parameters: the  $X$ ,  $Y$ ,  $Z$  coordinates of the two perspective centres and the angular orientation  $\omega$ ,  $\phi$ ,  $\kappa$ , of the projection systems. In analytical photogrammetry the twelve parameters can either be determined directly by a space resection of both photographs, (six plus six parameters) or indirectly by relative (five parameters) and absolute (seven parameters) orientation. In analogue photogrammetry, only the relative plus absolute orientation course can be taken.

The objective of relative orientation is to arrange the two projection systems with respect to each other in space so that all ray pairs associated with corresponding points in the two photographs intersect. The intersection points of the two projected rays define a spatial model.

In analytical photogrammetry the intersection of corresponding rays is enforced by the coplanarity condition. In stereoplotters the failure of intersections is seen in the viewing system as a mismatch of two corresponding image points. This mismatch, referred to as parallax, is resolved into two components, which are the x-parallax ( $px$ ), the separation of the two points in the direction of the  $X$  axis of the instrument and the y-parallax ( $py$ ), the separation in  $Y$  direction (see Figures 7-14a and 7-15). The x-parallax is a function of object point elevation and can be eliminated at any point in model space by changing the projection distance. (Raising or lowering the projection plane, as shown in Figure 7-14b). The y-parallax that remains, is the measure of non-coplanarity of the corresponding rays. Thus the condition of relative orientation to be enforced in stereoplotters is the elimination of y-parallaxes. This operation must be performed sequentially at five points in the overlap area (there are five relative orientation parameters) by rotations and translations of one or both of the projection systems.

In a universal stereoplotter each projection system has six degrees of freedom which physically model the six exterior orientation elements. These are the translations in  $X$ ,  $Y$ ,  $Z$  direction and the rotations  $\omega$ ,  $\phi$ ,  $\kappa$  around the coordinate axes as shown in Figure 7-15.

Before the relative orientation procedures are discussed, it is helpful to study the effect of each movement on the projected images in model space. Figure 7-16 shows the effect of the six projection system motions on the position of a symmetrical array of nine points. The total change in position of each point and the  $X$  and  $Y$  components of the movements are shown separately. Note the wide variety of effects these motions have in both magnitude and direction.

Of particular interests for relative orientation are the motions with Y-components, because these are useful for eliminating the y-parallaxes.

Six of the nine test points in Figure 7-16 fall within the overlap area, as shown in Figure 7-17 and are used as standardized point locations for relative orientation. Points 1 and 2 are located at or near the projection of the principal point of the two diapositives. Points 3, 4, 5 and 6 are near the four corners of the overlap, equidistant from the principal points. Figure 7-18 shows the Y-components of the movement at these six points as induced by the ten projector motions of relative orientation. (The two x-shifts are excluded since these have no y components).

In a fully manual operation, an empirical method is used for relative orientation whereby the y-parallax is cleared at points 1 to 5 sequentially. (Point 6 is used for check). The selection of the proper orientation element for clearing  $p_y$  at a particular point is governed by the following criteria:

- a) At each point  $p_y$  should be cleared by that orientation element which causes the maximum y-displacement at that point.
- b) The orientation element used at any subsequent point should not reintroduce y-parallax at previously cleared points.
- c) The orientation elements applied at the five points must be independent. Note that the Y and Z shifts and the  $\omega$  rotation of the left (L) and right (R) projectors are correlated. In addition the two  $\kappa$  rotations and the Y-shifts as well as the two  $\phi$  rotations and the Z shifts are also correlated. This is evident by examining Figure 7-18.

Relative orientation is accomplished either by moving both projectors, or by holding one projector fixed and only moving the other. The first method is called the two projector or *independent pair* method and the second one is the one projector or *depanent pair* method. Before the orientation commences, both projectors should be brought to a vertical position and the Y and Z settings equalized.

The following procedure is followed in the independent pair method:

The x-parallax is removed at the point operating at by changing the projection height before attempting to clear the y-parallax, and then

1.  $p_y$  is cleared at 1 with  $\kappa$ -rotation of projector R.
2.  $p_y$  is cleared at 2 with  $\kappa$ -rotation of projector L.
3.  $p_y$  is cleared at 3 with  $\phi$ -rotation of projector R.
4.  $p_y$  is cleared at 4 with  $\phi$ -rotation of projector L.

5.  $py$  is cleared at 5 with  $\omega$ -rotation of either projector and is overcorrected by introducing in the opposite direction about one-half of the  $y$ -parallax that existed at this point.
6. Steps 1 through 5 are repeated until all five points are parallax free.
7. point 6 is checked for  $py$  and any residual  $y$ -parallax found is distribute throughout the model.

Note that steps 1 to 4 do not disturb the previously oriented points. The  $\omega$  rotation in step 5, however, reintroduces  $y$ -parallaxes into the entire model. The  $\omega$  rotation has contributed to the original  $py$  value at every point and therefore it should have been applied as correction at every step. The effect of  $\omega$  was, however, ignored in the first four steps and all the  $py$  was removed by a single motion. The total  $\omega$  rotation (correction plus overcorrection) at point 5 intends to take care of the original amount of  $py$  that existed in the model at the start of the orientations process. The  $y$ -parallaxes that appear at points 1 to 4 represent the extra correction applied by ignoring initially the effect of  $\omega$  on the  $py$ .

The exact amount of the overcorrecting to be introduced by  $\omega$  depends on the type of camera used to take the photographs and on the location of point 5. The *overcorrection factor*  $K_o$  can be determined by the formula:

$$K_o = \frac{1}{2} \left( 1 - \frac{f^2}{d^2} \right)$$

and the *total correction factor*  $K_t$  by:

$$K_t = \frac{1}{2} \left( 1 + \frac{f^2}{d^2} \right)$$

where  $f$  is the principal distance and  $d$  is the distance from point 1 to point 5 measured on the diapositive. The projection height  $h$  is used instead of  $f$  when  $d$  is measured on the projection plane in model space.

Under ideal conditions the entire model should be parallax free after steps 1 to 4 have been repeated. In reality, however, several iterations are needed to complete the orientation depending how closely the assumptions are met on which the orientation procedure is based. These assumptions are that:

- a) the terrain is flat
- b) the six points form a regular grid, and
- c) the overcorrection is exact.

The steps of the one projector, dependent pair relative orientation are as follows:

1.  $p_y$  is cleared at 2 with Y translation,
2.  $p_y$  is cleared at 1 with K rotation,
3.  $p_y$  is cleared at 4 with Z translation,
4.  $p_y$  is cleared at 3 with  $\phi$  rotation,
5.  $p_y$  is cleared at 6 with  $\omega$  rotation and is overcorrected
6. repeat steps 1 through 5 until the five orientation points are parallax free.
7. check point 5 for  $p_y$ .

Usually the right-hand projector is chosen to perform the orientation.

The  $y$ -parallax equations derived in Section 4.5 are the mathematical foundations of the empirical relative orientation methods presented here. Equation 4-18 defines  $p_y$  at the six orientation points as a function of the five independent pair orientation elements. Reviewing this section gives further clarification of the procedures used in instruments.

Many stereoplotters have precise graduated circles and scales to measure the projector motions, and a numerical method of orientation can also be employed. In this case, the  $y$ -parallaxes are measured with a  $b_y$  or  $\omega$  motion at the six points, the orientation elements computed by equation 4-19 or 4-20, and the values set in the instrument. Usually a manual touch up is still necessary because the computation of the orientation elements is non-rigorous.

After relative orientation is completed, a true spatial model of the terrain exists which can be observed through the viewing system. Note that the model formation step that must follow the analytical relative orientation is not needed here since the intersection of corresponding rays is an integral part of the instrumental orientation process. The scale of the model thus created is, however, unknown and its orientation and position with respect to the object space coordinate system is arbitrary. These are defined in the absolute orientation.

#### 7.1.4.3 Absolute orientation

Absolute orientation has seven elements. These are the scale, the three angular orientation elements and the three translation elements of the model. In analytical photogrammetry a simultaneous solution of the seven parameter similarity transformation

(equation 4-13) takes care of absolute orientation. In analogue photogrammetry a sequential solution must be employed in the following steps:

1. scaling the model,
2. leveling the model,
3. X and Y translation,
4. azimuthal orientation, and
5. Z translation.

The model must include a minimum of two horizontal and three vertical control points to perform this orientation. These points are plotted on the map manuscript sheet at the required scale.

The scale of a model is controlled by the length of the base ( $b$ ) which is the distance in space between the two projection centers. The three components are  $bx$ ,  $by$  and  $bz$ . The model scale selectable is limited by the scale of the photographs and by the operational range of the particular stereoplotter.

In a fully manual operation, *scaling* (Step 1) is performed as follows: (Figure 7-19) The floating mark is set on one of the horizontal control points in the model, and the manuscript is moved until the plotted point is directly under the plotting pencil. The floating mark is then set on another horizontal control point, and the manuscript is rotated around the first control point until the line connecting the two control points meets the plotting pencil. The length of the base is then changed until the length of the control line in the model and on the manuscript are equal. This process also takes care of the  $X$ ,  $Y$  shift and the azimuthal rotation ( $\alpha$  or common  $\kappa$ ) of the model (Steps 3 and 4).

The required base setting can also be precalculated as:

$$bx^1 = bx \frac{D}{d}$$

where  $bx$  and  $bx^1$  are the existing and the required base settings, and  $D$  and  $d$  are the lengths of the control line in the manuscript and in the model respectively.

If the intended model scale is given, then the new base setting is calculated as

$$bx^1 = bx \frac{SF1}{SF2}$$

where  $SF1$  and  $SF2$  are the existing and the desired scale factor of the model.

If the  $Y$  and  $Z$  settings of the two projectors are not equal which is the case when the dependent pair relative orientation is employed, then the  $by$  and  $bz$  base components must also be changed by the same ratio as for  $bx$ . In the fully manual operation, this problem is solved by clearing the  $y$ -parallax, that appears after the  $bx$  component was scaled, at point 2 with a  $by$  motion and at point 4 or 6 with a  $bz$  motion. (Figure 7-20)

Leveling the stereomodel (Step 2) means to set the  $XY$  plane of the model horizontal (Figure 7-21). It is accomplished by the common rotations  $\Omega$  and  $\Phi$  whereby the entire model is rotated around its  $X$  and  $Y$  coordinate axes. (See Figure 7-15). The word common indicates that both projection systems are rotated as a unit. First the tilt of the model is determined by comparing the elevation of vertical control points as measured in the model with their known values. Then the  $\Omega$  and  $\Phi$  rotations are applied in one of the following three ways, depending on the construction of the instrument:

1. tilting the frame supporting the projectors (Figure 7-22),
2. tilting the map table to set it parallel with the model datum plane,
3. individual projector rotation whereby each projector is rotated sequentially by the same amount of and in the same direction. (Figure 7-31).

The first two methods rotate the whole model but the third method does not. In this case only the projectors rotate around their respective axes and the base which is also a part of the model, remains stationary. Therefore, a  $by$  and  $bz$  shift must follow the individual projector rotations as a corrective measure, as shown in Figure 7-23. This problem is solved by clearing the  $y$ -parallaxes that appear in the model after the individual projector rotations at point 2 with a  $by$  motion and at point 6 with a  $bz$  motion.

In the empirical method of absolute orientation the amount of  $\Omega$  and  $\Phi$  rotations needed to level the model is determined by the estimation. The dials of the rotations or the pitch of the levelling screws can be of assistance. Although three vertical control points, which form a large triangle, are sufficient for the leveling, a point near each corner of the model simplifies the orientation process and also provides a check point.

In the numerical method of absolute orientation, the required rotations are completed from the slope of the model and are set on the appropriate dials. For four control points as in Figure 7-24,

$$\tan \Omega = \frac{\Delta h_F - \Delta h_C}{L_{CF}} \quad \text{and} \quad \tan \Phi = \frac{\Delta h_E - \Delta h_F}{L_{EF}}$$

where the  $\Delta h$  values represent the discrepancies between the elevations read in the model and the elevations of the control points, and the  $L$  values are the lengths of the lines joining the control points. Point  $D$  is used as check point.

In case of three control points, the  $X$  and  $Y$  component of the model tilt must first be determined. According to Figure 7-25

$$\Delta h_4 = \Delta h_2 + \frac{L_{24}}{L_{23}} (\Delta h_3 - \Delta h_2) \quad \text{and}$$

$$\Delta h_5 = \Delta h_1 + \frac{L_{15}}{L_{13}} (\Delta h_3 - \Delta h_1)$$

The model rotations are then computed as

$$\tan \Omega = \frac{\Delta h_5 - \Delta h_2}{L_{25}} \quad \text{and} \quad \tan \phi = \frac{\Delta h_4 - \Delta h_1}{L_{14}}$$

Several stereoplotters have only nine degrees of freedom ( $\omega$ ,  $\phi$ ,  $\kappa$  left and right and  $b_x$ ,  $b_y$ ,  $b_z$ ) instead of twelve. The operation of these is restricted to the independent pair relative orientation and to the absolute orientation with individual projector rotations.

The  $Z$  translation (Step 5) is introduced by placing the floating mark on one of the vertical control points and then setting the height counter to the elevation of that point.

## 7.2 Analytical Plotters

Analytical photogrammetry has the advantage of

- rigorous application of corrections to measured image coordinates;
- no physical limitations posed to the photogrammetric solutions, such as orientation of the photo, principal distance, type of sensor, etc.
- high accuracy.

It is, however, not practical for mapping, since only point by point solution is possible.

Analogue instruments, on the other hand, place physical limitations on the type of photography that can be handled, on the corrections that can be applied to the measurements, and provide lower accuracy. Visualization of the stereo model and continuous measurement (plotting) of planimetric details and contours is, however, possible.

The analytical plotter is an instrument that combines the advantages of analytical and analogue photogrammetry. It consists essentially of a precision stereocomparator, which serves as the measuring and viewing system, an on line digital computer, which acts as the projection system, and a coordinatograph to execute the plotting. Although the model created and the photogrammetric solution. are mathematical, stereo viewing and point by point or continuous measurement are possible. Transformation between image, model and object coordinates is carried out analytically in the computer, in real time as the image is scanned by the operator. This instrument was invented by Dr. Helava at the National Research Council of Canada photogrammetric laboratory in Ottawa, in 1957.

The principle of the instrument is as follows: The XYZ movements in the stereomodel introduced by the operator through the hand wheels and the foot disk are picked up by encoders and transmitted to the computer. A real time program then computes the x,y coordinates in the two images that correspond to the particular model point, applies the necessary corrections, and moves the left and right measuring mark, with the help of servo motors, to the correct image locations. In this manner, a parallax free stereomodel is maintained in the viewing area at all times. The collinearity equations are used to calculate the left and right image coordinates as a function of the interior and exterior orientation elements and the model coordinates. A simplified flow-chart of this program is shown in Figure 7-26. This computation must be executed at least 30 times a second to assure a smooth movement of the measuring marks. The stereomodel is set up in the following manner

- **Interior Orientation:** The operator enters into the computer the calibrated principal distance and the calibrated coordinates of the fiducial marks, and measures the coordinates of the fiducial marks in the image. The position of the principal point and the parameters for the transformation from the instrument system to the image coordinate system are then computed. Correction parameters for lens distortion, refraction, earth curvature, etc. are also computed if the appropriate data has been entered.
- **Relative Orientation:** The operator measures the y-parallaxes at six or more points and the five relative orientation parameters are computed by least squares adjustment.
- **Absolute Orientation:** The operator measures the model coordinates of all control points and enters the corresponding ground coordinates. The seven parameters of the absolute orientation are then computed by least squares adjustment.

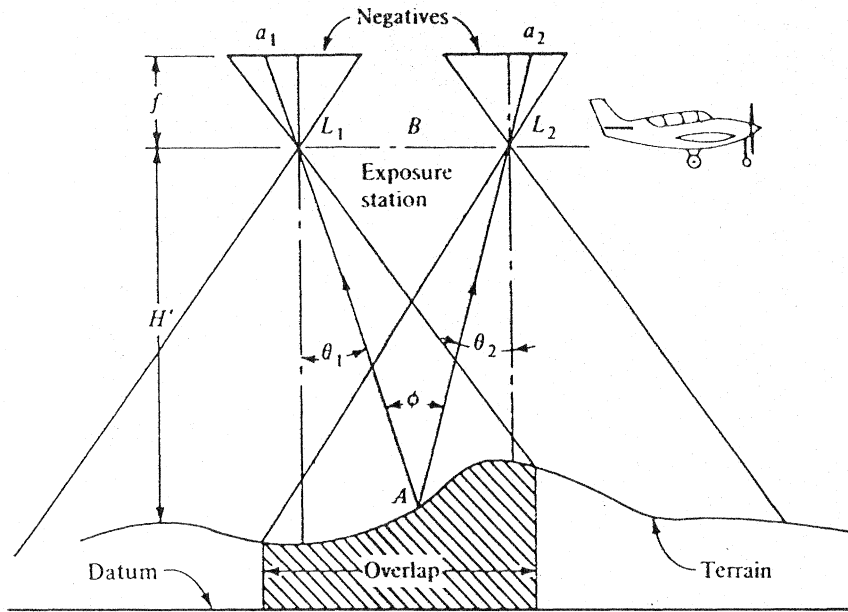
Note, that a measurement consists only of setting the measuring mark on the point. The readings are automatically entered into the computer via the encoders. If the approximate

location of points to be measured area known, such is the case for the fiducial marks and the relative orientation points, the computer can be pre-programmed to drive the measuring mark to the vicinity of these points. The operator must only perform the precise setting of the mark. (See also the description of the analytical plotters in Appendix II.)

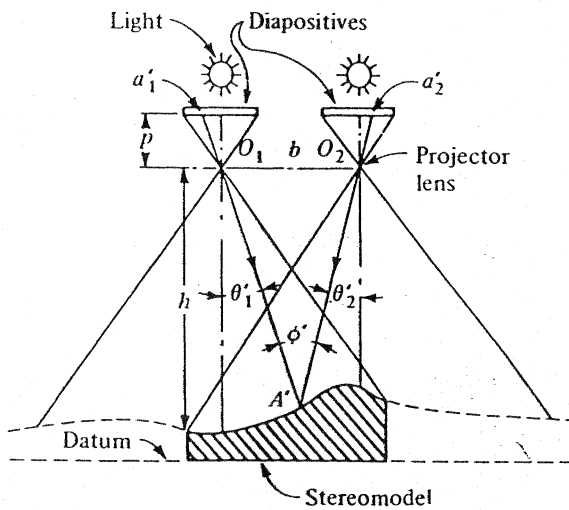
### 7.3 Digital Photogrammetric Workstations

Digital photogrammetry means to perform analytical photogrammetric operations on digital images. Photographs printed on film, glass or paper are digitized in image scanners and become a matrix of digital picture elements (pixels). The hardcopy image becomes a softcopy image which can readily be manipulated in a computer. Thus the term *softcopy photogrammetry* has emerged.

The measurements made on the digital data are processed by mathematical modeling according to the well known techniques of analytical photogrammetry. The analytical plotter is, however, replaced by an off-the-shelf computer graphics workstation. The high quality complex optical trains, the accurate mechanical positioning movements, the high precision encoders and the servo motors of the analytical plotter have disappeared. The images are viewed in stereo on the computer monitor with the help of a mirror stereoscope attachment, polarized glasses or liquid crystal shutter glasses. The measuring mark is formed by a few screen pixels grouped for easy pointing and moved around in the display with a mouse, to measure X and Y coordinate. The Z coordinate is obtained by adjusting the X-parallax between the two corresponding images with the help of the display software, activated by a mouse button. Hand wheels or foot disk are not necessary. This device is called *digital photogrammetric workstation* (DPW). It is suitable for the evaluation of any kind of imagery, metric or non-metric, which are acquired in digital form by aerial and satellite mounted remote sensing systems and CCD cameras, or are converted into digital form by image scanners. A detailed look at this new technology will be given in the next photogrammetry course.



(a)



(b)

Figure 7-1

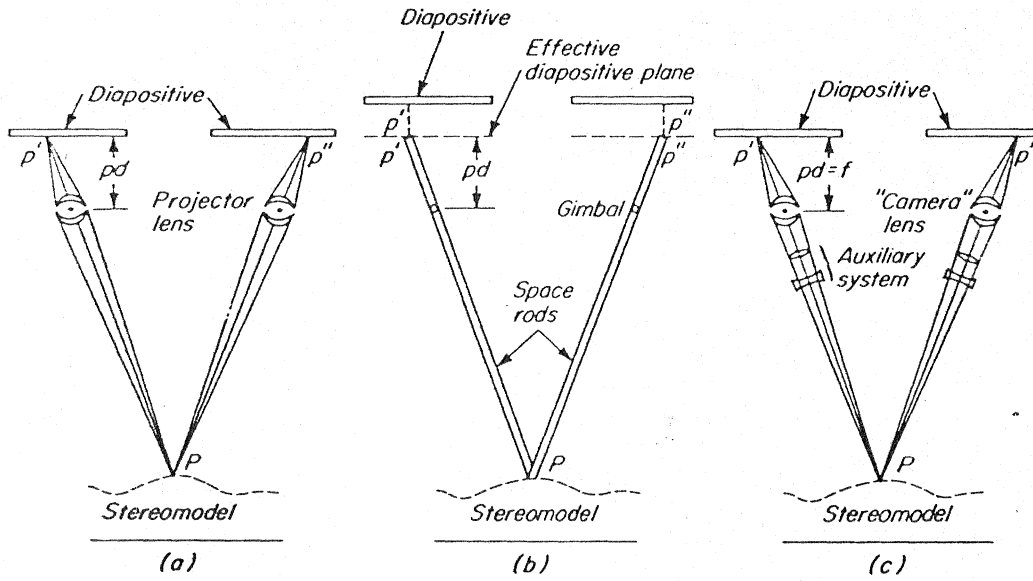


Figure 7-2

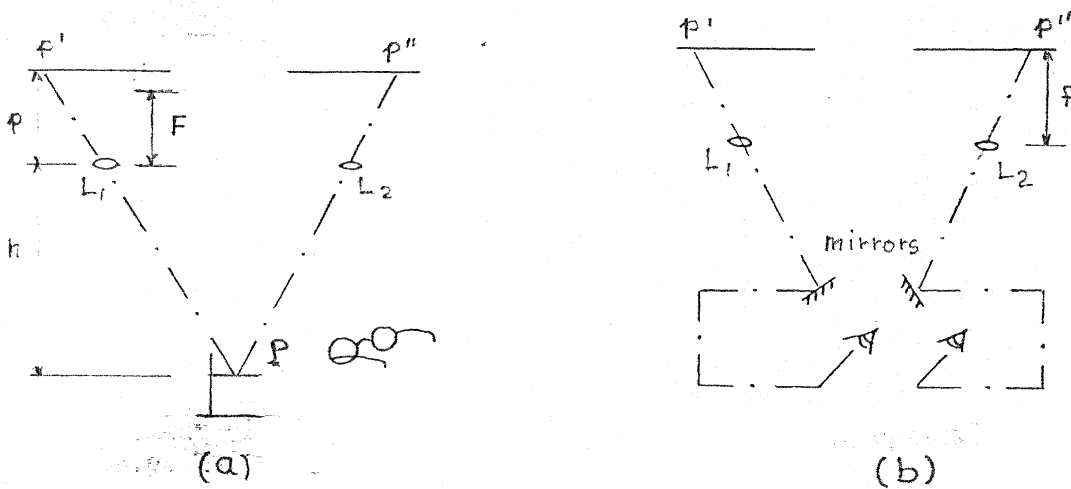


Figure 7-3

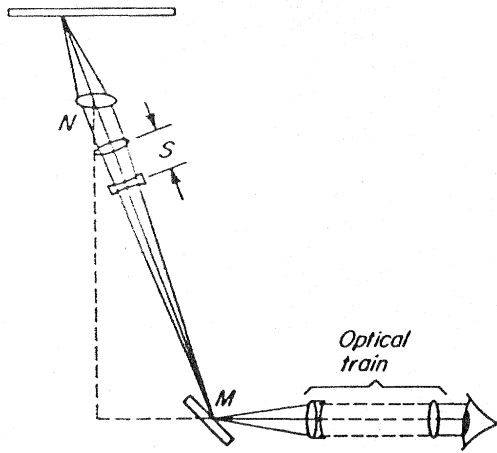


Figure 7-4

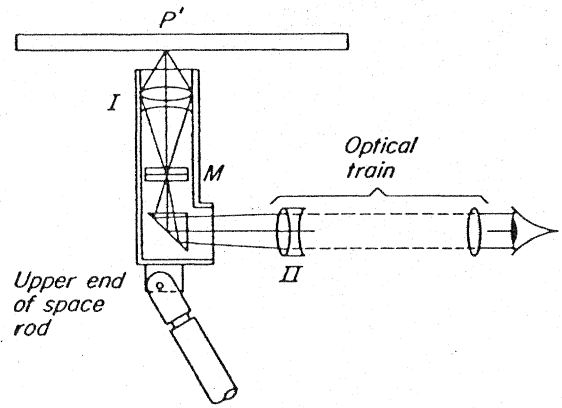


Figure 7-6

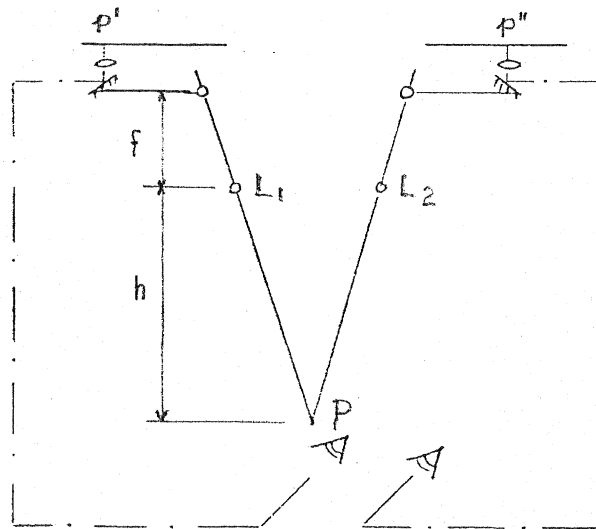


Figure 7-5

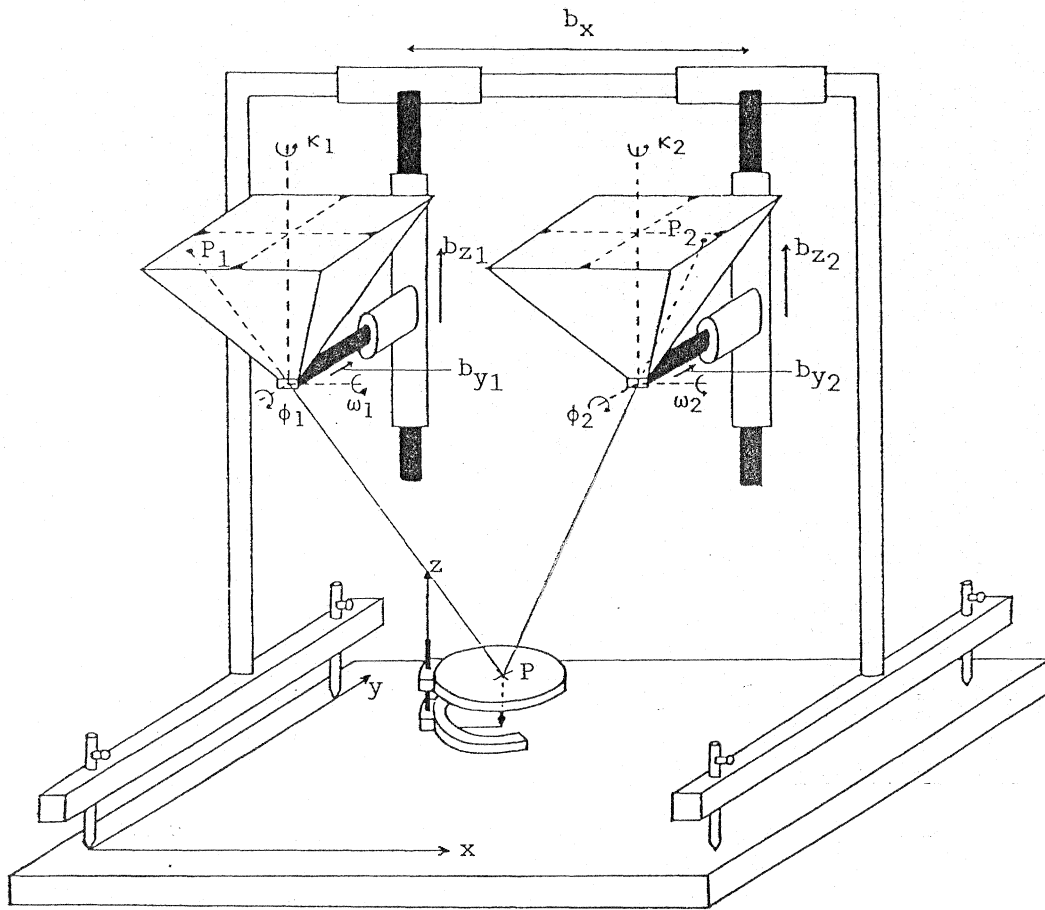


Figure 7-7

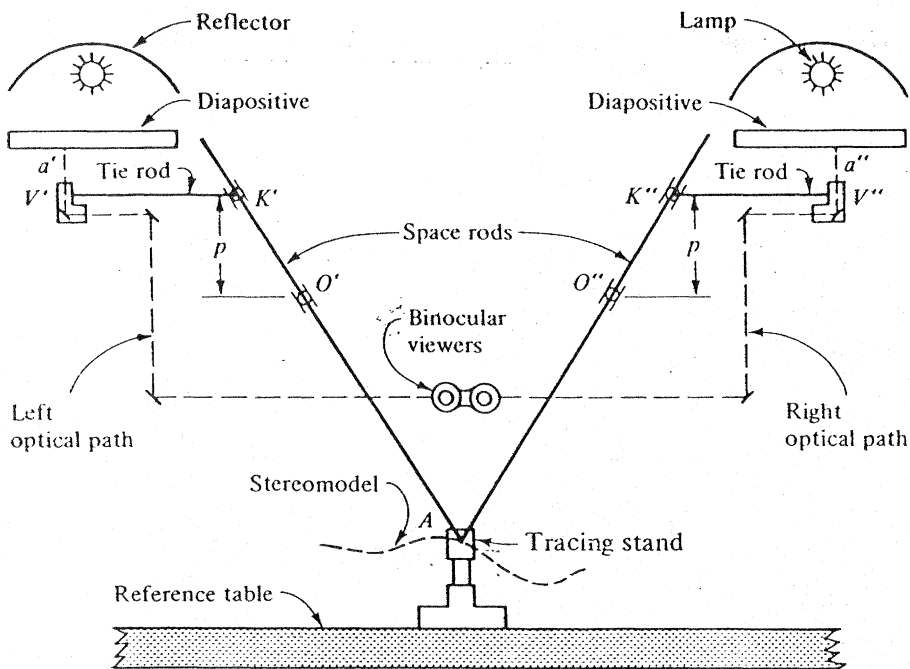


Figure 7-8

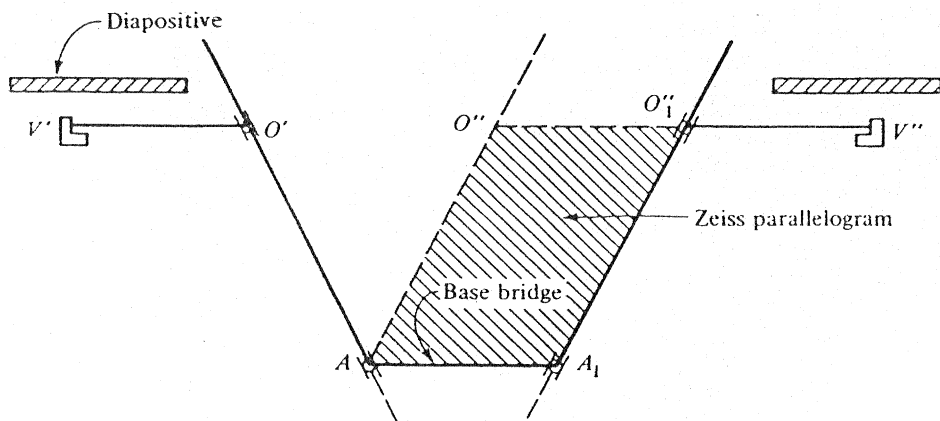


Figure 7-9

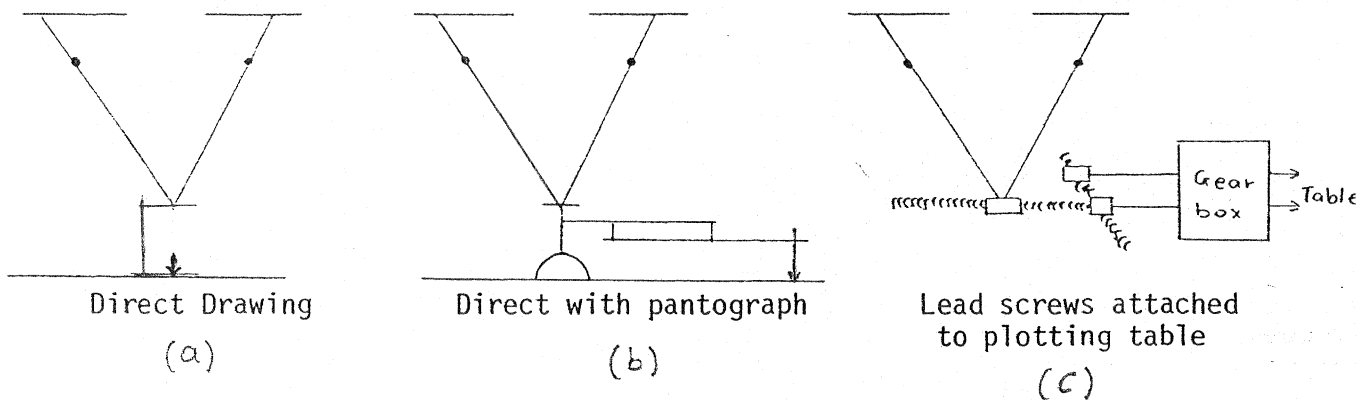


Figure 7-10

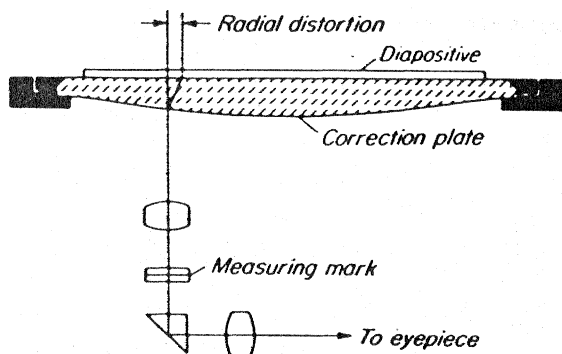


Figure 7-11. Use of aspheric correction plate for eliminating lens distortion.

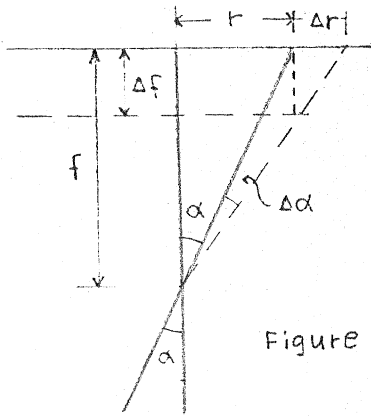
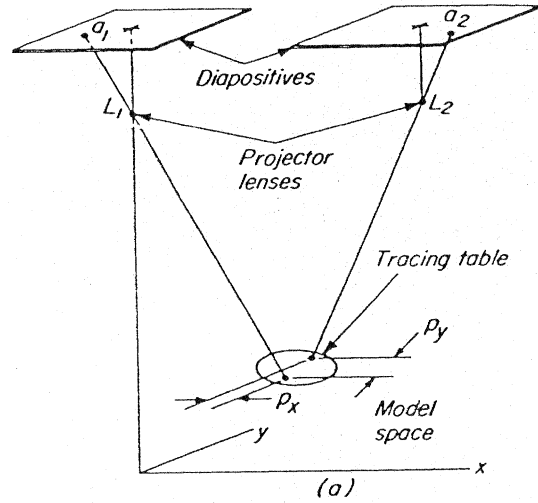


Figure 7-12



(a)

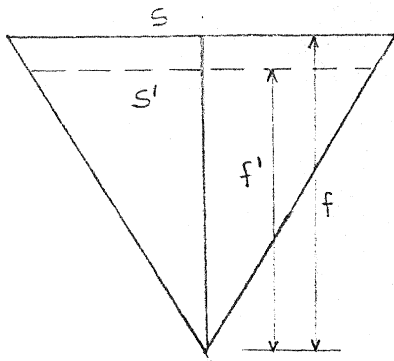
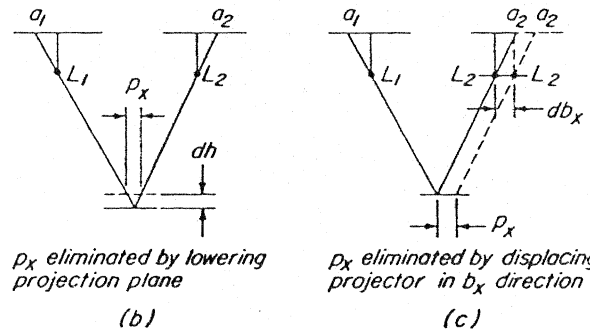


Figure 7-13



$p_x$  eliminated by lowering projection plane

(b)

$p_x$  eliminated by displacing projector in  $b_x$  direction

(c)

Figure 7-14 Nonintersecting rays from two projec

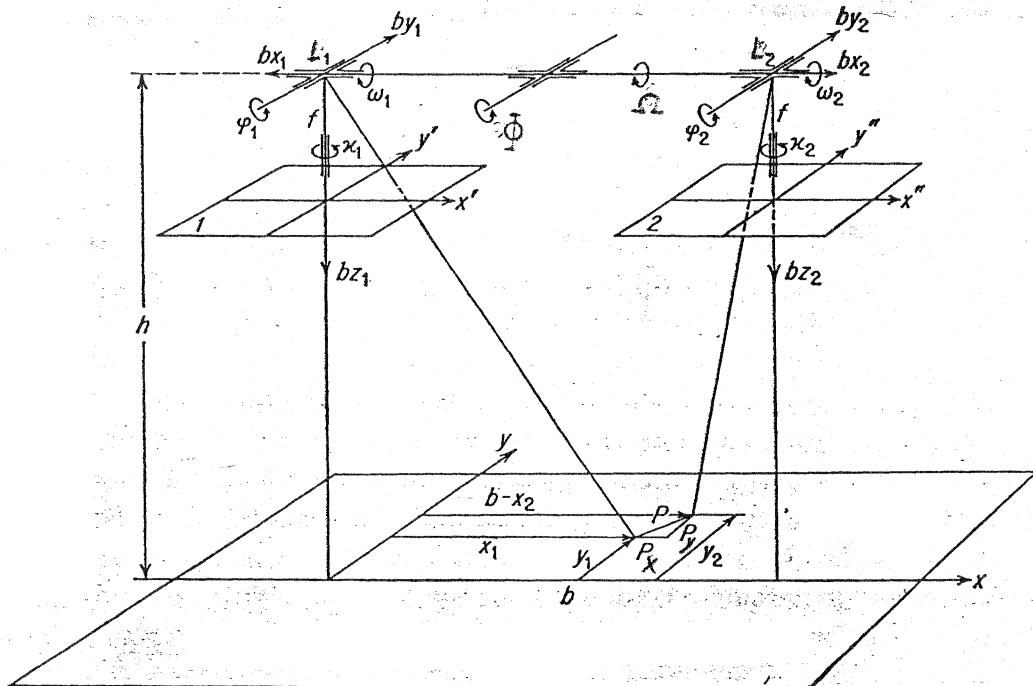


Figure 7-15

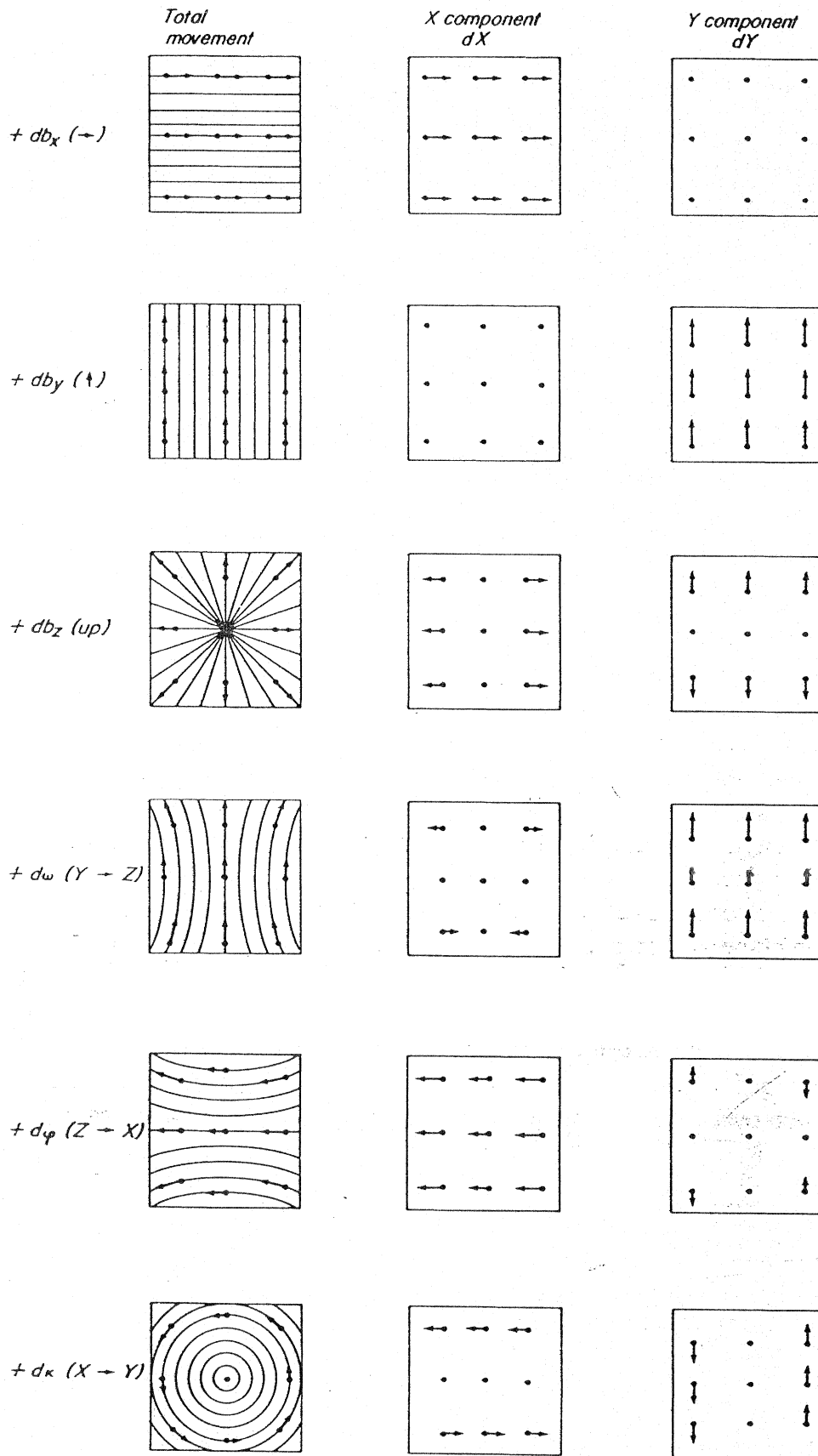


Figure 7-16 Effect of projector motions on movement of points in projection plane.

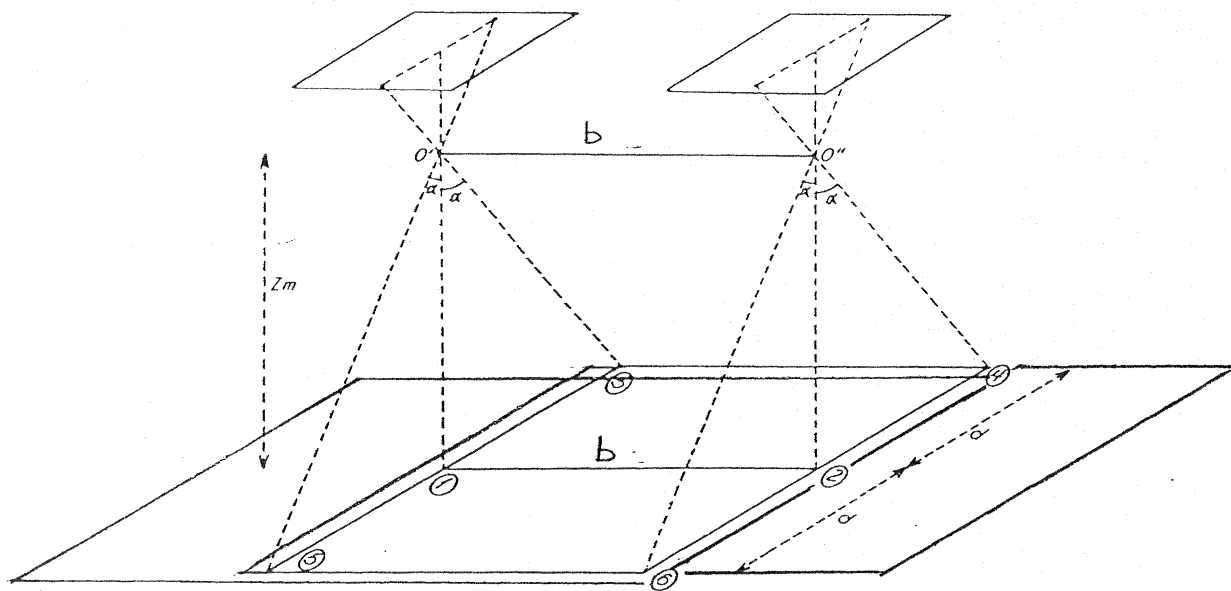


Figure 7-17a

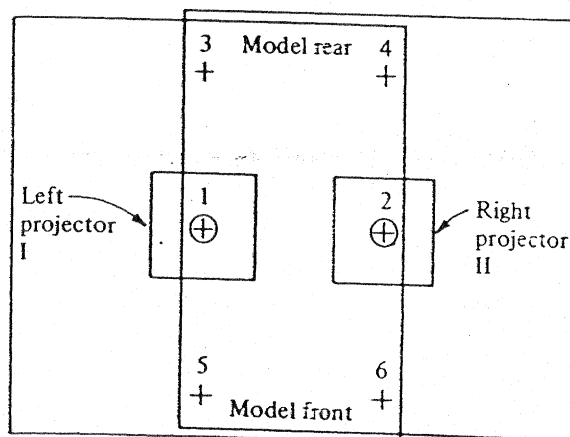
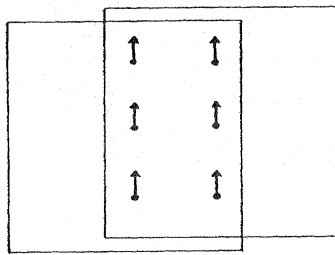
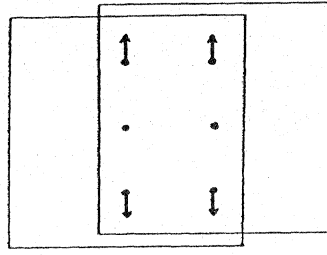


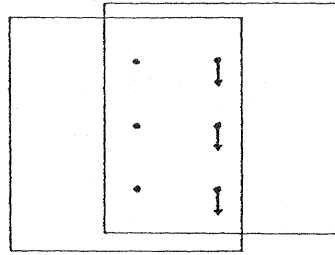
Figure 7-17b



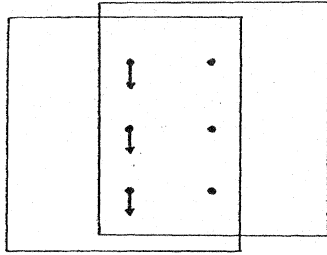
$$db_{y_1} = db_{y_2}$$



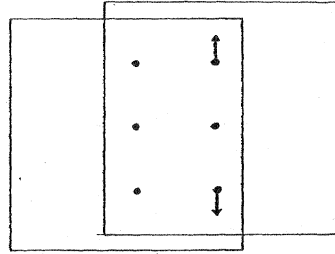
$$db_{z_1} = db_{z_2}$$



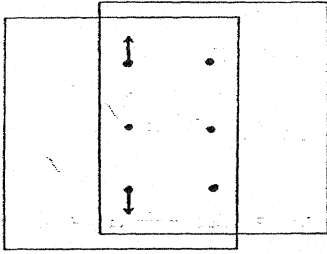
$$d\kappa_1$$



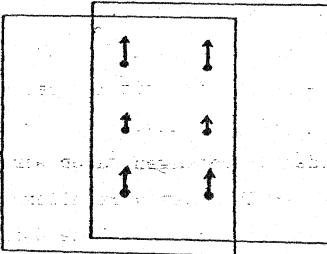
$$d\kappa_2$$



$$d\phi_1$$



$$d\phi_2$$



$$d\omega_2$$

Figure 7-18

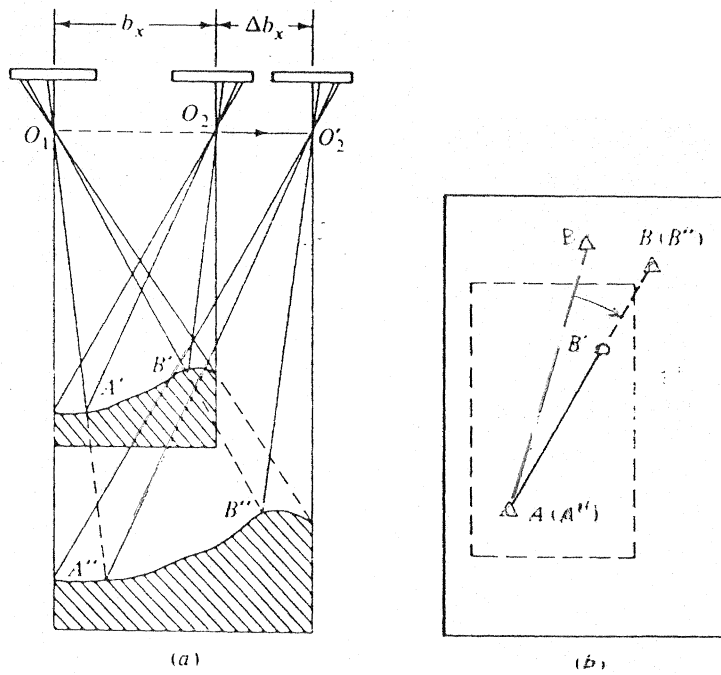


Figure 7-19

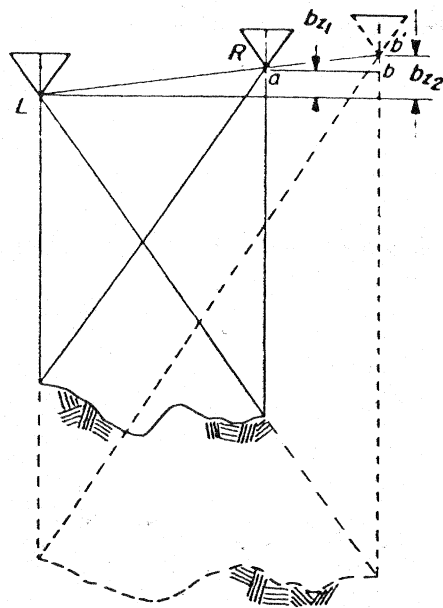


Figure 7-20 Effect of  $b_z$  component on scaling.

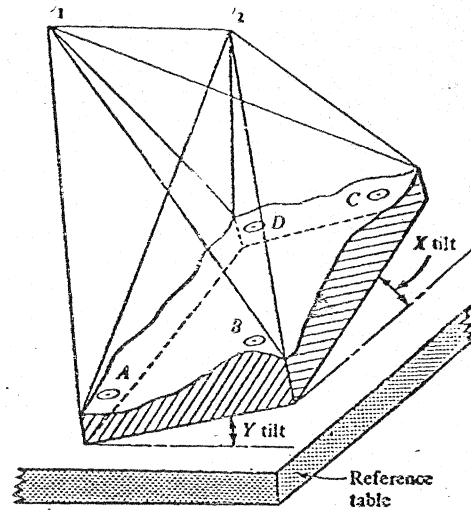


FIGURE 7-21  
Stereomodel that is not level (note X and Y components of tilt).

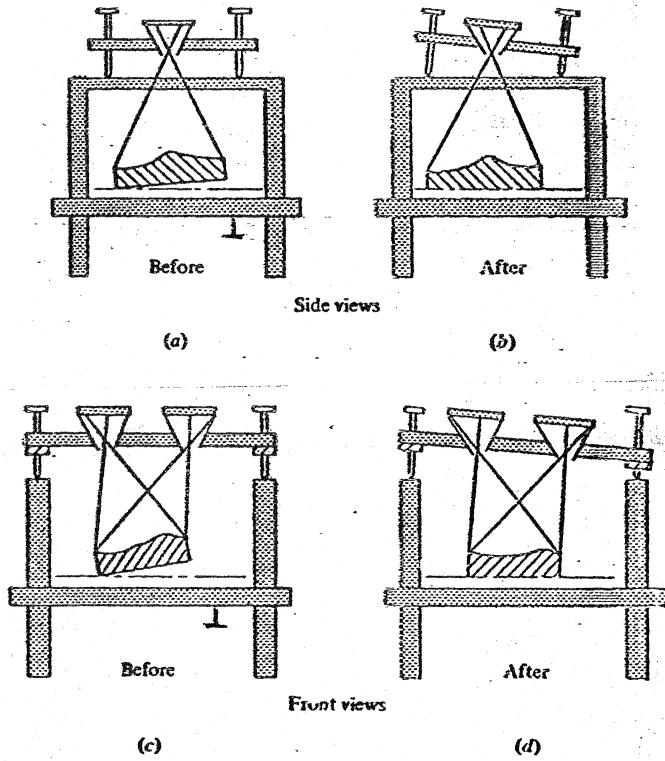


FIGURE 7-22  
(a) and (b) Correcting X tilt of a model by X tilt of projector bar. (c) and (d) Correcting Y tilt of a model by Y tilt of projector bar.



Figure 7-23

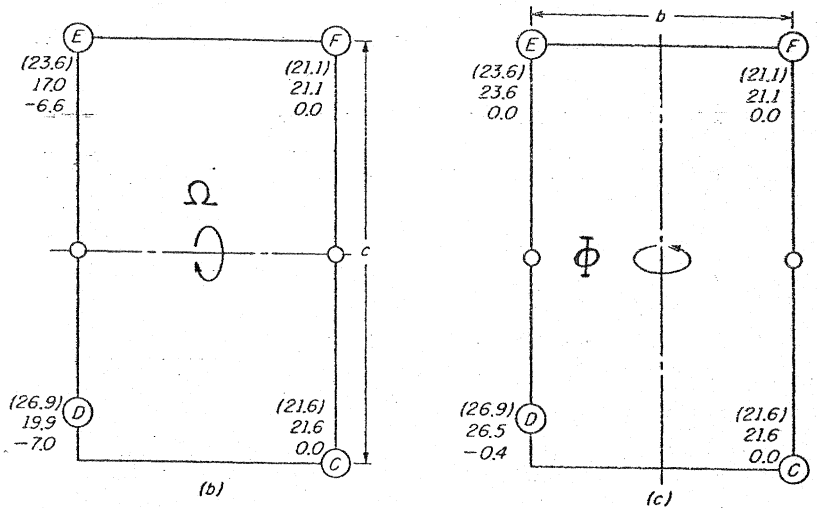
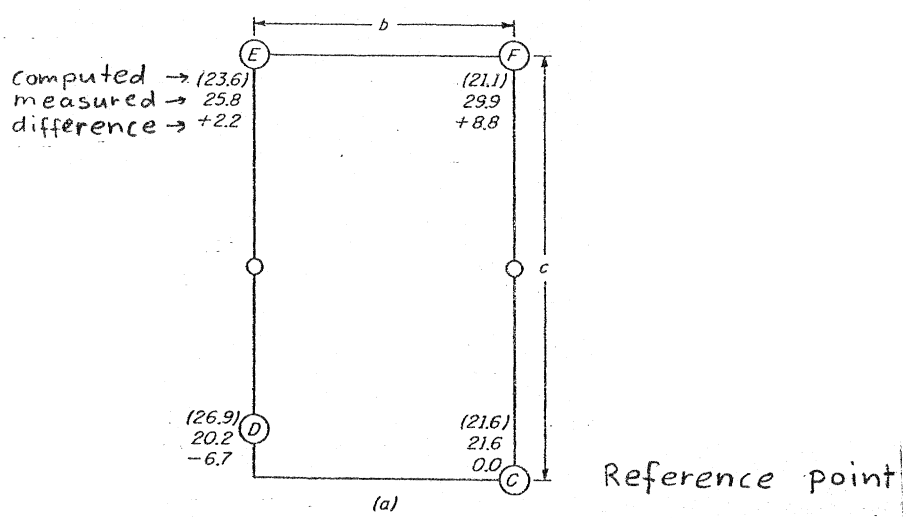


FIG. 7-24 Leveling analysis based on four vertical control points. (a) Readings on control prior to leveling. (b) Readings after rotation of model about X-axis. (c) Readings after rotation of model about Y-axis.

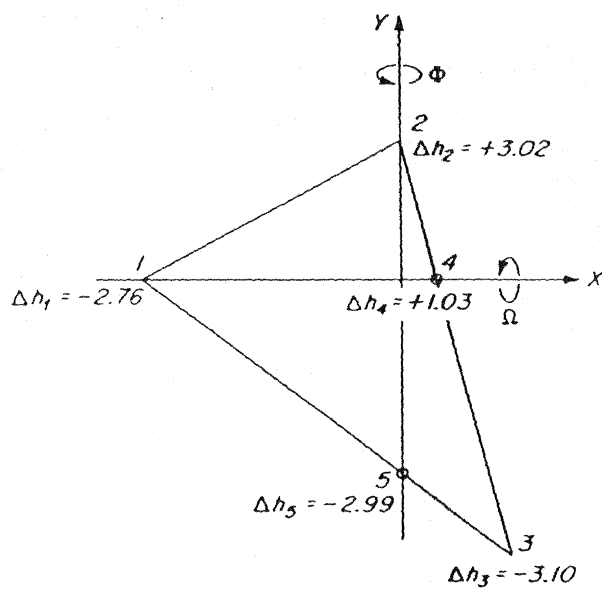


Figure 7-25 Leveling based on analysis of three vertical control points.

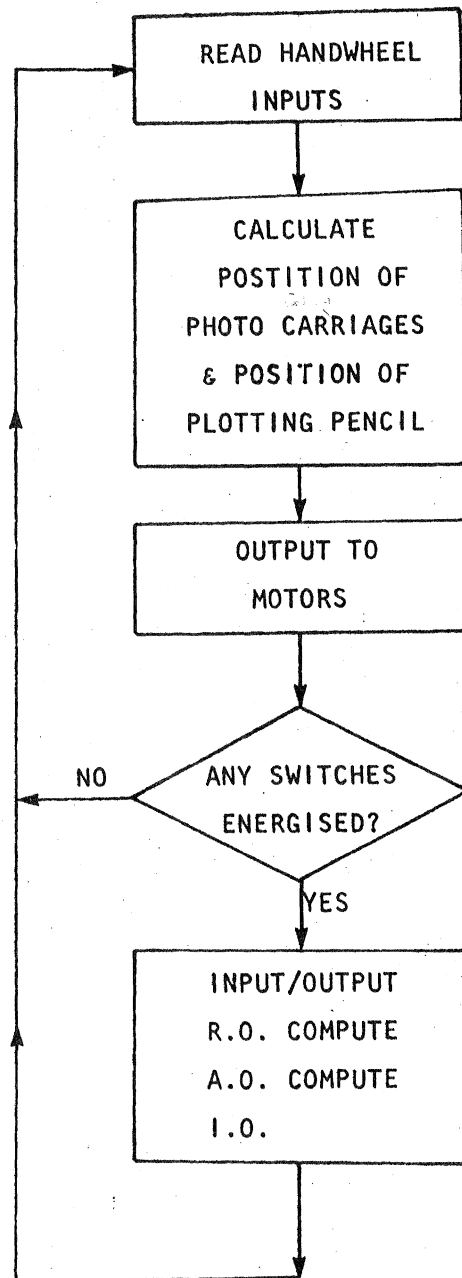


Figure 7-26 Simplified flow chart of real-time program to control movements in analytical plotters

## 8. MULTIPLE PHOTO ORIENTATION

### 8.1 Acquisition of Photographic Coverage

The geometric relationship between image, model and object space is established with the help of control points. These points, which have known X, Y and Z coordinates in the object space coordinate system, are used to determine the exterior orientation elements of a photograph or the absolute orientation elements of a spatial model. A minimum of three control points are needed to orient a photograph or a model. The object space or ground coordinates of these points could be obtained by direct measurements in object space. However, the acquisition of a large number of points would be required to control every photograph needed to cover a large area.. Needless to say, that such operation would be very costly and would negate the primary advantage of photogrammetry, which is the drastic reduction of field work in mapping.

Aerial photographs acquired for mapping are taken at regular intervals along a straight flight path to form a *strip* of photos. A large area is covered by several parallel strips to form a *block* of photographs. Spacing between photographs along a strip is such that a portion of successive photographs cover a common area of the terrain. This lapping along the line of flight is called *forward overlap* or simply *overlap*. (Figure 8-1). Overlaps provide the corresponding rays necessary for spatial positioning, model formation and stereoscopic viewing by space intersection. The amount of overlap is normally 60%. In this manner a continuous double coverage is assured and neighbouring spatial models overlap, which makes the connection of these models possible. The 60% forward overlap results in a 20% overlap of three successive photographs called *triple overlap* and in a 33% common coverage in neighbouring spatial models. Points in the triple overlap selected for model connection are called *pass points* (Figure 8-1).

The photographic coverage from adjacent flight lines are designed to provide a lateral overlap called *side lap*, which normally ranges between 20% and 30%. It assures an uninterrupted coverage and the connection of models in neighbouring strips to form a block of spatial models (Figure 8-2). Points in the sidelap selected for joining neighbouring strips are called *tie points*. Models assembled into a strip or block of spatial models can be regarded as a single model concerning ground control requirement, and can be transformed to the object space coordinate system as a unit.

## 8.2 Model Connection

Three methods can be employed for connecting spatial models:

- Bundle adjustment
- Independent model transformation
- Sequential solution.

The bundle adjustment method is the extension of the simultaneous resection solution for spatial positioning to a strip or block of photographs (see Section 4.3). A pair of observation equations are formed for every projection ray in a strip or block. It includes each ray associated with control, pass and tie points. A simultaneous solution of this equation system yields the exterior orientation elements of every photograph and the object space coordinates of all pass and tie points. It combines space resection and intersection and enforces the intersection of all rays of corresponding image points at the correct object space position (see Figure 8-3).

The bundle adjustment is the most rigorous solution of photogrammetric spatial positioning, but computationally the most demanding. Each ray provides two observation equations of the form of equation (5-3). For example Figure 8-3 shows a small block consisting of two strips, three photos each, or a total of six photographs. Points A, B, C, D are control points, d, e, f, g, h are pass points and b, f, j are tie points. Note that f serves both as pass and tie point. There are a total of 42 rays which give 84 observation equations. The total number of unknowns are:

$$6p + 3n = 69$$

where  $p$  is the number of photographs and  $n$  is the number of new points, those with unknown object space coordinates.

In the independent model transformation spatial models are formed by relative orientation using the overlapping photographs along a strip. Each model is referenced in its own provisional coordinate system. The models may be formed by analytical means, or set up in a stereoplotter. The independent models are joined together by three-dimensional similarity transformation based on pass and tie points (Equation 4-12). Note that the perspective centre of neighbouring photographs are also regarded as common model points and are included in the transformation (See Figure 8-4).

All models are now in a common but provisional coordinate system. This strip or block model is transformed as a unit to the object space coordinate system also by the

three-dimensional similarity transformation based on control points. Model connection and the adjustment to ground control can be performed simultaneously using Equation (4-12) or (5-6), (Figure 8-5).

The sequential solution of model connection is performed in three steps: scale transfer, rotation and translation. The coordinate system of the first model is selected as the coordinate system for the entire strip. Thus, the scale and orientation of the strip is defined by the scale and orientation of the first model.

The scale factor needed to scale model 2 to fit model 1 is computed as the mean ratio of distances between the pass points in the triple overlap, inducing the common perspective centre. The orientation of model 2 to model one is defined by the rotation matrix  $M_2$  which was obtained by the relative orientation of photo 2 to photo 1. The translation elements are the base components in model 1. The same procedure is followed to transform successive models to the previous one until the end of the strip is reached. The coordinates of all perspective centre must also be transformed.

The strip model formed in this manner is then adjusted to the available ground control points with three-dimensional similarity transformation. A simpler method of strip adjustment is by polynomials. The coefficients are based on the discrepancies between the measured coordinates of control points in the strip and their corresponding value in the object space system.

The sequential model connection can also be performed by analogue operations in a stereoplotter with multiple projectors such as a string of Balplexes the following way. The first two projectors are relatively oriented to form model 1 which is then absolutely oriented. Next, the third projector is relatively oriented to the second projector by the dependent pair method. Thereby, the absolute orientation is transferred from model 1 to model 2, with the exception of the scale. Scale transfer is achieved by changing the length of the base in model 2 until the elevation of a pass point in model 2 agrees with that in model 1. All three rays associated with this point are now intersecting at the same point in space (Figure 8-6). Model 1 and 2 are now connected and absolutely oriented.

The process described here is repeated for each successive projector and a strip mode is formed. If additional ground control points are available throughout the strip, a least squares adjustment is performed using polynomials. This procedure is often referred to as *bridging*. Models with ground control serve as bridge piers to support spans of uncontrolled models.

The model connection techniques described here are generally referred to as *aerial triangulation* or *aerotriangulation* and the fitting of strips or blocks of models to control points is called *strip and block adjustment*. It allows to generate object space coordinates of selected points based on only a framework of points surveyed in object space. These points can then serve for the absolute orientation of individual stereo models for map compilation. Aerotriangulation is also a useful method for the densification of survey control of networks or for the determination of the coordinates of specific points like property corners in cadastral surveying.

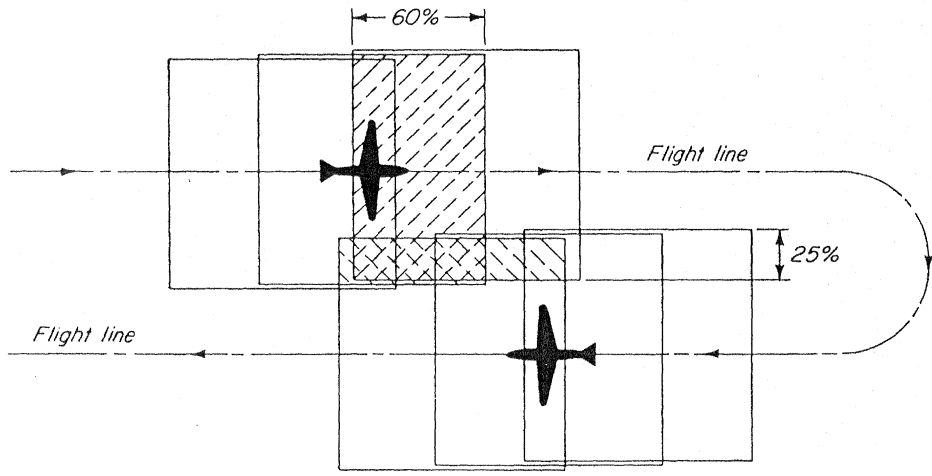


Figure 8-1a. Photographic overlap.

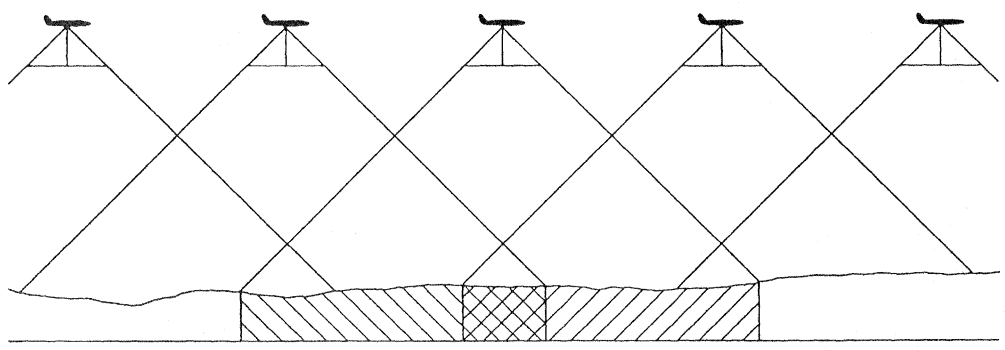


Figure 8-1b. Overlap along flight line.

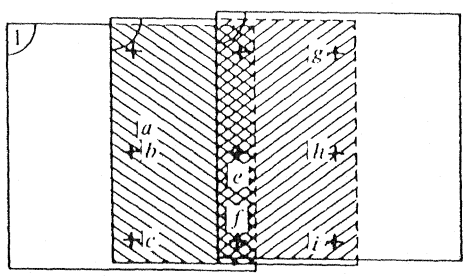
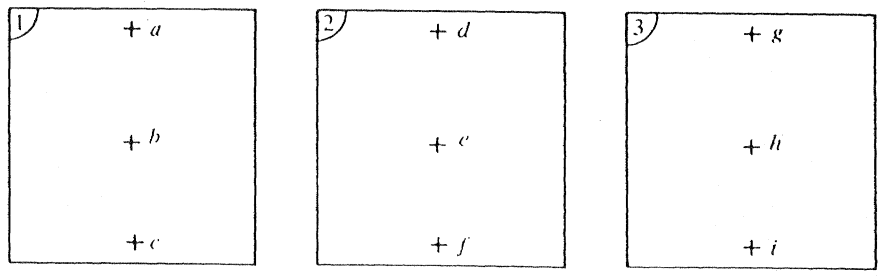
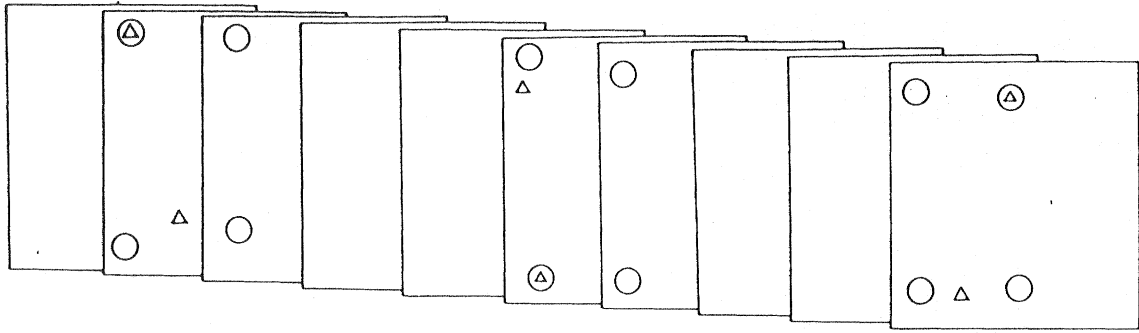
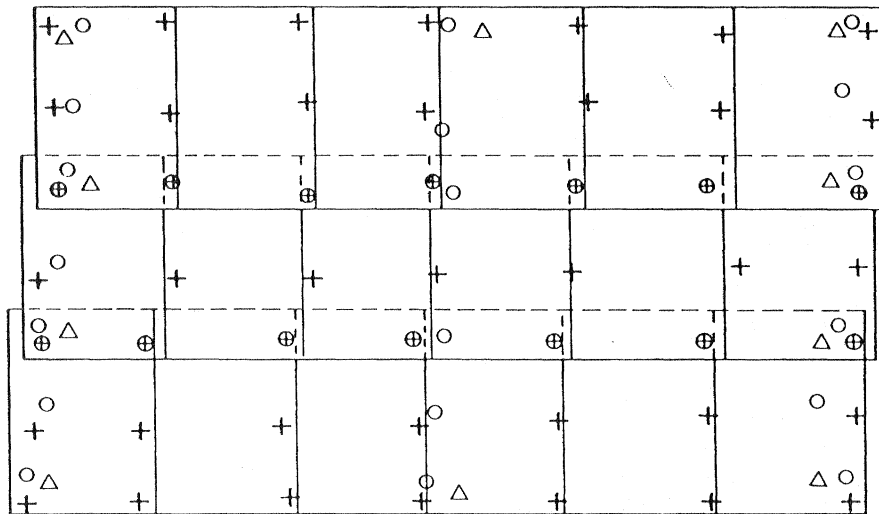


FIGURE 8-1c



- △ Horizontal control point
- Vertical control point
- ⊕ Horizontal and vertical control point

FIGURE 8-2 a



- △ Horizontal control points
- Vertical control points
- + Pass points
- ⊕ Tie points

FIGURE 8-2 b

Block of photos prepared for analytical control extension showing horizontal and vertical ground control points, pass points, and tie points.

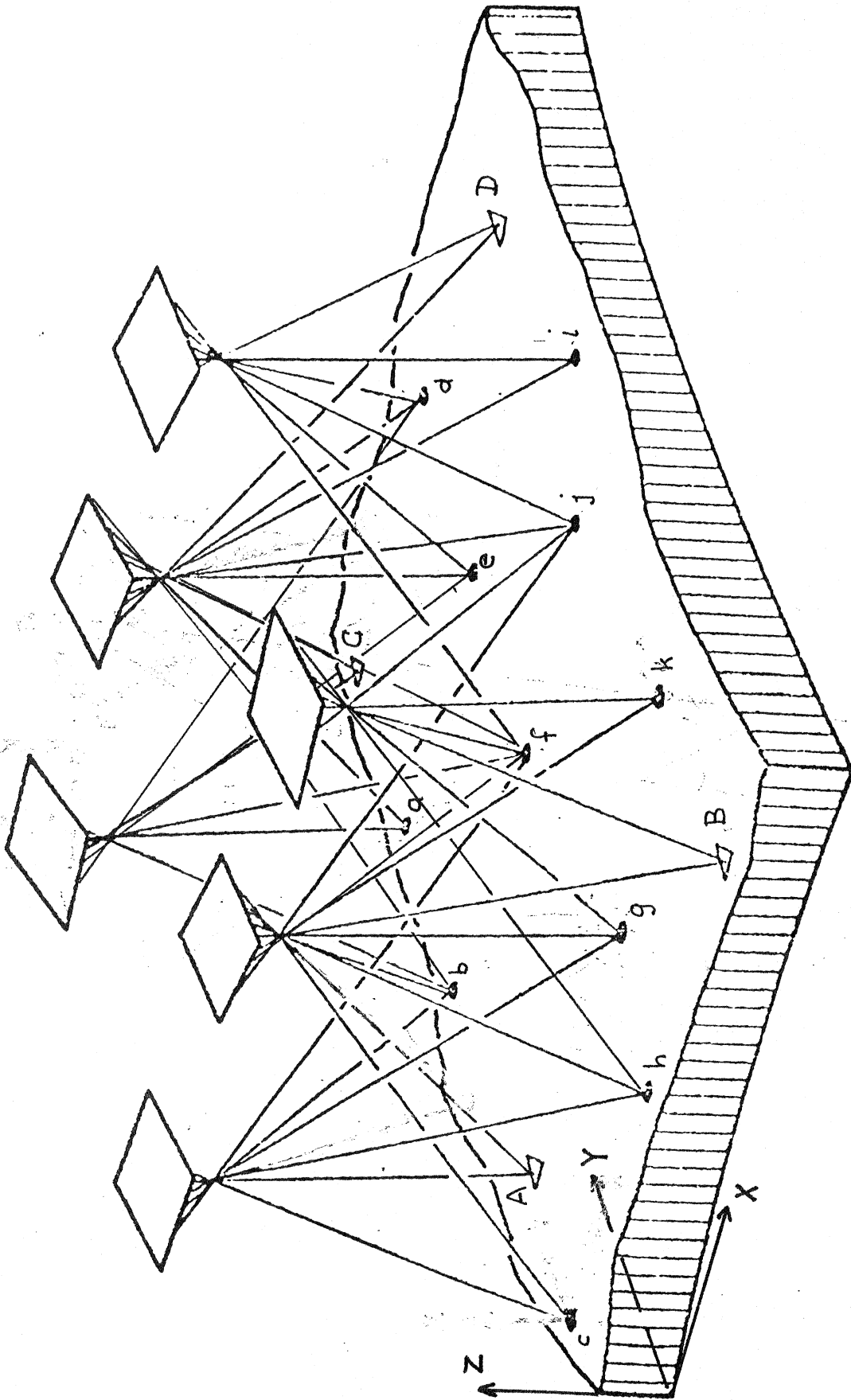


Figure 8-3

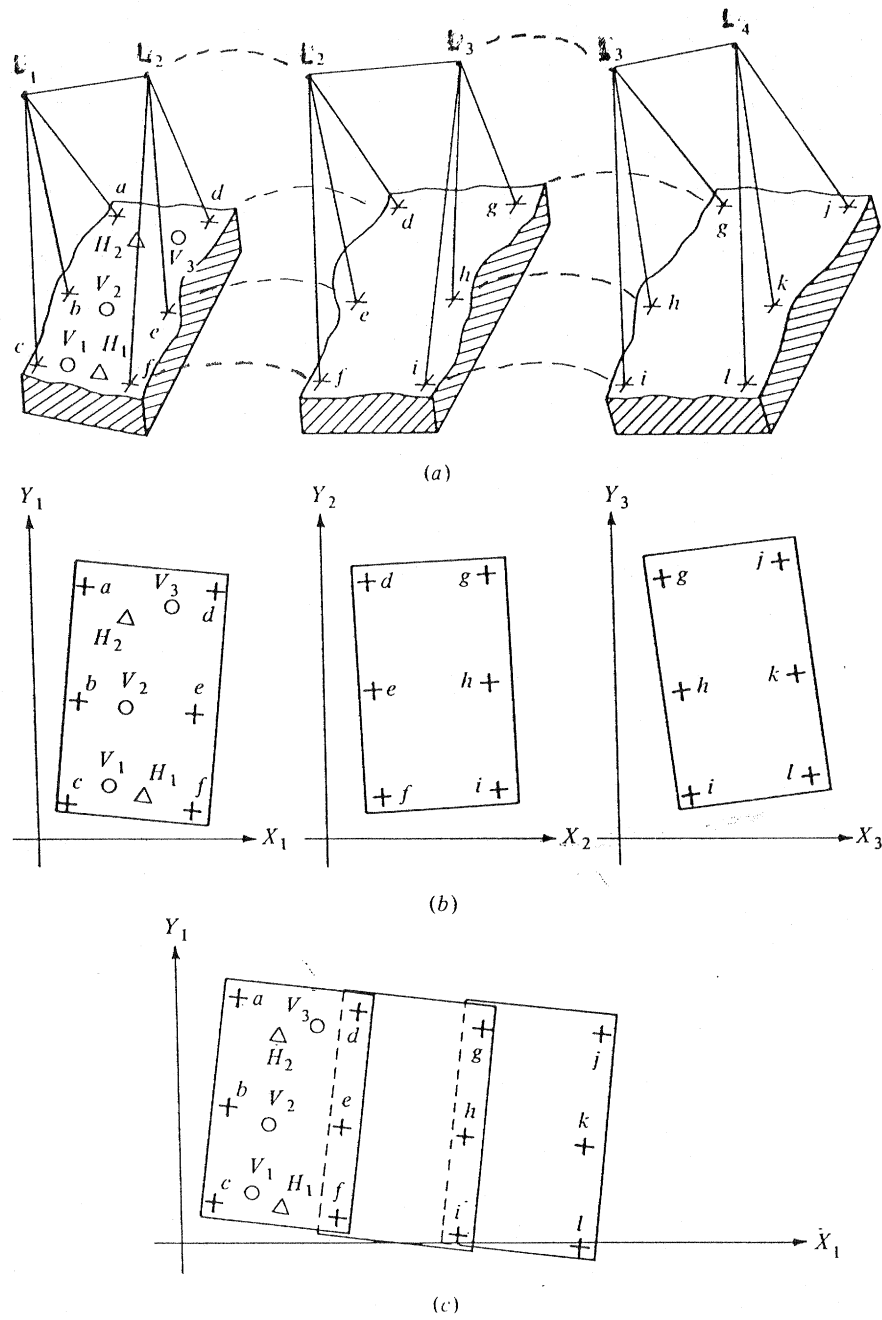


FIGURE 18-4

Independent model or semianalytical stereotriangulation. (a) Three adjacent relatively oriented stereomodels. (b) Individual arbitrary coordinate systems of three adjacent stereomodels. (c) Continuous strip of stereomodels formed by numerically joining the adjacent individual arbitrary coordinate systems into one system.

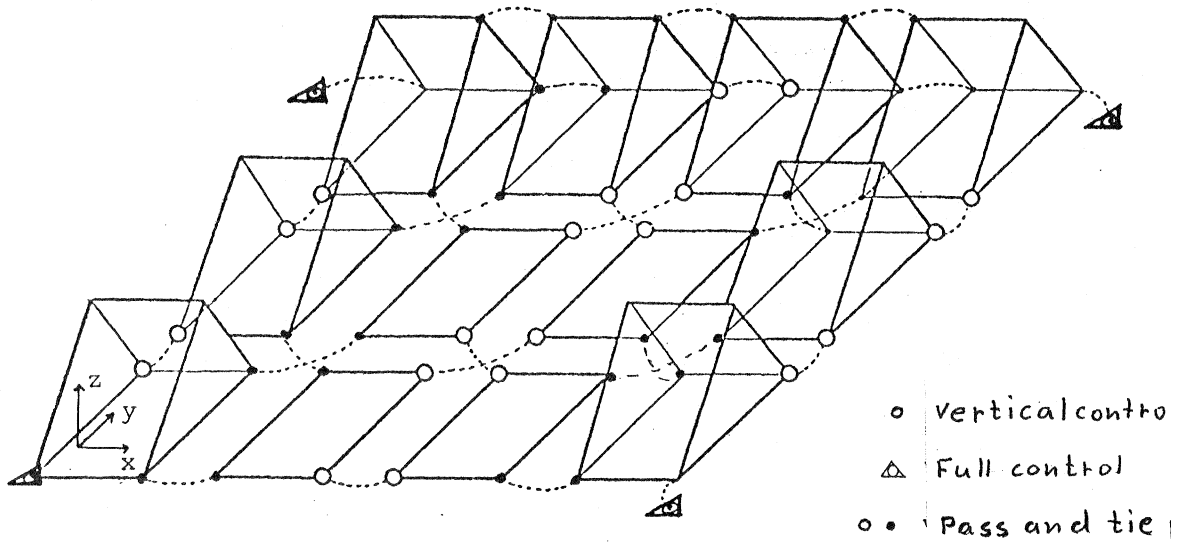


Figure 8-5

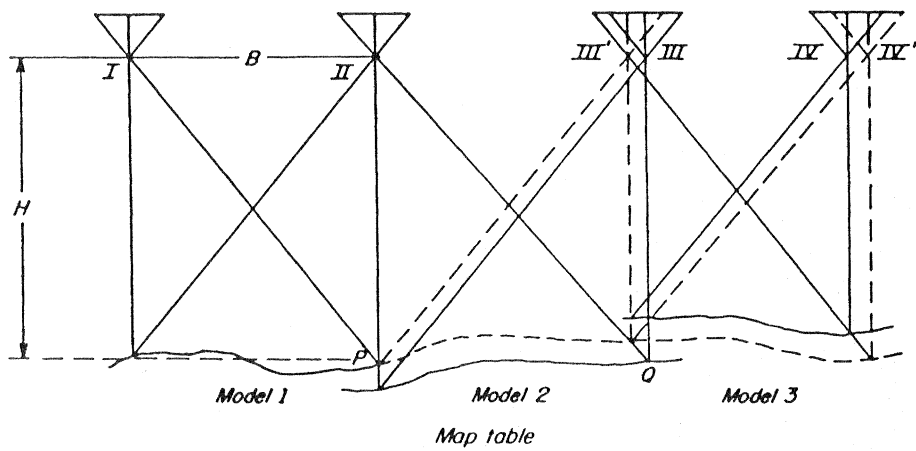


Figure 8-6. Bringing successive models to common scale.

**Appendix I**  
**LINEARIZATION OF THE PHOTOGRAMMETRIC**  
**EQUATIONS**

in which

$$\mathbf{B} = \begin{bmatrix} B_X \\ B_Y \\ B_Z \end{bmatrix} = \begin{bmatrix} X_{L_2} - X_{L_1} \\ Y_{L_2} - Y_{L_1} \\ Z_{L_2} - Z_{L_1} \end{bmatrix} = \text{base components} \quad (\text{C-9})$$

$$\mathbf{a}_1 = \begin{bmatrix} u_1 \\ v_1 \\ w_1 \end{bmatrix} = \mathbf{M}_1^t \begin{bmatrix} x - x_o \\ y - y_o \\ -f \end{bmatrix}_1 \quad (\text{C-10})$$

$$\mathbf{a}_2 = \begin{bmatrix} u_2 \\ v_2 \\ w_2 \end{bmatrix} = \mathbf{M}_2^t \begin{bmatrix} x - x_o \\ y - y_o \\ -f \end{bmatrix}_2 \quad (\text{C-11})$$

and  $\lambda_1$  and  $\lambda_2$  are two scale factors. The relationship given in equation C-8 represents three equations containing the two unknown scale factors  $\lambda_1$  and  $\lambda_2$ . If  $\lambda_1$  and  $\lambda_2$  are eliminated, only one equation remains which may be written in the form of a determinant:

$$F = \begin{vmatrix} B_X & B_Y & B_Z \\ u_1 & v_1 & w_1 \\ u_2 & v_2 & w_2 \end{vmatrix} = 0 \quad (\text{C-12})$$

or in a developed form it becomes

$$B_X(v_1 w_2 - v_2 w_1) - B_Y(u_1 w_2 - u_2 w_1) + B_Z(u_1 v_2 - u_2 v_1) = 0 \quad (\text{C-13})$$

Both equation C-12 and C-13 represent the coplanarity of the four points  $L_1, L_2$  (camera stations), and  $a_1, a_2$  (image points).

#### C-4 LINEARIZATION

All three types of conditions defined in the preceding sections of this Appendix involve equations which are nonlinear. It is very rare that they are used directly in a nonlinear numerical solution. Instead, it is customary to linearize the equations applying Taylor's series expansion and solving the resulting linear equations, then iterating the solution until the effect of the neglected higher-order terms is minimized.

If  $y = f(x)$  is a nonlinear function, the Taylor series expansion is given by

$$y = f(x^o) + \frac{dy}{dx} \Big|_{x^o} \Delta x + \frac{1}{2!} \frac{d^2 y}{dx^2} \Big|_{x^o} (\Delta x)^2 + \dots \quad (\text{C-14})$$

where  $x^o$  is the approximate value for  $x$  at which the function is evaluated. When using the series for linearization, only the first two terms (zero and first

order) on the right-hand side of equation C-14 are used. If  $y$  is a function of two variables  $x_1, x_2$ , that is,  $y = f(x_1, x_2)$  then the linearized form becomes

$$\begin{aligned} y &= f(x_1^o, x_2^o) + \frac{\partial y}{\partial x_1} \Big|_{x_1^o, x_2^o} \Delta x_1 + \frac{\partial y}{\partial x_2} \Big|_{x_1^o, x_2^o} \Delta x_2 \\ &= f(x_1^o, x_2^o) + j_1 \Delta x_1 + j_2 \Delta x_2 \\ &= y^o + [j_1 j_2] \begin{bmatrix} \Delta x_1 \\ \Delta x_2 \end{bmatrix} \end{aligned}$$

or,

$$y = y^o + \mathbf{J}_{yx} \Delta \mathbf{x} \quad (\text{C-15})$$

in which  $\mathbf{J}_{yx}$  is the Jacobian matrix of partial derivatives. Equation C-15 can be generalized to  $m$  functions  $\mathbf{y}$  in terms of  $n$  variables  $\mathbf{x}$ , that is  $\mathbf{y} = f(\mathbf{x})$ ; thus

$$\mathbf{y} \cong \mathbf{y}^o + \mathbf{J}_{yx} \Delta \mathbf{x} \quad (\text{C-16})$$

in which

$$\mathbf{y}^o = \begin{bmatrix} y_1^o \\ y_2^o \\ \vdots \\ y_m^o \end{bmatrix} = \begin{bmatrix} f_1(x_1^o, \dots, x_n^o) \\ f_2(x_1^o, \dots, x_n^o) \\ \dots \\ f_m(x_1^o, \dots, x_n^o) \end{bmatrix}$$

$$\mathbf{J}_{yx} = \frac{\partial \mathbf{y}}{\partial \mathbf{x}} = \begin{bmatrix} \frac{\partial y_1}{\partial x_1} & \dots & \frac{\partial y_1}{\partial x_n} \\ \vdots & \dots & \vdots \\ \frac{\partial y_m}{\partial x_1} & \dots & \frac{\partial y_m}{\partial x_n} \end{bmatrix} \text{ evaluated at } \mathbf{x}^o$$

$$\Delta \mathbf{x} = \begin{bmatrix} \Delta x_1 \\ \Delta x_2 \\ \vdots \\ \Delta x_n \end{bmatrix}$$

#### C-5 LINEARIZATION OF THE PROJECTIVITY EQUATIONS

The projectivity equations equation C-7 can be written in the functional form as

$$\begin{aligned} F_1 &= -u + \frac{a_1 u' + b_1 v' + c_1}{a_o u' + b_o v' + 1} = -u + \frac{r}{t} = 0 \\ F_2 &= -v + \frac{a_2 u' + b_2 v' + c_2}{a_o u' + b_o v' + 1} = -v + \frac{s}{t} = 0 \end{aligned} \quad (\text{C-17})$$



Consider as an example the sequence  $\omega \rightarrow \phi \rightarrow \kappa$  (see section A-3) where

$$\mathbf{M} = \mathbf{M}_\kappa \mathbf{M}_\phi \mathbf{M}_\omega$$

Therefore,

$$\frac{\partial \mathbf{M}}{\partial \omega} = \mathbf{M}_{\omega'} = \mathbf{M}_\kappa \mathbf{M}_\phi \frac{\partial \mathbf{M}}{\partial \omega}$$

but

$$\begin{aligned} \frac{\partial \mathbf{M}_\omega}{\partial \omega} &= \begin{bmatrix} 0 & 0 & 0 \\ 0 & -\sin \omega & \cos \omega \\ 0 & -\cos \omega & -\sin \omega \end{bmatrix} \\ &= \begin{bmatrix} 1 & 0 & 0 \\ 0 & \cos \omega & \sin \omega \\ 0 & -\sin \omega & \cos \omega \end{bmatrix} \begin{bmatrix} 0 & 0 & 0 \\ 0 & 0 & 1 \\ 0 & -1 & 0 \end{bmatrix} \end{aligned}$$

or

$$\frac{\partial \mathbf{M}_\omega}{\partial \omega} = \mathbf{M}_\omega \begin{bmatrix} 0 & 0 & 0 \\ 0 & 0 & 1 \\ 0 & -1 & 0 \end{bmatrix}$$

Then,

$$\mathbf{M}_{\omega'} = \mathbf{M} \begin{bmatrix} 0 & 0 & 0 \\ 0 & 0 & 1 \\ 0 & -1 & 0 \end{bmatrix} \quad (\text{C-26})$$

Next,

$$\frac{\partial \mathbf{M}}{\partial \phi} = \mathbf{M}_{\phi'} = \mathbf{M}_\kappa \frac{\partial \mathbf{M}_\phi}{\partial \phi} \mathbf{M}_\omega$$

in which

$$\begin{aligned} \frac{\partial \mathbf{M}_\phi}{\partial \phi} &= \begin{bmatrix} -\sin \phi & 0 & -\cos \phi \\ 0 & 0 & 0 \\ \cos \phi & 0 & -\sin \phi \end{bmatrix} \\ &= \begin{bmatrix} \cos \phi & 0 & -\sin \phi \\ 0 & 1 & 0 \\ \sin \phi & 0 & \cos \phi \end{bmatrix} \begin{bmatrix} 0 & 0 & -1 \\ 0 & 0 & 0 \\ 1 & 0 & 0 \end{bmatrix} \end{aligned}$$

Hence

$$\mathbf{M}_{\phi'} = \mathbf{M}_\kappa \mathbf{M}_\phi \begin{bmatrix} 0 & 0 & -1 \\ 0 & 0 & 0 \\ 1 & 0 & 0 \end{bmatrix} \mathbf{M}_\omega$$

But

$$\begin{aligned} \begin{bmatrix} 0 & 0 & -1 \\ 0 & 0 & 0 \\ 1 & 0 & 0 \end{bmatrix} \mathbf{M}_\omega &= \begin{bmatrix} 0 & \sin \omega & -\cos \omega \\ 0 & 0 & 0 \\ 0 & 0 & 0 \end{bmatrix} \\ &= \begin{bmatrix} 1 & 0 & 0 \\ 0 & \cos \omega & \sin \omega \\ 0 & -\sin \omega & \cos \omega \end{bmatrix} \begin{bmatrix} 0 & \sin \omega & -\cos \omega \\ -\sin \omega & 0 & 0 \\ \cos \omega & 0 & 0 \end{bmatrix} \end{aligned}$$

Hence

$$\mathbf{M}_{\phi'} = \mathbf{M} \begin{bmatrix} 0 & \sin \omega & -\cos \omega \\ -\sin \omega & 0 & 0 \\ \cos \omega & 0 & 0 \end{bmatrix} \quad (\text{C-27})$$

Alternatively,  $\mathbf{M}_{\phi'}$  can be derived as follows

$$\begin{aligned} \mathbf{M}_{\phi'} &= \mathbf{M}_\kappa \begin{bmatrix} -\sin \phi & 0 & -\cos \phi \\ 0 & 0 & 0 \\ \cos \phi & 0 & -\sin \phi \end{bmatrix} \mathbf{M}_\omega \\ &= \mathbf{M}_\kappa \begin{bmatrix} 0 & 0 & -1 \\ 0 & 0 & 0 \\ 1 & 0 & 0 \end{bmatrix} \mathbf{M}_\phi \mathbf{M}_\omega \\ &= \begin{bmatrix} 0 & 0 & -\cos \kappa \\ 0 & 0 & \sin \kappa \\ 1 & 0 & 0 \end{bmatrix} \mathbf{M}_\phi \mathbf{M}_\omega \end{aligned}$$

or

$$\begin{aligned} \mathbf{M}_{\phi'} &= \begin{bmatrix} 0 & 0 & -\cos \kappa \\ 0 & 0 & \sin \kappa \\ \cos \kappa & -\sin \kappa & 0 \end{bmatrix} \mathbf{M}_\kappa \mathbf{M}_\phi \mathbf{M}_\omega \\ &= \begin{bmatrix} 0 & 0 & -\cos \kappa \\ 0 & 0 & \sin \kappa \\ \cos \kappa & -\sin \kappa & 0 \end{bmatrix} \mathbf{M} \end{aligned} \quad (\text{C-28})$$

Finally

$$\frac{\partial \mathbf{M}}{\partial \kappa} = \mathbf{M}_\kappa' = \frac{\partial \mathbf{M}_\kappa}{\partial \kappa} \mathbf{M}_\phi \mathbf{M}_\omega$$

out

$$\frac{\partial \mathbf{M}_\kappa}{\partial \kappa} = \begin{bmatrix} -\sin \kappa & \cos \kappa & 0 \\ -\cos \kappa & -\sin \kappa & 0 \\ 0 & 0 & 0 \end{bmatrix} \\ = \begin{bmatrix} 0 & 1 & 0 \\ -1 & 0 & 0 \\ 0 & 0 & 0 \end{bmatrix} \mathbf{M}_\kappa$$

Hence

$$\mathbf{M}_\kappa = \begin{bmatrix} 0 & 1 & 0 \\ -1 & 0 & 0 \\ 0 & 0 & 0 \end{bmatrix} \mathbf{M} \quad (\text{C-29})$$

From equation 6-8, and dropping subscript  $A$ , let

$$\begin{bmatrix} U \\ V \\ W \end{bmatrix} = \mathbf{M} \begin{bmatrix} X - X_L \\ Y - Y_L \\ Z - Z_L \end{bmatrix} \quad (\text{C-30})$$

This may be partially differentiated with respect to any of the nine variables  $\omega, \phi, \kappa$  (implicit in  $\mathbf{M}$ )  $X_L, Y_L, Z_L$ , and  $X, Y, Z$ . As examples, one of each set of three are evaluated here, and the rest is left as exercise for the student.

$$\frac{\partial}{\partial \omega} \begin{bmatrix} U \\ V \\ W \end{bmatrix} = \frac{\partial \mathbf{M}}{\partial \omega} \begin{bmatrix} X - X_L \\ Y - Y_L \\ Z - Z_L \end{bmatrix} = \mathbf{M}^o \begin{bmatrix} 0 & 0 & 0 \\ 0 & 0 & 1 \\ 0 & -1 & 0 \end{bmatrix} \begin{bmatrix} X - X_L \\ Y - Y_L \\ Z - Z_L \end{bmatrix} \\ = \mathbf{M}^o \begin{bmatrix} 0 \\ Z - Z_L \\ Y_L - Y \end{bmatrix} \quad (\text{C-31})$$

$$\frac{\partial}{\partial Y} \begin{bmatrix} U \\ V \\ W \end{bmatrix} = \mathbf{M}^o \frac{\partial}{\partial Y} \begin{bmatrix} X - X_L \\ Y - Y_L \\ Z - Z_L \end{bmatrix} = \mathbf{M}^o \begin{bmatrix} 0 \\ 1 \\ 0 \end{bmatrix} = \begin{bmatrix} m_{12} \\ m_{22} \\ m_{32} \end{bmatrix} \quad (\text{C-32})$$

$$\frac{\partial}{\partial Z_L} \begin{bmatrix} U \\ V \\ W \end{bmatrix} = \mathbf{M}^o \frac{\partial}{\partial Z_L} \begin{bmatrix} X - X_L \\ Y - Y_L \\ Z - Z_L \end{bmatrix} = \mathbf{M}^o \begin{bmatrix} 0 \\ 0 \\ -1 \end{bmatrix} = \begin{bmatrix} -m_{13} \\ -m_{23} \\ -m_{33} \end{bmatrix} \quad (\text{C-33})$$

The elements of the  $\mathbf{B}$  matrix may now be evaluated using relationships similar to those in equation C-23, or,

$$\frac{\partial F_1}{\partial p} = \frac{f}{W} \left( \frac{\partial U}{\partial p} - \frac{U}{W} \frac{\partial W}{\partial p} \right) \quad \text{and} \quad \frac{\partial F_2}{\partial p} = \frac{f}{W} \left( \frac{\partial V}{\partial p} - \frac{V}{W} \frac{\partial W}{\partial p} \right) \quad (\text{C-34})$$

The partial derivatives of  $U, V, W$  in equation C-34 would be obtained from relations similar to those in equations C-31 to C-33. Assuming that the

sequence of variables is  $X_L, Y_L, Z_L, \omega, \phi, \kappa, X, Y, Z$ , the element  $b_{24}$  of  $\mathbf{B}$ , for example, would be

$$b_{24} = \frac{\partial F_2}{\partial \omega} = \frac{f}{W^o} \left( \frac{\partial V}{\partial \omega} - \frac{V}{W} \frac{\partial W}{\partial \omega} \right)^o \quad (\text{C-35})$$

The values of  $\partial V/\partial \omega$  and  $\partial W/\partial \omega$  are obtained from equation C-31 as

$$\frac{\partial V}{\partial \omega} = m_{22}^o (Z - Z_L)^o + m_{23}^o (Y_L - Y)^o$$

$$\frac{\partial W}{\partial \omega} = m_{32}^o (Z - Z_L)^o + m_{33}^o (Y_L - Y)^o$$

which may then be substituted into equation C-35 to yield the final form of the element  $b_{24}$ . All other elements of  $\mathbf{B}$  can be obtained in a similar manner, which is left as exercise for the student.

### C-7 LINEARIZATION OF THE COPLANARITY EQUATIONS

The coplanarity condition is given in the form of a determinant by equation C-12. The partial derivative of a determinant of order three with respect to a parameter  $p$  is equal to the sum of three determinants. If  $R_1, R_2, R_3$  are the three rows of a determinant  $D$ , then

$$\frac{\partial D}{\partial p} = \begin{vmatrix} \partial R_1/\partial p \\ R_2 \\ R_3 \end{vmatrix} + \begin{vmatrix} R_1 \\ \partial R_2/\partial p \\ R_3 \end{vmatrix} + \begin{vmatrix} R_1 \\ R_2 \\ \partial R_3/\partial p \end{vmatrix} \quad (\text{C-36})$$

Equation C-36 may be applied to equation C-12 to evaluate all partial derivatives necessary for its linearization. Since in most cases the coplanarity condition is used for relative orientation, there are usually *four* observed image coordinates  $x_1, y_1, x_2, y_2$  and *five* parameters. Therefore, the linearized form of equation C-12 is

$$\mathbf{A} \mathbf{v} + \mathbf{B} \Delta = \mathbf{f} \quad (\text{C-37})$$

1, 4, 4, 1    1, 5, 5, 1    1, 1

where

$$\mathbf{A} = [\partial F/\partial x_1 \quad \partial F/\partial y_1 \quad \partial F/\partial x_2 \quad \partial F/\partial y_2]$$

$\mathbf{v}$  = the vector of four observational residuals

$\mathbf{B}$  = the matrix of the partial derivatives of  $F$  with respect to the five specific parameters selected depending on the type of relative orientation.

$\Delta$  = corrections to the five specified parameters.

$$\mathbf{f} = -F^o = - \begin{bmatrix} B_x & B_y & B_z \\ u_1 & v_1 & w_1 \\ u_2 & v_2 & w_2 \end{bmatrix}$$

Each of the elements of **A** is composed of only one determinant since each image coordinate appears in only one row. For example

$$a_{13} = \frac{\partial F}{\partial x_2} = \begin{vmatrix} B_x & B_y & B_z \\ u_1 & v_1 & w_1 \\ \frac{\partial u_2}{\partial x_2} & \frac{\partial v_2}{\partial x_2} & \frac{\partial w_2}{\partial x_2} \end{vmatrix}$$

in which the partial derivatives shown may be evaluated from Eq. C-11 as

$$\frac{\partial}{\partial x_2} \begin{bmatrix} u_2 \\ v_2 \\ w_2 \end{bmatrix} = \mathbf{M}_2^T \begin{bmatrix} 1 \\ 0 \\ 0 \end{bmatrix} = \begin{bmatrix} m_{11} \\ m_{12} \\ m_{13} \end{bmatrix}_2$$

and hence

$$a_{13} = \begin{vmatrix} B_x & B_y & B_z \\ u_1 & v_1 & w_1 \\ (m_{11})_2 & (m_{12})_2 & (m_{13})_2 \end{vmatrix}$$

The other elements of **A** can be similarly evaluated.

The elements of **B** depend on whether relative orientation is dependent or independent. Independent relative orientation applies five rotational elements such as  $\omega_1, \phi_1, \kappa_1, \phi_2,$  and  $\kappa_2$ . For dependent relative orientation, one photograph and one base component (usually  $B_x$ ) are fixed. Therefore, the five parameters will be  $B_y, B_z, \omega_2, \phi_2, \kappa_2$ . Taking the latter case as an example the elements of **B** would be

$$b_{11} = \frac{\partial F}{\partial B_y} = \begin{vmatrix} 0 & 1 & 0 \\ u_1 & v_1 & w_1 \\ u_2 & v_2 & w_2 \end{vmatrix} = - \begin{vmatrix} u_1 & w_1 \\ u_2 & w_2 \end{vmatrix}$$

$$b_{12} = \frac{\partial F}{\partial B_z} = \begin{vmatrix} u_1 & v_1 \\ u_2 & v_2 \end{vmatrix}$$

$$b_{13} = \frac{\partial F}{\partial \omega_2} = \begin{vmatrix} B_x & B_y & B_z \\ u_1 & v_1 & w_1 \\ \frac{\partial u_2}{\partial \omega_2} & \frac{\partial v_2}{\partial \omega_2} & \frac{\partial w_2}{\partial \omega_2} \end{vmatrix}$$

$b_{14} = \partial F / \partial \phi_2$  and  $b_{15} = \partial F / \partial \kappa_2$  are evaluated similar to  $b_{13}$ . The partial derivatives in  $b_{13}$  are given by (from equations C-11 and C-26).

$$\begin{aligned} \frac{\partial}{\partial \omega_2} \begin{bmatrix} u_2 \\ v_2 \\ w_2 \end{bmatrix} &= \frac{\partial \mathbf{M}_2^t}{\partial \omega_2} \begin{bmatrix} x - x_0 \\ y - y_0 \\ -f \end{bmatrix}_2 = \left\{ \mathbf{M}_2^o \begin{bmatrix} 0 & 0 & 0 \\ 0 & 0 & 1 \\ 0 & -1 & 0 \end{bmatrix} \right\}^t \begin{bmatrix} x - x_0 \\ y - y_0 \\ -f \end{bmatrix}_2 \\ &= \begin{bmatrix} 0 & 0 & 0 \\ 0 & 0 & -1 \\ 0 & 1 & 0 \end{bmatrix} \left\{ \mathbf{M}_2^o \begin{bmatrix} x - x_0 \\ y - y_0 \\ -f \end{bmatrix}_2 \right\} = \begin{bmatrix} 0 & 0 & 0 \\ 0 & 0 & -1 \\ 0 & 1 & 0 \end{bmatrix} \begin{bmatrix} u_2 \\ v_2 \\ w_2 \end{bmatrix}_2 \end{aligned}$$

or

$$\frac{\partial}{\partial \omega_2} \begin{bmatrix} u_2 \\ v_2 \\ w_2 \end{bmatrix} = \begin{bmatrix} 0 \\ -w_2 \\ v_2 \end{bmatrix}_2$$

Consequently, the final form of the  $b_{13}$  element would be

$$b_{13} = \begin{vmatrix} B_x & B_y & B_z \\ u_1 & v_1 & w_1 \\ 0 & -w_2 & v_2 \end{vmatrix}_2$$

In a very similar manner the student may derive the remaining two elements  $b_{14}$  and  $b_{15}$ .

#### BIBLIOGRAPHY

- Lucas, J. R. 1963. Differentiation of the Orientation Matrix by Matrix Multipliers. *Photogrammetric Engineering* 29:708.  
 American Society of Photogrammetry. 1966. *Manual of Photogrammetry* 3rd ed. Menasha, Wisc.: George Banta Co., Chapter 10.

# Chapter 10

## Space Resection and Rectification of a Single Photograph

### 10-1 INTRODUCTION

The term *space resection* is the name given to the process in which the spatial position and orientation of a photograph is determined based on photographic measurements of the images of ground control points appearing on the photograph. An elementary type of *two-dimensional* resection is performed in the process of radial-line triangulation discussed in section 7-14. In this process, both the two-dimensional map position and the azimuthal orientation of the ray templet are established by fitting the templet rays to horizontal control points.

In space resection, the *three-dimensional* object space  $X_L, Y_L, Z_L$  coordinates of the exposure station are determined as well as the angular space orientation expressed by the orientation angles  $\omega, \phi, \kappa$ , or  $\alpha, t, s$  defined in section 6-6. In order to accomplish a space resection, the photograph must contain the images of at least three ground control points, not lying on or near a straight line, whose horizontal positions and elevations are known.

Although several space resection procedures have been devised over the years, the method described in the present chapter is rigorous and is based on the principle of collinearity of the photogrammetric ray presented in

section 6-7. The input to the method can be either coordinate measurements of the images made on a paper photograph corrected for film and paper distortions as discussed in section 7-3, or else the coordinates of the points obtained from a glass plate measured in a comparator and refined as explained in Chapter 9. The latter type of input will of course produce the superior results. The results of space resection are used in the analytical methods for the photogrammetric extension of horizontal and vertical control as discussed in Chapter 13. They are also used in some rectification methods.

The term *rectification* is the name given to the process by which a tilted or oblique photograph is transformed into an equivalent vertical photograph taken from the same exposure station. Rectification depends on a knowledge of the elements of the exterior orientation of the photograph. It can be performed either graphically as discussed in section 10-6, or instrumentally as explained in section 10-8. Point-to-point rectification can be performed analytically using the eight-parameter projective transformation equations given by equation A-11. As will be discussed, the orientation elements necessary for rectification are obtained either analytically by space resection using collinearity equations or else empirically by trial-and-error in a rectifier as explained in section 10-13.

### 10-2 SYSTEMS OF EXTERIOR ORIENTATION

Exterior orientation of a photograph has been previously defined as the object space coordinates  $X_L, Y_L, Z_L$  of the exposure station together with three orientation angles. The two systems of sequential rotations  $\omega, \phi, \kappa$  and  $\alpha, t, s$  are given in section 6-6. However, the sequence  $\phi, \omega, \kappa$  is frequently employed because it is quite commonly employed in stereoscopic plotting instruments.

### 10-3 SPACE RESECTION

Assume that the photographic coordinates of three ground control points have been measured and corrected for various systematic errors. Then, assuming that the photographic coordinate system origin has been reduced to the principal point, a pair of collinearity equations according to equation 6-15 can be written for each of the three points. Thus

$$\begin{aligned} x &= -f \left[ \frac{m_{11}(X_P - X_L) + m_{12}(Y_P - Y_L) + m_{13}(Z_P - Z_L)}{m_{31}(X_P - X_L) + m_{32}(Y_P - Y_L) + m_{33}(Z_P - Z_L)} \right] \\ y &= -f \left[ \frac{m_{21}(X_P - X_L) + m_{22}(Y_P - Y_L) + m_{23}(Z_P - Z_L)}{m_{31}(X_P - X_L) + m_{32}(Y_P - Y_L) + m_{33}(Z_P - Z_L)} \right] \end{aligned} \quad (10-1)$$

In these equations,  $x$  and  $y$  are the refined photographic coordinates of the control points;  $f$  is the known camera focal length or the principal distance of the photograph, and  $X_P, Y_P, Z_P$  are the known object space coordinates of the control point. These quantities are considered as fixed quantities, not subject to variation. The remaining terms are the unknown exposure station coordinates  $X_L, Y_L, Z_L$  and the unknown elements of the  $M$ -matrix defined in section 6-6 and formulated in equations 6-21 and 6-22 for the two common systems of orientation angles. These elements are defined by the three orientation angles, which together with the unknowns  $X_L, Y_L, Z_L$ , constitute six unknown parameters of the equations.

A direct solution of the six equations, two written for each of the three points, is not feasible because they contain the transcendental angular functions. The most practical solution is to determine a set of initial values for the unknown quantities ( $X_L^o, Y_L^o, Z_L^o, \omega^o, \phi^o, \kappa^o$ ) or ( $X_L^o, Y_L^o, Z_L^o, \alpha^o, t^o, s^o$ ); linearize the six equations by the Taylor series expansion, which will then contain six differentials of the parameters or corrections to the initial approximate values; solve for the differential corrections; add these to the original approximate values; and then iterate the solution of these six equations until they satisfy the collinearity equations within the desired accuracy. The development in this chapter will be confined to the  $\omega, \phi, \kappa$  system since it is the most frequently used.

An initial value for  $Z_L$  can be obtained from altimeter readings or by the scale relations given in section 7-4. Initial values for  $X_L$  and  $Y_L$  can be obtained simply by determining the average  $X$  and  $Y$  coordinates of the ground control points. For vertical photography,  $\omega^o$  and  $\phi^o$  can both be assumed as zero.

The angle kappa ( $\kappa$ ) is taken as the angle measured counterclockwise from the photographic position of the ground  $X$ -axis to the photographic  $x$ -axis as shown in Fig. 10-1. If the flight line is due east or west,  $\kappa^o = 0^\circ$  or  $180^\circ$ , respectively. If the flight line is due north or south,  $\kappa^o = +90^\circ$  or  $-90^\circ$ , respectively. Otherwise, an initial value can be obtained by computing the angle that one of the control lines makes with the ground  $X$ -axis, then computing the angle that the same line makes with the photographic  $x$ -

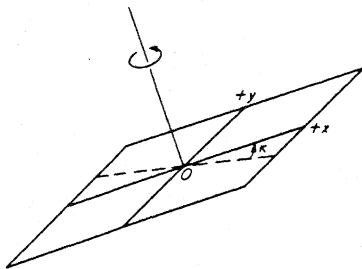


Figure 10-1. Definition of kappa angle.

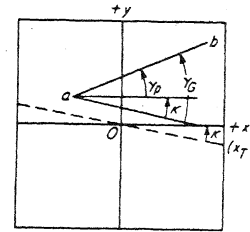


Figure 10-2. Kappa angle determined by direction of a line.

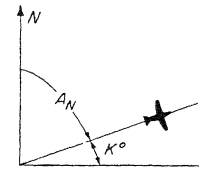


Figure 10-3. Relation between azimuth of flight line and kappa angle.

axis, and finally computing the difference in these angles. Thus, from Fig. 10-2,

$$\tan \gamma_P = \frac{y_b - y_a}{x_b - x_a} \quad \tan \gamma_G = \frac{Y_B - Y_A}{X_B - X_A}$$

and

$$\kappa^o = \gamma_G - \gamma_P \tag{10-2}$$

If the ground azimuth from north  $A_N$  of the line of flight is known, then, as shown in Fig. 10-3,

$$\kappa^o = 90^\circ - A_N \tag{10-3}$$

If an oblique photograph is to be resected, the approximate position of the ground nadir point must be determined. The initial angle approximations in the  $\alpha, t, s$  system are somewhat easier to determine than they are in the  $\omega, \phi, \kappa$  system. Although oblique resection is not discussed in this book, the principles are the same as they are for vertical photographs. The student should review section 6-11 and the appropriate sections of Chapter 7 before undertaking to resect an oblique photograph.

Equation 10-1 can be stated as

$$\begin{aligned} x &= F_x(X_L, Y_L, Z_L, \omega, \phi, \kappa) \\ y &= F_y(X_L, Y_L, Z_L, \omega, \phi, \kappa) \end{aligned} \tag{10-4}$$

Introducing the initial approximations of the six variables evaluates equation 10-4 to give  $F_{x_0}$  and  $F_{y_0}$ . Linearization by the Taylor series expansion gives

$$F_x = F_{x_0} + dF_x \tag{10-5}$$

$$F_y = F_{y_0} + dF_y$$

in which

$$\left. \begin{aligned} dF_x = dx &= \frac{\partial x}{\partial X_L} dX_L + \frac{\partial x}{\partial Y_L} dY_L + \frac{\partial x}{\partial Z_L} dZ_L + \\ &+ \frac{\partial x}{\partial \omega} d\omega + \frac{\partial x}{\partial \phi} d\phi + \frac{\partial x}{\partial \kappa} d\kappa \\ dF_y = dy &= \frac{\partial y}{\partial X_L} dX_L + \frac{\partial y}{\partial Y_L} dY_L + \frac{\partial y}{\partial Z_L} dZ_L \\ &+ \frac{\partial y}{\partial \omega} d\omega + \frac{\partial y}{\partial \phi} d\phi + \frac{\partial y}{\partial \kappa} d\kappa \end{aligned} \right\} \tag{10-6}$$

Thus,

$$\left. \begin{aligned} x &= F_{x_0} + A_1 dX_L + A_2 dY_L + A_3 dZ_L + A_4 d\omega + A_5 d\phi + A_6 d\kappa \\ y &= F_{y_0} + B_1 dX_L + B_2 dY_L + B_3 dZ_L + B_4 d\omega + B_5 d\phi + B_6 d\kappa \end{aligned} \right\} \tag{10-7}$$

in which  $x$  and  $y$  are the refined photographic coordinates;  $F_{x_0}$  and  $F_{y_0}$  are the values of the right-hand side of equation 10-1 obtained by substituting the initially assumed values of the six unknown parameters  $X_L^0$ ,  $Y_L^0$ ,  $Z_L^0$ ,  $\omega^0$ ,  $\phi^0$ , and  $\kappa^0$ ;  $dX_L$ ,  $dY_L$ ,  $dZ_L$ ,  $d\omega$ ,  $d\phi$ , and  $d\kappa$  are as yet unknown corrections to the initially assumed values; and the  $A$ 's and the  $B$ 's are the partial differential coefficients obtained by differentiation of equation 10-1. These partial differential coefficients are evaluated using the initially assumed values of the unknown parameters.

With three given complete control points, six linear equations can be formed, two for each point, by which the six unknown quantities,  $dX_L$ ,  $dY_L$ ,  $dZ_L$ ,  $d\omega$ ,  $d\phi$ , and  $d\kappa$  can be solved. These quantities are then added to the initial values, the values of  $F_{x_0}$  and  $F_{y_0}$  are again computed, the partial differential coefficients are again evaluated, and the six equations are again solved. Each time the process is iterated, the corrections become smaller. The process is stopped when the corrections are considered small enough to have no effect.

Linearization of equation 10-1 in order to obtain the partial differential coefficients contained in equation 10-6 is performed in section C-6 of Appendix C. Equation 10-7 can be expressed in matrix form as

$$\mathbf{B} \Delta = \mathbf{f} \tag{10-8}$$

6.6 6.1      6.1

in which

$$\mathbf{B} = \begin{bmatrix} \frac{\partial x}{\partial X_L} & \frac{\partial x}{\partial Y_L} & \frac{\partial x}{\partial Z_L} & \frac{\partial x}{\partial \omega} & \frac{\partial x}{\partial \phi} & \frac{\partial x}{\partial \kappa} \\ \frac{\partial y}{\partial X_L} & \frac{\partial y}{\partial Y_L} & \frac{\partial y}{\partial Z_L} & \frac{\partial y}{\partial \omega} & \frac{\partial y}{\partial \phi} & \frac{\partial y}{\partial \kappa} \end{bmatrix} \tag{10-9}$$

$$\Delta = \begin{bmatrix} dX_L \\ dY_L \\ dZ_L \\ d\omega \\ d\phi \\ d\kappa \end{bmatrix} \tag{10-10}$$

$$\mathbf{f} = \begin{bmatrix} (F_{x_0} - x) \\ (F_{y_0} - y) \end{bmatrix} = \begin{bmatrix} -\frac{fU^0}{W^0 - x} \\ -\frac{fV^0}{W^0 - y} \end{bmatrix} \tag{10-11}$$

The values of  $U^0$ ,  $V^0$ , and  $W^0$  in equation 10-11 are evaluated using the initial approximations by

$$\begin{bmatrix} U^0 \\ V^0 \\ W^0 \end{bmatrix} = \mathbf{M}^0 \begin{bmatrix} (X - X_L^0) \\ (Y - Y_L^0) \\ (Z - Z_L^0) \end{bmatrix} \tag{10-12}$$

in which  $\mathbf{M}^0$  is the numerical value of  $\mathbf{M}$  evaluated at the approximate values  $\omega^0$ ,  $\phi^0$ ,  $\kappa^0$  using equation 6-21.

The values of the corrections to the initial approximations are obtained from equation 10-8 as

$$\Delta = \mathbf{B}^{-1} \mathbf{f} \tag{10-13}$$

The computed corrections are added to the first (or current) set of approximate values to obtain updated approximations designated by subscript 1. Thus

$$\begin{aligned} X_{L_1} &= X_L^0 + \delta X_L & \omega_1 &= \omega^0 + \delta\omega \\ Y_{L_1} &= Y_L^0 + \delta Y_L & \phi_1 &= \phi^0 + \delta\phi \\ Z_{L_1} &= Z_L^0 + \delta Z_L & \kappa_1 &= \kappa^0 + \delta\kappa \end{aligned} \tag{10-14}$$

Matrices  $\mathbf{B}$  and  $\mathbf{f}$  are computed using these updated values, and equation 10-13 is again solved for the new set of corrections  $\Delta$ . The process is then repeated until the corrections become negligible.

If the images of more than three control points appear on the photograph to be resected, then more than the six minimum condition equations

$$d\kappa' = \frac{1}{3 \times 220} \left[ -0.88 - 1.64 - 1.00 \right. \\ \left. - \left( 3 \times 400 + \frac{2 \times 240^2}{400} \right) (-0.002899) \right] = +0.001203 \text{ rad}$$

$$d\phi'' = \frac{400}{2 \times 220 \times 240} (2.03 + 0.64) = +0.010114 \text{ rad}$$

$$d\kappa'' = \frac{1}{3 \times 220} \left[ 1.09 - 0.64 + 2.03 \right. \\ \left. - \left( 3 \times 400 + \frac{2 \times 240^2}{400} \right) (-0.002899) \right] = +0.010294 \text{ rad}$$

Converting the five angular values to grads, changing the algebraic signs, and adding to the initial values gives,

$$\omega' = 100.00 + 0.18 = 100.18^g$$

$$\phi' = 99.22 - 0.15 = 99.07^g$$

$$\kappa' = 397.96 - 0.08 = 397.88^g$$

$$\omega'' = 98.26^g \text{ (not used in orientation)}$$

$$\phi'' = 100.20 - 0.64 = 99.56^g$$

$$\kappa'' = 0.25 - 0.68 = -0.43^g = 399.57^g$$

## 11-8 ANALYTICAL RELATIVE ORIENTATION

The empirical and numerical methods for relative orientation discussed thus far are employed in the formation of a stereoscopic model in a plotting instrument. The model is then measured for the general purpose of map compilation. Many situations are encountered in photogrammetry, however, in which the model need not be formed, and only a limited number of object points must be located. In these situations, an  $x$ - $y$  comparator is used to measure the coordinates of the points of interest, and the photogrammetric solution is carried out analytically. Two successive photographs are then related to one another mathematically in the process known as analytical relative orientation.

In the analytical relative orientation process, the positions and orientations of both camera stations are determined with respect to an arbitrary object reference coordinate system. In addition, the object positions of as many points as there are measured image coordinates, are computed in this reference system.

In order to introduce the analytical orientation concept, the coplanarity condition (see section 6-13 and Appendix C) will be employed. This condition can be stated as follows:

$$b_x(v_1 w_2 - v_2 w_1) - b_y(u_1 w_2 - u_2 w_1) + b_z(u_1 v_2 - u_2 v_1) = 0$$

in which  $b_x$ ,  $b_y$ , and  $b_z$  are the base components, and

$$\begin{bmatrix} u_1 \\ v_1 \\ w_1 \end{bmatrix} = \mathbf{M}_1' \begin{bmatrix} x - x_o \\ y - y_o \\ -f \end{bmatrix}_1 \quad \begin{bmatrix} u_2 \\ v_2 \\ w_2 \end{bmatrix} = \mathbf{M}_2' \begin{bmatrix} x - x_o \\ y - y_o \\ -f \end{bmatrix}_2$$

With reference to Fig. 11-10 the coplanarity condition states simply that the exposure stations  $L'$  and  $L''$ , the image points  $a'$  and  $a''$  and the object point  $A$  all lie in the same plane. In the analytical solution, one camera position and photo orientation are assumed to be fixed with respect to the arbitrary reference coordinate system, and one component of the photo base is fixed to some arbitrary value. This latter condition fixes the scale of the object space. The second photograph is then allowed to take a position and orientation necessary to satisfy the coplanarity condition for a minimum of five object points.

Let the left-hand exposure station be taken as the origin of the arbitrary coordinate system. Then  $X_{L'} = 0$ ;  $Y_{L'} = 0$ ;  $Z_{L'} = 0$ . Further, let  $\omega' = \phi' = \kappa' = 0$ . Then the orientation matrix  $\mathbf{M}'$  for the left-hand photograph becomes the identity matrix  $\mathbf{I}$  for the arbitrary system. The arbitrary value of the base is designated  $b_{x_o}$ . The unknowns are therefore  $b_y''$ ,  $b_z''$ ,  $\omega''$ ,  $\phi''$ ,  $\kappa''$ . Assuming near-vertical aerial photography, approximate values for these five values may be taken as zero, that is,  $b_{y_o}'' = b_{z_o}'' = \omega_o'' = \phi_o'' = \kappa_o'' = 0$ . The elements of interior orientation are assumed to be known from camera calibration data.

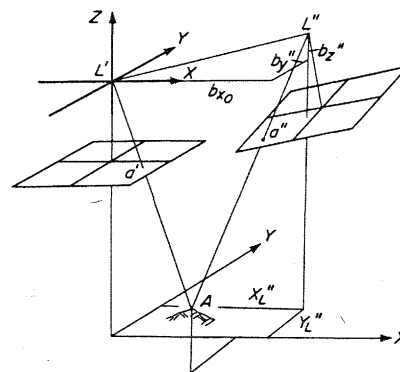


Figure 11-10. Coplanarity condition.

With the above data known or assumed, the elements of  $\mathbf{A}$ ,  $\mathbf{B}$ , and  $\mathbf{f}$  in equation C-37 may be numerically evaluated for each measured pair of conjugate image points. If only five well-distributed points are used, then only five linearized coplanarity condition equations will be available. This leads to a zero residual vector, that is,  $\mathbf{v} = 0$ , and the set of five equations becomes

$$\mathbf{B} \Delta = \mathbf{f} \quad (11-14)$$

5,5 5,1      5,1

equation 11-14 may be solved explicitly for the vector of corrections  $\Delta$  by

$$\Delta = \mathbf{B}^{-1}\mathbf{f} \quad (11-15)$$

The initial approximations are corrected using these corrections to give updated values for the five relative orientation elements as follows:

$$\begin{aligned} b_y'' &= b_{y_0}'' + \Delta b_y'' \\ b_z'' &= b_{z_0}'' + \Delta b_z'' \\ \omega'' &= \omega_0'' + \Delta\omega'' \\ \phi'' &= \phi_0'' + \Delta\phi'' \\ \kappa'' &= \kappa_0'' + \Delta\kappa'' \end{aligned} \quad (11-16)$$

Using these updated values, the matrices  $\mathbf{B}$  and  $\mathbf{f}$  are reevaluated and used to compute a new set of corrections. This process is then iterated until the corrections become insignificant.

In practice, analytical relative orientation is more frequently performed using more than five points. This results in redundant measurements that allow the relative orientation to be adjusted by the method of least squares. In this case, the residuals do not vanish. The vector of corrections is computed from the normal equations developed in Appendix B as follows

$$\Delta = [\mathbf{B}^T(\mathbf{AQA}^T)^{-1}\mathbf{B}]^{-1}[\mathbf{B}^T(\mathbf{AQA}^T)^{-1}\mathbf{f}] \quad (11-17)$$

in which  $\mathbf{Q}$  is the cofactor matrix of the observed image coordinates. If the coordinates of the image points are assumed to be uncorrelated and of equal precision,  $\mathbf{Q}$  is taken as the identity matrix. As in the case of the explicit solution given by equation 11-15, the solution for the corrections is iterated until no significant change occurs in the corrections.

The result of the analytical relative orientation is a set of  $XYZ$  coordinates of each exposure station and two orientation matrices  $\mathbf{M}'$  and  $\mathbf{M}''$  which relate the two photographs to the arbitrary object coordinate system. The coordinates of any point in the object coordinate system can then be computed by writing a pair of collinearity equations for each ray. The resulting four condition equations for each point are linearized as described in section C-6, Appendix C, and solved for the arbitrary object space  $XYZ$  coordinates. This procedure is detailed in section 13-13.

A small  $d\phi$  error causes the level datum to become slightly cylindrical. A small  $d\omega$  error introduces a diagonal warpage of the model. It is to be noted that if vertical control points are located in each of the four corners of the model, the effect of a  $d\omega$  error can be detected. However, this control configuration will *not* detect the effect of a  $d\phi$  error as can be seen by a study of Fig. 11-17. This latter error can only be detected by placing a fifth vertical control point somewhere in the middle of the model.

### 11-13 ANALYTIC ABSOLUTE ORIENTATION

As stated in section 11-1, in absolute orientation, a pair of relatively oriented photographs, and hence a three-dimensional model, is fitted to the ground control system by the three rotations of the model, three translations of the model, and a scale change. This fitting can be accomplished analytically through a program which performs the necessary spatial transformation. After relative orientation has been accomplished either instrumentally or analytically, the model coordinates of ground control points are measured, or computed analytically. These are then used to determine the seven elements or parameters necessary to transform the model coordinates into the ground coordinate system. This seven-parameter, or linear three-dimensional conformal, transformation developed in section A-3 of Appendix A is then used for absolute orientation of the model. The transformation is given by equation A-18 as

$$\mathbf{X}_G = s\mathbf{M}\mathbf{X} + \mathbf{k} \quad (11-22)$$

in which

$$\mathbf{X}_G = \begin{bmatrix} X_G \\ Y_G \\ Z_G \end{bmatrix} \text{ are the coordinates in the ground coordinate system}$$

$$\mathbf{X} = \begin{bmatrix} X \\ Y \\ Z \end{bmatrix} \text{ are the coordinates in the model coordinate system}$$

$s$  = the scale change from model space to object space

$\mathbf{M}$  = the orthogonal matrix that rotates the model coordinate system into the ground coordinate system. This matrix is formed in terms of the functions of three sequential rotations of the model:  $\Omega$ ,  $\Phi$ , and  $K$ .

$$\mathbf{k} = \begin{bmatrix} k_1 \\ k_2 \\ k_3 \end{bmatrix} \text{ are the three translations in the } X\text{-, } Y\text{-, and } Z\text{-directions respectively,}$$

In order to compute the seven parameters ( $s, \Omega, \Phi, K, k_1, k_2, k_3$ ), at least seven equations are required. Any model point whose three ground coordinates are known would yield three equations, which in the expanded functional form of equation 11-22 become,

$$\begin{aligned} F_1 &= X_G - s(m_{11}X + m_{12}Y + m_{13}Z) - k_1 = 0 \\ F_2 &= Y_G - s(m_{21}X + m_{22}Y + m_{23}Z) - k_2 = 0 \\ F_3 &= Z_G - s(m_{31}X + m_{32}Y + m_{33}Z) - k_3 = 0 \end{aligned} \quad (11-23)$$

Quite frequently, not all three ground coordinates are known; instead either the horizontal position ( $X, Y$ ) or the elevation ( $Z$ ) are given. When only the horizontal position of a point is known, the upper two equations in 11-23 can be written for that point. If only the elevation is known, then only the last equation can be written for the point. Thus, for the minimum control required for absolute orientation, that is two horizontal and three vertical control points, a total of seven equations can be written to solve for the seven unknowns. The linearized form of equation 11-23 for the minimum amount of control can be expressed as

$$\mathbf{BA} = \mathbf{f} \quad (11-24)$$

in which

$$\mathbf{B} = \begin{bmatrix} \frac{\partial F_1}{\partial s} & \frac{\partial F_1}{\partial \Omega} & \frac{\partial F_1}{\partial \Phi} & \frac{\partial F_1}{\partial K} & \frac{\partial F_1}{\partial k_1} & \frac{\partial F_1}{\partial k_2} & \frac{\partial F_1}{\partial k_3} \\ \frac{\partial F_2}{\partial s} & \frac{\partial F_2}{\partial \Omega} & \frac{\partial F_2}{\partial \Phi} & \frac{\partial F_2}{\partial K} & \frac{\partial F_2}{\partial k_1} & \frac{\partial F_2}{\partial k_2} & \frac{\partial F_2}{\partial k_3} \\ \frac{\partial F_3}{\partial s} & \frac{\partial F_3}{\partial \Omega} & \frac{\partial F_3}{\partial \Phi} & \frac{\partial F_3}{\partial K} & \frac{\partial F_3}{\partial k_1} & \frac{\partial F_3}{\partial k_2} & \frac{\partial F_3}{\partial k_3} \end{bmatrix} \quad (11-25)$$

$$\mathbf{A} = [\Delta s \quad \Delta \Omega \quad \Delta \Phi \quad \Delta K \quad \Delta k_1 \quad \Delta k_2 \quad \Delta k_3]^T \quad (11-26)$$

$$\mathbf{f} = -\mathbf{X}_G + s^o \mathbf{M}^o \mathbf{X} + \mathbf{k}^o \quad (11-27)$$

The superscript  $o$  in equation 11-27 indicates that  $\mathbf{f}$  is the value of the function computed from initial approximate values of the seven unknown parameters. For example,  $s^o$  can be computed using the length of a line between two control points in the model and the corresponding length on the ground. The rotation angles  $\Omega$  and  $\Phi$  can be initially assumed to be zero. The initial value of  $K$  can be computed as explained in section 10-3. The  $\mathbf{X}$  vector of one of the points can be multiplied by  $s^o$  (assuming  $\mathbf{M}^o$  to be a unit matrix) from which the initial translation approximations become,

$$\mathbf{k}^o = \mathbf{X}_G - s^o \mathbf{X}$$

or

$$\begin{aligned} k_1^o &= X_G - s^o X \\ k_2^o &= Y_G - s^o Y \\ k_3^o &= Z_G - s^o Z \end{aligned} \quad (11-28)$$

The values of the partial derivatives in equation 11-25 are evaluated as follows. (See Appendix C, section C-6 for the differentiation of  $\mathbf{M}$  with respect to the rotation angles.)

$$\frac{\partial}{\partial s} \begin{bmatrix} F_1 \\ F_2 \\ F_3 \end{bmatrix} = -\mathbf{M}^o \begin{bmatrix} X \\ Y \\ Z \end{bmatrix} \quad (11-29)$$

$$\frac{\partial}{\partial \Omega} \begin{bmatrix} F_1 \\ F_2 \\ F_3 \end{bmatrix} = -s^o \mathbf{M}^o \begin{bmatrix} 0 & 0 & 0 \\ 0 & 0 & 1 \\ 0 & -1 & 0 \end{bmatrix} \begin{bmatrix} X \\ Y \\ Z \end{bmatrix} = -s^o \mathbf{M}^o \begin{bmatrix} 0 \\ Z \\ -Y \end{bmatrix} \quad (11-30)$$

$$\frac{\partial}{\partial \Phi} \begin{bmatrix} F_1 \\ F_2 \\ F_3 \end{bmatrix} = -s^o \begin{bmatrix} 0 & 0 & -\cos K \\ 0 & 0 & \sin K \\ \cos K & -\sin K & 0 \end{bmatrix} \mathbf{M}^o \begin{bmatrix} X \\ Y \\ Z \end{bmatrix} \quad (11-31)$$

$$\frac{\partial}{\partial K} \begin{bmatrix} F_1 \\ F_2 \\ F_3 \end{bmatrix} = -s^o \begin{bmatrix} 0 & 1 & 0 \\ -1 & 0 & 0 \\ 0 & 0 & 0 \end{bmatrix} \mathbf{M}^o \begin{bmatrix} X \\ Y \\ Z \end{bmatrix} \quad (11-32)$$

$$\frac{\partial}{\partial k_1} \begin{bmatrix} F_1 \\ F_2 \\ F_3 \end{bmatrix} = \begin{bmatrix} -1 \\ 0 \\ 0 \end{bmatrix}; \quad \frac{\partial}{\partial k_2} \begin{bmatrix} F_1 \\ F_2 \\ F_3 \end{bmatrix} = \begin{bmatrix} 0 \\ -1 \\ 0 \end{bmatrix}; \quad \frac{\partial}{\partial k_3} \begin{bmatrix} F_1 \\ F_2 \\ F_3 \end{bmatrix} = \begin{bmatrix} 0 \\ 0 \\ -1 \end{bmatrix} \quad (11-33)$$

Equation 11-24 is solved for the vector of corrections  $\Delta$  in order to compute a better set of approximate values by the addition of the corrections to the initial approximations. Equations 11-29 through 11-33 are evaluated using these updated approximations and equation 11-24 is again solved. This process is iterated until  $\mathbf{f}$  becomes small enough to be considered negligible.

Usually there are more than the minimum number of control points available with which to solve for the parameters of absolute orientation. In such cases, the least squares method is used to obtain a best estimate of the seven parameters. The condition equations of equation 11-22 are linearized for one point into the general form

$$\mathbf{Av} + \mathbf{BA} = \mathbf{f} \quad (11-34)$$

Considering the ground coordinates to be fixed, then the matrix of coefficients of the residuals in equation 11-34 becomes

$$\mathbf{A} = \begin{bmatrix} \frac{\partial F_1}{\partial X} & \frac{\partial F_1}{\partial Y} & \frac{\partial F_1}{\partial Z} \\ \frac{\partial F_2}{\partial X} & \frac{\partial F_2}{\partial Y} & \frac{\partial F_2}{\partial Z} \\ \frac{\partial F_3}{\partial X} & \frac{\partial F_3}{\partial Y} & \frac{\partial F_3}{\partial Z} \end{bmatrix} \quad (11-35)$$

12

168

which from Eq. 11-23 becomes

$$\mathbf{A} = \begin{bmatrix} -sm_{11} & -sm_{12} & -sm_{13} \\ -sm_{21} & -sm_{22} & -sm_{23} \\ -sm_{31} & -sm_{32} & -sm_{33} \end{bmatrix}^0 \quad (11-36)$$

The vector of residuals is

$$\mathbf{v} = [v_x \quad v_y \quad v_z]^t \quad (11-37)$$

and  $\mathbf{f}$  is given by equation 11-27.

With the matrices  $\mathbf{A}$ ,  $\mathbf{B}$ , and  $\mathbf{f}$  evaluated at the initial set of approximations, the values of the first set of corrections  $\Delta$  is computed from an equation identical to equation 11-17. The corrections are then added to the original approximations for the seven parameters to get a new set of approximations. These updated approximate values are then used to evaluate new values for the matrices  $\mathbf{A}$ ,  $\mathbf{B}$ ,  $\mathbf{f}$  which in turn are used to compute a new  $\Delta$ . This procedure is repeated until the last vector of corrections is insignificantly small.

## BIBLIOGRAPHY

- 13
- American Society of Photogrammetry. 1966. *Manual of Photogrammetry*, 3rd ed. Menasha, Wisc.: George Banta Co. Chapters 9, 10, 13, and 14.
- Bender, L. U. 1967. Derivation of Parallax Equations. *Photogrammetric Engineering* 33:1175.
- Ghosh, S. K. 1971. Photo/Model/Map Scales. *Photogrammetric Engineering* 32:1154.
- Ghosh, S. K. 1968. *Theory of Stereophotogrammetry*. Columbus, Ohio: Ohio State University Bookstore.
- Harley, I. A. 1971. An Exact Procedure for Numerical Orientation of a Plotting Instrument *Photogrammetric Record* 7:27.
- Hothimer, J. 1961. Possibilities and Limitations for Elimination of Distortion in Aerial Photographs. *Photogrammetric Engineering* 27:136.
- Kasper, H. 1956. Graphical Determination of the Overcorrection Factor for Use in the Relative Orientation of Vertical Photographs in Any Terrain. *Photogrammetric Engineering* 22:239.
- Mroz, A. 1966. Relative Orientation. *Photogrammetric Record* 5:198.
- Oswal, H. L. 1967. Comparison of Elements of Relative Orientation. *Photogrammetric Engineering* 33:335.
- Talts, J. 1968. Accuracy of Stereomodels by Simulation. *Photogrammetric Engineering* 34:962.
- Tewinkel, G. C. 1953. Numerical Relative Orientation. *Photogrammetric Engineering* 18:841.
- Thompson, E. H. 1959. A Rational Algebraic Formulation of the Problem of Relative Orientation. *Photogrammetric Record* 3:152.
- Wood, R. 1974. The Application of the Programmable Calculator to Numerical Orientation. *Photogrammetric Record* 8:101.

## PROBLEMS

- 11-1. A Multiplex diapositive is made in a reduction printer which contains a lens with a 55.50-mm focal length. The principal distance of the Multiplex projector is 30.00 mm. The focal length of the aerial camera lens is 153.42 mm. Compute the optical distances  $A$  and  $B$  of Fig. 11-4(b).
- 11-2. If the image area on the aerial film negative of problem 11-1 measures 229 by 229 mm, what does the image area measure on the diapositive?
- 11-3. The focal length of the Multiplex projector lens of problem 11-1 is 27.69 mm. How far below the projector, to the nearest millimetre, is the plane of best focus of the projected diapositive image shown in Fig. 11-4(c) (the optimum projection distance)?
- 11-4. What is the size of the image area projected in the plane of best focus computed in problem 11-3?
- 11-5. Assuming a circle of confusion of 0.15-mm diameter, what is the depth of focus shown in Fig. 11-4(c) above and below the plane of best focus for the focal length and principal distance of the Multiplex given in problems 11-1 and 11-3 if the  $f$ /stop is  $f/45$ ?
- 11-6. Let Fig. 11-8 represent a pair of 9- by 9-in. photographs taken with a 6-in. focal length lens and containing 60% overlap. Points 1, 2, 4, and 3 form a square, as do points 1, 2, 6, and 5. If a Multiplex projector is used, what is the effect, in millimeters, of 3° swing of projector  $L$  on the  $y$ -displacement of point 4 in the plane of optimum definition? Of point 2?
- 11-7. If projector  $L$  in Fig. 11-8 is  $y$ -tilted 3°, what is the  $y$ -displacement, in millimetres, of point 4 in the plane of optimum definition?
- 11-8. If projector  $R$  in Fig. 11-8 is  $x$ -tilted 3°, what is the  $y$ -displacement, in millimetres, of point 3 in the plane of optimum definition? Of point 1?
- 11-9. A pair of Multiplex projectors are spaced so that the distance between their nodal points is 205 mm. A pair of conjugate points intersect on the tracing-table platen at a projection distance of 380 mm. What will be the  $x$ -displacement of the image of one point with respect to the other if the platen is moved upward 20 mm? Downward 20 mm?
- 11-10. In problem 11-9, the conjugate images coincide at a projection distance of 300 mm. Compute the  $x$ -displacements for an upward movement of 20 mm and a downward movement of 20 mm.
- 11-11. Compute the total effect in the projection plane lying 360 mm below a Multiplex projector lens on points 2, 3, and 4 of Fig. 11-8 if the left
- 169



**Appendix II**  
**PHOTOGRAMMETRIC INSTRUMENTS**

## 10-8 INSTRUMENTAL RECTIFICATION

Most photographic rectification is performed in order to produce rectified aerial photographs which have been brought to some uniform scale in order to produce high-quality mosaics. Photographic rectification is used also to produce scaled photo maps of flat-lying terrain in lieu of producing more expensive orthophotographs and orthophoto mosaics. In both of these applications, a continuous tone picture of the ground is needed. This is obtained by a complete rectification of all the imagery contained in the original tilted or oblique negative in the optical-mechanical instrument called the *rectifier*. The rectifier is somewhat similar to a photographic enlarger, except that in a rectifier, both the negative plane and the easel plane (or the lens plane and the easel plane) can tip and tilt. Furthermore, the negative can be shifted in the  $x$  and  $y$  directions in a rectifier.

Referring to Fig. 10-7, a tilted photograph is taken at exposure station  $L$  with a camera whose focal length is  $f$ . The negative and the resulting photograph, shown in their correct position, are both the same size and both contain the same tilt displacements. If the negative is transformed into an equivalent vertical photograph taken from the same exposure station and then enlarged by a magnification factor  $m$ , the principal distance of the resulting

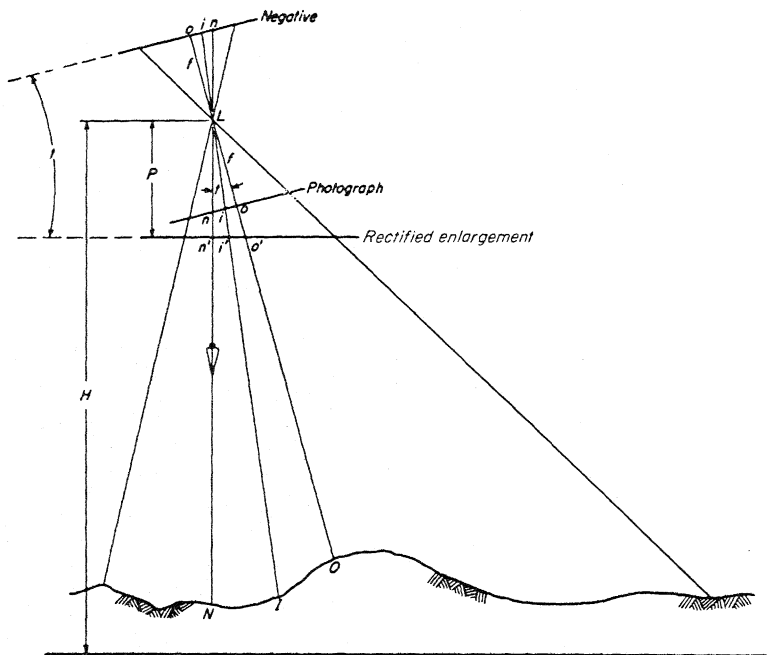


Figure 10-7. Tilted photograph and rectified enlargement.

vertical photograph will be  $p = mf$ . This rectification and enlargement can be accomplished in theory by placing the negative in a tilted plane, a sheet of enlarging paper in a horizontal plane called the easel plane, and a pinhole opening between the two planes, in such positions that the pinhole lies at a distance  $f$  from the negative plane and at a distance  $p$  from the easel plane, as shown in Fig. 10-8. A source of light over the negative would produce a point-to-point projective transformation of the negative images onto the enlarging paper, thus effecting the desired rectification.

The pinhole rectifier described above is unsatisfactory for several reasons, chief of which is the fuzziness of the image due to the finite size of the pinhole and the unreasonably long exposure time required. An enlarger lens is thus required. In Fig. 10-9, an enlarger is used to change the magnification of an untilted photograph in the ratio  $t/s$  using a lens with a focal length  $F$  according to the lens equations given by equations 2-7 and 2-8. In order to convert this enlarger to a rectifier, the negative and easel planes (or the lens and easel planes) must be able to tilt. This requires that the optical condition called the *Scheimpflug condition* be satisfied. The Scheimpflug condition states that in order to maintain sharp focus between the negative plane and the easel plane when these planes are not parallel, the negative plane, the plane of the lens, and the easel plane must intersect along one line. The plane of the lens is the plane perpendicular to the optical axis of the lens and passing through the optical center of the lens.

In Fig. 10-10, which is a section of a rectifier, the negative plane makes an angle  $\alpha$  with the lens plane. The focal length of the projector is designated as  $F$ . The distance  $F$  measured along the optical axis upward along  $Ld$  from  $L$  defines the position of point  $V$ . The line  $VL$  in turn fixes the direction of the easel plane in the following way. Since  $V$  lies at a distance  $F$  from the lens at  $L$ , measured along the optical axis, it is in the focal plane of the lens, and its image is formed at infinity. Therefore, the easel plane must be parallel with the line  $VL$ , forming the angle  $\beta$  with the lens plane. Otherwise, a bundle of rays from  $V$  will form an image at a finite distance in the easel plane. Further-

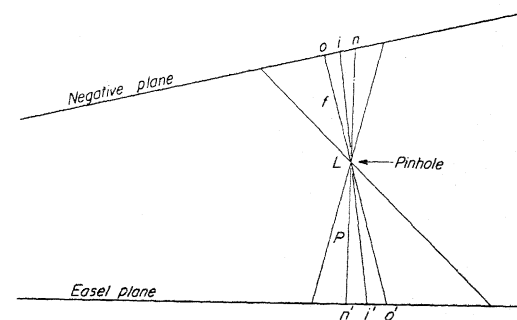


Figure 10-8. Pinhole rectification.

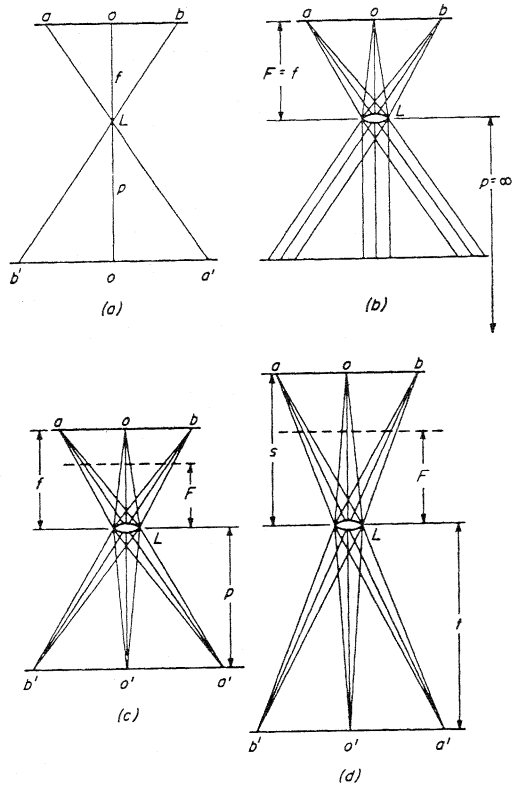


Figure 10-9. Photographic enlargement. (a) Pinhole enlargement,  $m = p/f$ . (b) Enlargement set for infinity focus,  $F = f$ . (c) Enlarger set for  $m = p/f$ . (d) Enlarger set for  $m = t/s$ , with  $F$  independent of  $f$ .

more, by the Scheimpflug condition, the easel plane must intersect the negative plane along the line formed by the intersection of the negative plane and the lens plane. The point trace of this line in the plane of Fig. 10-10 is at  $S$ .

Point  $W'$  is defined by the distance  $F$  below the lens. Since  $W'$  lies in the focal plane of the lens, it represents the point where a bundle of rays lying in the plane of Fig. 10-10 and coming from infinity will be brought to focus in the easel plane. The line  $W'L$  must therefore be parallel with the negative plane.

With the positions of the negative plane, the lens plane, and the easel plane fixed, a bundle of rays from point  $a$  will come to focus at  $a'$  and rays from point  $b$  will come to focus at  $b'$ . The points  $a'$  and  $b'$  are so located that

$$\frac{1}{x} + \frac{1}{x'} = \frac{1}{F} \quad \text{and} \quad \frac{1}{y} + \frac{1}{y'} = \frac{1}{F}$$

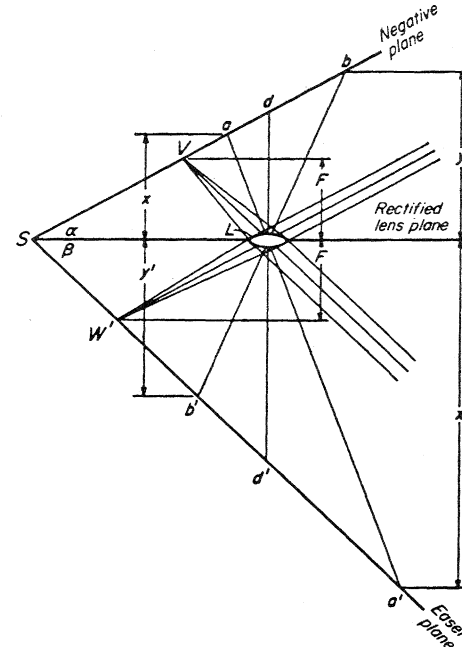


Figure 10-10. Scheimpflug condition.

### 10-9 GEOMETRY OF THE RECTIFIER

In order to allow for a continuous range of tilt angles, magnifications, and camera focal lengths, a rectifier must be designed to permit changes in angles  $\alpha$  and  $\beta$  of Fig. 10-10, and also to permit changes in the distances  $dL$  and  $d'L$ . The relationship between the rectifier elements shown in Fig. 10-10 is obtained from the original photography configuration shown in Fig. 10-7 by means of a set of equations called the *rectifier equations*.

In Fig. 10-11,  $L_C$  is the exposure station of a tilted photograph,  $f$  is the camera focal length, and  $p = mf$  is the principal distance of the rectified photograph. These quantities correspond to those shown in Fig. 10-7. Point  $S$  is the axis of perspective between the negative plane and the plane of the rectified photograph. Point  $V$  is the vanishing point of the tilted photograph for lines that lie parallel to the principal plane of the photograph. It represents the image of objects lying at infinity. Thus  $L_C V$  must be parallel to the plane of the rectified enlargement (plane  $SA$ ). Point  $W$  is the vanishing point in the rectified enlargement for objects that would be photographed at infinity in the plane of the tilted photograph. Thus  $WL_C$  must be parallel to the negative plane. These two points are unique and cannot change their relationship with  $L_C$  and  $S$ . Consequently, the figure  $SVL_C W$  must always

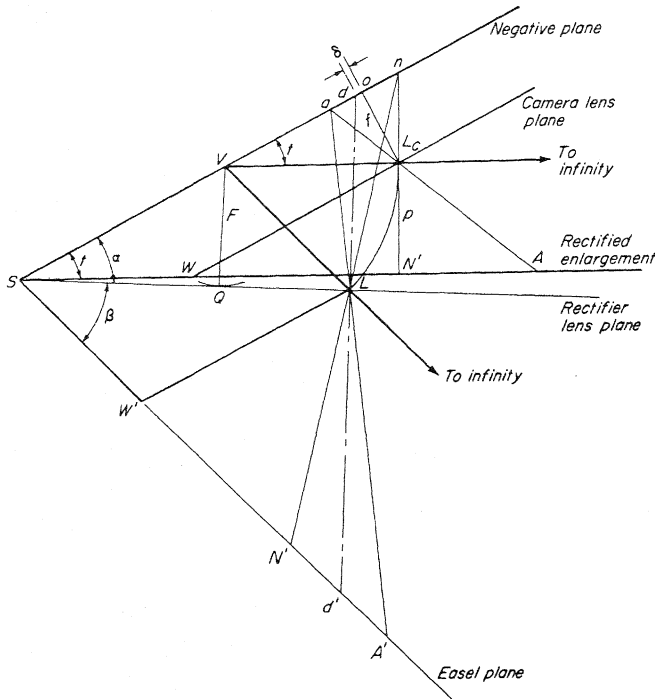


Figure 10-11. Rectifier geometry.

remain as a parallelogram of the same side lengths in whatever configuration is selected for the rectifier components.

Assume that a given rectifier lens has a focal length  $F$  as shown in Fig. 10-10 and is placed at  $L$  in Fig. 10-11 in order to make  $VL = VL_C$ . The rectifier lens plane is  $SL$  which is tangent to an arc from  $V$  with a radius equal to  $F$  at point  $Q$ . In order to be able to construct such an arc, the following relationship must be satisfied

$$F \leq p \csc t, \quad p = mf \tag{10-18}$$

Also, in order that the arc  $L_C L$  meets the line  $SQ$ , the following must be satisfied

$$F \leq f \csc t \tag{10-19}$$

In order to accommodate both an enlargement and a reduction, then equation 10-18 must be satisfied in the rectifier.

The easel plane of the rectifier must be parallel to  $VL$  if  $V$  still represents the vanishing point. Thus,  $SVLW'$  is a parallelogram of sides equal in length

to those of the original parallelogram  $SVL_CW$ . Points  $S$ ,  $V$ , and  $W'$  of Fig. 10-11 correspond to the same points in Fig. 10-10.

The image of negative point  $a$  projected through lens  $L_C$  appears at  $A$  on the plane  $SA$  of the rectified enlargement. When projected through the rectifier lens at  $L$  it appears on the easel plane at  $A'$ . From similar triangles  $aVL_C$  and  $aSA$ ,

$$SA = VL_C \frac{Sa}{Va}$$

but since  $VL_C = VL$ ,

$$SA = VL \frac{Sa}{Va}$$

The two triangles  $aVL$  and  $aSA'$  are also similar. Thus

$$SA' = VL \frac{Sa}{Va}$$

or  $SA = SA'$ . Since  $a$  is any point, the above analysis is true for any point in the negative plane. This demonstrates that the rectification of the negative in the easel plane (plane  $SA'$ ) is identical to its rectification in the plane of the original rectified enlargement (plane  $SA$ ).

The axis of the rectifier lens intersects the negative plane at point  $d$ . This is displaced from the principal point  $o$  along the principal line a distance  $\delta$  shown in Fig. 10-11. Since the principal plane of the negative is in the plane of the figure, it is obvious that the negative must be able to be rotated and shifted in two directions in its own plane. Similarly, the enlarging paper has the same three degrees of freedom on the easel in order to locate its absolute position in a map system.

In addition to the six degrees of freedom cited above, four other elements of the rectifier must be varied. These are shown in Fig. 10-11 as:

1. The angle  $\alpha$  between the negative plane and the lens plane
2. The angle  $\beta$  between the easel plane and the lens plane
3. The distance  $Ld$  along the optical axis between the lens and the negative plane
4. The distance  $Ld'$  between the lens and the easel

All the above elements total 10 degrees of freedom. However, only eight parameters are required to relate the negative plane to the easel plane as discussed in sections 10-7 and 10-8. But  $Ld$  and  $Ld'$  are related by the lens equation, and  $\alpha$  and  $\beta$  are related by the Scheimpflug condition. Thus, there are eight independent elements or degrees of freedom in a rectifier. Since the rectified enlargement or reduction is not usually related to a map coordinate system in a rectifier, three degrees of freedom can be eliminated. The rectifier is thus designed around only five degrees of freedom.

174

If the rectifier is designed so that the lens is fixed in position (called a *fixed-lens* rectifier), the rectifier equations are given as follows:

$$\sin \alpha = \frac{F \sin t}{mf} \tag{10-20}$$

$$\sin \beta = \frac{F \sin t}{f} = m \sin \alpha \tag{10-21}$$

$$Ld = F \left( 1 + \frac{\tan \alpha}{\tan \beta} \right) = F \frac{\sin(\alpha + \beta)}{\cos \alpha \sin \beta} \tag{10-22}$$

$$Ld' = F \left( 1 + \frac{\tan \beta}{\tan \alpha} \right) = F \frac{\sin(\alpha + \beta)}{\sin \alpha \cos \beta} \tag{10-23}$$

$$\delta = \frac{f}{\sin t} \left( \cos t - \frac{\cos \beta}{\cos \alpha} \right) \tag{10-24}$$

in which  $\delta$  is the amount by which the negative must be shifted along the principal plane of the negative in order to bring point  $d$  on the optical axis of the rectifier lens.

The negative is placed in the negative holder and rotated until the principal plane of the photograph lies in the principal plane of the rectifier. The negative is then shifted through the distance  $\delta$ , positive upward. The other settings are then made in the rectifier, following which the rectified photograph is produced.

The settings of the rectifier may be computed from the orientation elements following a space resection, or from readings taken in a stereoscopic plotting instrument. In most rectifier production, however, the settings are arrived at empirically as discussed in section 10-13. If the orientation matrix  $\mathbf{M}$  is known, the tilt and swing can be obtained by the following:

$$\begin{aligned} \cos t &= m_{33}, & \text{from which } t \text{ is computed} \\ \left. \begin{aligned} \sin s &= -\frac{m_{13}}{\sin t} \\ \cos s &= -\frac{m_{23}}{\sin t} \end{aligned} \right\} & \text{from which } s \text{ is computed} \end{aligned} \tag{10-25}$$

### 10-10 AUTOMATIC RECTIFIERS

An automatic rectifier is a rectifier so constructed that it automatically maintains the relationship between the object distance and the image distance expressed in equation 2-7, and at the same time fulfils the Scheimpflug condition. The object-image relationship is maintained by an inversor, one

design of which is described in section 3-10. The Scheimpflug condition is satisfied by means of a Carpentier inversor, which causes the negative plane, the easel plane, and the lens plane to intersect along a common line.

A Carpentier inversor is shown schematically in Fig. 10-12. The member  $dA$  is fixed perpendicular to the negative plane, and the member  $Bd'$  is fixed perpendicular to the easel plane. Point  $A$  is located at a distance  $a$  from the axis of rotation of the negative plane, this distance being measured parallel to the lens axis  $dLd'$ . Point  $B$  is located at a distance  $a$  from the axis of rotation of the easel plane. The member  $AB$  pivots about a fixed point  $C$ , which is located at a distance  $a$  from the optical center of the lens. Both point  $A$  and point  $B$  are constrained to move along a horizontal line so as to maintain the distance  $a$ . A change of the angle  $\alpha$  to  $\alpha'$  causes a corresponding change of  $\beta$  to  $\beta'$ , and also movement of the common point of intersection  $S$  to  $S'$ . Coupled with the Carpentier inversor is the inversor that maintains the object-image relationship.

The automatic rectifier is provided with five basic motions and has corresponding dials or graduations for setting off computed or assumed values.

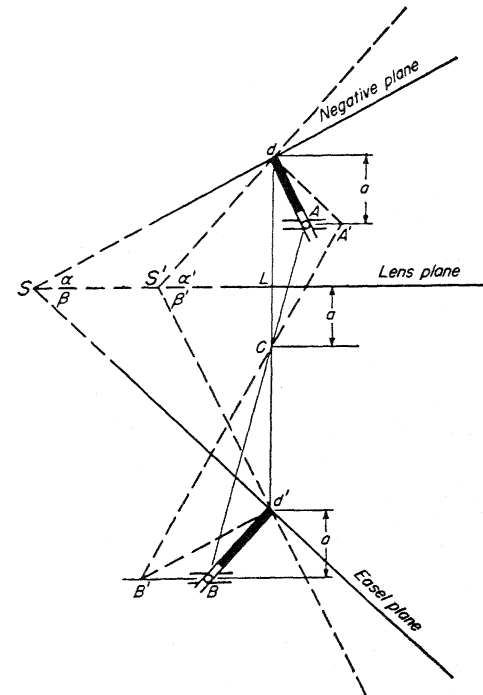


Figure 10-12. Carpentier inversor.

These motions provide for the required magnification; the swing of the negative so as to place the principal plane of the negative in the principal plane of the rectifier; the offset motion in the direction of the principal plane; an offset motion normal to the direction of the principal plane; and the rotation of the easel plane with respect to the lens plane.

The automatic rectifier shown in Fig. 10-13 maintains critical focus by means of a combination *Pythagorean-Carpentier* inverter. The Pythagorean inverter performs the same function as does the Peaucellier inverter. The rectifier is of the fixed-lens type. By means of automatic calculators, any three settings of the rectifier establish the remaining two settings in the instrument. The negative is automatically displaced in the direction of the principal plane of the photograph through the small distance  $\delta$ .

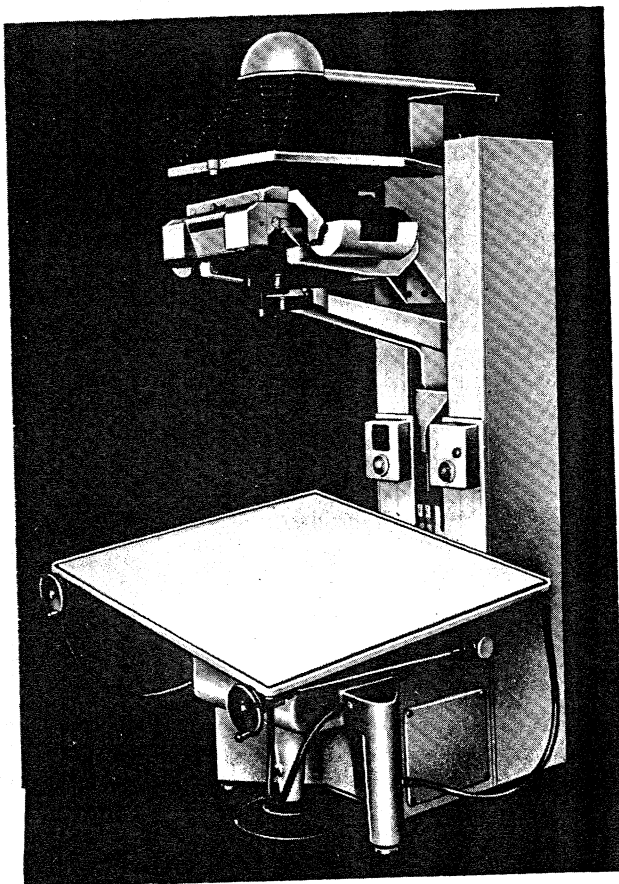


Figure 10-13. Zeiss SEG 5 rectifier. Courtesy of Carl Zeiss, Oberkochen.

#### 10-11 CONTROL FOR EMPIRICAL RECTIFIER ORIENTATION

Settings of an automatic rectifier may be arrived at by a trial-and-error method called empirical rectification. As preparation for the method, the easel plane must contain the map positions of at least four images appearing on the photograph. These map positions must then be modified to account for the relief displacement of each control point. One of the most common methods of obtaining the control is through the use of a radial-line triangulation system developed in the desired scale of the rectified photographs as discussed in section 7-14.

The easel control can take the form of a planimetric or topographic map which has been enlarged or reduced to the desired scale of the rectified photography. This type of control allows for the rectification of low and high obliques as well as near verticals since radial-line triangulation is not required.

If the rectified photograph is to be used as an accurate photo map, the ground must be fairly flat in order to avoid relief displacements. The map control should then be obtained by direct field surveys in the area.

#### 10-12 EFFECT OF RECTIFIER MOTIONS ON EASEL POINTS

The effects of the five rectifier motions on the image of a square figure projected from the negative onto the easel are shown in Fig. 10-14. The quadrilateral  $ABCD$  is the original figure obtained on the easel when there is a downward slope of the easel as indicated in view (a). The effect of magnification is shown in the same view. The four points  $A$ ,  $B$ ,  $C$ , and  $D$  have been displaced outward to points  $A'$ ,  $B'$ ,  $C'$ , and  $D'$  along radials from the point at which the easel is pierced by the optical axis of the lens. Points  $A$  and  $B$  on the upward side have not been displaced so much as have points  $C$  and  $D$  on the downward side. In views (b), (c), (d), and (e), the quadrilateral  $A'B'C'D'$  is the net result of each of the four motions after the line  $A'B'$  has been made to coincide with the line  $AB$  by a change in magnification, a rotation of the sheet on the easel, or a shift of the sheet, or a combination of these three. In this way the effects of the motions are reduced to their effects on points  $C$  and  $D$  only.

In Fig. 10-14(b), the negative has been rotated about the principal point, this rotation corresponding to a swing motion. Point  $C$  has swung from  $C''$  to  $C'$ , while point  $D$  has swung from  $D''$  to  $D'$ . After the line  $A'B'$  has been made to coincide with  $AB$  by swinging the easel sheet and changing the magnification, the net effect of the negative swing motion is seen at points  $C$  and  $D$ . The side  $AD$  has shortened to  $A'D'$ , while the side  $BC$  has lengthened to  $B'C'$ . The sides  $A'D'$  and  $B'C'$  do not converge quite so much as do the sides  $AD$  and  $BC$ . Furthermore, side  $C'D'$  is no longer parallel to side  $A'B'$ .

In Fig. 10-14(c) the tilt of the easel has been increased. So, after  $A'B'$  has been made to coincide with  $AB$ , points  $C$  and  $D$  are seen to have moved

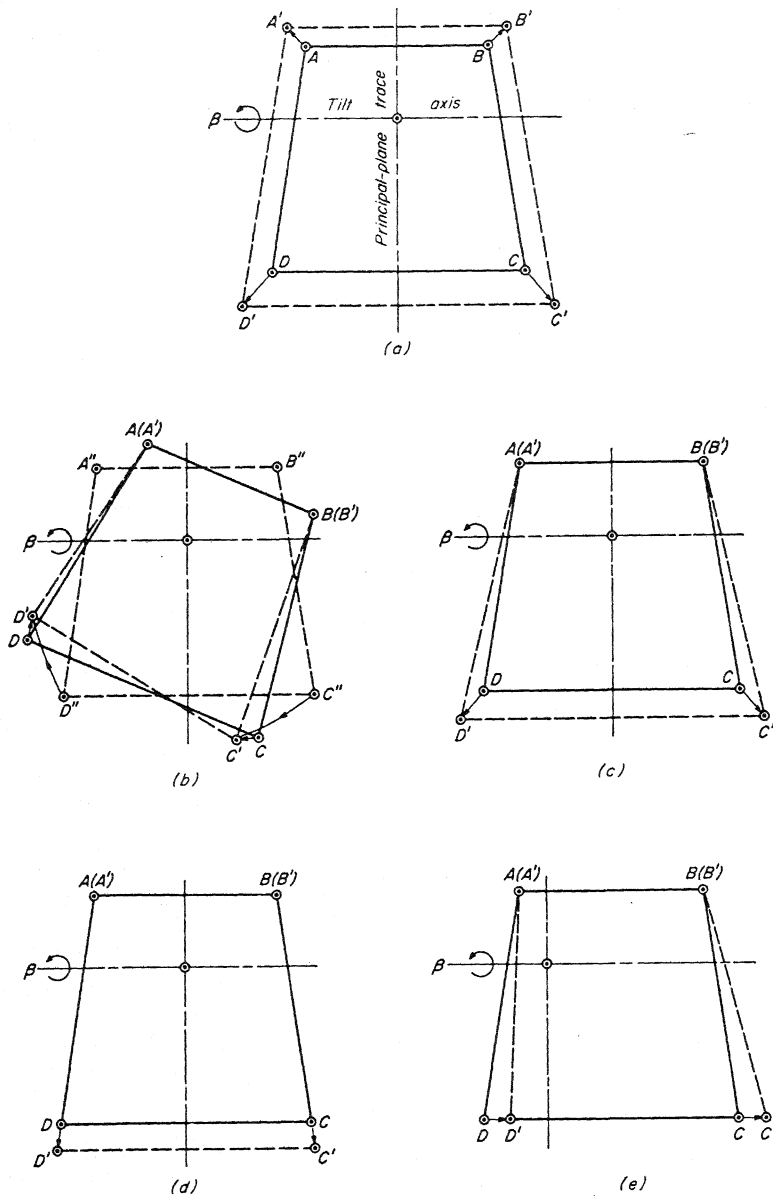


Figure 10-14. Deformation of the easel image. (a) Magnification. (b) Swing. (c) Easel tilt. (d) Y displacement. (e) X displacement. Copyright 1966, American Society of Photogrammetry. Reproduced with permission.

outward to  $C'$  and  $D'$ . The entire quadrilateral has been elongated in a direction perpendicular to the tilt axis of the easel, and the convergence of the sides has increased.

In Fig. 10-14(d) the negative has been displaced in a direction parallel to the principal plane of the rectifier and in a direction toward the intersection of the negative plane and the easel plane. This movement is designated as a  $Y$ -displacement. The displacements  $CC'$  and  $DD'$  are in a direction opposite to that of the negative, and along the lines  $BC$  and  $AD$  as shown.

In Fig. 10-14(e) the negative has been displaced to the left in a direction parallel to the tilt axis of the easel. This movement is termed an  $X$ -displacement. Such a displacement causes a deformation of the figure similar to a shear deformation. The net displacements of the points are to the right and in a direction parallel to the tilt axis of the easel.

### 10-13 EMPIRICAL ORIENTATION OF THE RECTIFIER

Let it be assumed that a square  $abcd$ , whose corners represent four control points or pass points on the negative, is projected onto the easel of a rectifier that is set for unit magnification and for zero tilt. With these settings the projection of the image of the square onto the easel will appear as shown in Fig. 10-15(a) at  $abcd$ . The easel control quadrilateral  $ABCD$  has been located to the desired datum scale as previously outlined. The problem is to orient the projected image of  $abcd$  so that it fits the control quadrilateral.

In Fig. 10-15(a), the image has undergone a magnification that makes side  $A'B'$  fit side  $AB$ . Note that  $C'$  and  $D'$  must now be displaced in a direction away from line  $AB$  and outward from the center of the format. An analysis of Fig. 10-14 will show that an easel tilt will produce a certain amount of the desired displacement. If at this stage  $C$  and  $D$  were required to be displaced toward  $AB$  and inward toward the center, the entire negative would have to be swung approximately  $180^\circ$ . The line  $CD$  would then become the control line.

In Fig. 10-15(b), the easel has been tilted simultaneously with an increase in magnification (to hold the control line). As a result,  $C$  has been slightly overcorrected to  $C'$ , while  $D$  has been greatly overcorrected to  $D'$ .

In Fig. 10-15(c), a swing and a slight change in magnification have caused line  $C'D'$  to lie nearly parallel to  $CD$ . If  $AB$  were parallel to the tilt axis of the easel at this stage, the swing would be increased until  $C'D'$  was, in fact, parallel to  $CD$ . The effect of an  $X$ -displacement, as shown in Fig. 10-15(d), is to cause lines  $AD$  and  $A'D'$  and lines  $BC$  and  $B'C'$  to nearly coincide. If at this stage  $AB$  were parallel to the tilt axis of the easel, the  $X$ -displacement would be increased until these lines did, in fact, coincide.

In Fig. 10-15(e), a  $Y$ -displacement and a change in magnification cause points  $C'$  and  $D'$  to coincide with the easel control points  $C$  and  $D$ , respectively. The easel control sheet is now replaced by enlarging paper, and an exposure is made. The result is a rectified photograph brought to the desired scale.

# Chapter 11

## Theory and Techniques of Orientation

### 11-1 INTRODUCTION

Two different *types* of orientation are considered in photogrammetric operations. These are interior orientation and exterior orientation. These two orientations are achieved by two *processes* of orientation called *relative orientation* and *absolute orientation*. Interior orientation has been defined as that set of three elements ( $x_o, y_o, f$ ) which recover the geometry of the bundle of rays inherent in each photograph as that which existed at the instant of exposure. Exterior orientation has been defined as that set of six elements ( $X_L, Y_L, Z_L, \omega, \phi, \kappa$ ) which fix the spatial position and attitude of each individual bundle (each photograph) with respect to the ground (or object) coordinate system. The interior orientation elements are usually known from the camera calibration data. On the other hand, the exterior orientation elements must be determined for each exposure, either directly by means of auxiliary sensors (see section 4-13) or else indirectly by means of ground control points as discussed in Chapters 10 and 13.

Relative orientation is the process by which a pair of overlapping photographs are related to one another in some arbitrary space to correspond with their coorientation at the time of photography. The relative orientation process solves for five orientation elements. These are either five angular

178

relations between the two individual bundles representing the photographs or else three rotational and two translational elements. The result is the formation of a three-dimensional model in arbitrary space and at an arbitrary scale.

Absolute orientation is the process by which a pair of relatively oriented photographs, and hence the three-dimensional model, is related to the ground control system. This consists of solving for seven absolute orientation elements. They are the scale of the three-dimensional model, three translations of the model, and three rotations of the model. It is to be noted that if the elements of exterior orientation of each of the two overlapping photographs ( $\omega_L, \phi_L, \kappa_L, X_L, Y_L, Z_L, \omega_R, \phi_R, \kappa_R, X_R, Y_R, Z_R$ ) are known, the relative (five parameters) and absolute (seven parameters) orientation are also known.

Relative and absolute orientation are accomplished either instrumentally or analytically. Both empirical and numerical methods are employed in the instrumental solutions to the orientation problem. This chapter will begin with the empirical techniques employed in a very simple stereoscopic plotting instrument because it is somewhat easier to visualize than the numerical and analytical methods. Also, the empirical methods are employed in the majority of photogrammetric mapping projects.

A stereoscopic plotting instrument shown in its most elementary form in Fig. 11-1, is an optical mechanical instrument of high precision. To use such an instrument, a pair of overlapping photographs are first placed in a pair of carriers and are oriented to ground control. Then the rays from the two photographs are projected anaglyphically (see section 5-9) and are caused to intersect in the measuring space of the instrument to form a theoretically perfect model of the terrain. The instrument will be referred to simply as a plotter. The photograph carriers are called projectors in some instruments and are referred to as cameras in other instruments. The model of the terrain will be referred to simply as a model.

The model formed by the projection of rays from the two projectors is at a known scale, which is established by the scale used for plotting the ground control. The horizontal scale and the vertical scale are the same. The operator may view the model stereoscopically, that is, in three dimensions by using colored spectacles (see section 5-9). A measuring mark, located in the middle of the tracing table, and visible to the operator at all times, is used to measure the model in all three dimensions. When aerial photographs are used, the real or apparent up-and-down motion of the measuring mark is a measure of elevation, to the scale of the model, and the movement of the mark in a horizontal plane is a measure of the change in the  $X$ - and  $Y$ -coordinates between points, to the scale of the model.

The space position of the measuring mark in the model can be read on instrument  $X, Y, Z$  scales and then recorded manually, or can be automatically recorded, to give the space position of any point appearing in the model, to the scale of the model. The horizontal movement of the measuring

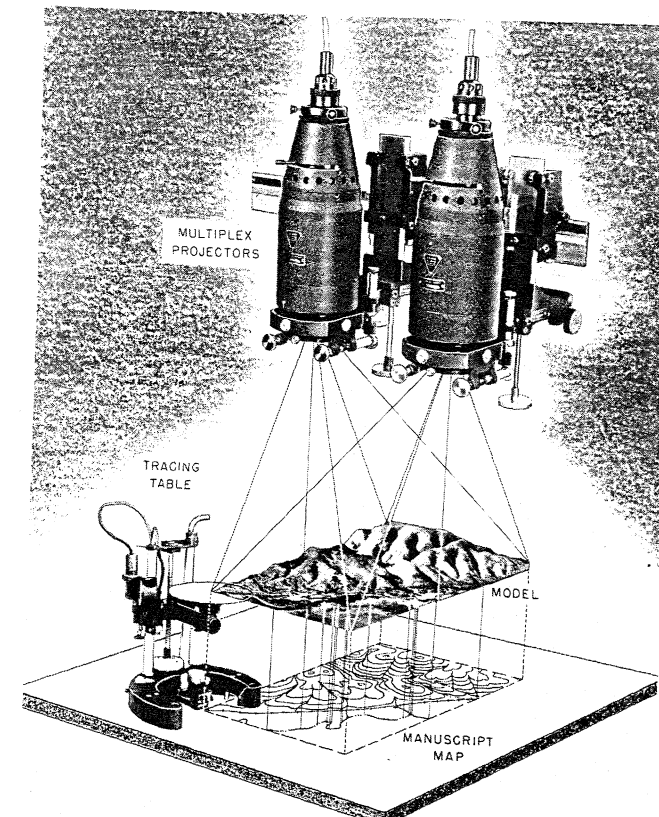


Figure 11-1. Elementary stereoscopic plotting instrument. Bausch and Lomb Multiplex. Courtesy of US Geological Survey.

mark throughout the model is transmitted to a plotting pencil that traces out the map positions of the features appearing in the overlap area of the two photographs forming the model. The plotting pencil may move at the same scale as the model, or it may move at a larger or a smaller scale than the model, the relative movement depending on the type of plotter.

The position of a contour line is traced out by the plotting pencil when the  $Z$ -position of the measuring mark is held fixed at the desired elevation of the contour line. In this way the operator locates points of equal elevation in the model by a continuous trace along the surface of the model. The contour lines thus plotted, together with the planimetric features previously mentioned, are plotted in orthographic projection on a map sheet, producing a topographic map at the desired scale.

Figure 11-1 is a schematic diagram of two Multiplex projectors that depicts the basic ideas introduced above. The pair of projectors are suspended from a horizontal bar, which represents the general direction of the line of flight. A pair of reduced diapositives are placed in the two projectors above the projector lenses. As will be discussed later, the amount of reduction of the original negative from a 9 by 9 in. (23 by 23 cm) size down to the size of the diapositive depends on the principal distance of the projector lens, which is about 30 mm, and on the focal length of the aerial camera lens that took the photographs.

Each of the two projectors has six motions, three translational motions and three rotational motions, which correspond to the six elements of exterior orientation for each photograph. The three translational motions are shown in Fig. 11-2. Each projector may be moved independently in a direction parallel to the supporting bar, that is, in the direction of the flight line. This motion is referred to as the *X-motion*. Each projector may also be moved independently in a horizontal direction and perpendicular to the supporting bar. This motion is referred to as the *Y-motion*. Moreover, each projector may be moved independently in a vertical direction and perpendicular to the supporting bar. This motion is called the *Z-motion*. The three translation motions are used to establish the air base in the plotting instrument between two projectors. They are thus referred to as base component motions  $b_x$ ,  $b_y$ , and  $b_z$ .

The three rotational motions of each projector are also indicated in Fig. 11-2. A projector may be rotated about a line generally parallel with the supporting bar and passing through the emergent nodal point of the projector lens. This rotation is called omega, ( $\omega$ ), and is sometimes referred to as *x-tilt*. The projector may be rotated similarly about a horizontal line that is perpendicular to the supporting bar and passes through the emergent

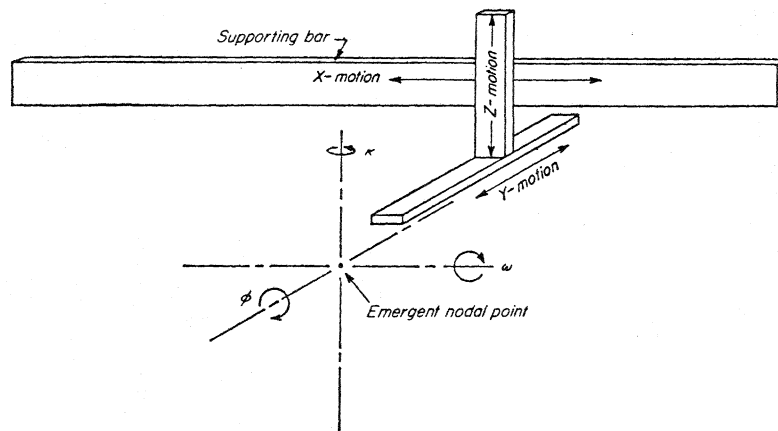


Figure 11-2. Motions of Multiplex projector.

nodal point of the projector lens. This rotation is called phi, ( $\phi$ ), and is also called *y-tilt*. The projector may also be rotated about the optical axis of the projector lens. This rotation is called the swing of the projector, or kappa ( $\kappa$ ). It should be noted that the axes of rotation are mutually perpendicular. The  $\phi$ -axis is the primary rotational axis of the Multiplex instrument. Its direction with respect to the supporting bar remains unchanged, whereas both the  $\omega$ -axis, which is secondary, and the  $\kappa$ -axis (optical axis), which is tertiary, are rotated during the orientation process.

The six motions of each projector are used to orient the projectors in their correct space positions and attitudes with respect to the map sheet that contains ground control points.

## 11-2 INTERIOR ORIENTATION

In order to reconstruct the bundle of rays produced at the time of photography, the proper elements of interior orientation in the projectors must be established. The operational steps involved are as follows:

1. Prepare the diapositive to the correct size
2. Eliminate the radial distortion of the aerial camera lens
3. Center the principal point of the diapositive on the optical axis of the projector lens
4. Set off the principal distance in the projector

The diapositive is a reproduction with positive tone made from the original film negative. It is either the same size as the original negative or else a reduction to a smaller format. The full size diapositive is prepared either by contact printing or by 1 to 1 projection printing in a reduction printer. The reduced size diapositive must be made in a reduction printer, two types of which are shown in Fig. 11-3. A small cross representing the principal point is imaged on the diapositive at the intersection of the fiducial lines in the reduction process.

Elimination of radial-lens distortion is accomplished in several different ways, depending on the type of stereoscopic plotting instrument. The method employed for the Multiplex used a lens in the reduction printer containing the same distortion characteristics as the Metrogon camera lens, which was used in conjunction with Multiplex mapping. Other methods used to eliminate lens distortion are discussed in Chapter 12.

The diapositive is placed in its carrier and shifted in both directions to make the principal point cross coincide with optical axis of the projector lens. This is accomplished using a special centering device. This accomplishes step 3 above.

The Multiplex has a fixed principal distance between the diapositive and the rear nodal point of the projector lens. The reduction process must therefore relate the camera focal length to this fixed distance in order to complete step 4 above. In Fig. 11-4(a) the camera focal length is  $f$ , and in Fig.

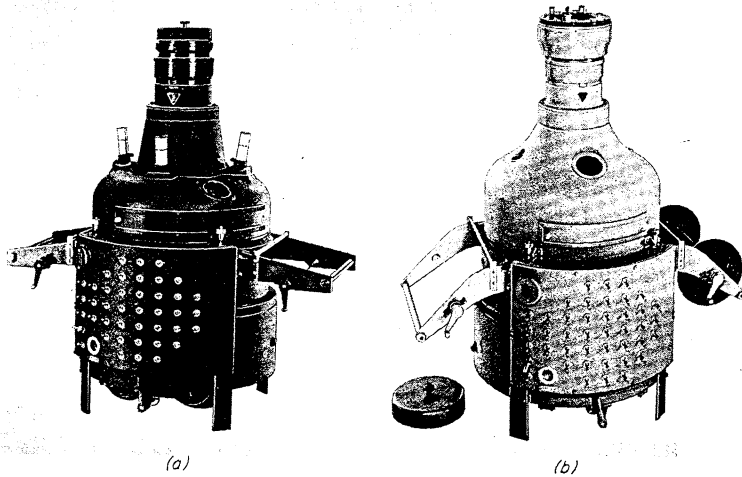


Figure 11-3. (a) Multiplex reduction printer. (b) Balplex reduction printer (see section 12-8). Courtesy of Bausch and Lomb Optical Co.

11-4(c) the principal distance of the diapositive is  $p$ . As indicated in view (a), a ray of light from ground point  $E$  enters the camera lens at an angle  $\alpha$  with the optical axis of the camera lens, and appears at  $e$  on the negative. As represented in view (b), the negative has been reduced in a reduction printer by projection through the base (see section 3-10), to make a diapositive with negative geometry and containing image  $e'$ . As indicated in Fig. 11-4(c), the diapositive is projected through the projector lens, and the ray from  $e'$  is projected to  $E'$  in the plane of best focus. The ray  $e'E'$  makes the same angle with the optical axis of the projector lens as the ray  $Ee$  made with the optical axis of the camera lens at the time of exposure. In order to recreate this true angular relationship, the distances  $A$  and  $B$  in Fig. 11-4(b) must bear the following relationship:

$$\frac{A}{B} = \frac{f}{p} \tag{11-1}$$

in which  $A$  is the optical distance in the reduction printer from the plane of the negative to the front nodal point of the reduction-printer lens;  $B$  is the optical distance from the emergent nodal point of the reduction-printer lens to the diapositive plane;  $f$  is the focal length of the aerial camera lens, modified to allow for uniform film deformations; and  $p$  is the principal distance of the projector lens.

In many stereoscopic plotting instruments using full size contact or 1 to 1 diapositives, the variation in focal lengths encountered in different projects is accommodated by physically changing the principal distance in

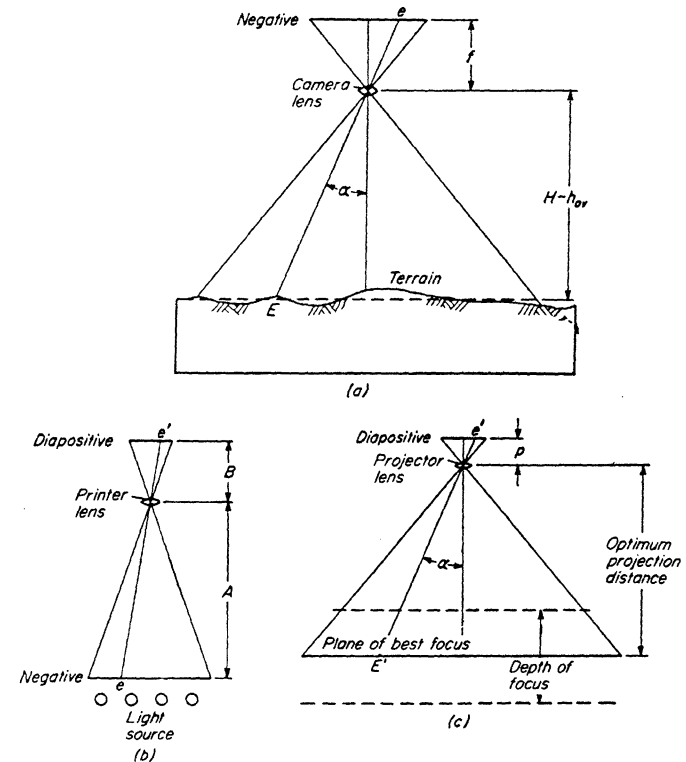


Figure 11-4. Relationship between aerial negative and diapositive in reduction process.

the instrument between the diapositive plane and the projection center of the diapositive. This is discussed in Chapter 12.

On examination of Fig. 11-4(a) and (c), it is seen that the orientation of the diapositive in the projector must be the same as the orientation of the negative in the camera. That is, the right-to-left and front-to-back relationships must be the same. This is accomplished by printing through the back of the film when making the diapositive. Then, when the diapositive is placed in the projector, with the emulsion down, the diapositive image is in the same orientation in the projector as the negative image was in the aerial camera. When the diapositive is projected this way, the image of the ground will be correct right-to-left and front-to-back.

### 11-3 RELATIVE ORIENTATION

After the interior orientation of each diapositive has been accomplished, the corresponding rays from the two projectors will not generally intersect

one another when projected into the model space. This situation is shown in Fig. 11-5(a). The two rays  $L_1a_1$  and  $L_2a_2$  fail to intersect in a point when they reach the projection plane, which is represented by the top of the tracing table in the Multiplex. The mismatch is resolved into two components  $p_x$  and  $p_y$ , which are called *x-parallax* and *y-parallax*. As developed in Chapters 5 and 7, *x-parallax* is a function of elevation and can be eliminated at each point in the model space simply by raising or lowering the projection plane as shown in Fig. 11-5(b), or else by displacing one or the other projector in the  $b_x$  direction as shown in Fig. 11-5(c). The *y-parallax* that remains at each point in the model is systematically eliminated in the operational process of relative orientation. This process involves the rotation and translation of one or both of the projectors.

In order to study the effect of each translation and rotation on the elimination of *y-parallax* in the model, refer to Fig. 11-6. A diapositive containing nothing but nine points located in a square symmetrical array is placed in one of the projectors, and all rotational elements are set to zero. At this position, the optical axis of the projector is vertical, and the array of points projected onto a horizontal plane is similar to that on the diapositive except for a scale change due to projection. Starting from this zero position of the projected points, a small (differential) change is introduced in each of

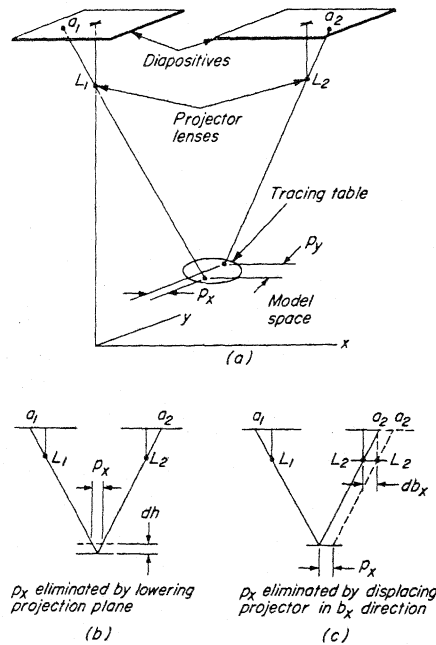


Figure 11-5. Nonintersecting rays from two projectors.

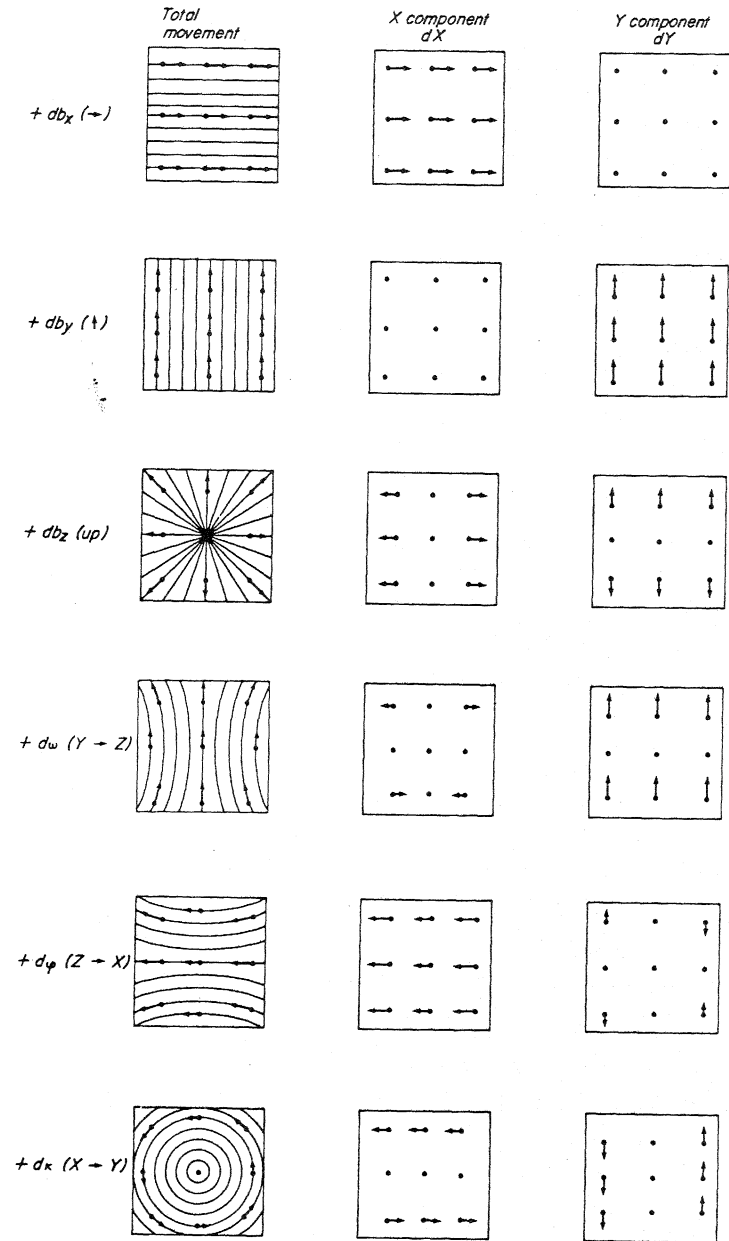


Figure 11-6. Effect of projector motions on movement of points in projection plane.

the six orientation elements. Figure 11-6 shows the total movements from the zero position due to the change in each element. The  $X$ - and  $Y$ -components of these movements are also shown.

A translation  $db_x$  causes an equal amount of shift of all the points in the  $X$ -direction. This movement has no effect on  $y$ -parallax because it produces no  $Y$ -component. On the other hand a translation  $db_y$  causes an equal amount of shift in the  $Y$ -direction at all points.

A  $db_z$  translation upward (positive) has the effect of increasing the scale of the projected array of images. The central point, which is directly on the projector optical axis, does not undergo any movement. The other eight points, however, move radially outward from the central point in proportion to their distance from the central point. The  $X$ -component is seen to be equal but of opposite direction in the two outer columns of points, and the  $Y$ -component is equal but of opposite direction in the two outer rows of points. It is to be noted that no  $Y$ -displacement has been introduced along the middle row of points due to the  $db_z$  translation.

The effect of an  $\omega$ -rotation is shown in Fig. 11-7. The six points shown in the figure correspond to the middle and right columns of points in Fig. 11-6. The three points in the middle column lie in a vertical plane containing the projection center. Their projected images are seen to be displaced along a straight line. The outer two points move more because they are farther from the projection center than the middle point. Any one of the three rays projected through the right column of points is an element of a cone whose axis is the  $X$ -axis of the projector. As the projector is rotated, the element sweeps through a conical surface, which intersects the horizontal projection plane in a hyperbola. These three points, as well as those lying in the left column, therefore, move through small portions of hyperbolic arcs in the projection plane as shown in Fig. 11-7. A  $d\omega$  rotation causes a  $Y$ -displacement of all nine points. Those in the two outer rows are displaced equally in the  $Y$ -direction. Those in the middle row are displaced equally, but by a smaller amount than the outer points. In other words, the  $y$ -parallax effect of  $d\omega$  is

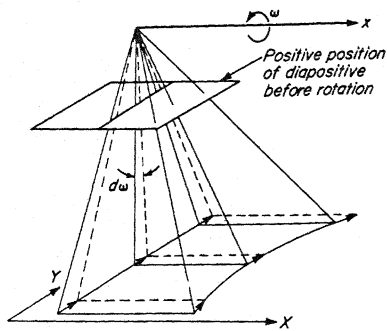


Figure 11-7. Effect of  $\omega$ -rotation on projected points.

more pronounced in the back and front edges of the model than along the center.

A  $d\phi$  rotation is identical to that of a  $d\omega$  rotation with the results rotated  $90^\circ$  as can be seen by studying Fig. 11-6. Of particular significance is the fact that this orientation element produces a  $Y$ -displacement only in the four outer-corner points. These relatively small  $Y$ -displacements are accompanied by rather large  $X$ -displacements, a fact which becomes significant in performing relative orientation.

Since  $d\kappa$  is a rotation about the  $Z$ -axis or the optical axis of the projector, the rays describe a vertical cone, and the projected points move along concentric circles whose center is the projector's nadir point. The  $X$ - and  $Y$ -displacements are shown in Fig. 11-6.

From the above discussion, it is seen that selective differential changes of the orientation elements at different model points can be used to eliminate existing  $y$ -parallaxes. The amount of differential changes can be arrived at empirically, based on the visual effect of the motions at selected points in the model. They can also be computed mathematically based on measured  $y$ -parallaxes at the selected points by the so-called differential formulas developed in section 11-6.

Relative orientation can be accomplished either by moving both projectors, or by holding one projector fixed and only moving the second projector. The first method is referred to as *independent* relative orientation and is the one most frequently used in practice. It is also referred to as the "swing-swing" method. The second method is referred to as *dependent* relative orientation. This method is used when the orientation of one projector must not be disturbed as in control extension (see Chapter 13).

#### 11-4 EMPIRICAL INDEPENDENT RELATIVE ORIENTATION

The points selected for relative orientation, whether performed empirically or numerically, are standardized at six points in the stereoscopic model. These points, called the orientation points, are shown in Fig. 11-8. This diagram shows the overlap area of the projected images of two diapositives. Point 1 is the projection of the principal point of the left hand diapositive. The left projector is designated  $L$ . Point 2 is the projection of the principal point of the right-hand projected diapositive. The right projector is designated  $R$ . Points 3, 4, 5, and 6 lie at the four corners of the *neat* model. If the plotter operator has placed a pair of diapositives into projectors.  $L$  and  $R$  and has centered them, and he now turns on the projector lamps, the colored images from the two projectors will overlap one another in the measuring space beneath the projectors.

Before any orientation is attempted, both projectors should first be brought to a vertical position by eye, using the  $\omega$  and  $\phi$  motions. Then the  $b_y$ - and  $b_z$ -settings should be equalized by reference to the scales provided, it being assumed that the two photographs are vertical and that they have been

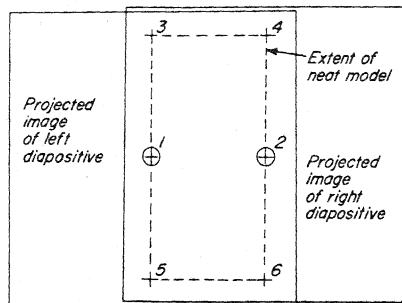


Figure 11-8. Location of orientation points. The neat model extends from one principal point to the next in the direction of the flight line and is approximately twice as wide normal to the direction flight.

taken from the same flying height. These settings also make the air base parallel to the supporting bar, this position being convenient for the orientation process.

The selection of which orientation elements to use in order to eliminate  $y$ -parallax at a particular orientation point is governed by the following two criteria.

1. For a given point, clear the  $y$ -parallax by that orientation element which causes a maximum  $Y$ -displacement at the point.
2. At any subsequent point, use the orientation element which will not, as far as possible, introduce  $y$ -parallax at a previously cleared point.

Adhering to the above criteria, the operational sequence follows. The operator brings the tracing table to the vicinity of point 1. Without wearing the colored spectacles, he will see a mismatching of the red image and the blue-green image coming from the two Multiplex projectors.

The displacement of conjugate images in the  $X$ -direction at point 1 is removed by raising or lowering the platen. This displacement will be called  $\Delta x$ -parallax to distinguish it from absolute parallax ( $x - x'$ ). The  $y$ -parallax between the conjugate images is removed by a  $\kappa$  rotation of projector  $R$ . A study of Fig. 11-6 will indicate that a swing of projector  $R$  imparts a  $Y$ -motion to the image of point 1 projected from projector  $R$ . The necessary amount of swing is indicated by visual coincidence between the red and blue-green images of a well-defined image at point 1.

The tracing table is moved to point 2, and the  $\Delta x$ -parallax is removed by raising or lowering the platen. The  $y$ -parallax is now removed by swinging projector  $L$ , as indicated by Fig. 11-6. This swing, or  $\kappa$ , does not, or should not, introduce  $y$ -parallax at point 1, because projector  $L$  is rotated around that point. The  $y$ -parallax is thus cleared at the two principal points.

The tracing table is moved to point 3, and the  $\Delta x$ -parallax is removed by

raising or lowering the platen. The  $\phi$  rotation of projector  $R$  is used to clear the  $y$ -parallax. As  $\phi$  is introduced, a considerable amount of  $\Delta x$ -parallax will be introduced at point 3. This must be removed by raising or lowering the platen simultaneously with the removal of  $y$ -parallax by use of the  $\phi$  motion of projector  $R$ . An examination of Fig. 11-6 will indicate that this motion should introduce no  $y$ -parallax at either of the principal points, 1 and 2, thus satisfying the second criterion.

If the vertical movement of the tracing table limits the removal of  $\Delta x$ -parallax, one of the two projectors must be translated in the  $X$ -direction to accomplish the same thing. This  $b_x$  motion has no effect on  $y$ -parallax and consequently has no effect on relative orientation. Its effect is to raise or lower the entire stereoscopic model relative to the tracing table, and to reduce or enlarge the model. (See Fig. 11-11).

The tracing table is moved to point 4, and the platen is raised or lowered to eliminate the  $\Delta x$ -parallax at the point. A  $\phi$ -rotation of projector  $L$  will move the image coming from projector  $L$  in the  $Y$ -direction as well as in the  $X$ -direction. But this motion should introduce no  $y$ -parallax at the principal points nor at point 3. Therefore, a  $\phi$ -rotation of projector  $L$  and a simultaneous raising or lowering of the platen will remove the  $y$ -parallax and the  $\Delta x$ -parallax of point 4. At this stage of orientation, points 1, 2, 3, and 4 have been cleared of  $y$ -parallax.

The tracing table is now moved to either point 5 or point 6, and  $\Delta x$ -parallax is removed by raising or lowering the platen. An  $\omega$ -rotation of either projector will introduce  $y$ -parallax at all four of the previously cleared points as shown by a study of Fig. 11-6. Since an  $\omega$ -rotation of either projector will produce the same effect, then only one  $\omega$ -rotation is independent. If it is assumed that the  $y$ -parallax at point 5 has been precisely cleared by an  $\omega$ -rotation of projector  $R$ , then the  $y$ -parallax introduced at points 3 and 4 will be equal in amount to that which had existed at point 5 but will be in the opposite direction. Only about two-thirds of this amount will be introduced at points 1 and 2, because these two points are not affected quite so much by  $\omega$ -rotation as are points 3 and 4. A reorientation to clear the  $y$ -parallax at points 1 through 4 will again introduce  $y$ -parallax at point 5.

A careful analysis of the effects of the rotational motions indicates that the following procedure is more effective: If point 5 is overcorrected to introduce  $y$ -parallax in the opposite direction equal to about one-half of the original  $y$ -parallax, then a reorientation to clear the  $y$ -parallax at points 1 through 4 should very nearly if not completely clear the  $y$ -parallax at point 5. The effect of the two swing motions in the reorientation of points 1 through 4 is to reduce the  $y$ -parallax at the principal points to zero and to reduce the  $y$ -parallax at points 3, 4, and 5 to about one-third of the original  $y$ -parallax, but now the displacements at points 3 and 5 are in opposite directions. Hence, a  $\phi$ -rotation of projector  $R$  will eliminate the  $y$ -parallax at points 3 and 5 simultaneously. A  $\phi$ -rotation of projector  $L$  will eliminate the remaining  $y$ -parallax at point 4.

The amount of overcorrection to be introduced by the  $\omega$ -rotation depends on the type of the camera and the nature of the topography. It is greatest for normal-angle photography, decreasing for wide-angle and super-wide-angle photography. Referring to Fig. 11-8, if  $a$  is the distance from point 1 to point 5 measured on the original photograph and  $f$  is the focal length, the overcorrection factor  $k$  can be approximated by the following expression

$$k = \frac{1}{2} \left( 1 + \frac{f^2}{a^2} \right) \quad (11-2)$$

#### Example 11-1

Given a focal length of 152 mm, and  $a = 98$  mm, and the estimated  $y$ -parallax at point 5 is 0.80 mm. Compute the amount of overcorrection.

#### SOLUTION

By equation 11-2,

$$k = \frac{1}{2} \left( 1 + \frac{152^2}{98^2} \right) = 1.70$$

The overcorrection is thus  $1.70 \times 0.80 = 1.36$  mm. An  $\omega$ -rotation must therefore be introduced to cause a  $y$ -parallax of  $1.36 - 0.80 = 0.56$  mm in the direction *opposite* to the original  $y$ -parallax. The height of point 5 and the slope of the topography at the point has an effect on the amount of overcorrection to be applied. This is empirically arrived at by the experienced operator after the first or second iteration.

To recapitulate this orientation process, the steps will be briefly stated in the order of their performance.

1. Clear  $y$ -parallax at 1 with  $\kappa$ -rotation of projector  $R$ .
2. Clear  $y$ -parallax at 2 with  $\kappa$ -rotation of projector  $L$ .
3. Clear  $y$ -parallax at 3 with  $\phi$ -rotation of projector  $R$ .
4. Clear  $y$ -parallax at 4 with  $\phi$ -rotation of projector  $L$ .
5. Introduce one-half of the  $y$ -parallax existing at point 5 or 6 in the opposite direction with  $\omega$ -rotation of either projector.
6. Repeat steps 1 through 5 until no parallax exists at the five points.

When the adjustment just outlined has been completed, the sixth point should be checked. If it contains  $y$ -parallax, then the  $y$ -parallax has not really been cleared at all of the original five points.

When the orientation by matching red and blue-green images has been refined until no apparent  $y$ -parallax can be detected, the operator puts on the spectacles and checks each point by bringing the measuring mark to the model surface at the five points. If  $y$ -parallax exists, he will detect a slight

$y$ -displacement of the two images of the measuring mark received by the eyes. The residual  $y$ -parallax is cleared by trimming the adjustments slightly until the split image of the measuring mark disappears at all the points. At this stage, the entire model is assumed to be free from  $y$ -parallax, and relative orientation is completed.

A review of the above procedure shows that independent relative orientation determines five of the six possible rotations between the two projectors. The sixth rotation element is the  $\omega$ -rotation of one or the other of the two projectors. Note that only five orientation points are necessary to complete the independent relative orientation. The sixth point is used only as a check. In practice, an experienced operator can usually distribute any residual  $y$ -parallax at the check point throughout the rest of the model by introducing small false rotational motions. This can also be done numerically by the method of least squares as shown in Section 11-7.

### 11-5 EMPIRICAL DEPENDENT RELATIVE ORIENTATION

When dependent relative orientation must be used in order to preserve the orientation of one of the projectors, the rotational and translational motions of the other projector must be used. As in the independent case, five orientation points are satisfied with five projector motions. Since the  $b_x$  motion has no effect on  $y$ -parallax, these motions are  $\omega$ ,  $\phi$ ,  $\kappa$ ,  $b_y$ , and  $b_z$ .

The following technique is used for dependent relative orientation when, say, the left projector is held fixed. The orientation points are those shown in Fig. 11-8. Assume that  $\Delta x$ -parallax is removed at each point before attempting to remove  $y$ -parallax.

1. Clear  $y$ -parallax at 2 using  $b_{yR}$ .
2. Clear  $y$ -parallax at 1 using  $\kappa_R$ . Note that this does not introduce  $y$ -parallax at point 2 as shown in Fig. 11-6.
3. Clear  $y$ -parallax at 4 using  $b_{zR}$ . Note that this does not cause  $y$ -parallax at either points 1 or 2.
4. Clear  $y$ -parallax at 3 using  $\phi_R$ . This does not introduce  $y$ -parallax at either points 1, 2, or 4.
5. Overcorrect the  $y$ -parallax at point 6 using  $\omega_R$ .
6. Repeat steps 1 through 5 until no  $y$ -parallax exists at the five orientation points.
7. Check for  $y$ -parallax at point 5. If  $y$ -parallax exists, the other orientation points should be checked for residual  $y$ -parallaxes.

After the above procedure has been completed, the orientation is touched up while viewing the model stereoscopically (using the colored glasses in the case of the Multiplex projectors).

The procedures described in these two sections to perform relative orientation apply to most stereoscopic plotting instruments.

## 11-9 INSTRUMENTAL ABSOLUTE ORIENTATION

The purpose of absolute orientation is to bring a stereoscopic model to the desired map scale, and to place the model in its correct orientation with respect to the datum for elevations and to the horizontal control plotted on the map sheet. Absolute orientation in an instrument is accomplished in two distinct phases, called *scaling* and *leveling*. In order that a model may be scaled, the model must contain two horizontal control points whose positions have been plotted on the map sheet at the desired map scale. In order that a model may be leveled, the model must contain a minimum of three, but preferably four or five, noncollinear vertical control points.

Before the scaling operation is discussed, it is advisable to consider the effect of a  $b_x$  motion of either of two projectors on the stereoscopic model which has been obtained by relative orientation. In Fig. 11-11, in which the illumination system is not shown, projectors  $L$  and  $R$  have been relatively oriented to form a stereoscopic model indicated by the solid outline in the measuring area beneath the projectors. It is assumed that the readings of the  $Y$ -motion and the  $Z$ -motion are the same on both projectors, that is,  $b_y = b_z = 0$ . If projector  $R$  is moved to the right by an  $X$ -motion, the original base  $b_{x_1}$  has been increased by an amount  $\Delta b_x$  to give a new base  $b_{x_2}$ . At the same time, the original flying height represented by  $h_1$  above the model terrain has been increased by an amount  $\Delta h$  to give  $h_2$ . Since projector  $R$  has been moved parallel with itself, then  $h_2/h_1 = b_{x_2}/b_{x_1}$ . The ratio  $b_{x_2}/b_{x_1}$ , is the increase in the scale of the stereoscopic model.

The effect of a  $b_z$  base component on scaling is shown in Fig. 11-12. Denoting the initial value as  $b_{z_1}$ , if projector  $R$  is now moved from  $a$  to  $b$  by a  $b_x$  motion,  $y$ -parallax will be introduced into the model because the images

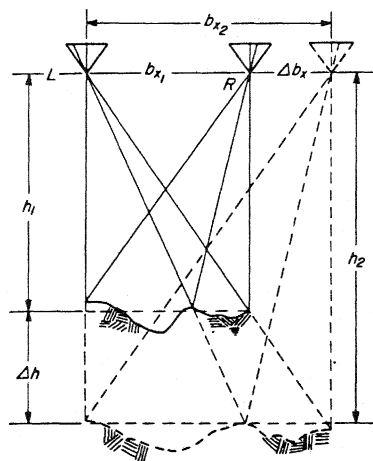


Figure 11-11. Effect of  $b_x$  component on scaling.

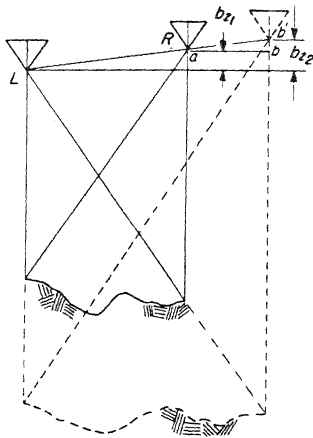


Figure 11-12. Effect of  $b_z$  component on scaling.

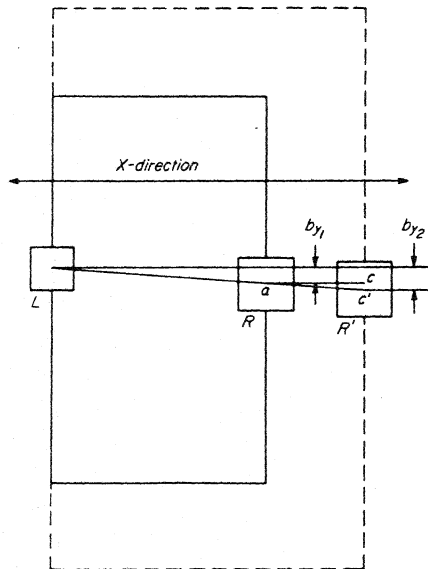


Figure 11-13. Effect of  $b_y$  component on scaling.

coming from projector R have been displaced inward relative to the new (larger) scale of the model. A Z-motion of projector R represented by  $bb'$  will eliminate the y-parallax over the entire model. The new  $b_z$  component  $b_{z2}$  is related to  $b_{z1}$  by the relationship  $b_{z2}/b_{z1} = b_{x2}/b_{x1}$ .

The effect of a  $b_y$  base component on scaling is shown in Fig. 11-13.

The solid rectangle is the outline of the neat model before scale change. The  $b_y$  base component after relative orientation but before scale change is shown as  $b_{y1}$ . If projector R is now moved from a to c by a  $b_x$  motion, y-parallax in the same direction and of an amount equal to the distance  $cc'$  will be introduced over the entire model. A Y-motion of projector R will eliminate this y-parallax. The new  $b_y$  component designated  $b_{y2}$  is related to  $b_{y1}$  by the relationship  $b_{y2}/b_{y1} = b_{x2}/b_{x1}$ . The large dashed rectangle is the outline of the neat model after the scale change.

The preceding two paragraphs reveal why it is convenient to equalize the  $b_y$  and  $b_z$  settings of the two projectors before independent relative orientation is performed. This is, of course, not possible when performing dependent relative orientation since  $b_y$  and  $b_z$  base components will nearly always exist. If the model is examined after scaling and y-parallax exists along the line from 1 to 2 of Fig. 11-8, this is caused only by the  $b_y$  component. Thus, the y-parallax is eliminated along this line by a  $b_y$  motion of one of the projectors. Then any remaining y-parallax will be (or should be) symmetrical with respect to the line joining points 1 and 2. This y-parallax is cleared by a  $b_z$  motion of one of the projectors.

### 11-10 SCALING THE MODEL

When a model is to be scaled, the map sheet containing the plotted positions of at least two horizontal control points is placed on the map table. The plotting pencil of the tracing table is placed on one of the map control points, and the entire map sheet is slid, carrying the tracing table with it, until the measuring mark receives the model image of the control point. This position of the tracing table is shown as point  $A_1$  in the upper diagram of Fig. 11-14.

With the map sheet fixed in position, the tracing table is moved to the second control point in the model. The orthographic projection  $B_1$  of this point on the map sheet, compared with the map position of the point, will indicate the necessary amount of rotation of the map sheet and the necessary scale change. The map sheet is rotated about the point  $A_1$  as the center until the position of the line  $AB$  as viewed in the model is in the same direction as the map position of  $AB$ . The base is now enlarged or reduced by an X-motion of one of the projectors (or both), until the distance  $AB$  as determined by a measurement in the model is the same as the map distance  $AB$ . This is a trial-and-error procedure, because the map sheet must be shifted and rotated each time the scale is changed.

The above trial-and-error process for scaling a model must be used if the instrument, such as the Multiplex, does not contain precise linear scales from which to obtain the values of the base components and for determining the precise model coordinates of the control points. However, when using an instrument with the appropriate scales, the process of scaling is quite simplified. The model coordinates of the control points are used to compute the model length of the line joining the points. If the ground elevations of the

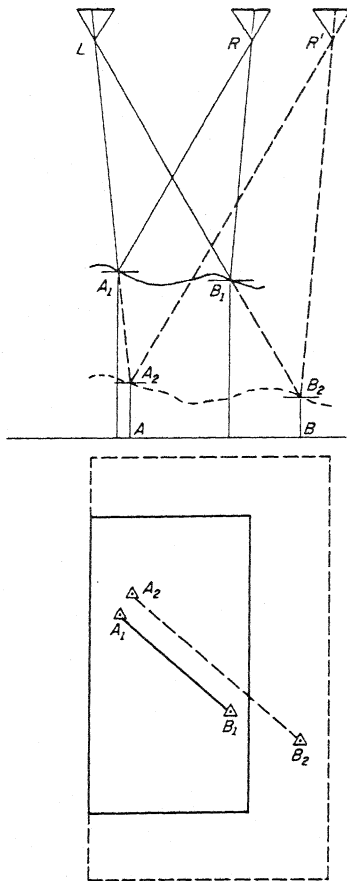


Figure 11-14. Scaling to horizontal control points.

two control points are not known, then the model length is determined by model  $x$  and  $y$  coordinates only. If the ground elevations of both points are known then the model length is determined by the model  $x$ ,  $y$ , and  $z$  coordinates. The model length can then be compared with what it is supposed to be, and the necessary base changes can be made.

Example 11-4

After an initial relative orientation, the base components are:  $b_{x_1} = 225.00$  mm;  $b_{y_1} = -8.16$  mm;  $b_{z_1} = +6.76$  mm. The data for two horizontal/vertical control points are as follows:

POINT	GROUND $X$ (m)	GROUND $Y$ (m)	ELEV. (m)	MODEL $x$ (mm)	MODEL $y$ (mm)	MODEL $z$ (mm)
1	670,296.3	223,343.7	1243.66	302.55	716.25	144.66
2	670,766.9	223,347.2	1275.24	325.70	318.02	172.22

The map scale is 1/1200. Compute the base components necessary to bring the model to the map scale.

SOLUTION

The ground spatial length is given as

$$D = [(X_2 - X_1)^2 + (Y_2 - Y_1)^2 + (Z_2 - Z_1)^2]^{1/2} = 471.67 \text{ m.}$$

The correct model spatial length is then  $471.67/1200 = 0.39306 \text{ m} = 393.06 \text{ mm}$ . The model spatial length following initial relative orientation is:

$$d_o = [(302.55 - 325.70)^2 + (716.25 - 318.02)^2 + (144.66 - 172.22)^2]^{1/2} = 399.85 \text{ mm}$$

Thus, since the initial model length is too long, the base components must be reduced by the factor  $393.06/399.85$ .

$$b_{x_2} = 225.00 \times \frac{393.06}{399.85} = 221.18 \text{ mm}$$

$$b_{y_2} = -8.16 \times \frac{393.06}{399.85} = -8.02 \text{ mm}$$

$$b_{z_2} = +6.76 \times \frac{393.06}{399.85} = +6.65 \text{ mm}$$

If the elevations of the ground control points were not known, the computations would then be as follows:

$$D = [(X_2 - X_1)^2 + (Y_2 - Y_1)^2]^{1/2} = 470.61 \text{ m}$$

The correct model length =  $470.61/1200 = 0.39218 \text{ m} = 392.18 \text{ mm}$

$$d_o = [(302.55 - 325.70)^2 + (716.25 - 318.02)^2]^{1/2} = 398.90$$

The new base components are then

$$b_{x_2} = 225.00 \times \frac{392.18}{398.90} = 221.21 \text{ mm.}$$

$$b_{y_2} = -8.16 \times \frac{392.18}{398.90} = -8.02 \text{ mm.}$$

$$b_{z_2} = +6.76 \times \frac{392.18}{398.90} = +6.65 \text{ mm.}$$

The difference in the  $b_x$  components between the two solutions is caused by the model not being leveled at this stage.

11-11 LEVELING THE MODEL

When scaling has been performed as outlined in section 11-10, the model usually will not be at precisely the correct scale because it is tipped and tilted relative to the datum for elevations. After the model has been leveled to fit vertical control, the scale should be checked to determine whether or not any scaling refinements are required.

Since interior orientation has been established by making the correct reduction (or setting off the correct principal distance) and by centering the diapositives in their carriers, the horizontal and vertical scales of the model formed by a pair of projectors are precisely the same. On the basis of this fact, the correct settings of the tracing-table platen can be computed for any desired scale. Modern tracing tables contain gears which can be introduced to give a direct reading in feet or metres of elevations to a particular scale of the model (and the map). The elevation readings may be changed without moving the platen up and down. This provision is necessary in order that the counter may be indexed to a vertical control point in the process of leveling.

The selected model scale (see section 11-10) is set in the tracing table or elevation counter. The measuring mark is brought into contact with each of the vertical control points in the model. The model elevations are read and recorded. Imagine the model to contain three vertical control points 1, 2, and 3 as shown in Fig. 11-15. Let  $\Delta h_1$ ,  $\Delta h_2$ , and  $\Delta h_3$  represent the discrepancies between the elevations read in the model and the correct values of these elevations. A line parallel with the X-axis of the instrument is drawn through point 1 and intersects the line 2-3 at point 4. The discrepancy in the elevation at point 4 can be obtained by interpolation. That is,

$$\Delta h_4 = \Delta h_2 + \frac{L_{2-4}}{L_{2-3}}(\Delta h_3 - \Delta h_2) \tag{11-18}$$

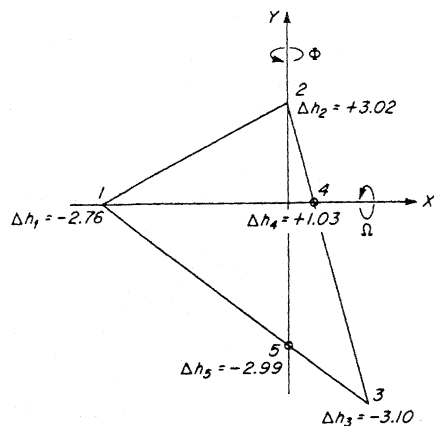


Figure 11-15. Leveling based on analysis of three vertical control points.

in which  $L_{2-4}$  and  $L_{2-3}$  are the lengths of the lines joining points 2 and 4, and 2 and 3, respectively.

Similarly, a line parallel with the instrument Y-axis is drawn through point 2 to intersect with line 1-3 at point 5. The discrepancy in the elevation at point 5 is obtained by interpolation. Thus

$$\Delta h_5 = \Delta h_1 + \frac{L_{1-5}}{L_{1-3}}(\Delta h_3 - \Delta h_1) \tag{11-19}$$

Due regard must be given to the algebraic signs of the  $\Delta h$ 's in equations 11-18 and 11-19.

The model rotations  $\Omega$  and  $\Phi$  can then be computed from the slopes of the two lines 1-4 and 2-5 as follows.

$$\tan \Omega = \frac{\Delta h_5 - \Delta h_2}{L_{2-5}} \tag{11-20}$$

$$\tan \Phi = \frac{\Delta h_4 - \Delta h_1}{L_{1-4}} \tag{11-21}$$

All values of the lengths of the lines and the elevation discrepancies must be in the same units, that is, either instrument units or in ground units. The algebraic sign of  $\Omega$  and  $\Phi$  is best determined in practice by an analysis of the direction through which the model must be tipped and tilted in order to raise portions of the model and lower other portions.

Example 11-5

Given the following data pertaining to the points shown in Fig. 11-15

POINT	$\Delta h$ (mm)	LINE	LENGTH (mm)
1	-2.76	1-3	260
2	+3.02	2-3	234
3	-3.10	2-4	76
		1-5	174
		1-4	163
		2-5	176

Compute the amount of  $\Omega$ - and  $\Phi$ -rotations required to level the model.

SOLUTION

By equation 11-18,

$$\Delta h_4 = +3.02 + \frac{76}{234}(-3.10 - 3.02) = +1.03 \text{ mm}$$

By equation 11-19,

$$\Delta h_5 = -2.76 + \frac{174}{260}(-3.10 + 2.76) = -2.99 \text{ mm}$$

By equation 11-20,

$$\tan \Omega = \frac{-2.99 - 3.02}{176} = -0.03415$$

$$\Omega = -1^\circ 57' 20'' = -2.173^\circ$$

By equation 11-21,

$$\tan \Phi = \frac{1.03 + 2.76}{163} = 0.02325$$

$$\Phi = 1^\circ 20' 00'' = 1.480^\circ$$

The front of the model must be raised by the  $\Omega$ -rotation, and the left side of the model must be raised by the  $\Phi$ -rotation.

In the Multiplex-type instrument, the entire model is rotated about the  $X$ - and  $Y$ -instrument axes in the leveling process by means of leveling screws. These screws either rotate the frame supporting the projectors while the map table remains stationary as in the usual arrangement, or else they tip and tilt the map table while the support frame remains stationary. In either case, the model moves as a unit with respect to the map table, which defines the vertical datum, and both the relative orientation and model scale are preserved. The  $\Omega$ - and  $\Phi$ -rotations imparted to a Multiplex model are shown schematically in Fig. 11-16. The left view is a side view of the model, which is rotated through angle  $\Omega$  in order to level the model front-to-back. The right view is a front view of the model, which is rotated through the angle  $\Phi$  in order to level the model side-to-side. These simpler instruments do not contain circular scales by which to rotate the model through the necessary angles. The angular rotations are functions of the pitch of the leveling screws and the distance between them, as illustrated in the following example.

#### Example 11-6

The pitch of the leveling screws in Fig. 11-16 is 2.30 mm. The distance front to back between the screws shown in Fig. 11-16(a) is 635 mm. The distance side to side between the screws shown in Fig. 11-16(b) is 813 mm.

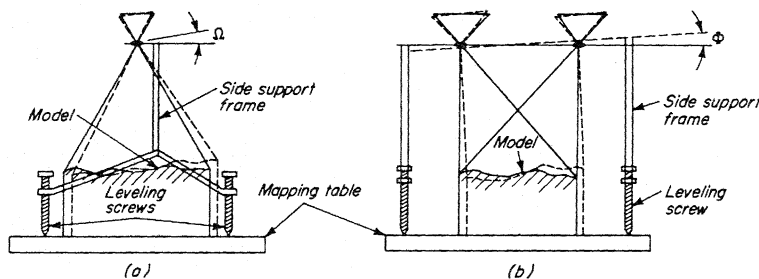


Figure 11-16. Leveling a model by  $\Omega$  and  $\Phi$  rotations of supporting frame.

How much should the front screws be turned in order to level the model of example 11-5 front to back (without turning the back screws)? How much should the screws on the left side be turned (without turning those on the right side) in order to level the model side to side?

#### SOLUTION

The angle  $\Omega_o$  through which the model is rotated front to back for each turn of the leveling screws is given by

$$\tan \Omega_o = \frac{2.30}{635} = 0.00362$$

Thus, since  $\tan \Omega$  (from example 11-5) is 0.03415, then

$$n_\Omega = \frac{0.03415}{0.00362} = 9.43 \text{ turns, raising the front of the frame.}$$

The angle  $\Phi_o$  through which the model is rotated side to side for each turn of the leveling screws is given by

$$\tan \Phi_o = \frac{2.30}{813} = 0.00283$$

Then, since  $\tan \Phi$  (from example 11-5) is 0.02325,

$$n_\Phi = \frac{0.02325}{0.00283} = 8.22 \text{ turns, raising the left side of the frame}$$

#### 11-12 MODEL DEFORMATION

A stereoscopic model can always be made to fit three vertical control points since three points are sufficient to define the datum plane. However, it is not always possible to level a model using four or more vertical control points. Assuming that the ground control is not in error and that the vertical control point has been correctly identified in the model, the main source of the discrepancy is due to model deformation. The model deformation in turn is caused by inexact relative orientation between the two photographs or projectors.

The individual effects of the orientation elements are shown graphically in Fig. 11-17. A small  $db_x$  error causes a slight scale error and does not affect elevations by any appreciable amount unless the terrain relief is considerable. This error raises or lowers the model a small amount which is allowed for by proper indexing of the elevation counter.

A small  $db_y$  error has no effect on elevations, but simply introduces  $y$ -parallax throughout the model. A  $db_z$  error of either or both projectors has the effect of tipping the model in the  $X$ -direction. This error is overcome in the leveling process. The  $dk$  error tilts the model in the  $Y$ -direction. This error is also overcome in the leveling process.

STEREOPHOTOGRAMMETRY

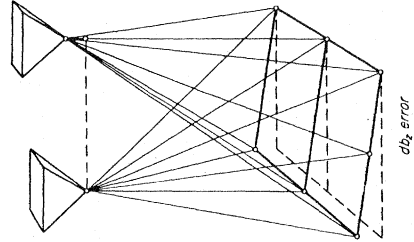
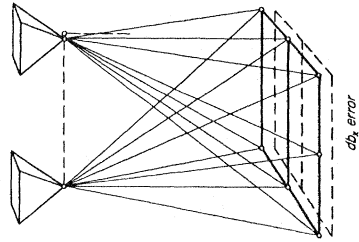
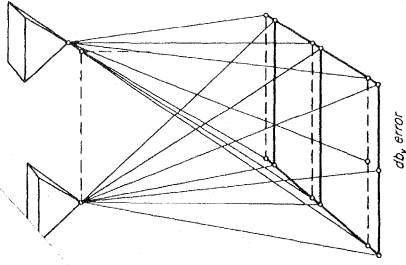
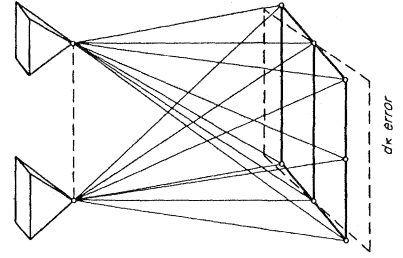
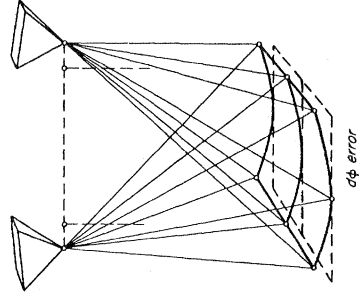
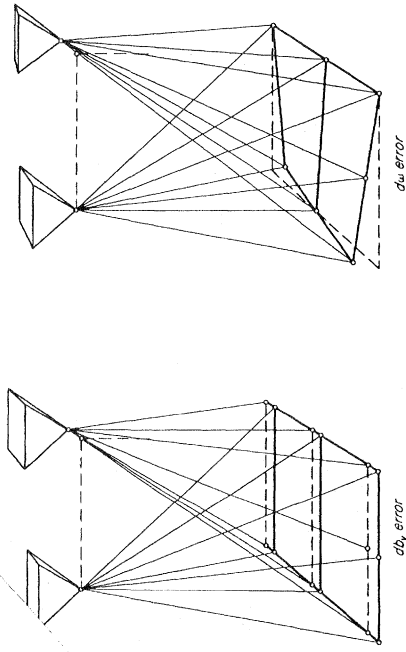


Figure 11-17. Effects of relative orientation errors on model.

# Chapter 12

## Stereoscopic Plotting Instruments

### 12-1 INTRODUCTION

The main function of a stereoscopic plotting instrument, discussed briefly in section 11-1, is the formation of a three-dimensional model of the ground at a known scale which can be measured by the operator in order to compile a topographic map. The *stereo model* can also be measured to obtain numerical information in the form of profiles and *XYZ* coordinates of random or regularly spaced points, the latter process being referred to as digitizing the model. Discrete points in the model can be measured in order to determine ground coordinates and elevations of points in a boundary survey.

Some types of plotters can be used to join a sequence of models together instrumentally in the form of a strip for the purpose of extending ground control. This is called either *analog triangulation* or *stereotriangulation*, and is explained in Chapter 13.

The plotter can also be used to form a model in some arbitrary spatial orientation and scale. A sequence of models thus formed, referred to as independent models, can then be joined together mathematically in order to extend ground control. This process is referred to as *independent model triangulation*, and is also explained in Chapter 13.

Aside from the aerial camera itself, the stereoscopic plotting instrument

is the most important instrument employed in the practice of photogrammetry. The design of a plotter can be relatively simple, as in the case of the Multiplex described in Chapter 11, or can be quite complex. This chapter will discuss the essential features of the different designs from the standpoint of the orientation processes described in Chapter 11, and as they impose limitations on planning the aerial photography to be used in them.

A stereoscopic plotting instrument embodies four main components. These are: (1) the projection system; (2) the viewing system; (3) the measuring system; and (4) the tracing system. These components vary among plotters, but their functions are all the same.

### 12-2 PROJECTION SYSTEMS

The projection system projects the images of conjugate points on a pair of diapositives into the model space of the instrument. Three types of projection systems are employed and are the basis for the most important classification of plotters. They are: the direct-optical; the mechanical; and the optical-mechanical systems. These three systems are diagrammed conceptually in Fig. 12-1.

In the direct-optical projection system, the diapositive images  $p'$  and  $p''$  are projected into the model space by means of a low-distortion projector lens, and form an image at  $P$ . As discussed in section 11-2, the principal distance of the diapositive is matched to the principal distance of the projector lens in a reduction printer. In order to maintain acceptable sharpness of the projected images through the vertical range of the model, the lenses contain diaphragms with very small apertures (see section 2-16). Each instrument with this type of projection system has a characteristic vertical range beyond which the image sharpness is no longer acceptable.

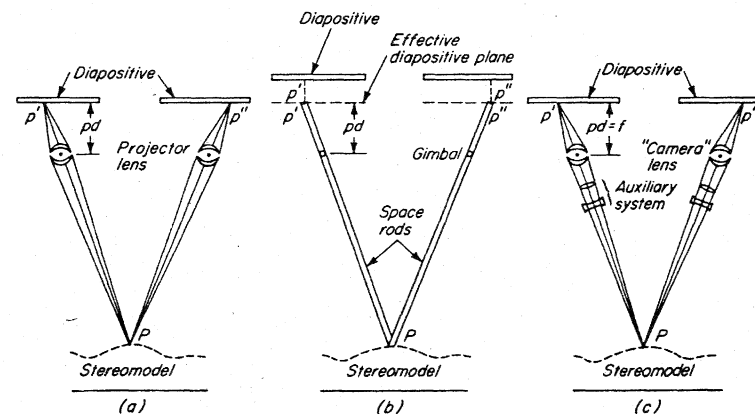


Figure 12-1. Projection systems. (a) Direct-optical. (b) Mechanical. (c) Optical-mechanical.

The mechanical projection system shown in Fig. 12-1(b) employs a pair of precision *space rods* that pass through gimbals located at the perspective centers of the diapositives. The distance between the *effective plane of the diapositives* to the gimbals is set off mechanically to coincide with the principal distance of the diapositives. The points  $p'$  and  $p''$  are projected orthogonally down to the upper ends of the space rods (to be described later). They are then projected mechanically along the axes of the space rods to fix the position of model point  $P$ . The transfer of the image point from the diapositive to the effective upper end of the space rod is accomplished in several different ways. The method diagramed in Fig. 12-1(b) is shown here because of its close analogy to the principle of direct-optical projection. Space rods can be identified in the instruments shown in Figs. 12-5, 12-16, 12-19, and 12-23.

The optical-mechanical projection system employs projector or "camera" lenses which nominally match the lens of the aerial camera used to acquire the photography. If it can be imagined that the lenses used in the projectors exactly match the focal length and distortion characteristics of the aerial camera lens, then points  $p'$  and  $p''$  would be projected out through the lenses to infinity in precisely the correct directions. That is, they recreate backward the directions of the original rays coming into the camera at the instant of exposure. This concept is called the *Porro-Koppe* principle, and was adhered to quite closely in the past. Modern instruments incorporating the optical mechanical projection system, such as the Thompson-Watts Plotter and the Zeiss C8 Stereoplanigraph described in section 12-17, use other methods for recreating the original ray paths.

After the rays pass through the lens, they are collimated, that is, they are parallel with one another. They are then projected through an auxiliary lens system which brings them to focus on a reference surface in the model at  $P$ , which contains the measuring mark. The mechanical aspect of this type of projection system derives from the fact that the reference mark must be moved mechanically in all three directions in order to recover a model point, or to define the model surface.

### 12-3 VIEWING SYSTEMS

The viewing systems employed in direct-optical stereo plotters are either the anaglyphic, polarizing, or stereo-image alternator systems. These systems were described in Chapter 5 (see Figs. 5-19 and 5-20).

Mechanical projection instruments employ an orthogonal view of the diapositive, which is then directed to the eyepiece of the instrument by an optical train. One system is shown schematically in Fig. 12-2. Objective lens I projects the image  $p'$  from the diapositive onto the reference surface containing the measuring mark at  $M$ . This mark lies in the focal plane of objective lens II. The rays are turned by the prism and are then projected through objective II into the optical train, which carries the image to the observer's eye. Two such systems, one for each eye, allow the diapositives to

be viewed stereoscopically. Lens I, reference mark  $M$ , the prism, and lens II all move as a unit. This movement causes the upper end of the space rod, which is attached to this assembly, to describe a plane that is parallel to the plane of the diapositive. This plane was referred to above as the effective plane of the diapositive. The complete projection and viewing systems of the Wild Autographs A10 and A7 are shown in Figs. 12-22 and 12-25, respectively.

The Zeiss Stereoplanigraph C8 is virtually the only optical-mechanical instrument used in the United States at the present time. Its viewing system is a combination goniometer-optical train system. In Fig. 12-3(a), imagine the eye to occupy the position of the reference mark with the auxiliary system removed. The eye could then move around under the projector lens and view different parts of the diapositive. This is identical to goniometric viewing (see Fig. 4-25) except that the measuring telescope is replaced by the eye. In the instruments, the image formed by the auxiliary system on the reference mark is carried to the observer's eye by means of an optical train as shown schematically in Fig. 12-3(b). Since the reference mark is mechanically moved around under the projector lens, then Fig. 12-3(b) is conceptually the same as Fig. 12-3(a). The complete projection and viewing system of the Zeiss Stereoplanigraph is shown in Fig. 12-30.

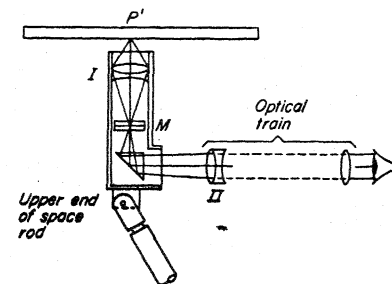


Figure 12-2. Orthogonal viewing of diapositive in mechanical-projection instrument.

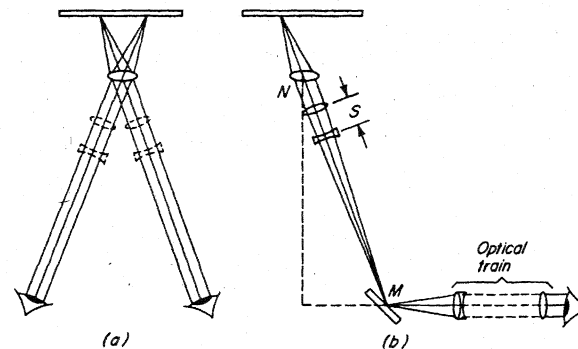


Figure 12-3. Goniometric viewing of diapositive.

### 12-4 STEREO MODEL VERSUS STEREO IMAGE

The term *stereo model*, or simply *model*, is used frequently with reference to the surface generated by the infinite positions of point  $P$  in Figs. 12-1(a), (b), and (c). A distinction must be made between this surface and the stereoscopic view of the overlapping diapositives seen by the operator. In the direct-optical instruments such as the Multiplex, the stereo model as defined above is identical to the stereoscopic view seen by the observer. In the mechanical and optical-mechanical instruments, however, the observer does *not* see the stereo model as defined above. The stereo model is formed by the projection. The *stereo image* is seen by the observer through the viewing system. This is similar to the stereo image seen under a stereoscope. Thus in a direct-optical instrument the stereo image and the stereo model are one and the same, but in the mechanical or optical-mechanical instrument, they are completely different.

### 12-5 MEASURING SYSTEMS

Two basic measuring systems are used in stereoplotters. The first system, used with direct-optical projection instruments, employs a single luminous mark located in the center of a white platen which is a part of the tracing table of the instrument. This platen can be identified in Fig. 11-1. The mark is a floating mark that is viewed simultaneously with viewing the model. The up-and-down motion of the platen is recorded on a counter on the tracing table, either in feet or in metres. The older tracing tables, many of which are still in use, contain millimetre scales whose readings can be converted to feet or metres according to the desired model scale. The  $X$  and  $Y$  displacements of the measuring mark cannot be measured directly unless the instrument is fitted with an  $X$ - $Y$  coordinatograph. (See section 12-6.)

The second measuring system incorporates two measuring marks exactly like the half-marks of the parallax bar. These marks are located, one in each optical path, between the diapositive and the eyepiece of a mechanical or optical-mechanical instrument. For example, the measuring mark is located at  $M$  in Fig. 12-2 in a mechanical projection instrument and at  $M$  in Fig. 12-3(b) in an optical-mechanical projection instrument.  $X$  and  $Y$  motion are imparted to these marks either freehand or by handwheels on the instruments. Referring to Fig. 12-1(b), if the intersection of the space rods at  $P$  is moved to the left, the upper ends of the space rods are moved to the right, pivoting about the gimbals, thus scanning the diapositive in the  $X$ -direction. A movement of  $P$  in or out of the plane of the drawing displaces the upper ends of the space rods in the  $Y$ -direction. Thus, since the measuring mark moves with the upper end of the space rod as shown in Fig. 12-2, then any motion imparted to  $P$  is also imparted to the pair of measuring marks. On some instruments, the  $X$  and  $Y$  movements of the marks can be read from precise  $X$  and  $Y$  scales attached to the instrument. These movements can also be automatically recorded by various types of encoders.

Measurement in the vertical direction is based on the same principle as vertical measurement of the floating mark using the parallax bar. Referring again to Fig. 12-1(b), if  $P$  is moved vertically upward or downward, the upper ends of the space rods and thus the measuring marks would move in opposite  $X$ -directions. This changes the  $x$ -parallax of the marks. Since the measuring marks and the diapositives are viewed stereoscopically, the single floating mark appears to move vertically in the stereo image seen by the operator. The vertical movement of  $P$  is read on the elevation scale of the instrument or else is automatically recorded.

### 12-6 TRACING SYSTEMS

If an instrument uses a tracing table as shown in Fig. 11-1, then the map features are traced directly from the stereo model by means of a pencil located directly beneath the measuring mark. The basic idea is presented in

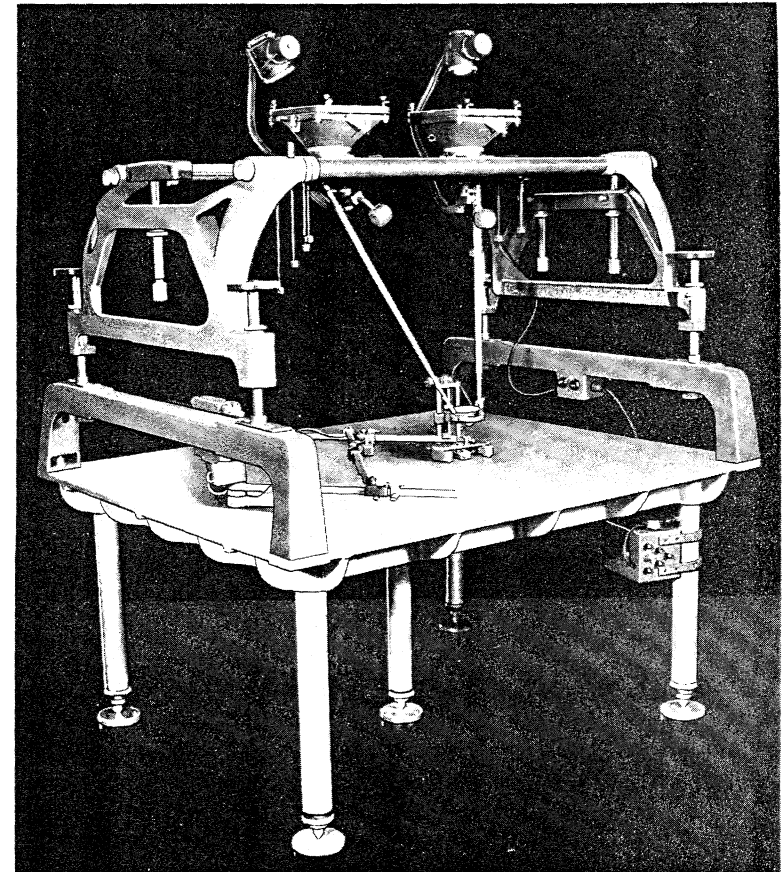


Figure 12-4. Early Kelsh plotter.

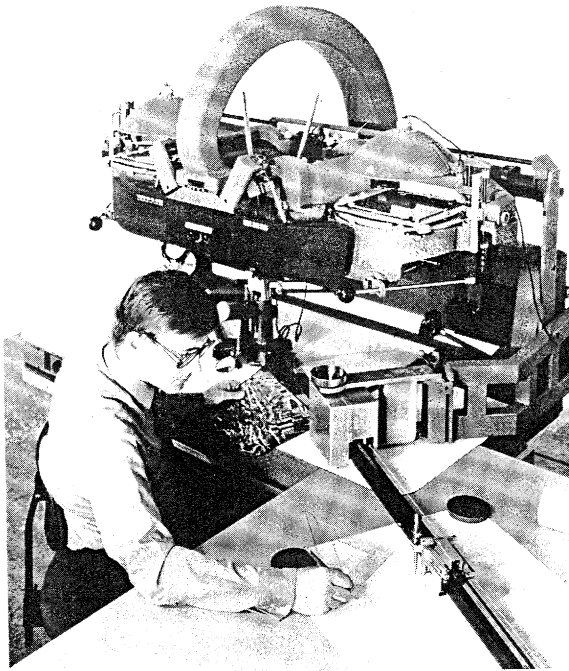


Figure 12-5. Wild Aviograph B8S showing linear pantograph and plotting table. Courtesy of Wild Heerbrugg Instruments, Inc.

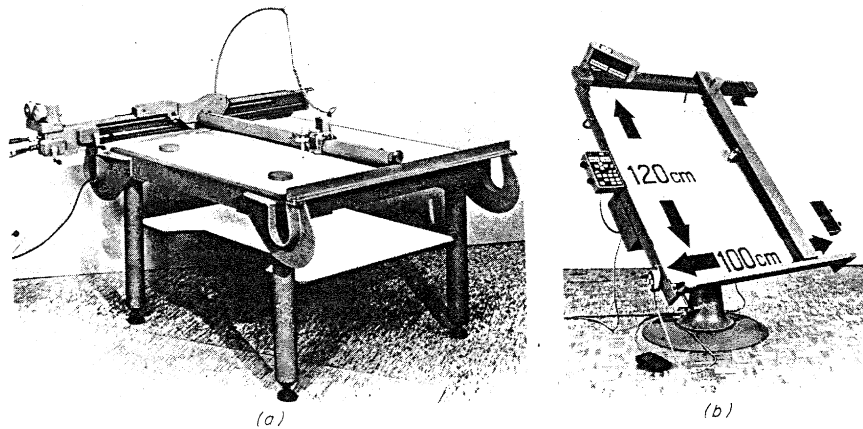


Figure 12-6. Coordinatographs. (a) Mechanical connection to instrument motions. (b) Electrical connection to instrument motions. Courtesy of Wild Heerbrugg Instruments, Inc.

section 11-1. The tracing is therefore at the same scale as the model. A *pantograph* can be connected to the tracing table as shown in Fig. 12-4. This permits an enlargement or (usually) a reduction from the model scale to the map compilation scale. A linear pantograph is used in the instrument shown in Fig. 12-5 to accomplish the same thing.

If the measuring mark is moved by means of a pair of *X*- and *Y*-hand-wheels, these movements must be transferred to the map sheet mounted on a coordinatograph, two types of which are shown in Fig. 12-6. The connection between the instrument and the coordinatograph can be seen in Fig. 12-21. The relation between the model scale and the map compilation scale can be increased or decreased by means of interchangeable gears. Then as the hand-wheels on the instrument are turned in order to follow a map feature, the motions are geared up or down and impart corresponding motions to the coordinatograph pencil, which draws out the enlarged or reduced features on the map sheet.

## 12-7 MULTIPLEX PLOTTER

Many of the features of the Multiplex instrument were described in Chapter 11 in conjunction with the orientation techniques. A cross section of one of the projectors is shown in Fig. 12-7. The function of the condenser lenses is to concentrate as much light as possible at the diaphragm opening of the projector lens, bearing in mind that this opening is very small. The optimum projection distance for best focus is 360 mm as shown. The optics permit satisfactory sharpness through a total vertical range of about 180 mm. This range represents the depth of focus of the image, which is fixed by the focal length of the projector lens, the object and image distances, the diaphragm opening, and the acceptable circle of confusion as explained in section 2-16.

The method of accomplishing interior orientation was discussed in section 11-2. This includes the preparation of the diapositive with the proper reduction through a reduction printer lens which eliminates the radial lens distortion contained in the negative, and centering the diapositive principal point on the projector lens axis.

Independent relative orientation of the Multiplex projectors is accomplished by the three rotational motions of each projector, and dependent relative orientation is performed using both the rotational and translational motions of one of the projectors as described in sections 11-4 and 11-5. The method of scaling and leveling the resulting model was discussed in detail in sections 11-9, 11-10, and 11-11.

The vertical range permitted in the Multiplex represents one-half the flying height above the average elevation of the ground. Either the model scale (and thus the mapping scale, assuming no pantograph) must be designed to fit the flying height of the photography and the vertical relief in the area, or else the flying height must be chosen to fit a preselected model scale,

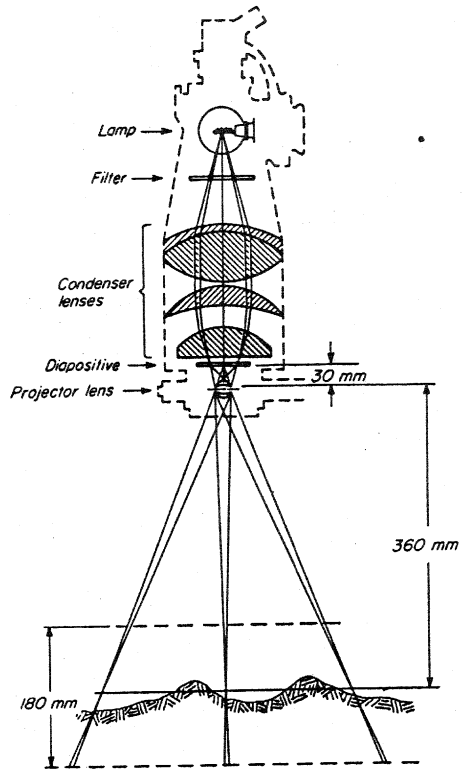


Figure 12-7. Multiplex projector. Copyright 1966, American Society of Photogrammetry. Reproduced with permission.

taking into account the vertical relief. This is illustrated by way of the following numerical examples.

Example 12-1

The flying height above the average terrain elevation is 6500 m. The relief ranges from 700 m above to 300 m below the average elevation. What is the largest and the smallest scale which can be accommodated in the Multiplex? What is the optimum scale?

SOLUTION

Figure 12-8(a) shows the model in the position of the largest scale and Fig. 12-8(b) shows it in the position of the smallest scale. At the largest scale, the lowest point should be no more than 450 mm below the projector lenses

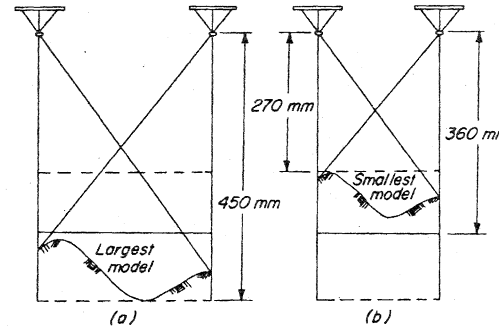


Figure 12-8. Maximum and minimum scales in Multiplex model.

according to Fig. 12-7. The flying height above the lowest point is  $6500 + 300 = 6800$  m. Thus

$$\text{largest model scale} = \frac{450 \text{ mm}}{6800 \text{ m}} = \frac{1}{15,110}$$

At the smallest scale, the highest point should be no closer than 270 mm to the projector lenses. The flying height above the highest point is  $6500 - 700 = 5800$  m. Thus

$$\text{smallest model scale} = \frac{270 \text{ mm}}{5800 \text{ m}} = \frac{1}{21,480}$$

The optimum scale is obtained by placing the average elevation of the model at the optimum projection distance. Thus

$$\text{optimum model scale} = \frac{360 \text{ mm}}{6500 \text{ m}} = \frac{1}{18,055}$$

Example 12-2

If Multiplex mapping is to be compiled at a scale 1 in. = 500 ft, what flying height above the average terrain must be maintained during photography? What range of relief can be accommodated in the Multiplex model?

SOLUTION

Converting the engineer's scale to representative fraction form 1/6000, and placing the average elevation at the plane of best focus gives

$$\frac{360 \text{ mm}}{H_{av}} = \frac{1}{6000}; \text{ and } H_{av} = \frac{6000 \times 360}{304.8} = 7087 \text{ ft}$$

(Note: 304.8 converts millimetres to feet.) At a scale of 1/6000, the range of relief is

$$\Delta h = \frac{6000 \times 180}{304.8} = 3543 \text{ ft}$$

Examples 12-1 and 12-2 demonstrate the wide flexibility in the choice of scales and relief which can be accommodated in the Multiplex instrument. This much flexibility is not obtainable however in the direct-optical instruments used at the present time (see sections 12-8 and 12-9).

12-8 BALPLEX PLOTTER

The Balplex plotter, shown in Fig. 12-9, is similar in all respects to the Multiplex except for the size of the diapositives and the method of illuminating them. It is a direct-optical instrument in which the model is viewed either anaglyphically or else using the stereo image alternator. The measuring and tracing systems are identical to the Multiplex, except that the Balplex frequently employs a pantograph attached to the tracing table for plotting the map at a reduced scale.



Figure 12-9. Balplex 760 plotter. Courtesy of Bausch and Lomb Optical Co.

A section of the Balplex projector is shown in Fig. 12-10. The diapositive is illuminated by light from a lamp reflected from an ellipsoidal reflector surface, the function of which is explained in section 2-3. This arrangement eliminates the need for bulky condenser lenses while at the same time providing uniform illumination over the diapositive.

The principal distance of the Balplex projector is 55 mm, compared with a 30-mm principal distance in the Multiplex projector. The Balplex diapositive consequently is larger than the Multiplex in the ratio 55/30. A special reduction printer shown in Fig. 11-3 is used to make the diapositives. Camera lens distortion is eliminated by means of a correction plate located between the negative and the printer lens as diagramed in Fig. 12-11. The plate is ground aspheric to correct for a particular radial distortion pattern. Thus, a different correction plate is needed for each type of aerial camera lens.

The Balplex plotter is made in two sizes. The first is the original instrument designed for topographic map compilation by the US Geological

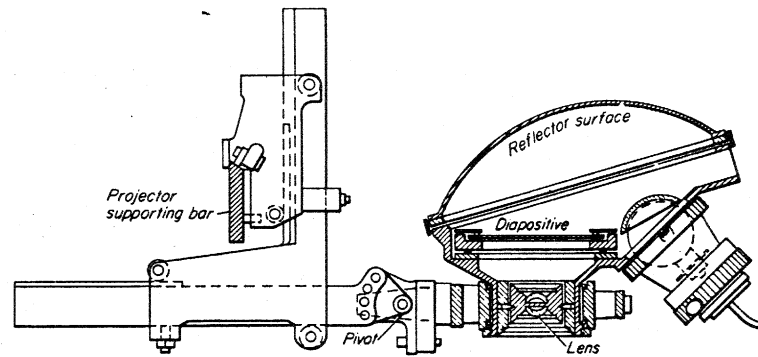


Figure 12-10. Section through Balplex projector.

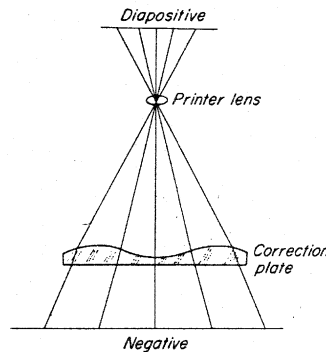


Figure 12-11. Correction plate used in reduction printer.

Survey, which is referred to by that agency as the ER55 (Ellipsoidal Reflector, 55-mm principal distance). The optimum projection distance of the ER55 is 525 mm. The vertical range of usable focus is about 240 mm.

The commercial version is the Balplex 760 whose optimum projection distance is 760 mm. It thus creates a model at a larger scale than the ER55 using the same photography. The vertical range of usable focus is about 220 mm.

Each Balplex projector is provided with a gross rotational motion about a line parallel to the supporting bar through the point marked "pivot" in Fig. 12-10. This motion permits the Balplex to use diapositives made from oblique photographs. The plane of optimum focus can be made to lie parallel to the map table by tilting the projector lens about a line passing through the upper nodal point so as to satisfy the Scheimpflug condition stated in section 10-9.

Orientation and map-compilation procedures with the Balplex are identical to those described for the Multiplex. The greater diapositive area, the longer projection distance, and the larger model provide greater accuracy than that obtainable with the Multiplex from the same aerial photography.

## 12-9 KELSH-TYPE PLOTTER

A large number of direct-optical plotters which use full-sized diapositives have been manufactured in which the design generally follows that of the instrument developed by Harry Kelsh in the late 1940s. One of the early versions of the Kelsh plotter is shown in Fig. 12-4. Some of these plotters are designed so that two different diapositive carriers can be used interchangeably on the same frame. One carrier has a nominal principal distance of 152.4 mm, and the other has a nominal principal distance of 210 mm. These instruments can thus accommodate both normal- and wide-angle photography. Normal-angle photography is used extensively for mapping heavily forested areas because it allows the operator to see the ground in the stereo model easier than when wide-angle photography is used.

Interior orientation is accomplished in the projected rays by one of two methods. In the first method, the diapositive is made at a 1 to 1 ratio in a reduction printer containing a lens distortion correction plate. Provision is made in the printer to accommodate different camera focal lengths. Since the Kelsh projector lenses are practically distortion-free, the projected cone of rays are correct.

In the second method, the diapositive is prepared either 1 to 1 in a fixed reduction printer without a correction plate or else by contact printing of the diapositive (see section 3-9). The correct principal distance is then set off on the projectors to match the camera focal length. The lens distortion is eliminated by means of a cam that raises or lowers the projector lens, thus changing the principal distance to match the distortion.

In its basic configuration, each projector contains three rotational motions, but only the  $b_x$  translational motion with which to scale the model. Relative orientation is thus performed by the independent method described in section 11-4. Some versions of the instrument contain small  $b_y$  and  $b_z$  motions. The entire frame can be tipped and tilted by means of footscrews, in order to level the model.

The illumination of the diapositives is provided by two small lamps located above the diapositives. These lamps swing in arcs about the center of the projector lenses, the motions being imparted to the lamp support arms by means of the guide rods attached to the tracing table. This arrangement can be seen in Fig. 12-4. Only a small portion of each diapositive is illuminated at any time, and that portion is projected through the lens and down onto the tracing-table platen. As the tracing table is moved about in the model area, the lamps are rotated in their arcs so as to maintain the illumination and keep the images from the two diapositives on the platen. The model is viewed either anaglyphically, with the stereo-image alternator, or using the polarized platen viewer, PPV (see Chapter 5).

The optimum projection distance (which varies in different designs) is about 30 in. or 760 mm for the wide-angle projectors and about 33 in. or 840 mm for the normal-angle projectors. The usable depth of focus is about 8 or 9 in (200–230 mm). Technical specifications relating to the Kelsh plotters may be obtained from the manufacturer.

## 12-10 ZEISS DOUBLE PROJECTION PLOTTER

The Zeiss double projection plotter (DP) shown in Fig. 12-12 is a direct-optical instrument that employs 1 to 1 scale diapositives. The entire model area is illuminated during projection. The instrument uses the anaglyph method of viewing. By changing projector lenses, enlargement from diapositive scale to map scale can be either  $1.6\times$ ,  $2.0\times$  or  $2.5\times$ . The model is oriented by the independent method because the instrument contains only the  $b_x$  motion. Leveling is performed with a common  $\Phi$ -rotation together with the  $\omega'$  and  $\omega''$  rotations. The optimum projection distance and the usable vertical range depend on which set of lenses is being used. The tracing table of the DP-1 is moved freehand while that of the DP-2 is moved by means of X- and Y-handwheels. The DP-3 (not shown) is the same as the DP-2 except that the handwheel motions drive the pencil chuck of a separate coordinatograph allowing a wide range of plotting scales for the same photography.

The tracing table platen is fixed vertically. The relative up and down motion of the measuring mark is made by raising and lowering the two projectors and thus the entire model with respect to the tracing table. This has the advantage that map features can be drawn freehand directly on the map sheet without the use of the tracing table. This is of considerable advantage in revising planimetry on existing maps.

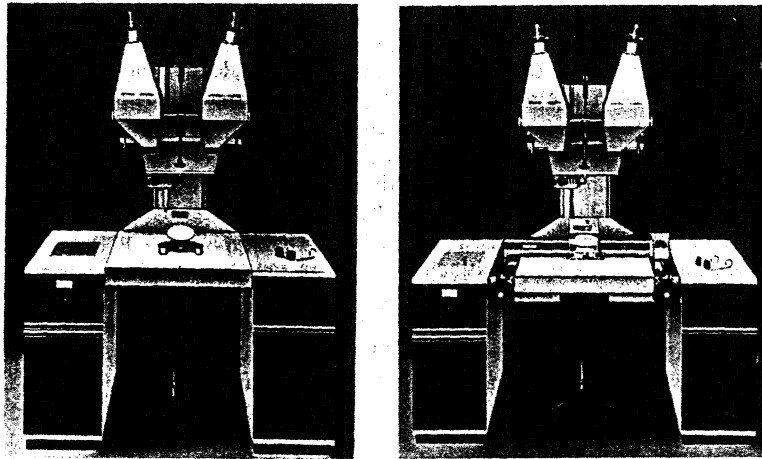


Figure 12-12. (a) Zeiss DP-1 double projection plotter with freehand movement of tracing table. (b) Zeiss DP-2 with handwheel movement of tracing table. Courtesy of Carl Zeiss, Oberkochen.

12-11 WILD AVIOGRAPH B8S

The Aviograph B8S, shown in Fig. 12-5, is a mechanical projection instrument that accepts full size diapositives and can accommodate both wide-angle and superwide-angle photography. A schematic view of the projection and viewing system is shown in Fig. 12-13. Each diapositive carrier on which the diapositive is centered has three rotational motions,  $\omega'$ ,  $\phi'$ , and  $\kappa'$  for the left diapositive, and  $\omega''$ ,  $\phi''$ , and  $\kappa''$  for the right diapositive. These rotations are used to accomplish relative orientation. The base  $b$ , which can be read on a scale, is established as the distance between the pivot points of the space rods. These two pivot points are the effective perspective centers of the diapositives about which the  $\omega$  and  $\phi$  rotations take place as shown. Note that they lie *inside* of and *above* the diapositive stages. This places the diapositives in a positive rather than a negative position as in the direct-optical projection instruments. The lower pivot points  $g'$  and  $g''$  are constrained to move in planes which define the effective diapositive planes. These are shown in Fig. 12-14. The vertical distance between the effective perspective centers at  $L'$  and  $L''$  and the effective diapositive planes is set off in the instrument equal to the calibrated focal length of the aerial camera lens. Lens distortion can be eliminated, if required, by using aspheric correction plates to support the diapositives as shown in Fig. 12-15.

The arrangement for projecting a point on the diapositive and the measuring mark into a relatively simple optical train is shown in Fig. 12-2. However, instead of being moved by the upper end of the space rod as shown in Fig. 12-2, the objective-mark assembly is moved on a cross slide system of

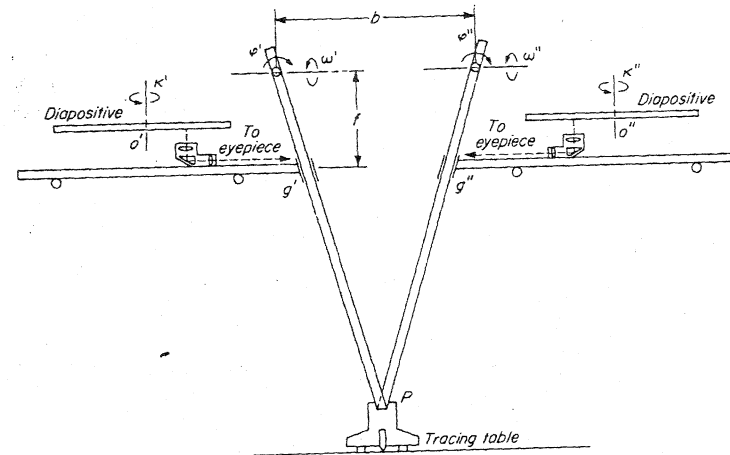


Figure 12-13. Schematic diagram of projection and viewing in Wild Aviograph B8S.

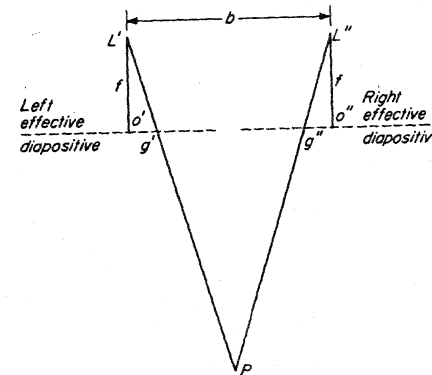


Figure 12-14. Principle of projection in Wild Aviograph B8S.

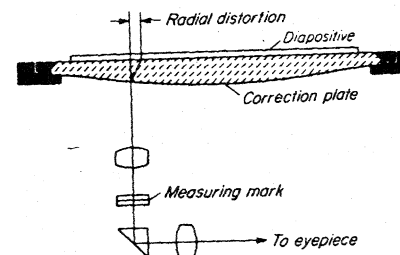


Figure 12-15. Use of aspheric correction plate for eliminating lens distortion.

tubular supports, which can be identified in Fig. 12-5. As the tracing table is moved to the right, the viewing objectives are also moved to the right under the diapositives, allowing the operator to scan the stereoscopic image in the  $X$ -direction. Similarly, moving the tracing table toward or away from the operator permits him to scan in the  $Y$ -direction. If the operator raises or lowers the intersection point at the tracing table, the objectives are moved in opposite  $X$ -directions, increasing or decreasing the parallaxes of the measuring marks. This causes the floating mark to appear to move up and down in the stereo image.

The entire model of the B8S is tilted side-to-side about a common  $\Phi$ -axis during the leveling process. Front-to-back tilting of the model is accomplished by rotating the individual diapositive carriers an equal amount by the  $\omega'$  and  $\omega''$  rotations. The values of  $\Phi$ ,  $\omega'$ , and  $\omega''$  which must be set off in order to level the model are obtained by an analysis of the measured vertical control points, as explained in section 11-11.

The Wild B8S is capable of being digitized in all three directions although this is not necessary for map compilation. The map can be compiled at model scale or enlarged or reduced by means of the linear pantograph shown in Fig. 12-5.

The vertical range that can be accommodated in the stereo model is not limited by optical performance but rather by mechanical constraints in the instrument. When using wide-angle photography, the maximum projection distance is 350 mm measured from the lowest position of the tracing table up to the base. The elevation range is 138 mm.

#### Example 12-3

Solve example 12-1 using a Wild B8S instrument.

#### SOLUTION

Since the flying height above the lowest point is 6800 m, then

$$\text{largest model scale is } \frac{350 \text{ mm}}{6800 \text{ m}} = \frac{1}{19,430}$$

The distance from the base to the upper limit of the tracing table is  $350 - 138 = 212$  mm. The flying height above the highest point is 5800 m.

$$\text{smallest scale is } \frac{212 \text{ mm}}{5800 \text{ m}} = \frac{1}{27,360}$$

There is no optimum scale in the B8S except to the extent that the largest convenient scale permits more precise plotting because of the mechanical advantage involved.

The possible scale ranges shown in example 12-3 can of course be extended upward or downward by means of the pantograph by a factor of

2.5 each way. Thus, the largest scale as given in Example 12-3 can be increased to 1/7770, and the smallest scale can be reduced to 1/68,400.

#### 12-12 KERN PG2

The Kern PG2 instrument shown in Fig. 12-16, is a mechanical projection instrument in which the effective perspective centers are located in *front* of and *below* the diapositive carriers. The diapositives are thus in a negative position. The perspective centers can be identified as the upper pivot points of the space rods in the figure.

During relative orientation, each diapositive can be rotated in  $\kappa$  about its own principal point. However, the  $\omega$ - and  $\phi$ -rotations are imparted to the space rods rather than to the diapositive carriers. Furthermore, an  $\omega$  rotation can only be given to the left space rod, and a  $\phi$ -rotation only the right. The fifth component needed to perform relative orientation is obtained by an inclination of the base bridge of the instrument.

In Fig. 12-17, imagine two diapositives to be located above the two fixed perspective centers at  $L'$  and  $L''$ . The space rods  $p'L'g'$  and  $p''L''g''$  do not intersect at the lower end, but are separated by the base bridge whose length is  $S - b$  in which  $S$  is a fixed value representing the distance between  $L'$  and  $L''$ , and  $b$  is the stereo-model base. The base  $b$  can be identified by imagining the right-hand space rod to be moved parallel with itself to an intersection at  $g'$  as shown by the dashed line  $Lg'$ . The parallelogram  $LL''g''g'$  thus formed is called the *Zeiss parallelogram* and is incorporated in several kinds of plotting instruments primarily to overcome mechanical space limitations

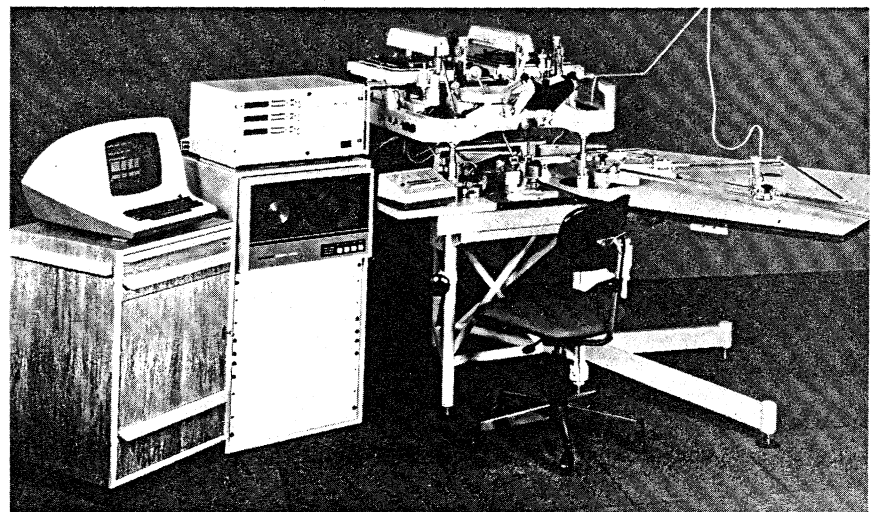


Figure 12-16. Kern PG2 stereoplotting instrument. Courtesy of Kern Instruments, Inc.

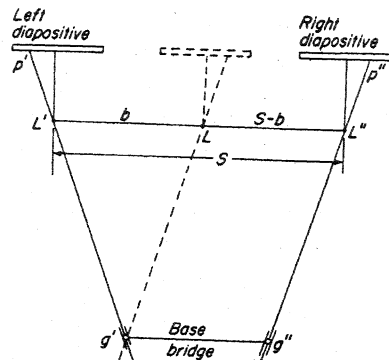
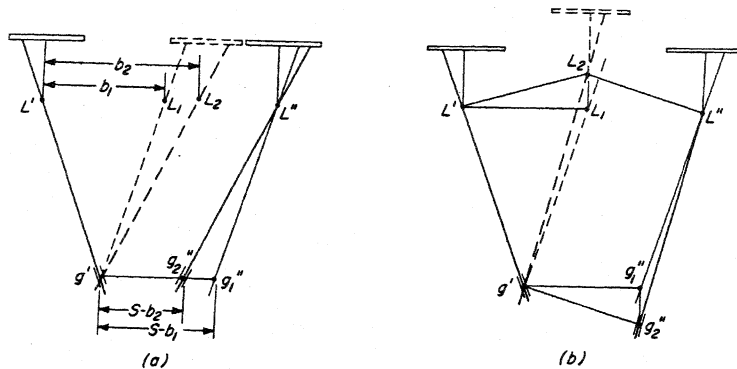


Figure 12-17. Zeiss parallelogram.

Figure 12-18. (a) Increasing base by decreasing length of base bridge.  
(b) Lowering right pivot point in effect raises right projector.

and to simplify the mechanical motions. It also permits base-in base-out operations on certain instruments as explained in section 13-6.

In the Kern PG2, the motions of points  $g'$  and  $g''$  are confined to the  $X-Z$  plane, which is also the plane of the figure. If the distance  $g'g''$  is decreased, the base  $b$  is increased correspondingly, from  $b_1$  to  $b_2$  as shown in Fig. 12-18(a). This preserves the Zeiss parallelogram during the scaling operation. If  $g''$  of Fig. 12-17 is lowered to  $g_2''$  as shown in Fig. 12-18(b), the effect is to raise  $L$  from  $L_1$  to  $L_2$  in order to preserve the Zeiss parallelogram  $L_2L''g_2''g'$ . The distance  $L_1L_2$  is the  $b_2$  component of the base, which is the fifth component used for relative orientation. These five components are  $\kappa'$ ,  $\kappa''$ ,  $\omega'$ ,  $\phi''$ , and  $b_2$ ; the latter element is referred to on the instrument as  $B\Phi$ . Relative orientation of the PG2 is somewhat different than the procedures described in sections 11-3 and 11-4 since the motions necessary for those methods are not available.

If the negatives and consequently the diapositives show differential shrinkage in the  $x$ - and  $y$ -directions, these can be allowed for in the PG2 by setting off different principal distances in the  $x$ - and  $y$ -direction for each diapositive.

The  $X$ - and  $Y$ -movements of the viewing system are split between the diapositives that move together as a unit in the  $X$ -direction, and a portion of the optics, which views the diapositive orthogonally and moves in the  $Y$ -direction.

The numerical value of the base can be read from a base scale. This facilitates the scaling process as described in section 11-10. The stereo model is leveled by tipping and tilting the drawing table relative to the instrument.

Compilation is performed on a separate drawing table. Translation of the  $X-Y$  freewheeling motion of the tracing table to the drawing table is made through one of a variety of pantographs available for the instrument.

One of the distinguishing features of the PG2 is the ability to read directly the  $X, Y, Z$  coordinates of the perspective centers of the instrument. This is necessary for independent model triangulation as discussed in section 13-8.

### 12-13 ZEISS PLANIMAT

The Zeiss Planimat, shown in Fig. 12-19, is a mechanical-projection instrument which uses full-size diapositives. It will accept camera focal lengths of 88, 152, 210, and 305 mm. Lens distortion correction, if necessary, is made by aspheric plates which support the diapositives. The effective perspective centers are located *behind* and *above* the diapositive holders. These can be identified as the upper gimballs through which the space rods pass. This places

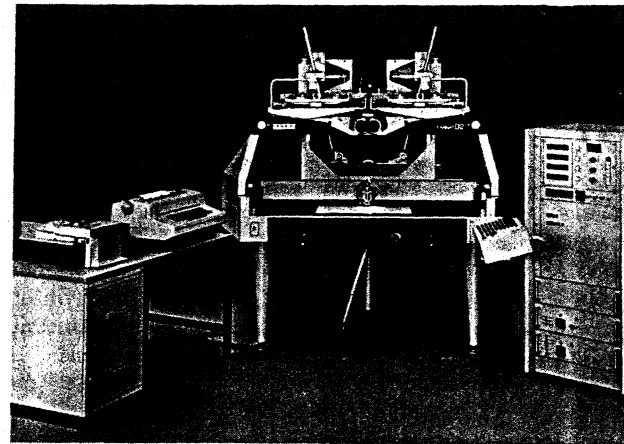


Figure 12-19. Zeiss D2 Planimat. Courtesy of Carl Zeiss, Oberkochen.

the diapositives in the positive position. The Zeiss Planimat incorporates the Zeiss parallelogram as shown in the schematic diagram of Fig. 12-20. The design principle is shown in this diagram. The viewing system is fixed while the diapositives are displaced in  $X$  and  $Y$  for viewing. The diapositive carriers are rotated about three axes to provide the  $\omega', \phi', \kappa', \omega'', \phi'', \kappa''$  angles. The lower pivot of the left space rod can be raised and lowered as shown in Fig. 12-20. This provides the  $b_z$  base component as demonstrated in Fig. 12-18(b). The lower pivot of the right space rod can be moved horizontally in the  $Y$ -direction, as shown in Fig. 12-20. A movement toward the reader will in effect displace the right perspective center away from the reader, and vice versa. This provides the  $b_y$  base component. Thus, relative orientation can be performed by both the independent and the dependent methods. The values of  $p_y$  at the orientation points can be precisely measured by means of the  $b_y$  scale. Relative orientation can thus be performed numerically as described in section 11-7 and as illustrated by example 11-3.

The diapositive principal distance is set off equal to the focal length of the camera lens by displacing the perspective centers vertically. The effective diapositive plane is the surface generated by movement of the middle gimbals identified as  $g'$  and  $g''$  in Fig. 12-20 as the base carriage below is moved around in  $X$  and  $Y$ . The camera focal length  $f$  is accommodated as shown. The movement of the base carriage is provided by a precision cross-slide system shown schematically in Fig. 12-20. The  $Y$ -motion is primary, the  $X$ -motion is secondary, and the  $Z$ -motion is tertiary. The  $X$  and  $Y$  motions are driven by handwheels, and the  $Z$ -motion is driven by a foot disk. As the base carriage

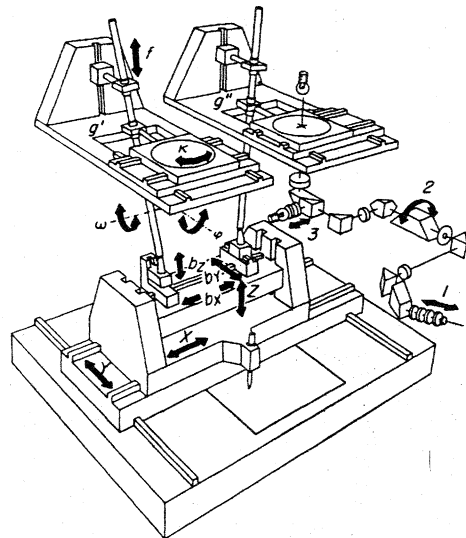


Figure 12-20. Schematic view of Zeiss Planimat.

is moved, the space rods pivot about the perspective centers, forcing the diapositives to move. As the base bridge is moved vertically, the diapositives are forced outward or inward with respect to one another, causing a change in  $x$ -parallax of the measuring mark.

The vertical range of the instrument for wide angle photography ( $f = 152$  mm) measured down from the perspective centers is from 193 to 463 mm.

Example 12-4

Solve example 12-1 using the Zeiss Planimat and wide-angle photography.

SOLUTION

Since the flying height above the lowest point is 6800 m, then

$$\text{Largest model scale is } \frac{463 \text{ mm}}{6800 \text{ m}} = \frac{1}{14,690}$$

The flying height above the highest point is 5800 m. Thus

$$\text{Smallest model scale is } \frac{193 \text{ mm}}{5800 \text{ m}} = \frac{1}{30,050}$$

Scaling is performed numerically as described in section 11-10. Leveling is accomplished by tilting and tipping the diapositive carriers and by rotating the base as described in section 12-16 for the Wild Autograph A7.

Plotting in the Zeiss Planimat can be performed either directly in front of the operator at the stereo-model scale, or else at an enlarged or reduced scale on the separate drawing coordinatograph. All three instrument coordinates can be fully digitized.

12-14 WILD AUTOGRAPH A10

The Wild Autograph A10, shown in Fig. 12-21, is functionally similar to the Zeiss Planimat except for the placement of the perspective centers. These are the middle cardans of the space rods shown schematically in Fig. 12-22, and are seen to lie *between* and *below* the diapositives. This places the diapositives in the negative position. The diapositives are displaced in the  $X$ -direction and the optics are displaced in the  $Y$ -direction while viewing.

The instrument provides for the three rotations of each diapositive, a  $b_y''$  base component and a  $b_z'$  base component. Most of the features of the instrument, including the optical train can be identified in Fig. 12-22. Principal distances from 88 to 308 mm can be accommodated in the instrument. The  $Z$ -range is from 130 to 450 mm.

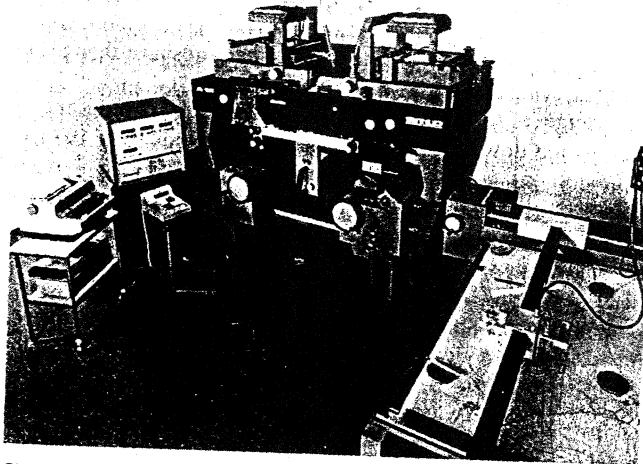


Figure 12-21. Wild Autograph A10. Courtesy of Wild Heerbrugg Instruments, Inc.

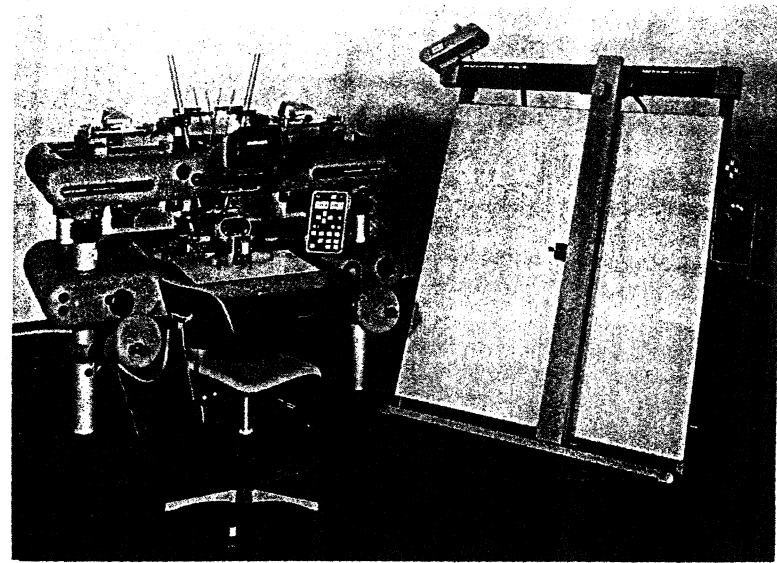


Figure 12-23. Wild Aviomap stereoplotter. Courtesy of Wild Heerbrugg Instruments, Inc.

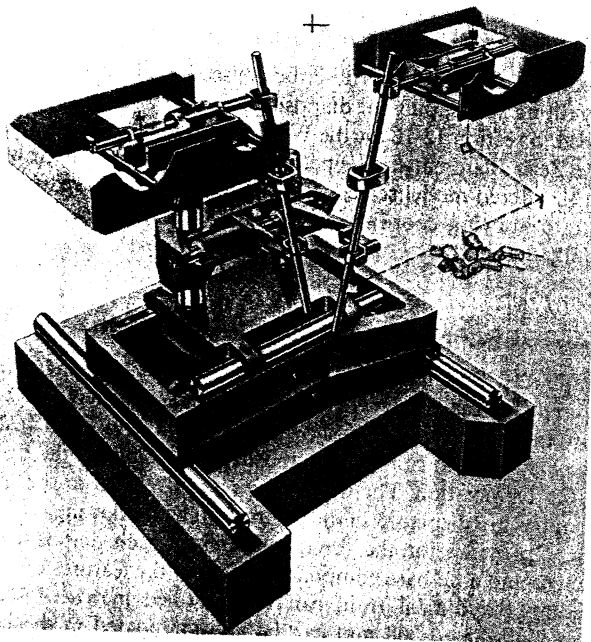


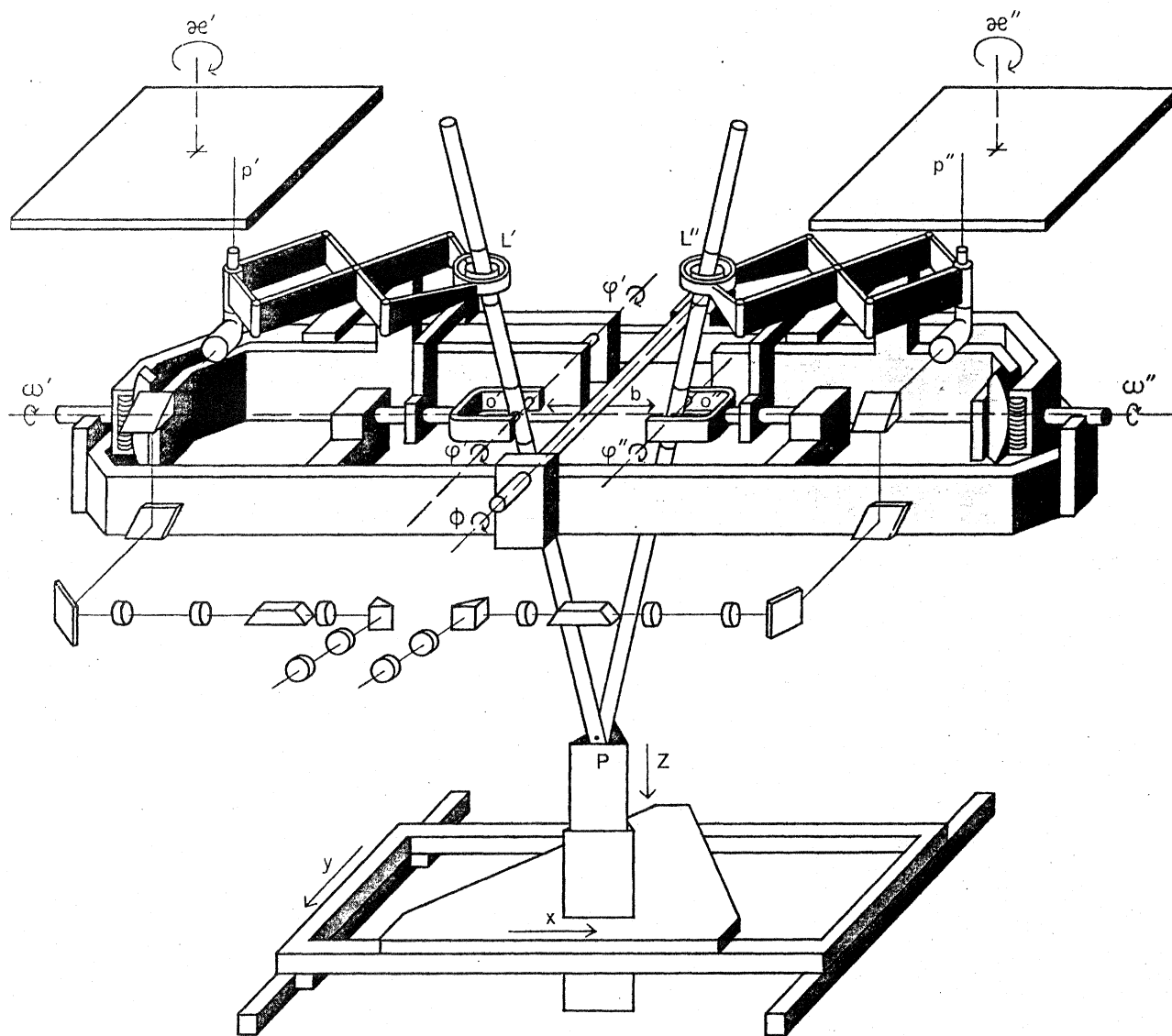
Figure 12-22. Schematic view of Wild Autograph A10.

#### 12-15 WILD AVIOMAP

The Wild Aviomap shown in Fig. 12-23 is a mechanical projection instrument that uses full size diapositives ranging from normal-angle to superwide-angle photography. The perspective centers are located *between* and *below* the diapositives, thus placing the diapositives in the negative position. It is similar in many respects to the Wild Autograph A10. However, it can be used in the freewheeling mode in which the carriage travels on air bearings.

#### 12-16 WILD AUTOGRAPH A7

The Wild Autograph A7, shown in Fig. 12-24 is a mechanical projection instrument accepting full size diapositives with focal lengths ranging from 98 to 215 mm. It differs from all the previously described instruments in one very important aspect. The A7 is capable of extending control through a flight strip of diapositives by the method of stereotriangulation described in section 13-6. This is made possible by means of an optical switch at the eyepiece, which allows either eye to observe either the left or the right diapositive, and by alternatively switching the base from the usual "base-in" position to an outside "base-out" position by means of the Zeiss parallelogram. The use of the optical switch and the two positions of the base will be described in section 13-6.



Functional diagram of the Wild A8 Autograph

## 16-7 ANALYTICAL PLOTTERS

One of the main tasks of all stereoplotters is to establish the projective relationship between each model point and its corresponding image points on the stereopair of photographs. In all the plotters discussed in Chapter 12, this relationship is realized by analog means, either optically, or mechanically, or optically-mechanically. On the other hand, in the analytical plotters, the projective relations are implemented analytically. For this reason, an integral part of each analytical plotter is a digital computer. The computer performs, on real-time basis, the computations necessary to continually satisfy the mathematical relationships between the model points and their respective image points given by equation 6-15. Substitution of the digital computer for mechanical and optical parts increases the accuracy, flexibility, and versatility of the plotting instrument.

The analytical plotter should have an inherently higher accuracy than any conventional plotter. First of all, since no attempt is made to recreate an analog model of both the position and attitude of the camera stations, the construction of the optical-mechanical component of the analytical plotter is greatly simplified. It is, in fact, essentially that of a stereocomparator. Another inherent capability that contributes to increased accuracy is the provision for compensation of systematic image errors in the digital computer (see Chapter 9). With the flexibility provided by having an on-line computer, any systematic error that can be mathematically modeled can be corrected. Also, the computer can readily accommodate redundant information, such as extra fiducials, reseau points, and more points than the minimum necessary for relative and absolute orientation.

With regard to versatility, design limitations on the analytical plotter are many times less stringent than on conventional plotters. For example, the focal length can range from 1 or 2 cm, to 1 or more metres, and the angles  $\omega$  and  $\phi$  of  $30^\circ$  or  $40^\circ$  can be accommodated. Plotting scales can be extremely variable, say 50 times the photo scale. In addition, the availability of a com-

puter makes possible the calculation of such things as direct distances between points, angles between lines, areas of enclosed figures, and so on. Finally analytical plotters are the only plotters that can plot from panoramic and continuous-strip photography.

In its basic form, an analytical plotter contains the components shown in Fig. 16-10. The four main components are: (1) the stereocomparator where the two plates are inserted; (2) a digital computer; (3) a coordinatograph; and (4) the operator's console. Perhaps the easiest way to understand the basic concept of the analytical plotter is to proceed through the steps of its operation. The plates are inserted into the plate holders and roughly oriented. The principal distance for each plate (which may not necessarily be the same for both plates) is then entered into the computer. This is equivalent to making the principal distance settings in an analog plotter.

Next, the values of lens distortion corrections, atmospheric refraction and earth curvature corrections, and calibrated fiducial mark and reseau coordinates are entered into the computer storage. The operator now sets the measuring mark on the fiducial marks of each plate in turn, signaling the computer to receive these values as plate coordinates. The computer then computes the position of the principal point together with the directions of the coordinate axes of each plate. Any one of the various transformations discussed in Chapter 9 can be used in these computations based on redundant fiducial marks. This completes interior orientation. At this point, the computer has established a separate photographic coordinate system for each plate as shown in Fig. 16-11. These systems are then related to a "model" coordinate system by relative and absolute orientation.

Relative orientation is accomplished in a manner similar to analytical relative orientation given in section 11-8. The operator selects a procedure such as dependent relative orientation of, say, photo 2 (on the right) to

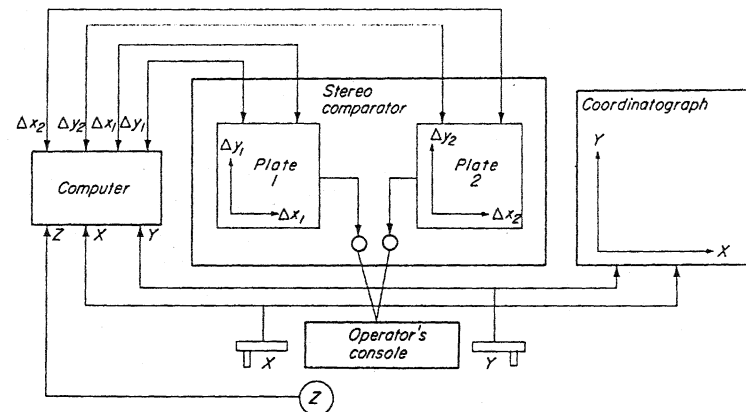


Figure 16-10. Components of an analytical plotter.

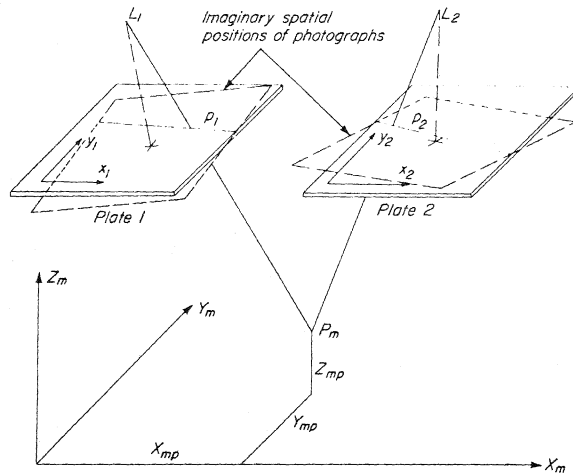


Figure 16-11. Photographic and model coordinate systems in analytical plotter.

photo 1. He then enters the approximate values of the five elements  $\omega''$ ,  $\phi''$ ,  $\kappa''$  and  $b_y''$  and  $b_z''$  which he estimates from an examination of the photographs. He then proceeds to any model point and clears the  $y$ -parallax using  $p_y$  (for photo 2) and presses a button to signal the computer to refine and store the plate coordinates  $x_1, y_1, x_2, y_2$ , of the corresponding image points. Most analytical plotters will accommodate 25 or more such parallax points. Once five or more points are thus measured, the computer uses the linearized collinearity equations (see equation C-25) in order to determine the five orientation elements.

The computer memory will now contain all 12 exterior orientation elements of the two photographs relative to a model coordinate system defined by (in this instance) the coordinate system of the left-hand photograph. The measuring mark is moved around in this model system by means of two handwheels and a foot disk (or some mechanical equivalent). From these displacements, the computer determines the instantaneous model  $X_m, Y_m$ , and  $Z_m$  coordinates of the model point occupied by the measuring mark. These model coordinates, together with the stored elements of interior orientation and the 12 elements of exterior orientation of both photographs, are then used to compute, in real time, the photographic plate  $x_1, y_1, x_2, y_2$  coordinates of the instantaneous model point, using the collinearity equations. As soon as the plate coordinates are computed, they are used to generate signals to servo motors which drive the photo stages in  $x$  and  $y$  such that the conjugate images with the calculated photo coordinates (which must now contain all the effects of systematic errors) are brought precisely under the half-marks of the viewing optics.

This presents to the operator a continuous stereoscopic view of the two photographs in the immediate vicinity of the measuring mark. The calculations are performed so rapidly that the operator senses no delay between his turning of the handwheels and foot disk and the apparent movement of the floating mark in the model. The computer also controls the optics that allow for differential magnification (to accommodate scale differences between conjugate images) and differential rotation of the two images. These controls are based on the stored interior orientation elements of each photograph and on the two individual photographic coordinate systems.

The model as viewed by the operator is not a complete analog model as constructed by the stereoscopic plotting instruments discussed in Chapter 12. Rather, it is incrementally constructed for the viewing of only a small portion by the operator at any time. All of the underlying projective relations are mathematically implemented by the computer.

In order to perform absolute orientation, the operator enters the ground coordinates of a sufficient number of control points (minimum of two horizontal and three vertical) and records their corresponding model coordinates by placing the floating mark on each control point. A seven-parameter transformation, (see equation A-18 and section 11-13) is computed iteratively, using least squares if more than minimum control is available. The computed seven parameters are then used to transform the exterior orientation elements of the two photographs such that they now relate to the ground control system instead of the model system. Thus, if  $x_1, y_1, x_2, y_2$  for any point is known, its ground coordinates can be computed. Conversely, if the ground coordinates are known, the plate coordinates can be determined. The ground coordinate system is defined in the instrument by the handwheel and foot disk encoder displacements at some arbitrary scale.

After absolute orientation has been accomplished, the measuring mark now occupies a point in the ground coordinate system. The operator traces out planimetric features and contour lines just as in the analog instruments described in Chapter 12. The displacements of the measuring mark can be stored as profiles, digitized contour lines, or digital terrain models, or they can be transmitted to a coordinatograph by servo motors in order to produce a map or chart.

The basic concept of the analytical plotter as explained above was invented in 1957 by U.K. Helava who was at that time with the National Research Council of Canada. Since then, many models and systems of the analytical plotter have been developed and built by a number of photogrammetric firms in both North America and Europe. Most of the plotters are built on the Helava concept in which the  $X_m, Y_m, Z_m$  model point coordinates generate pulses and compute: (1) four photo shifts, as diagrammed in Fig. 16-10, which are effected by four servo motors; and (2) two plotting table shifts which are also executed by servos.

A historical review of the analytical plotters through 1974 is given in Table 16-1. Presently available analytical plotters are listed in Table 16-2.

Table 16-2 COMPARISON OF PRESENTLY AVAILABLE ANALYTICAL INSTRUMENTS

MANUFACTURER AND YEAR	MODEL	COMPUTER	CORE STORAGE	DISK STORAGE	CONTROL	DIGITIZATION INCREMENT	ADDITIONAL HARDWARE	CYCLE TIME
Bendix, 1976	US 1	PDP 11/35	24K, 16 bit	1.2M 16 bit	CRT	1 $\mu$ m	multilevel interrupt	900 ns
Instronics-Gestalt, 1976	Anaplot	PDP 11/45	32K, 32 bit	2 $\times$ 1.2M 32 bit	CRT, panel	1 $\mu$ m	double precision floating point, multilevel interrupt	—
Matra, 1976	Traster 77	Telmech. solar 16-40	32K, 16 bit	2 $\times$ 2.5M 8 bit	CRT	0.5 $\mu$ m	coded linear encoders	750 ns
OMI, 1975	AP/C-3T	PDP 11/35	24K, 16 bit	1.2M, 16 bit	panel	2 $\mu$ m	multilevel interrupt	900 ns
OMI, 1976	AP/C-4	PDP 11/03	24K, 16 bit	cassette	CRT	2 $\mu$ m	—	1.2 $\mu$ s
Zeiss Oberkochen, 1976	Planicomp C 100	HP 21 MX	24K, 16 bit → 128K	4.9M, 8 bit	panel CRT	1 $\mu$ m	floating point multilevel interrupt	650 ns
Jenoptik, 1976	Stereo-dicomat	Kongsberg SM 4	16K, 16 bit	—	Teletype	0.625 $\mu$ m step	—	—
Galileo, 1976	Digital stereo cartograph	PDP 11/05	12K, 16 bit	—	Teletype	1 $\mu$ m step	—	900 ns
Zeiss Oberkochen, 1976	Stereocord	HP 9810 or HP 9830	ROM 51 words ROM 1760 words cassette	—	HP 9810 or HP 9830	10 $\mu$ m	—	—
K. & E/H. Dell Foster 1976	RSS-300-11	—	—	—	—	—	—	—

531

Copyright 1977, American Society of Photogrammetry. Reprinted with permission of the American Society of Photogrammetry.

## 530 PHOTOGRAMMETRY

Table 16-1 DEVELOPMENT OF ANALYTICAL INSTRUMENTS THROUGH 1974

YEAR	MODEL	MANUFACTURER	SPECIAL FEATURES	USERS
INVENTION				
1957	U. Helava			
PROTOTYPE AND EARLY MODELS				
1963	AP-1	NRC Ottawa	delay line memory	private
1963	AS-11A	O.M.I.-Bendix	D.D.A.	military
1964	AP/C	O.M.I.-Bendix	delay line memory	private
INTERMEDIATE MODELS				
1968	AS-11A-1	O.M.I.-Bendix	BX 272—core	military
1972	AP/C-3	O.M.I.-I.B.M.	IBM 1130—core	private
SPECIAL MODELS				
1968	UNAMACE	Bunker-Ramo	TRW automatic image correlation	military
1968	AS-11B-1	Bendix-O.M.I.	BX 272 automatic image correlation	military
1974	TA 3/P1	O.M.I.-Bendix	PDP 15 automatic image correlation	military
1972	Gestalt	Hobrough Ltd.	Nova automatic image correlation	private
DIGITAL STEREOCARTOGRAPH				
1972	D.S.	Galileo	Laben minicomputer	private
IMAGE SPACE PLOTTER				
1974	A.P.P.S.	E.T.L., Fort Belvoir	HP 9810	military

Copyright 1977, American Society of Photogrammetry. Reprinted with permission of the American Society of Photogrammetry.

The most marked difference shown in the two tables is the changeover from special purpose to general purpose computers. The tables also show two categories of analytical plotters: (a) those which were designed and built for the military and which were dominant until 1976; and (b) those produced for commercial use which proliferated in 1976.

The OMI Analytical Plotter AP/C4, shown in Fig. 16-12, is a direct descendent of the original AP-1 plotter developed at the National Research Council of Canada. The individual  $x$  and  $y$  displacements required to satisfy the collinearity condition for all model points is split between the optics which move in the  $x$ -direction and the diapositive stages which move in the  $y$ -direction. These displacements are measured through linear glass scale optical encoders. The stereoscopic model is viewed through binocular eyepieces and motion is imparted to the measuring mark by turning a pair of handwheels and a foot disk. Communication and interaction between the operator and the computer/instrument is made via a CRT terminal. A series

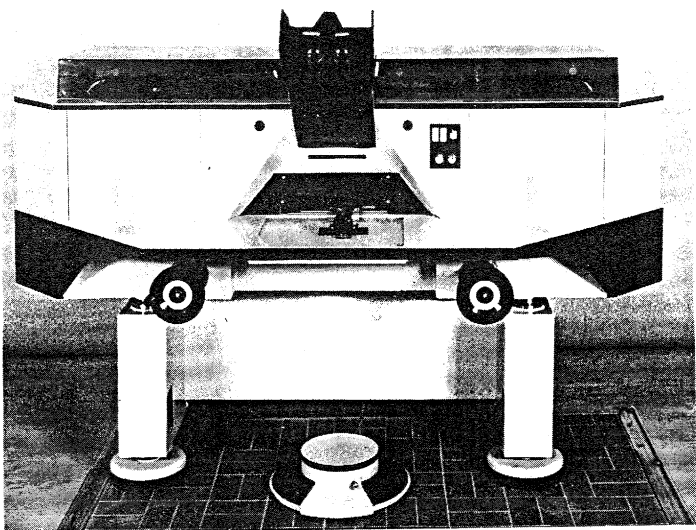


Figure 16-12. OMI Analytical Plotter AP/C4. Courtesy of OMI Corp. of America.



Figure 16-13. Matra Optique Traster 77 Analytical plotter. Courtesy of Matra-Division Optique.

of instructions or interrogations is displayed on the face of the CRT tube to which the operator reacts or responds when performing such tasks as interior, relative, and absolute orientation.

The Matra Traster 77 shown in Fig. 16-13 operates basically on the Helava concept. Small sections of conjugate areas of the diapositives are

projected onto one another at great magnification on the face of a large screen directly in front of the operator. The projector light has been cross-polarized so that the operator views the stereo image, together with a projected measuring mark, in three dimensions by viewing through polarized glasses. Displacement of the measuring mark in  $X$  and  $Y$  is accomplished by rotating an air-cushioned ball with the right hand. A drum is turned with the left hand to move the measuring mark in the  $Z$ -direction. The individual  $x$  and  $y$  displacements required for collinearity are imparted to the diapositive stages by means of lead screws. Measurement of these displacements is made with respect to  $X$  and  $Y$  linear glass encoders. A CRT display is located on one side of the stereoviewing screen. This is used to interact with the computer when performing the different functions. A television screen is located to the other side of the stereoviewing screen. This displays the progress of the drawing as it is developed on the drawing table, via a video camera which moves with the pencil holder.

Descriptions of most of the analytical plotters available at the time of publication of this text (1979) can be found in the November, 1977 issue of *Photogrammetric Engineering and Remote Sensing*.

## 16-8 TOTALLY DIGITAL SYSTEMS

The totally digital system is a sequential process in which the photographs are first digitized, and then the data are processed in large computers. Such a system is exemplified by the experimental Digital Automatic Map Compilation System, DAMCS, which was developed by International Business Machines. In this system, the scanning of the photographs was done by a modified STK-1 stereocomparator. The digital photo densities were stored on magnetic tape. Modern precision microdensitometers and high-speed scanner-printers perform the same task. The number of gray shades was limited to 64 in the DAMCS, although current scanners can quantize up to 1024 gray shades. The data on the magnetic tape are then read into a large computer and digitally manipulated. Using the values of the camera parameters and the input digital data, the photographs are differentially rectified digitally. In the process, conjugate images are located by statistically matching the data using the cross-correlation technique explained in section 16-3. After the image matching is performed, parallax differences are converted to terrain elevation differences. The output of the computer is another magnetic tape which is then used to produce orthophotos and contour manuscripts. In printing the manuscripts, the scanner is used to perform the reverse function, that is, to paint a latent image onto a sensitized film by the light source from a CRT that has been modulated by the computer-fed data. The orthophotograph is exposed by modulating the light to the required density level, and the contours are printed by exposing the light at all spots that fall at the predetermined contours.

**Appendix III**  
**LABORATORY PROJECTS**

**September, 1996**

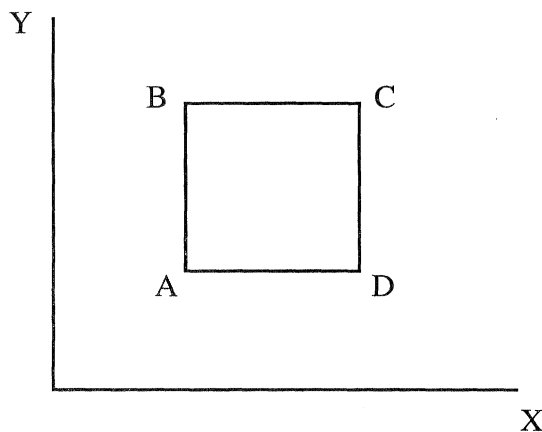
## SE 3303 Photogrammetry I

### Lab. #1: Familiarization with Geometric Transformations

1. List the six possible sequences of rotations around three mutually perpendicular axes.
2. Form the resultant rotation matrix  $M_T$ , if the first rotation occurs around the Z ( $\kappa$ ) the second rotation around the Y ( $\varphi$ ) and the third around the X ( $\omega$ ) axes.
3. Given are the coordinates of a point P in a three-dimensional Cartesian coordinate system: X, Y, Z. This coordinate system is first rotated by angles  $\omega_1, \varphi_1, \kappa_1$  to form system  $X_1, Y_1, Z_1$  and then is rotated again by  $\omega_2, \varphi_2, \kappa_2$  to establish the  $X_2, Y_2, Z_2$  system. (First and second means the sequence of the rotations). Calculate the coordinates of P in the  $X_1, Y_1, Z_1$  and in the  $X_2, Y_2, Z_2$  systems. Find the orientation of the  $X_2, Y_2, Z_2$  axes with respect to the X, Y, Z system. Use the  $M_T$  matrix formed in Question 2.

$$\begin{array}{lll}
 P_X = -43.461\text{m} & \omega_1 = -1.2553^\circ & \omega_2 = -0.1553^\circ \\
 P_Y = -83.699\text{m} & \varphi_1 = 0.0937^\circ & \varphi_2 = -0.9768^\circ \\
 P_Z = 152.670\text{m} & \kappa_1 = -0.7631^\circ & \kappa_2 = -91.1901^\circ
 \end{array}$$

4. What would the rotation angles of the  $X_2, Y_2, Z_2$  axes with respect to the X, Y, Z system be, if the numerical values of the matrices obtained in Question 3. would be valid for the case when  $\omega$  is the first,  $\varphi$  the second and  $\kappa$  the third rotation?
5. Show graphically the effect of an active four-parameter similarity transformation and a six-parameter affine transformation on the square A,B,C,D in this figure.



**Total Value:** 20 marks (2% of final course mark).

## SE 3303 Photogrammetry I

### Lab. #2: Rotations in Three Dimensions.

- Form the rotation matrices  $M_{r1} = M_x M_y M_z$  and  $M_{r2} = M_y M_x M_z$  with the following three sets of rotation angles:  $\phi = \omega = \kappa = 1^\circ; 5^\circ$  and  $30^\circ$ .  
There are a total of six matrices to be formed.
- Extract the three rotation angles from each matrix formed in Qu.1. with  $30^\circ$  rotation, which would be valid for the other sequence of rotation. (Extract from the numerical form of  $M_{r1}$  the angles which would be valid for the rotation sequence  $M_{r2} = M_y M_x M_z$  and vica versa.)  
Compare these values to  $30^\circ$  and draw conclusions.
- Form the 1st. order approximation of  $M_{r1}$  and  $M_{r2}$  using each of the rotation angles given in Qu.1. What conclusions can you draw?
- The coordinates of a point P are as follows:  
 $x = 90.00$  mm,  $y = 90.00$  mm,  $z = 150.00$  mm.  
Compute the coordinates of this point rotated by  $M_{r1}$  and  $M_{r2}$  as formed with each of the three angles given in Qu.1. (There are six sets of coordinates to be computed).  
What conclusions can you draw?  
Compute the coordinates rotated by each of the 1st. order approximations of the matrices formed in Qu.3. Are the differences in the results obtained with the rigorous and the approximate matrices significant, if a precision of 0.02 mm is required?
- Given are the X and Y coordinates of three point clusters, A, B and C as follows:

Pt	<u>Cluster A</u>		<u>Cluster B</u>		<u>Cluster C</u>			
	XA	YA	XB	YB	XC	YC		
A1	10.0	40.0	B1	30.0	60.0	C1	40.0	60.0
A2	40.0	70.0	B2	60.0	70.0	C2	80.0	70.0
A3	70.0	40.0	B3	70.0	40.0	C3	80.0	40.0
A4	40.0	10.0	B4	40.0	30.0	C4	40.0	30.0
A5			B5	20.0	40.0	C5	20.0	40.0
A6			B6	40.0	80.0	C6	60.0	80.0
A7			B7	80.0	60.0	C7	100.0	60.0
A8			B8	60.0	20.0	C8	60.0	20.0

- Plot each cluster on graph paper to see the geometric shape formed by these points. Identical number codes, e.g. A2, B2, C2, signify corresponding points.
- Transform Cluster B to Cluster A by similarity and affine transformation, as well as Cluster C to Cluster A also by similarity and affine transformation to find the transformed coordinates of points 5 to 8.
- Plot each transformed point cluster. Examine the geometric shapes that resulted and draw conclusions on the effects of the two types of transformation used.

Analyse the results of each question and make comments as appropriate.

**Note:** The Photogrammetric Program Package installed on the Novell network should be used for the solution, supplemented by hand calculations, as necessary.

**Submission:**

- Annotated computer printout.
- Comments and conclusions in point form.

**Total Value:** 20 marks (2% of final course mark).

## SE 3303 Photogrammetry I

### **Lab. #3: Processing of Image Coordinate Measurements**

Given are a set of image space coordinates measured on a pair of overlapping aerial photographs (Photos #8798 and #8799), as listed on Data Sheets 1.

Transform the measured image coordinates from the comparator (instrument) system to the image coordinate system, based on the measured and the calibrated coordinates of the fiducial marks, listed on Data Sheets 1. Use the affine or the projective transformation.

Apply corrections to the transformed image coordinates of both photos for: film distortion, radial lens distortion, atmospheric refraction and earth curvature. The camera calibration data and other pertinent information are provided on Data Sheet 2.

#### **Submission:**

- a) A tabulated listing of each correction, the sum of the corrections and the corrected image coordinates.
- b) Comments on the significance of the individual corrections and that of the total corrections.

**Total Value:** 30 marks (3% of final course mark).

## SE 3303 Photogrammetry I

### **Lab. #4: Analytical Perspective Rectification**

1. Given are the image space coordinates of Photos #8798 and #8799 processed in Lab #3, and the ground coordinates of certain points, as listed on Data Sheet 3. Compute the planimetric object space (ground) coordinates ( $X$ ,  $Y$ ) of points 1050 and 1151 by:

- (a) Space resection of each photograph, followed by reprojection onto a horizontal plane, set at the average terrain elevation (25 marks);
- (b) Projective transformation of each photograph onto a horizontal plane (25 marks).

2. Given are the  $X$  and  $Y$  coordinates of two point clusters, A and D as follows:

Pt	<u>Cluster A</u>		<u>Cluster D</u>	
	XA	YA	XD	YD
A1	10.0	40.0	D1	36.00 56.00
A2	40.0	70.0	D2	94.29 71.43
A3	70.0	40.0	D3	90.00 35.00
A4	40.0	10.0	D4	38.18 30.91
A5			D5	20.00 40.00
A6			D6	60.00 80.00
A7			D7	140.00 60.00
A8			D8	60.00 20.00

- (a) Plot each cluster on graph paper to see what geometric shape these points form. Points with identical number code, e.g. A2, B2, C2, are corresponding points.
- (b) Transform Cluster D to Cluster A by affine and projective transformation, to find the transformed coordinates of points 5 to 8.
- (c) Plot each transformed point cluster. Examine the geometric shapes that result and draw conclusions on the effects of the three types of transformation used. (10 marks for Question 2.)

The Photogrammetric Program Package installed on the Novell network should be used for the solution, supplemented by writing additional computer programs, or by performing hand calculation, as necessary.

#### **Submission:**

- (a) A step-by-step description of the procedures followed in each method, including the equations used;
- (b) A tabulated list of input, intermediate and final values;
- (c) Annotated copy of computer outputs;
- (d) Analysis (comparison) of the results.

**Total Value:** 60 marks (6% of final course mark).

**SE 3303 Photogrammetry I****Lab #5: Computation of Object Space Coordinates**

1. Given are the image space coordinates of Photos #8798 and #8799 processed in Lab #3, and the ground coordinates of certain points, as listed on Data Sheet 3. Compute the object space (ground) coordinates (X, Y,Z) of points 1050 and 1151 by:

- (a) Space resection of the each photograph followed by space intersection (30 marks);
- (b) A modular solution consisting of analytical relative orientation, model formation and absolute orientation (30 marks);

The Photogrammetric Program Package installed on the Novell network should be used for the solution, supplemented by writing additional computer programs, or by performing hand calculation, as necessary.

**Submission:**

- (a) A detailed, step-by-step description of the procedures followed in each method, including the equations used;
- (b) ;
- (c) Annotated copy of computer outputs;
- (d) Analysis (comparison) of the results.

**Total Value:** 60 marks (6% of final course mark).

## SE 3303 Photogrammetry I

### **Lab. #6: Numerical Orientation**

Given are the image space coordinates of Photos #8798 and #8799 processed in Lab #3, and the ground coordinates of certain points, as listed on Data Sheet 3. Determine the object space (ground) coordinates (X, Y, Z) of points 1050 and 1151 using approximate numerical solutions as follows:

1. Calculate the dependent pair relative orientation elements of the stereo pair using the y-parallax equation. (Note that the equations in the lecture notes express the orientation elements as errors).
2. Calculate the model coordinates of all image points based on the relative orientation elements. (It is sufficient to use the 1st order approximation of the rotation matrix to form the model coordinates).
3. Determine the residual y-parallax at each orientation point in the model formed in Qu 2.
4. Select three ground control points and perform the absolute orientation of the model using the sequential method. (Note, that two of the equations must be set up for the Z coordinates).
5. Calculate the object space coordinates of the two unknown points. (You have to use the rigorous form of the Rodrigues matrix. Assume that  $B_x$  is equal to the photo base, B.)
6. Compare the results obtained in this assignment with those in Lab. #3., and draw conclusions.

#### **Submission:**

A tabulated list of input, intermediate and final values

**Total Value:** 40 marks (4% of final course mark).

## SE 3303 Photogrammetry I

### **Lab. #7: Familiarization with Analogue Stereo-plotters**

1. Examine the Balplex stereo-plotter in Room E-17 and the Wild A10 stereo-plotter in Room E-16 and familiarize yourself with the following main components of a stereo-plotter:
  - projection and illumination system,
  - viewing system
  - tracing and measuring system.
2. Note the physical (analogue) implementation of the analytical concepts of interior and exterior orientations, collinearity and coplanarity conditions, and space intersection.
3. List all possible projector motions available in both instruments.
4. Examine the gimbal suspension in both instruments and note which the primary, secondary and tertiary axis of rotation is. What is the proper sequence for combining these three rotations to form the resultant  $M_T$  rotation matrix for these instruments?
5. In the Balplex, study the effect of the six projector motions on the position in the projection plane of the nine marked grid intersections. Draw a series of diagrams to illustrate these effects.
6. Perform the relative orientation of the grid plates in the Balplex according to the two projectors (independent pair) and the one projector (dependent pair) method. (See the lecture notes).
7. (a) Perform the absolute orientation in the following manner:  
Determine the scale of the grid model under the assumption that the length of the diagonal of one grid square is 900 m on the ground.  
  
(b) Change the model scale to 1:10 000.  
  
(c) Level the model. Any grid intersection can serve as vertical control since all grid intersections have the same elevation. Use the individual projector rotations to simulate the common projector rotations. (See the lecture notes).

#### **Submission:**

- a) Brief description of the construction of each instrument.
- b) A short discussion on the analogue versus the analytical photogrammetric operations based on the observations made in 2.
- b) Appropriate response to Items 3. to 5.

**Total Value:** 20 marks (2% of final course mark).

## DATA SHEET 1

## S.E. 3312 ANALYTICAL PHOTOGRAMMETRY

## 1. Calibrated Fiducial Coordinates

<u>Point</u>	<u>X (mm)</u>	<u>Y (mm)</u>
1	105.999	106.002
2	106.011	-106.000
3	-105.991	-106.000
4	-106.001	106.002

## 2. Observed comparator coordinates of fiducial marks.

<u>Point</u>	<u>Photo 8798</u>		<u>Photo 8799</u>	
	<u>X (mm)</u>	<u>Y (mm)</u>	<u>X (mm)</u>	<u>Y (mm)</u>
1	405.482	402.597	405.029	402.587
2	405.611	190.561	405.098	190.550
3	193.569	190.428	193.076	190.473
4	193.458	402.474	193.018	402.513

## 3. Observed comparator coordinates of control points.

<u>Point</u>	<u>Photo 8798</u>		<u>Photo 8799</u>	
	<u>X (mm)</u>	<u>Y (mm)</u>	<u>X (mm)</u>	<u>Y (mm)</u>
1149	205.680	380.074	--	--
1049	196.559	296.969	--	--
849	196.405	197.374	--	--
850	294.048	198.735	206.713	211.229
1050	293.997	292.230	205.778	302.632
1150	294.541	385.240	205.363	399.061
1151	384.197	382.791	298.793	396.929
1051	383.379	291.247	296.268	301.961
851	383.065	199.833	294.374	212.431
852	--	--	386.290	216.738

## DATA SHEET 2

S.E. 3312. ANALYTICAL PHOTOGRAMMETRY

Camera Calibration Data

1. Focal Length: 153.000 mm
2. Radial lens distortion polynomial coefficients:

$$\Delta r = k_0 r + k_1 r^3 + k_2 r^5 + \dots$$

( $\Delta r$  is in micrometres)

( $r$  is in millimetres).

$$k_0 = -0.1299737 \quad k_1 = 4.378912 \text{ E-5} \quad k_2 = -2.60268\text{E-9}$$

Photo Information

3. Flying Height: approx. 3100 m above datum  
Average terrain elevation: 450m

Miscellaneous

4. Earth Radius: approx. 6370 km.

## DATA SHEET 3

## S.E. 3312. ANALYTICAL PHOTOGRAMMETRY

## 1. Ground Coordinates of control points in U.T.M. System.

<u>Point</u>	<u>X(m)</u>	<u>Y(m)</u>	<u>Z(m)</u>
1149	438817.956	3629823.735	452.403
1049	437300.055	3629956.293	451.253
849	435567.275	3629920.910	451.990
850	435568.736	3628224.783	452.466
1150	438915.736	3628201.190	455.420
1051	437178.798	3626605.042	455.246
851	435566.790	3626654.696	452.178
852	435620.929	3624989.483	453.948